GEM TN-93-452

GEM Collaboration Council Meeting SSCL

August 5, 1993

Abstract:

Agenda, attendees, and presentations of the GEM Collaboration Council Meeting held at the SSC Laboratory on August 5, 1993.

GEM COLLABORATION COUNCIL MEETING

REVISED AGENDA

August 5, 1993

9:00 AM	Greetings, Announcements	Yost
9:10	Status of the collaboration	Barish
10:00	Project Manager's Report	Sanders
10:30	Break	
10:40	Calorimetry	Willis
11:20	Muon System	Taylor
11:50	Tracker System	Baltay/Thomas
12:20 PM	Lunch	
1:20	B Physics with GEM	Yamamoto
1:40	Pattern Recognition in GEM Muon System	Dingus
2:00	Simulation results since TDR	Womersley
2:20	FCAL test results from BNL	Rutherfoord
2:40	Computing Report	Word
3:00	Status of the Laboratory	Schwitters
3:30	Adjourn	

gem

γeμ

Presentation by:

G. Yost

August 5, 1993

GEM Council Meeting

Reminder: Future Council dates:

Sept 30

Dec 2

General Collaboration

Meeting:

Nov 1, 2, 3

Gatlinburg, TN

Parks Vista Hotel

(615) 436-9211

ORNL will organize the meeting.

Big Printing of the TDR:
in 2 weeks (± 1 week);
every collaboration member will
receive a copy.

NIS site tour and tunnel
tour tomorrow.

Meet here @ 7:30 AM for
safety orientation.
Transportation to depart 8:00.
Only 30 people in tunnel;
must be clear by 9:30.

Tunnel tour sign-up at
reg. desk.

gem

γeμ

Presentation by:

B. Barish

8/5/93.

GEM

SSC Status

Senate
Mangmt
#

GEM Status

FY93 #

Detector Progress / Evolution
- Configuration Control
- Design Progress

PLANS FY94 –
- Fermilab Test Beam "Sector Test" Proposal
- Engineering Design
- Magnet

CALORIMETER WITH FEM - A & B

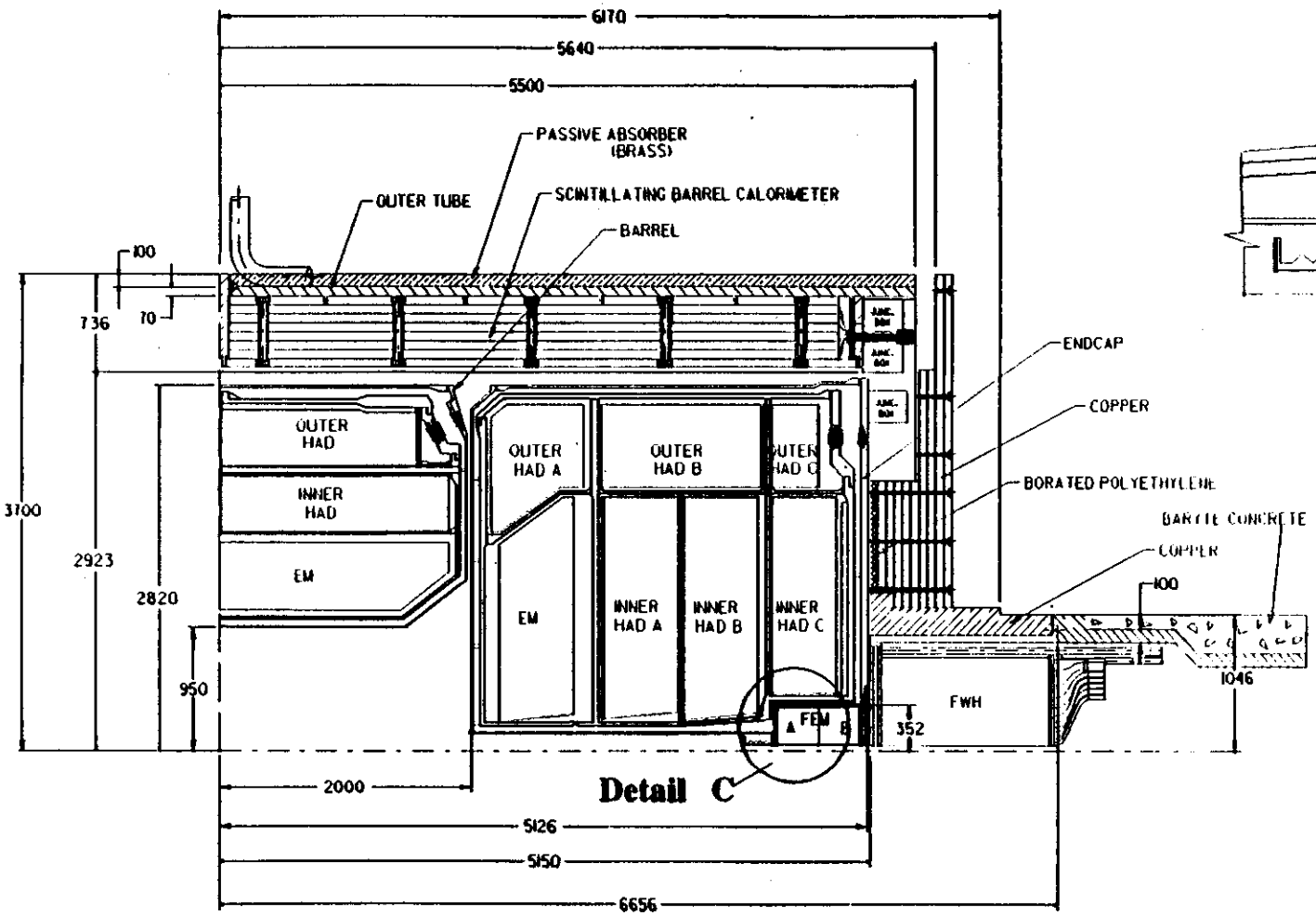

Detail C

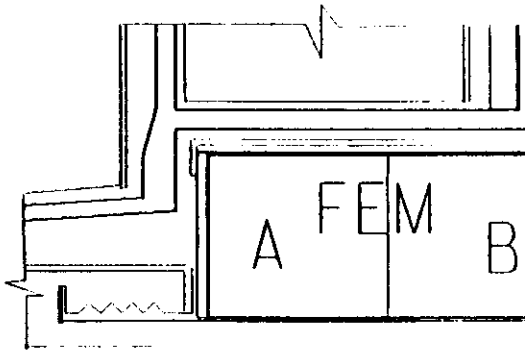

(tdrfcal/930802/xc

GEM CALORIMETER WITH SEPARATE FORWARD CALORIMETER

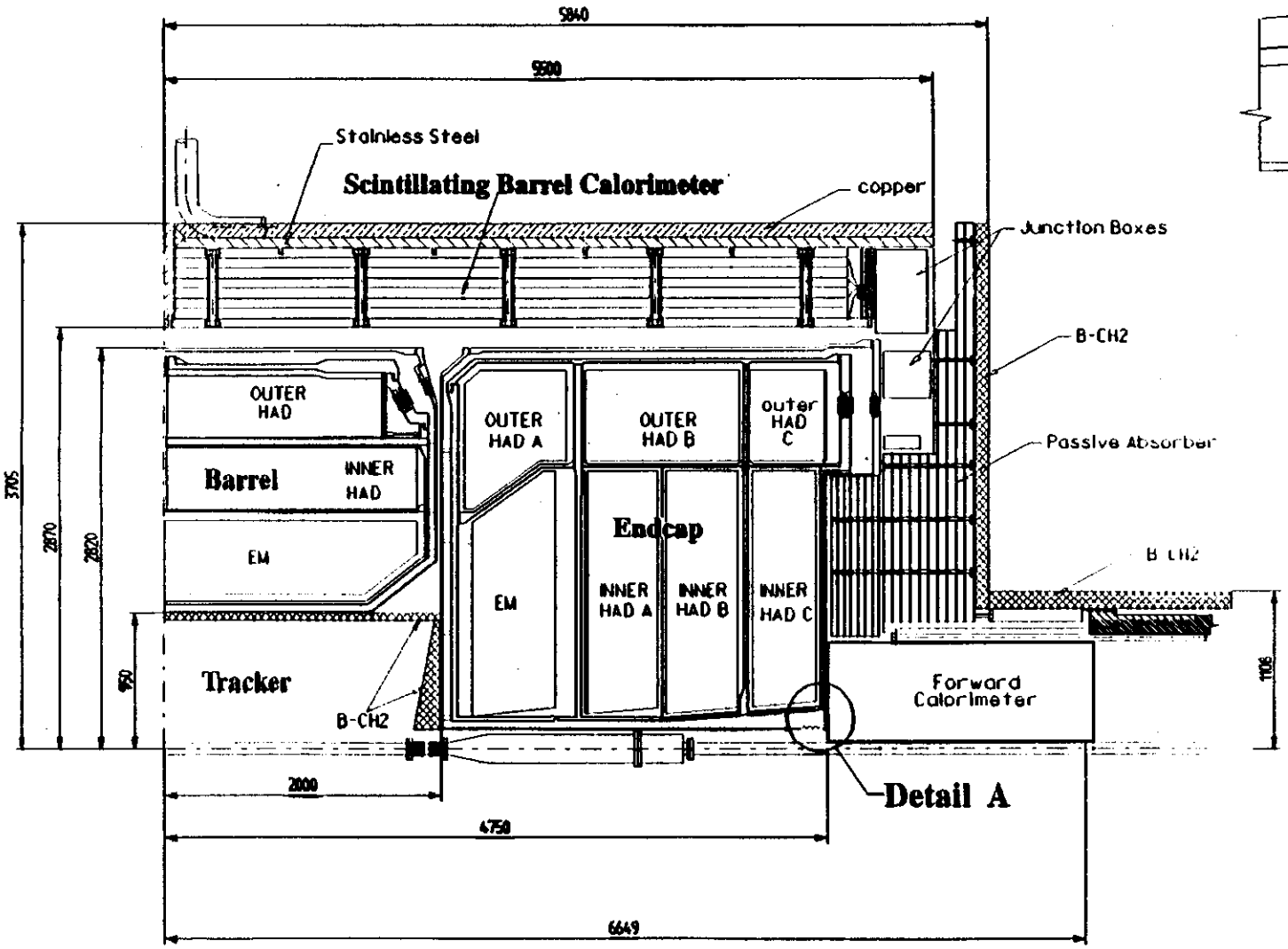

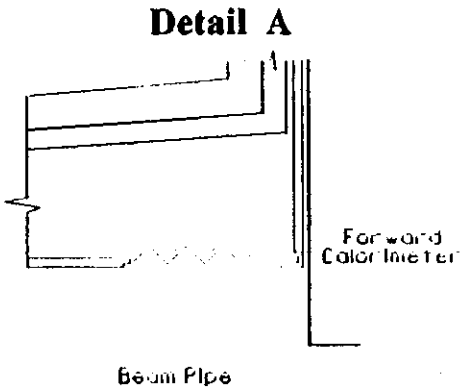

(lmfwcal 930802/sc)

GEM DETECTOR
PROPOSED PARAMETERS

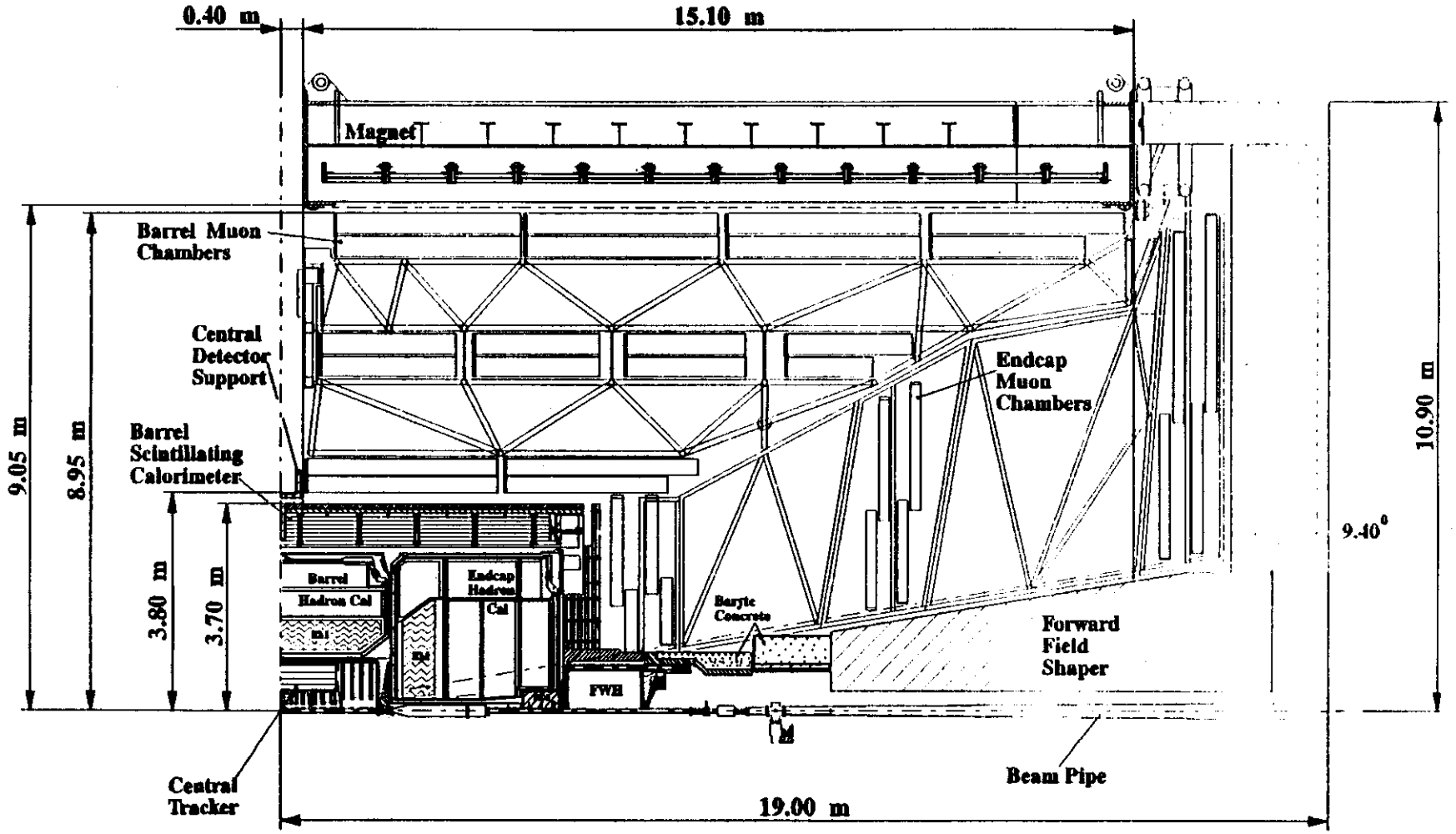

(PROpr/930803/

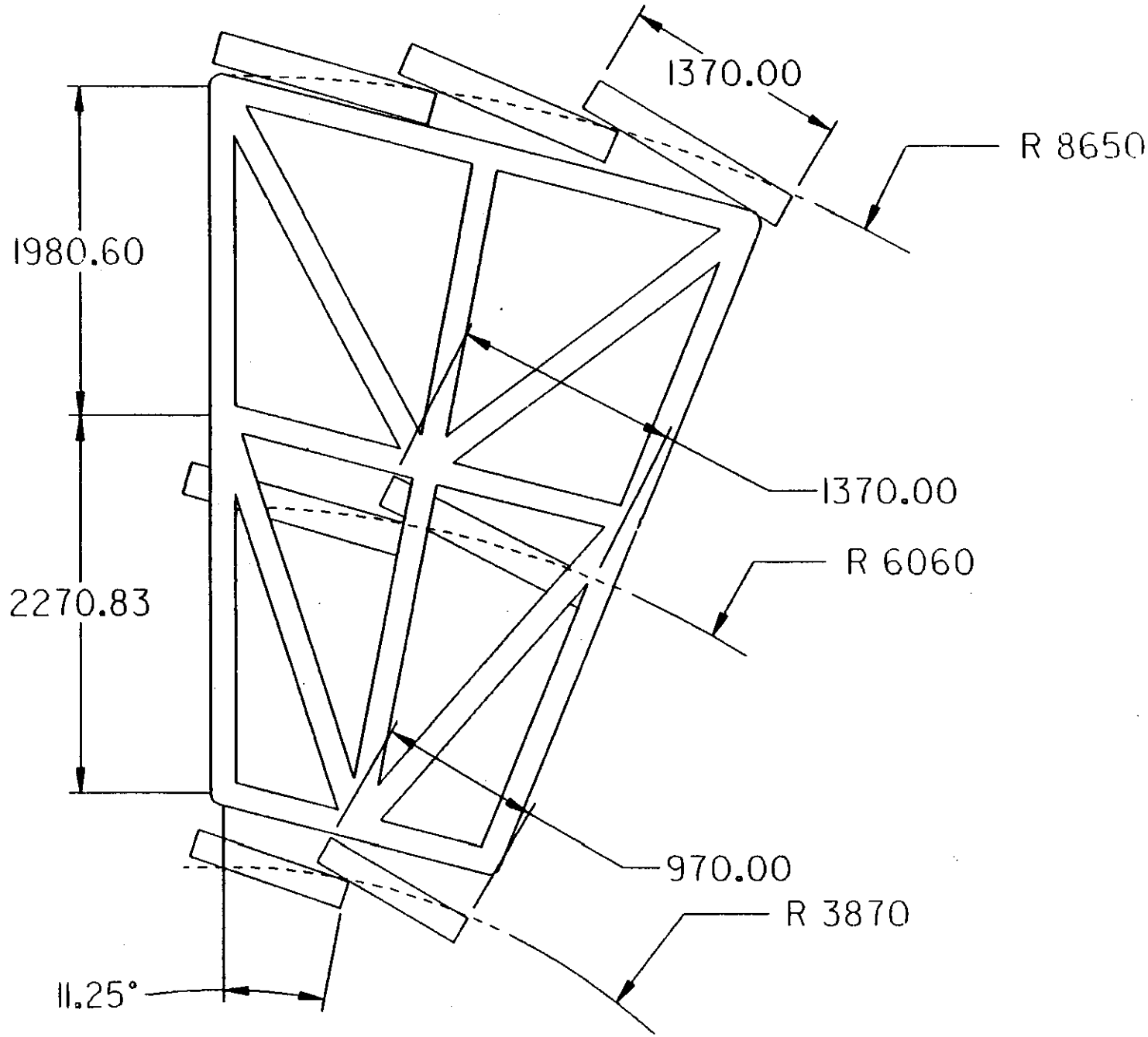
1370.00
R 8650
1980.60
1370.00
R 6060
2270.83
970.00
R 3870
11.25°

gem

γeμ

Presentation by:

W. Willis

FNAL TEST

"MARCH '95"

= NOVEMBER '95 ?

PHASE	SCOPE
TDR	TEST CAL. TRANSITION
PAC RPT	ASKS REALISTIC * CT w/ ELECTRONICS * CAL " + STRIPS * μ FULL SCALE + ELECTRONICS + ALIGN.
"SUSPENDED ANIMATION"	"18° SECTOR" WHAT IS IT?

Test Beam Cryostat & Transporter

-Bill Wisniewski

GEM TEST BEAM CRYOSTAT
MODULE ARRANGEMENT

Rev: 6/11/93

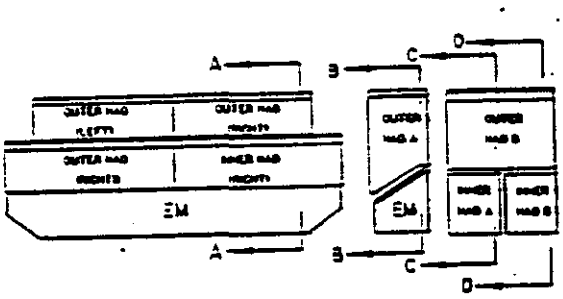

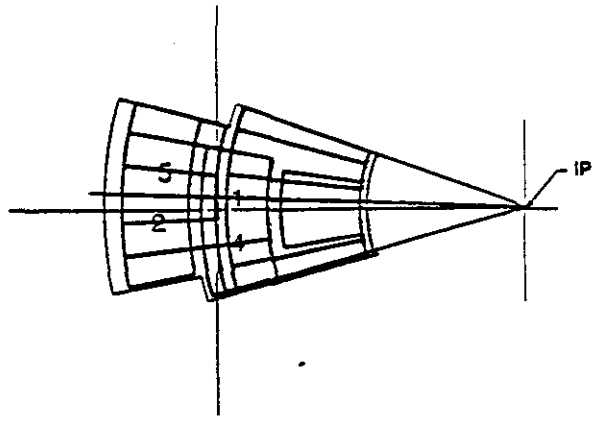

COMPOSITE VIEW
ROTATED 90°

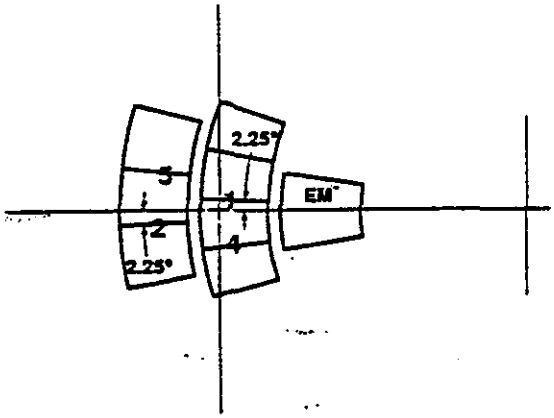

SECTION A-A (BARREL)
ROTATED 90°

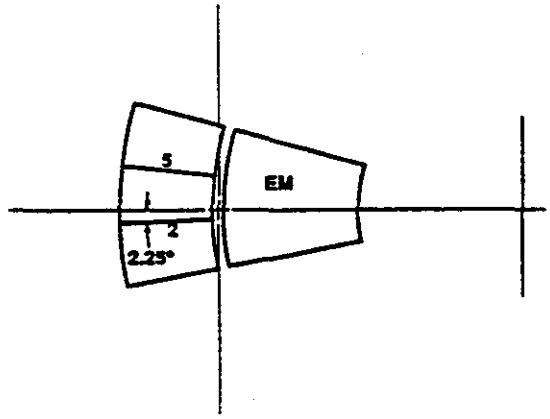

SECTION B-B (ENDCAP)
ROTATED 90°

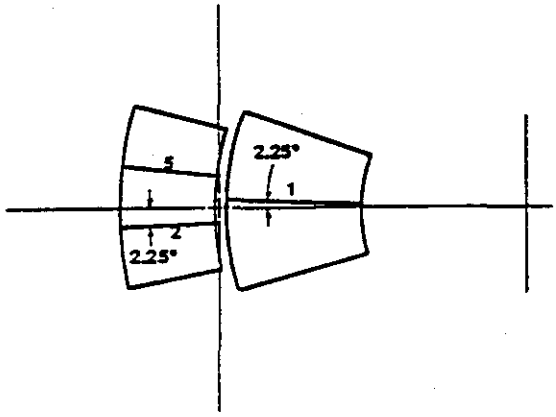

SECTION C-C (ENDCAP)
ROTATED 90°

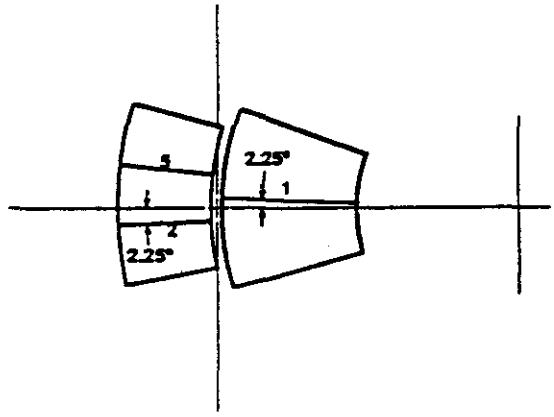

SECTION D-D (ENDCAP)
ROTATED 90°

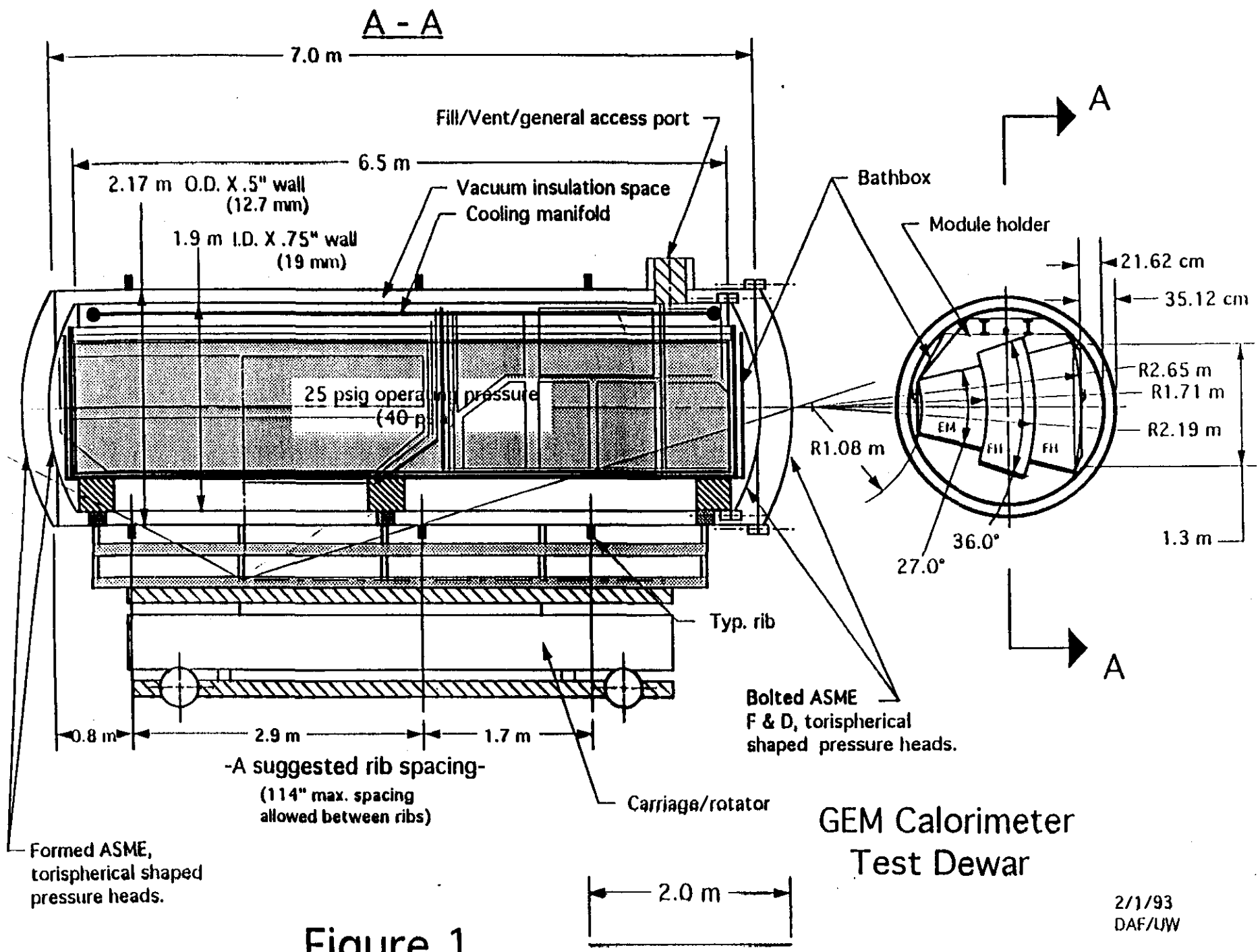
A - A
7.0 m
6.5 m
Fill/Vent/general access port
2.17 m O.D. X .5" wall
(12.7 mm)
1.9 m I.D. X .75" wall
(19 mm)
Vacuum insulation space
Cooling manifold
Bathbox
Module holder
A
21.62 cm
35.12 cm
R2.65 m
R1.71 m
R2.19 m
EM
FH
FH
R1.08 m
36.0°
27.0°
1.3 m
25 psig operating pressure
(40 psi)
Typ. rib
Bolted ASME
F & D, torispherical
shaped pressure heads.
0.8 m
2.9 m
1.7 m
-A suggested rib spacing-
(114" max. spacing
allowed between ribs)
Carriage/rotator
Formed ASME,
torispherical shaped
pressure heads.
2.0 m
GEM Calorimeter
Test Dewar
2/1/93
DAF/UW

Figure 1

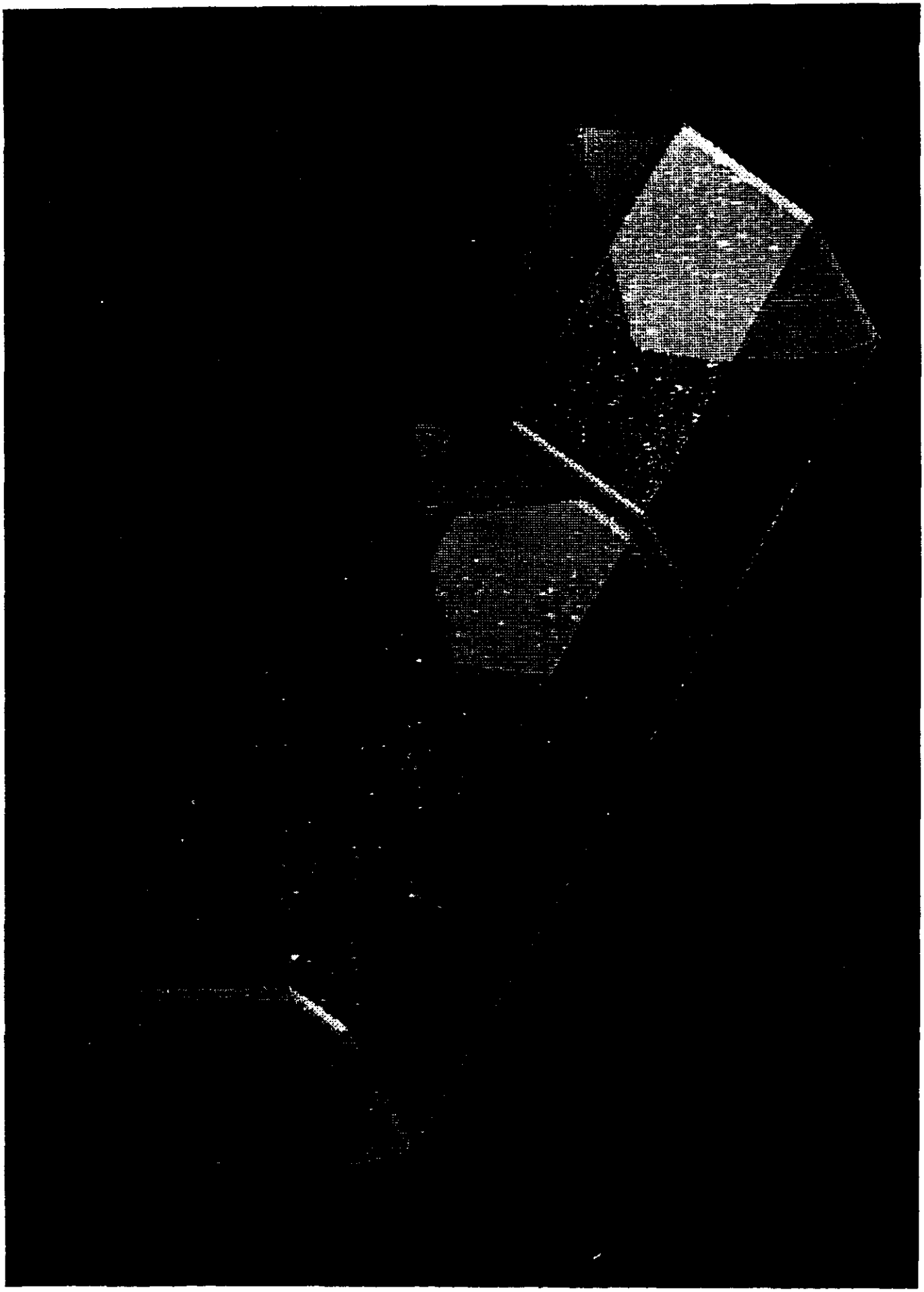

Cryostat Outer Vessel Unwrapped View
(Heads Not Shown; Head Depth = 17.17")

Rev: 7/8/93

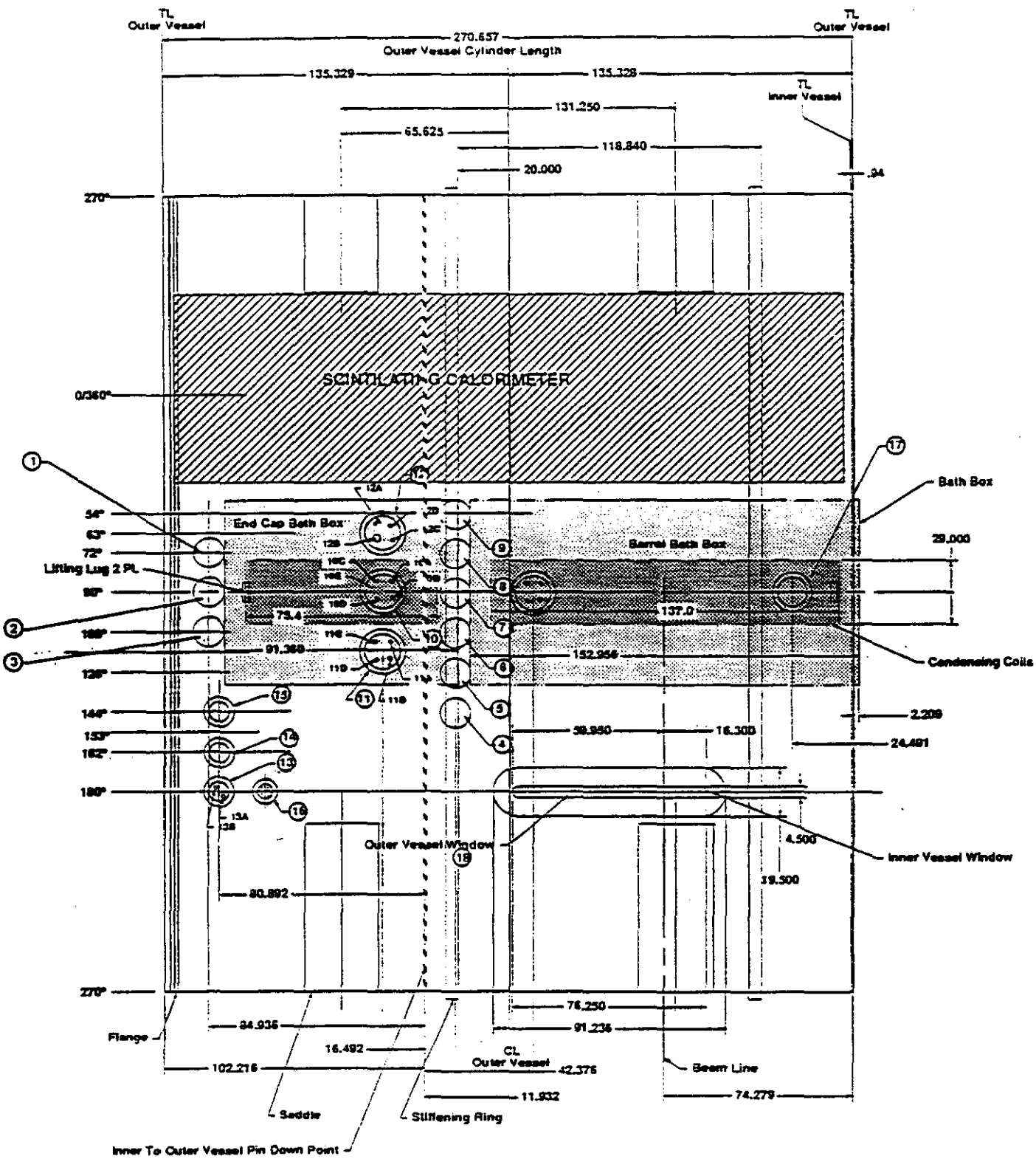

Problems:
1. Stiffening Ring interferes with center ports
2. Signal feedthru ports are now 12.0" dia and old spacing (shown) probably will not work.

Notes
1. Axial thermal shrinkage at any point on inner vessel can be calculated by mutiplying length from pin point by -.00454.
2. Inner vessel radial shrinkage is.41".

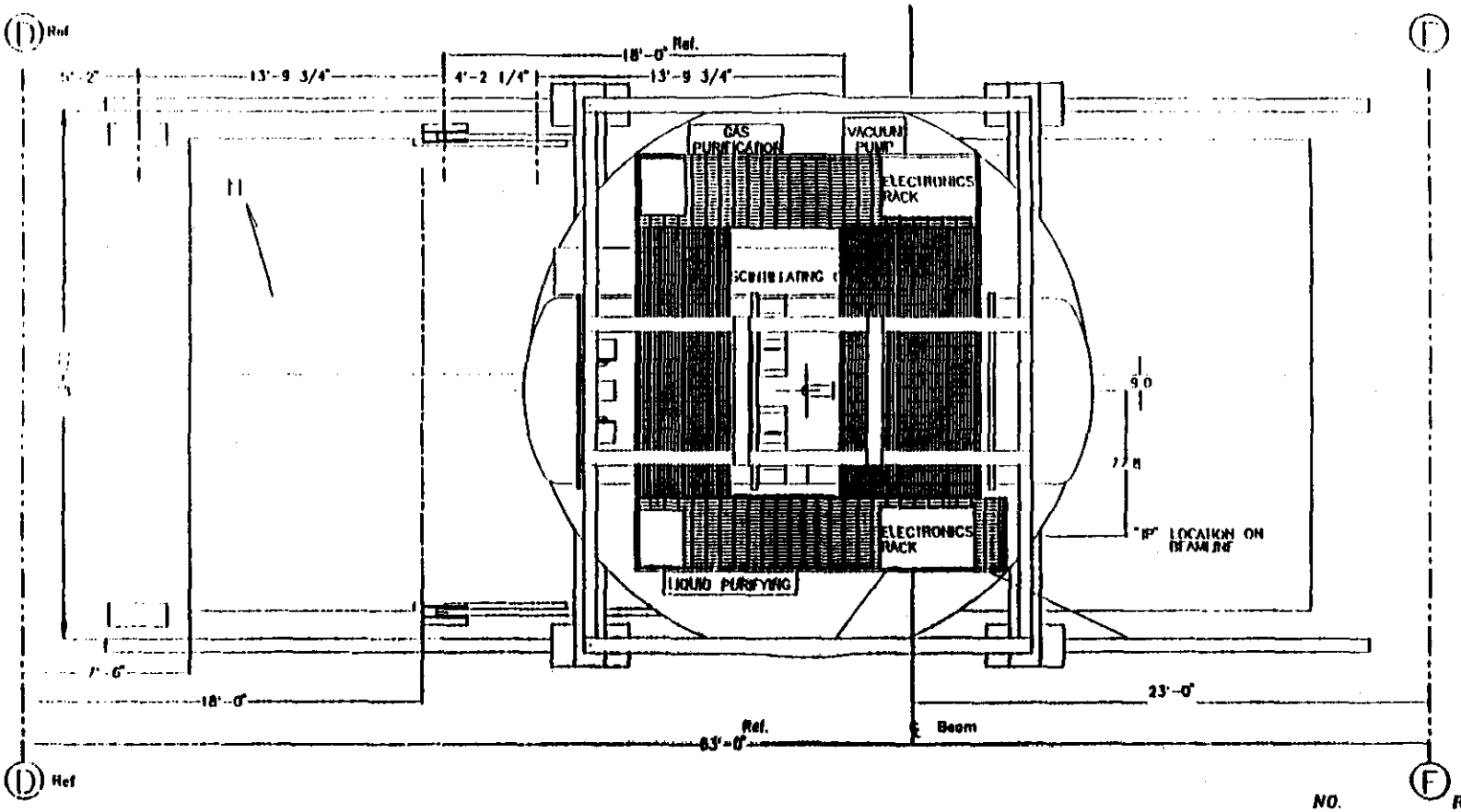

NO. REVISIONS

DEPT. OF PHYSICS AND ASTRO
UNIVERSITY OF ROCHESTE
SIDNEY W. BARNES RESEARCH LA

DWG. TITLE
CONCEPT 'D' PLAN VIEW

DR. Don Spielak	DATE: JULY 14, 93	FO
C'K'D	DATE:	

REMOVE ALL BURRS & SHARP
TOLERANCES UNLESS OTHERWISE

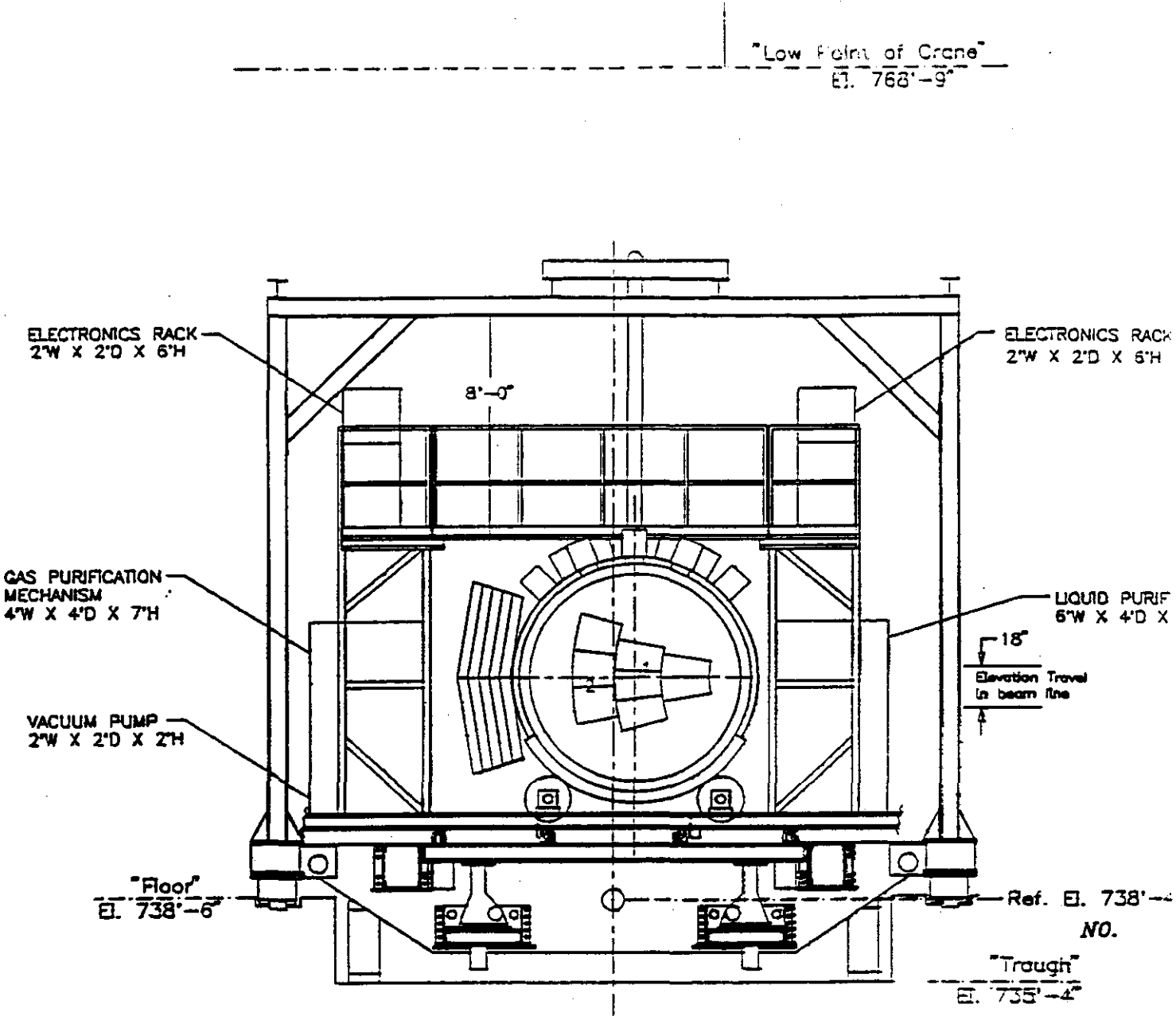

SI

DWG. TI

DR. D

C'K'D

DECIMAL

SCALE
NTS

PLAN FOR R+D - TEST

DOCUMENT

* HARVEY NEWMAN HAS 3 FIRST CUT DOCS NOW -
* HE WILL ISSUE GUIDE LINES SOON - FOR FIXING SCOPE, INTEGRATION, ETC
* REAL FIRST DRAFTS ~ 2 SEPT.
* EXECUTIVE COMMITTEE REVIEW 9 SEPTEMBER
* FINAL, WITH BUDGET + SCHEDLE AT GEM MEETING 30 SEPTEMBER

⇒ * TEXAS PROPOSALS!!! ⇐

gem

γeμ

Presentation by:

F. Taylor

F.E.Taylor August 5, 1993

STATUS of GEM MUON SYSTEM

Recent Activities:

(1) Perform the most essential R&D

- engineering plans for production CSC
  - chamber workshop at SSCL
- construction of full-scale CSC
  - parts being sent to Dubna
- fabricate electronics needed for CSC prototype
  - BNL (cathode) BU (anode)
- alignment R&D
  - video-bar code, stretched wire, plans for ATS
- simulation of detector performance
  - hit-level MC, coverage/new geometries, calorimeter thickness, $\Delta E\mu$ correction

(2) Optimization of muon system - cost and performance

(3) Formulate plans for FNAL test beam

- definition of goals
- equipment needed
- integration with calorimeter and CT
- schedule and costs

(4) Answer PAC questions

Chamber Engineering

(1) fabrication of cathode panels

- flat to ± 100μm over area 1.2 x 3.5 m^2
- cathode precision + intra-layer alignment ± 50μm
- low mass and cheap

(2) fabrication of chamber frames

- improve the baseline G-10 design with lower ρ

(3) integration with system

- where to attach to support structure
- placement of electronics, cooling, cabling

(4) construction of full-scale prototype at Dubna

- test electrical characteristics
- mechanical properties (sag, weight)

(5) fabrication of small-scale prototypes

- strip width studies
- endcap geometry
- Lorentz angle

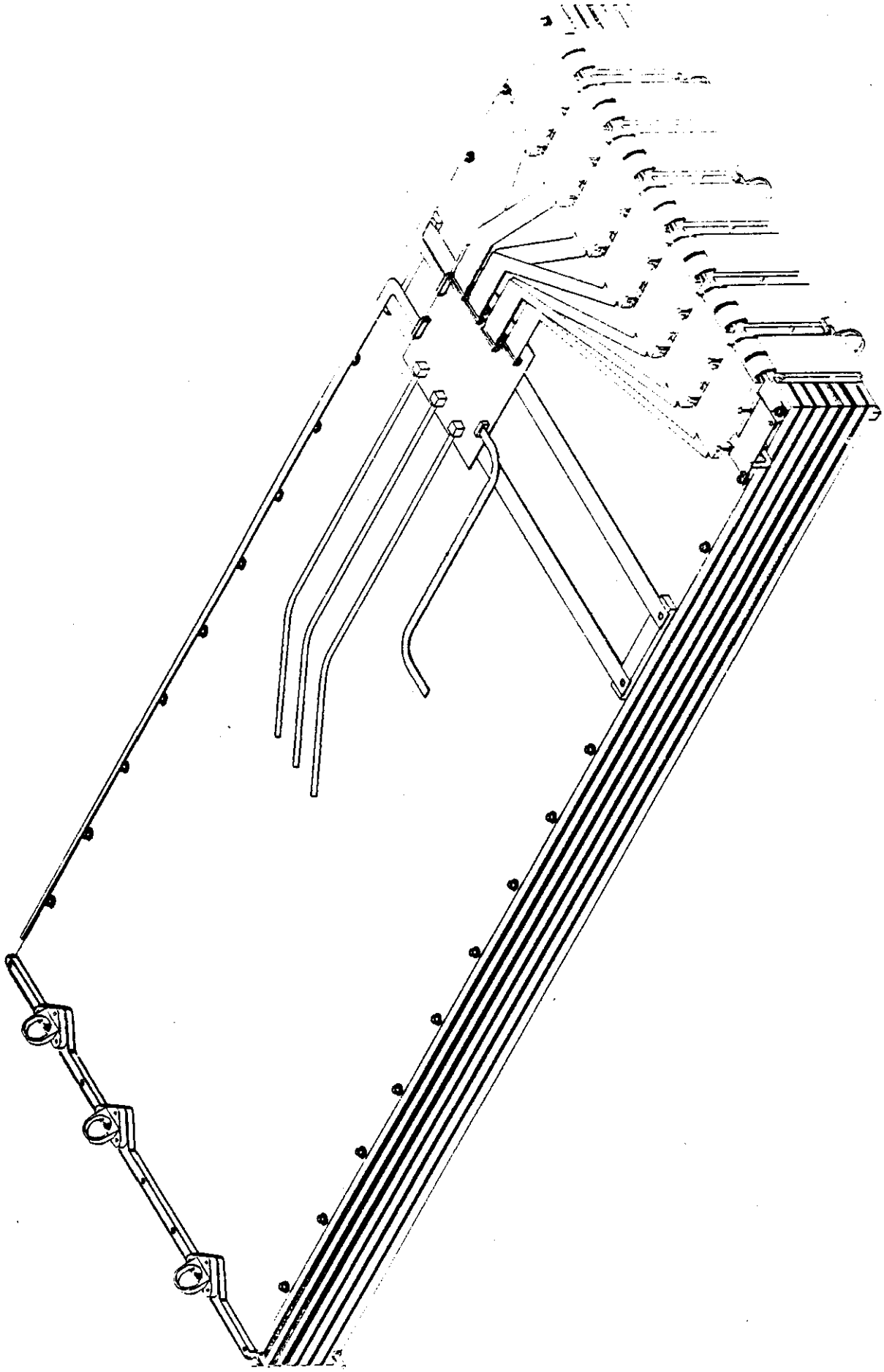

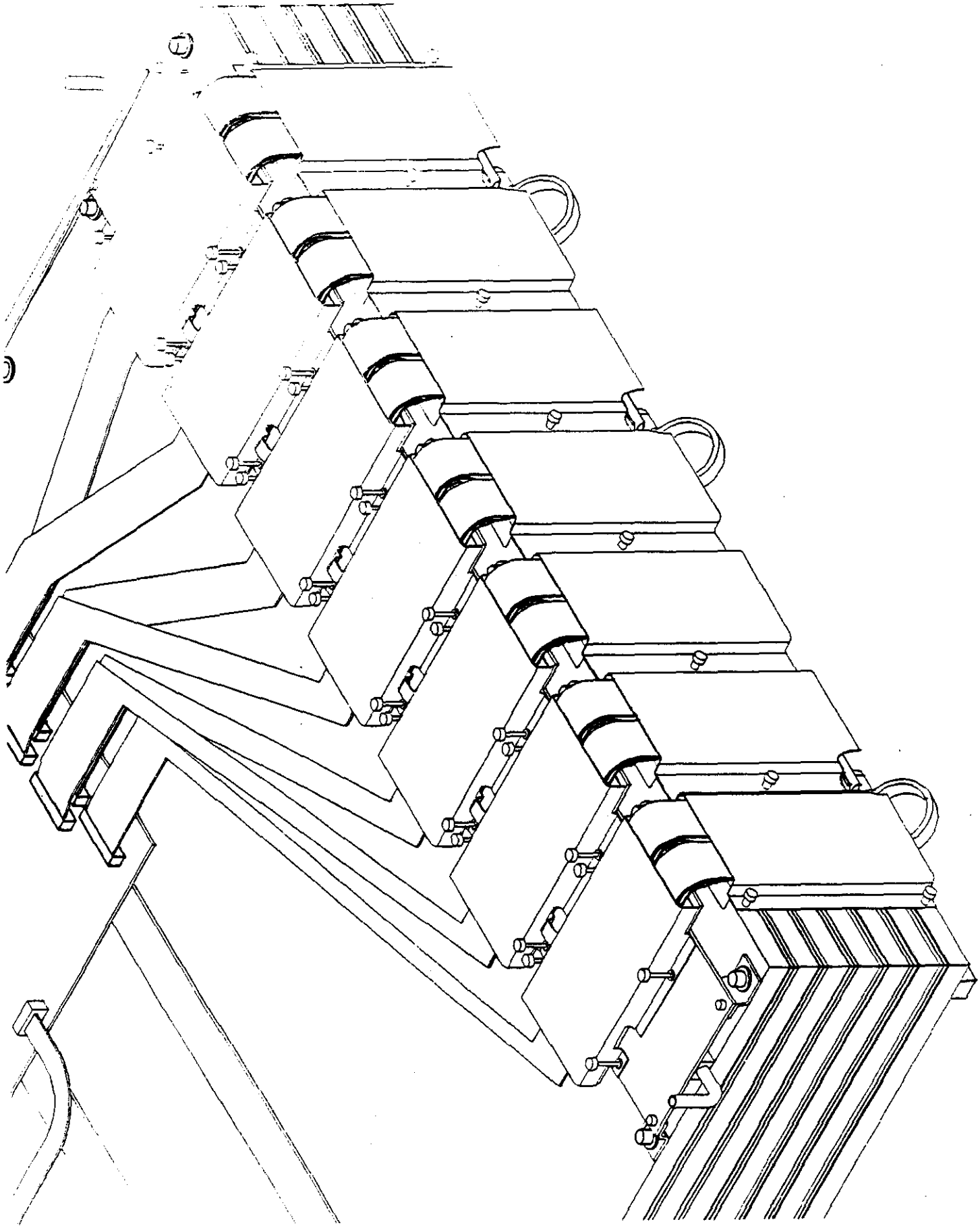

Optimization of Muon System

(1) axial-projective alignment scheme

- can reduce the θ gaps in barrel
  [present barrel loss $\Delta\eta \approx 0.17$]
  [goal: at least 1 SL coverage everywhere.]
- tests with wire readout promising
  [Andrei Korytov et al.]
- computations of sagitta error within baseline
  [Yuri Gerstein et al.]

(2) segmentation in ϕ ["why 48/TDR ?" Igor Golutvin]

- consider SL1:SL2:SL3 = 32:32:48
  - smaller number of chambers/uniform size
  - reduces X_0 in middle SL (less frames)

but:
  - how to align ?
  - how to support ?

(3) longer lever arm

- but smaller calorimeter => larger punch-through

(4) higher B-field

- massive re-engineering needed ?

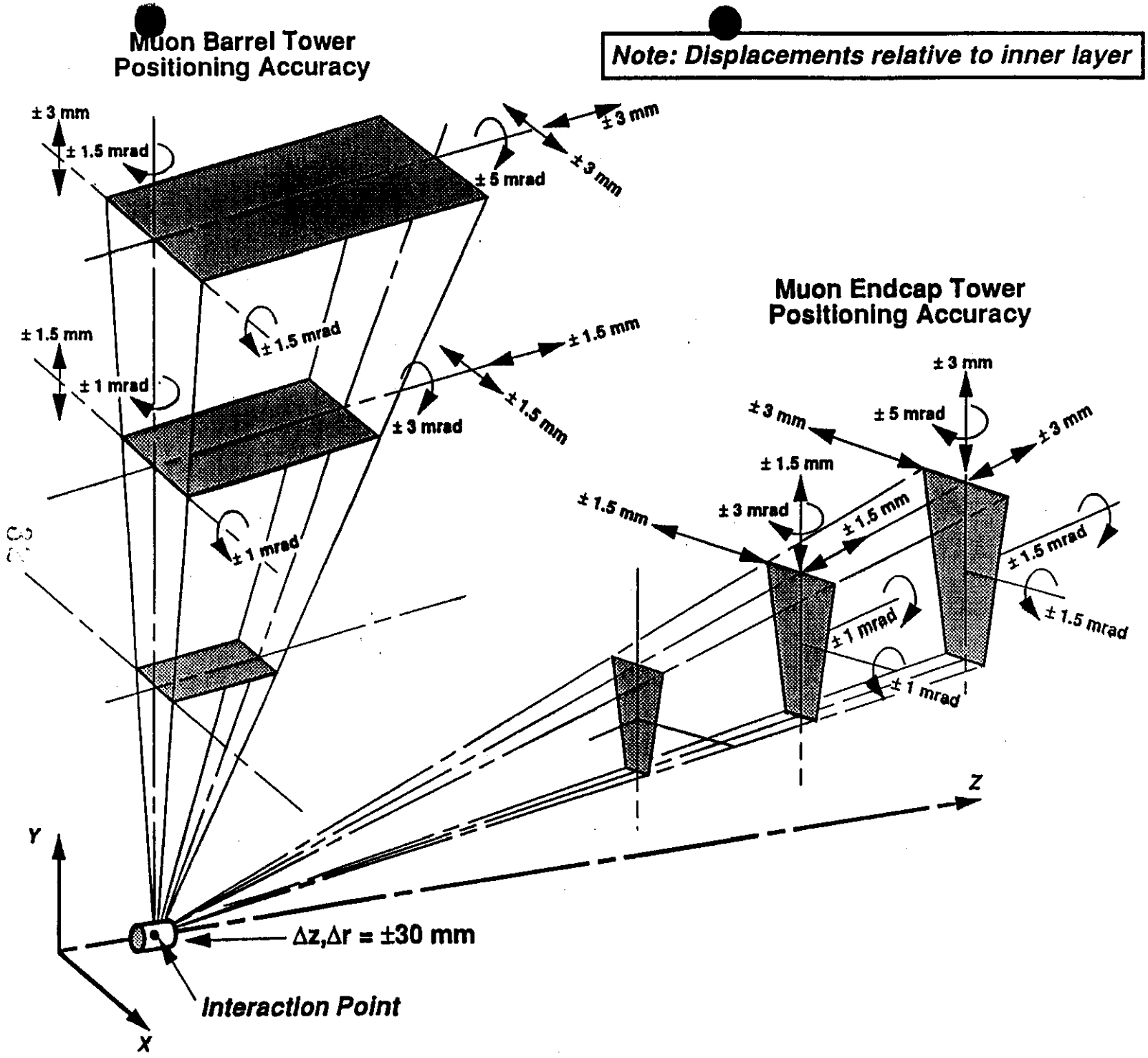
Muon Barrel Tower
Positioning Accuracy
Note: Displacements relative to inner layer
± 3 mm
± 1.5 mrad
± 5 mrad
± 3 mm
± 3 mm
± 1.5 mrad
± 1.5 mm
± 1 mrad
± 3 mrad
± 1.5 mm
± 1.5 mm
± 1 mrad
Muon Endcap Tower
Positioning Accuracy
± 3 mm
± 3 mm
± 5 mrad
± 3 mm
± 1.5 mm
± 1.5 mm
± 3 mrad
± 1.5 mm
± 1.5 mrad
± 1 mrad
± 1.5 mrad
± 1 mrad
Z
Y
X
Δz,Δr = ±30 mm
Interaction Point

GEM DETECTOR PARAMETERS
BASELINE 2

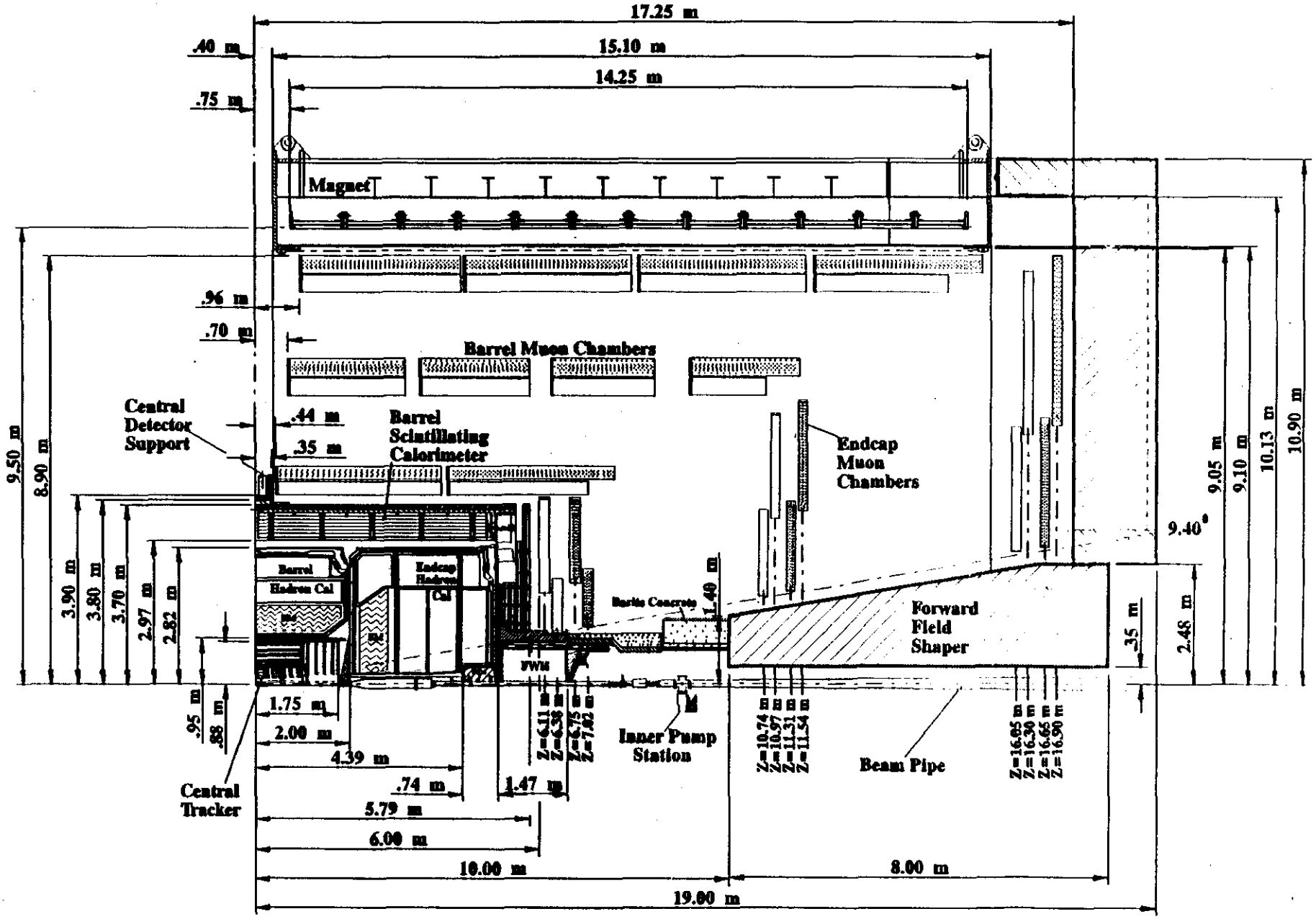

(DETpars/2/0/26/ZC)

(a)

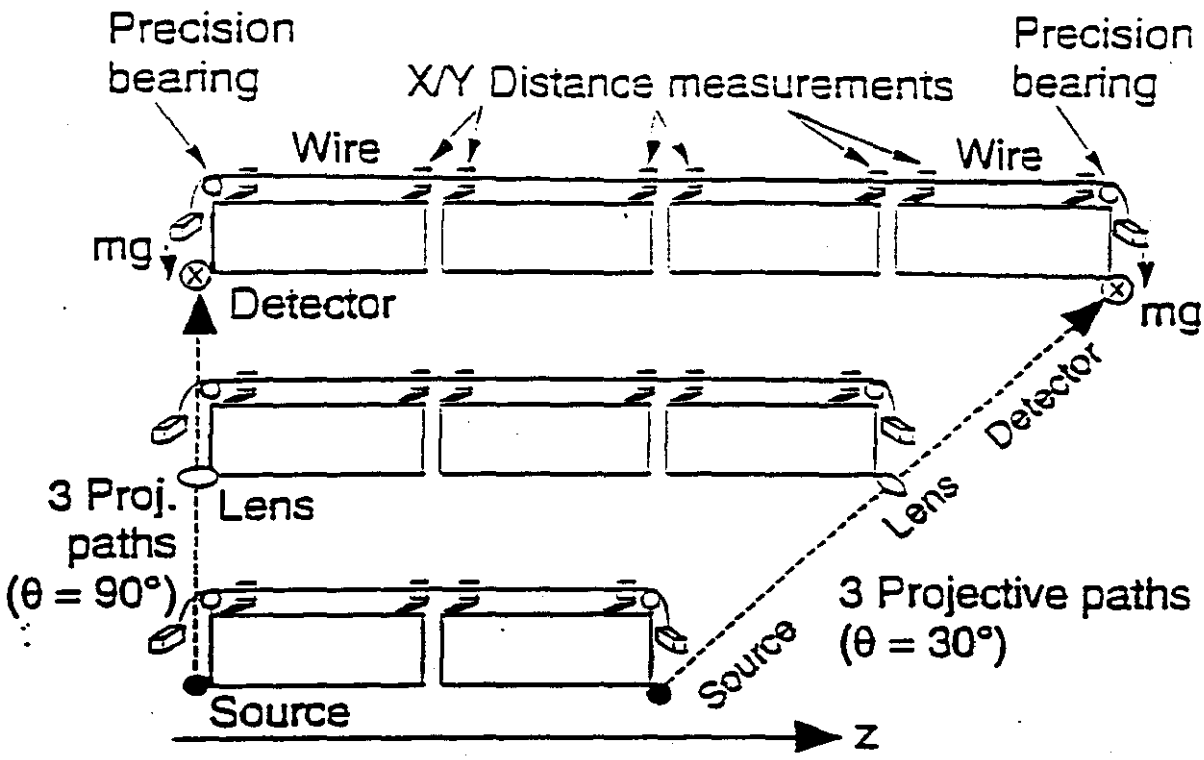
Precision bearing
X/Y Distance measurements
Precision bearing
Wire
Wire
mg
Detector
mg
Detector
3 Proj. paths (θ = 90°)
Lens
Lens
3 Projective paths (θ = 30°)
Source
Source
z

(b)

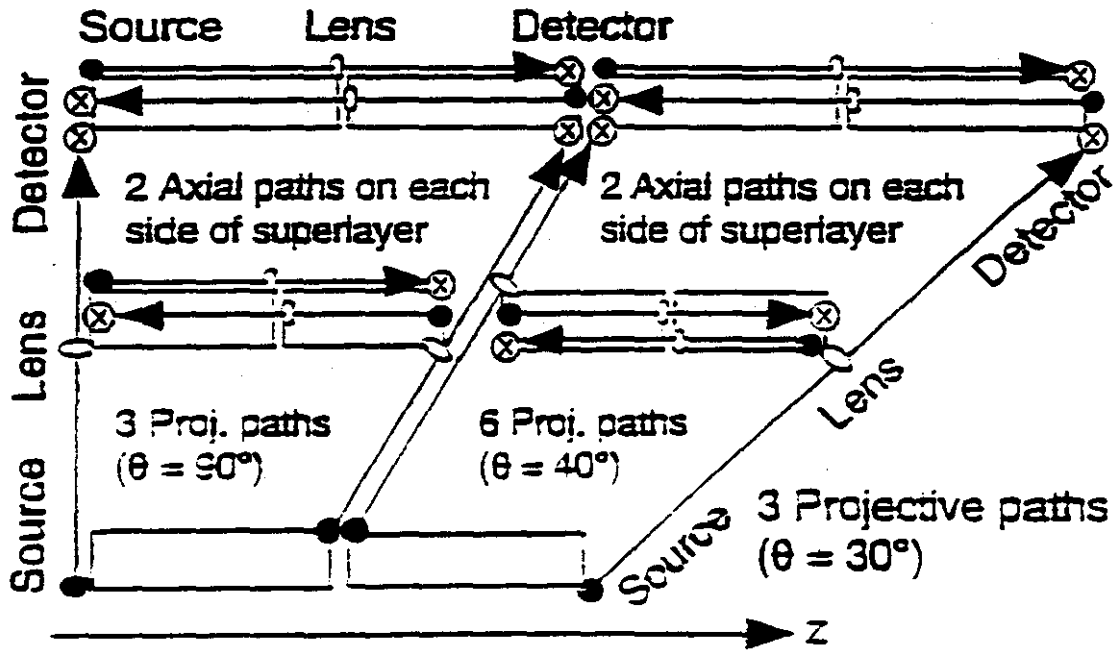
Source
Lens
Detector
Detector
2 Axial paths on each side of superlayer
2 Axial paths on each side of superlayer
Detector
Lens
Lens
3 Proj. paths (θ = 90°)
6 Proj. paths (θ = 40°)
3 Projective paths (θ = 30°)
Source
Source
z

TIP-03890

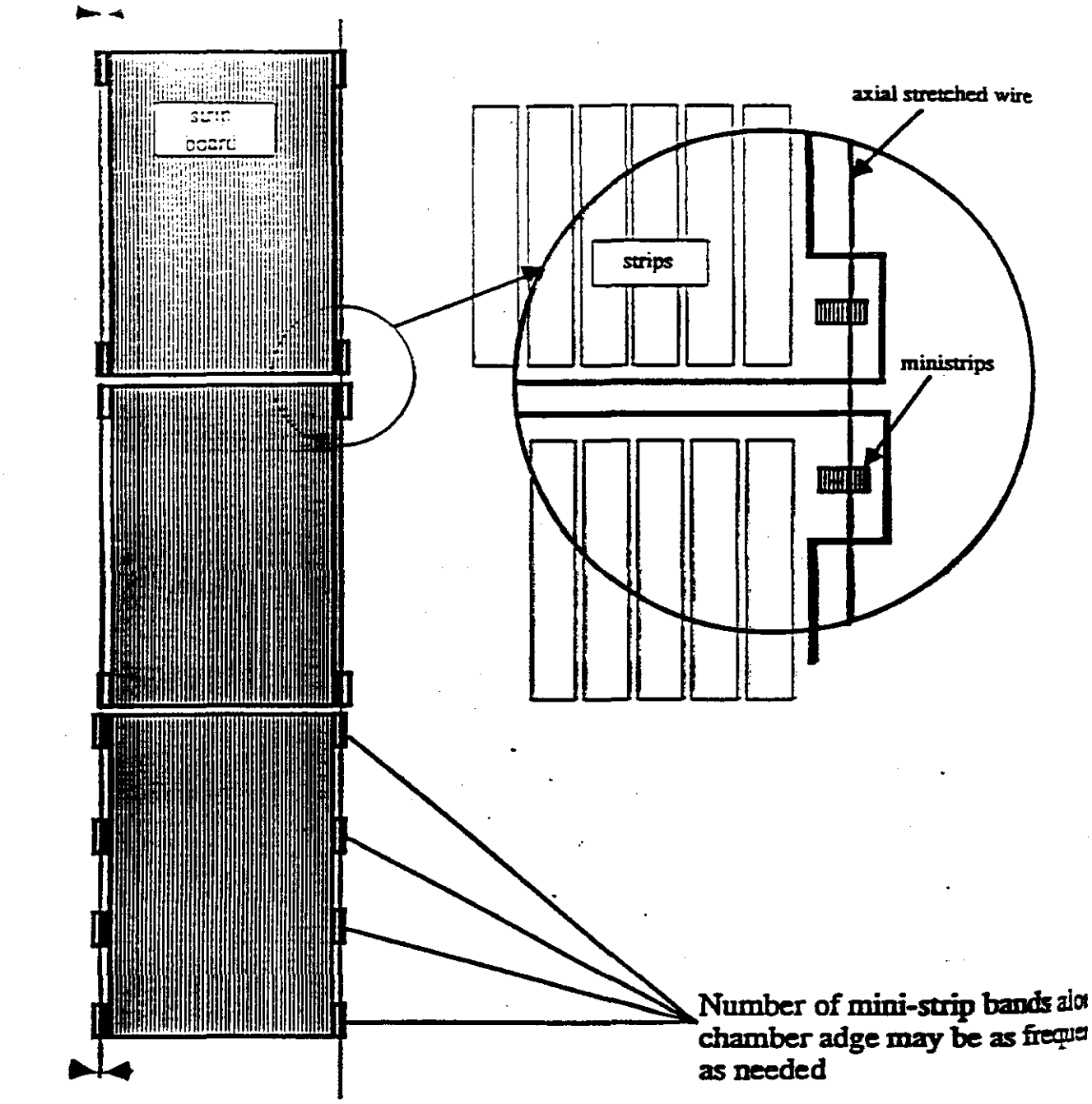

wire fixture
is NOT attached to
strip boards

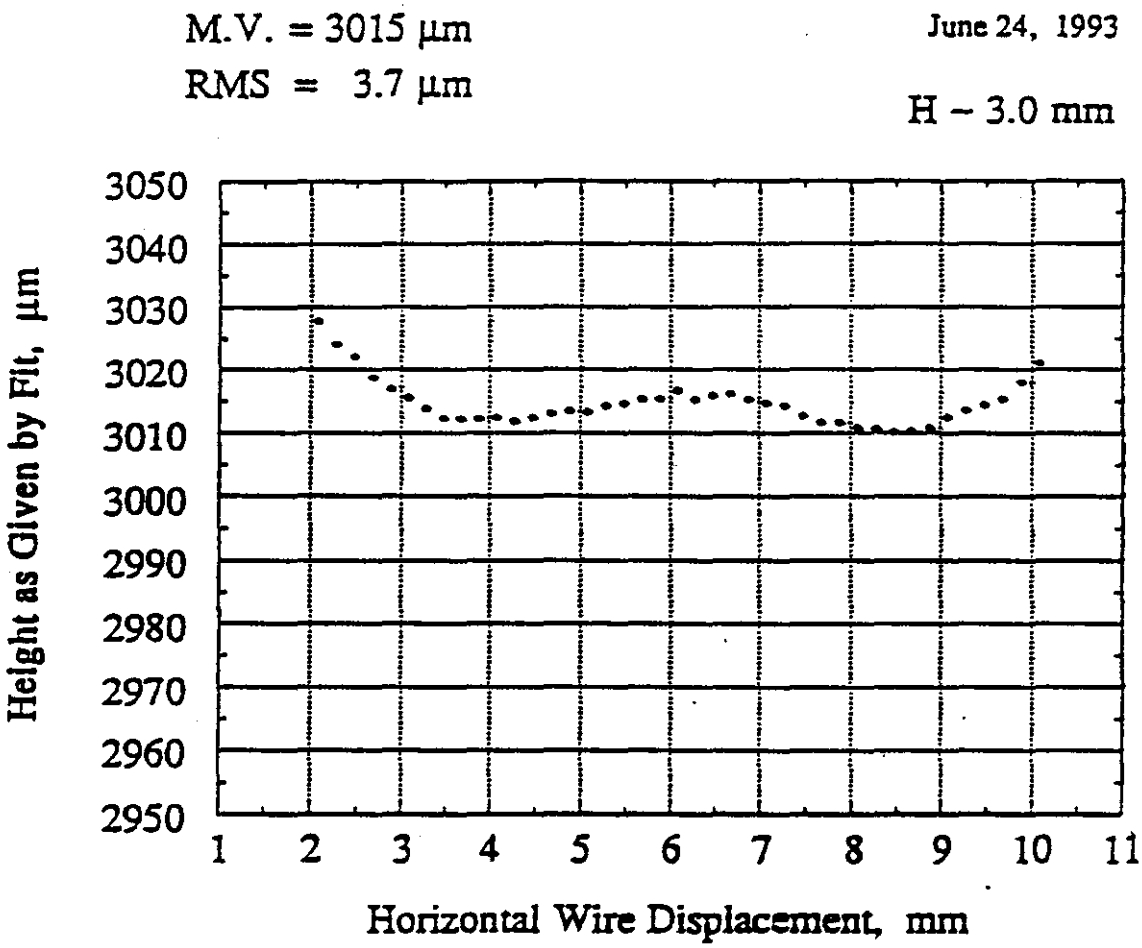
M.V. = 3015 µm
RMS = 3.7 µm
June 24, 1993
H – 3.0 mm
Height as Given by Fit, µm
3050
3040
3030
3020
3010
3000
2990
2980
2970
2960
2950
1
2
3
4
5
6
7
8
9
10
11
Horizontal Wire Displacement, mm

Alignment Test Stand (ATS) Objectives

- Provide a "Test Bed" for proposed projective alignment hardware.
- Provide variable temperature conditions as would be seen in GEM.
- Measure the effects of air disturbances on the actual structure.
- Test actual hardware designs for chamber/structure interface.
- Develop alignment procedures, testing and certification.
- Demonstrate the physical constraints of the various alignment schemes.
- Test positioning actuators and kinematic mounting schemes.
- Test bed for using X rays for global alignment.

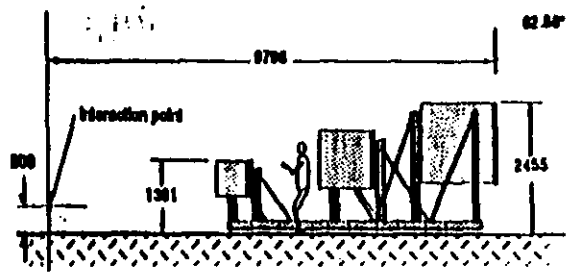

Mechanical Design and Fixturing

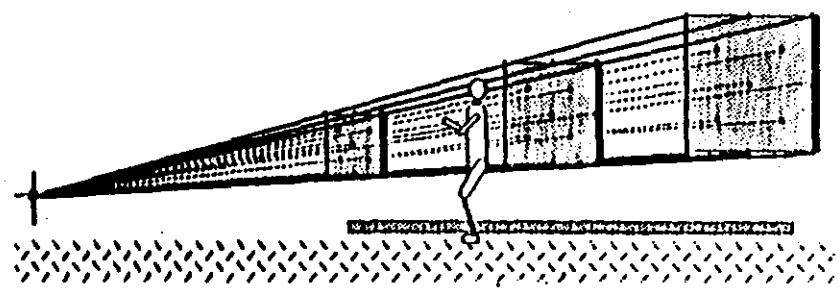
Projective Alignment Lines of Sight

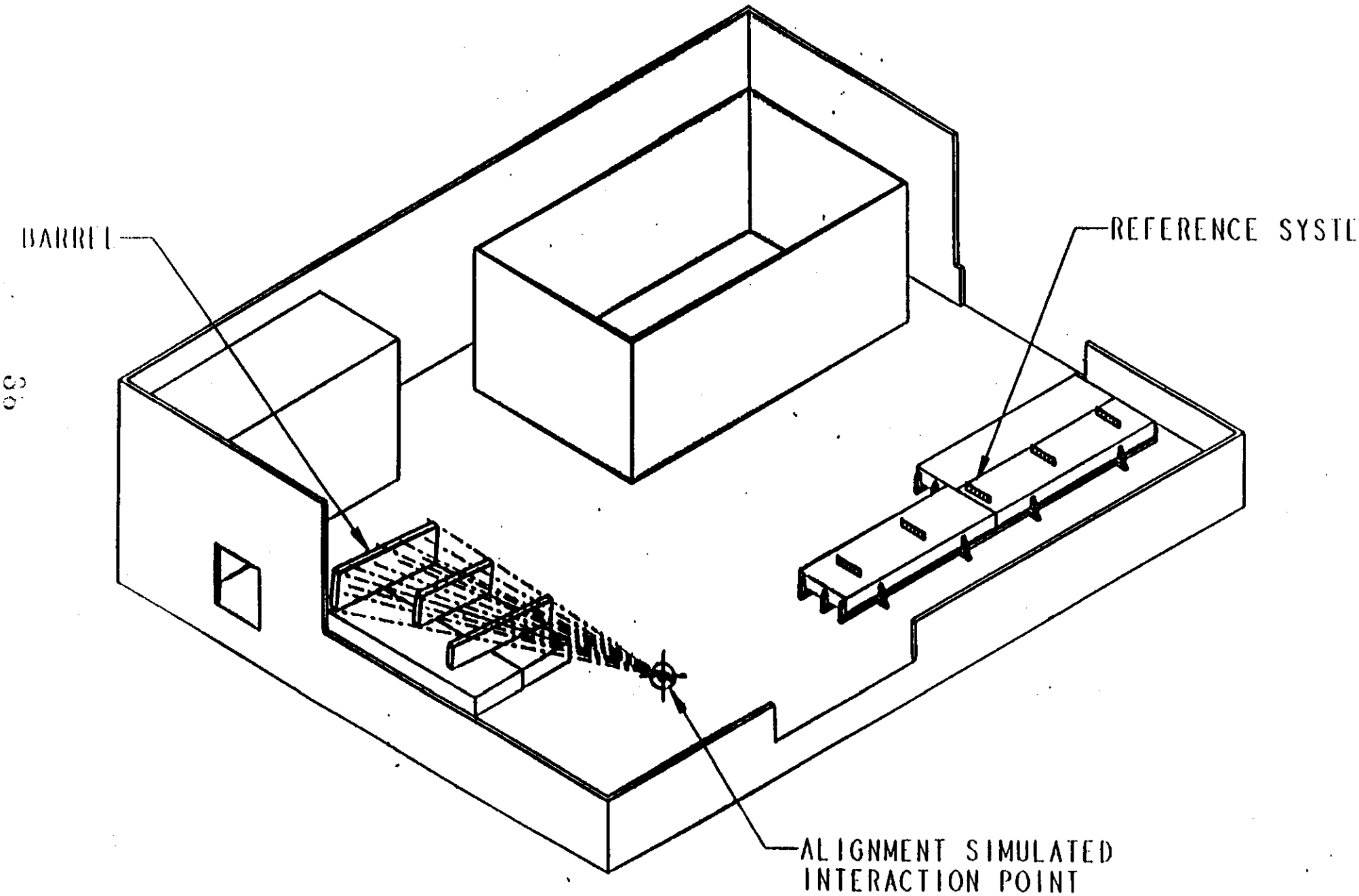
BARREL
REFERENCE SYSTE
ALIGNMENT SIMULATED
INTERACTION POINT

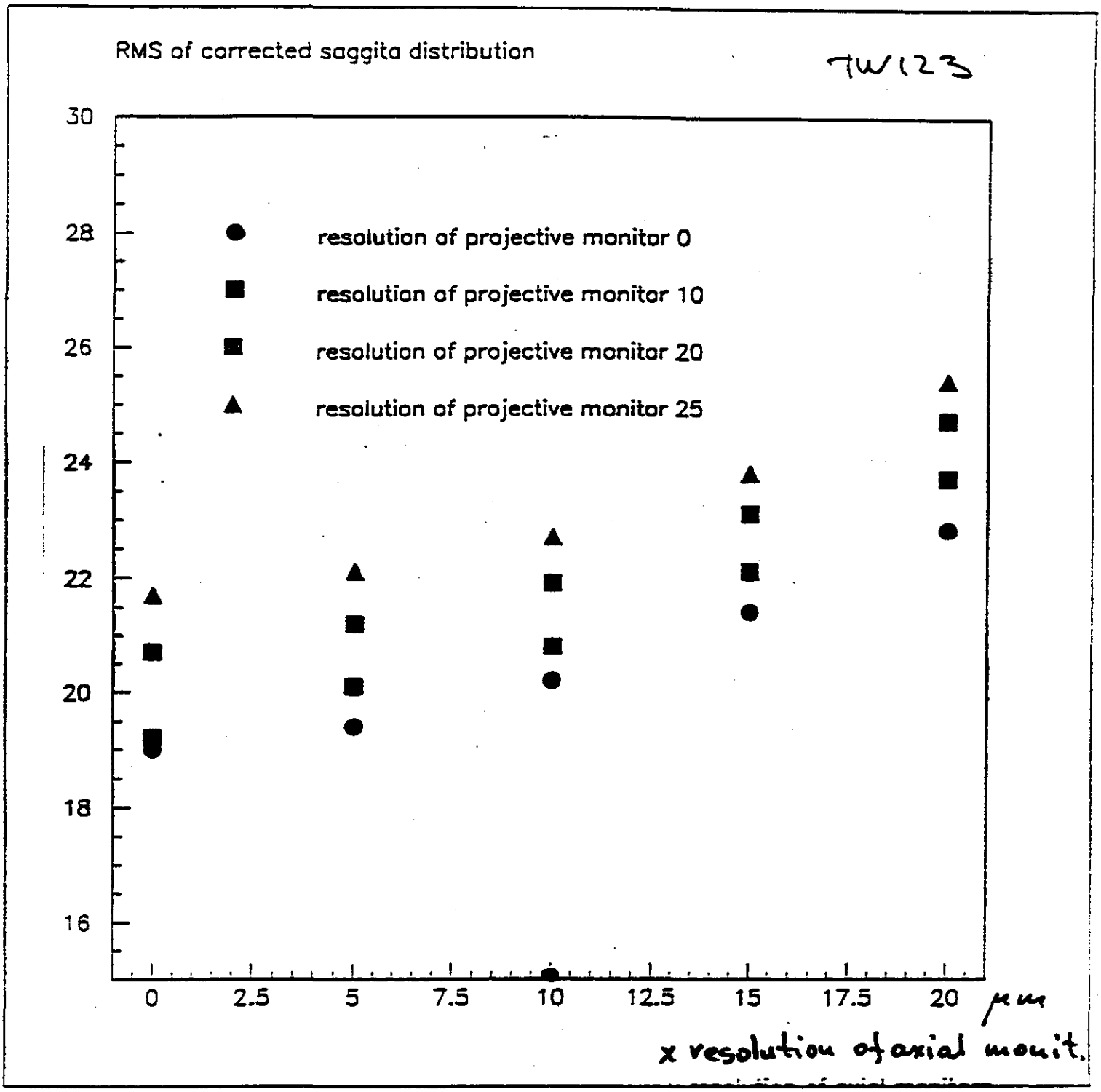

All other parameters - BASELINE

Table 1.

		method	proj. monitors resolution	non-projectivity	proj.mon + non-project.	axial mon. resolution	All
pure projective	tower 1	2.2	13.1	18.6	21.6		23.3
	tower 2	2.5	12.5	18.6	19.4		22.4
	tower 3	3.0	13.1	20.2	22.8		22.8
	tower 4	3.2	12.4	19.1	22.7		24.9
optical ax. mon	tower 12	4.1	10.6	15.9	19.3	5.7	22.5
	tower 34	3.5	11.1	17.7	19.0	4.8	21.5
wire	tower 1234	5.6	11.7	14.0	16.1	13.2	22.2
	tower 123	6.0	12.0	13.4	17.6	12.	22.1

tower 123 - gapless configuration with 3 chambers in second SL

OK!

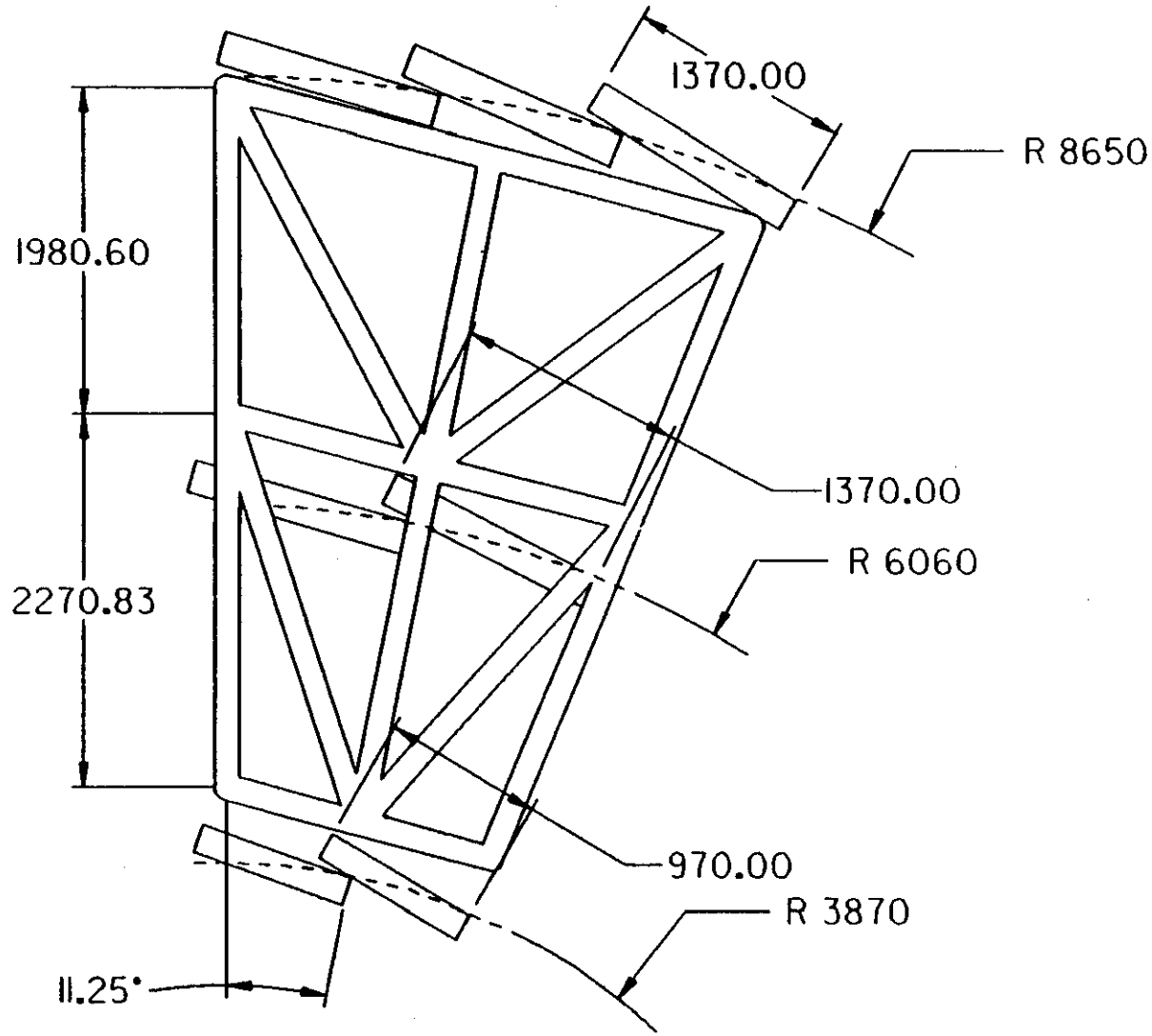
1370.00
R 8650
1980.60
1370.00
R 6060
2270.83
970.00
R 3870
11.25°

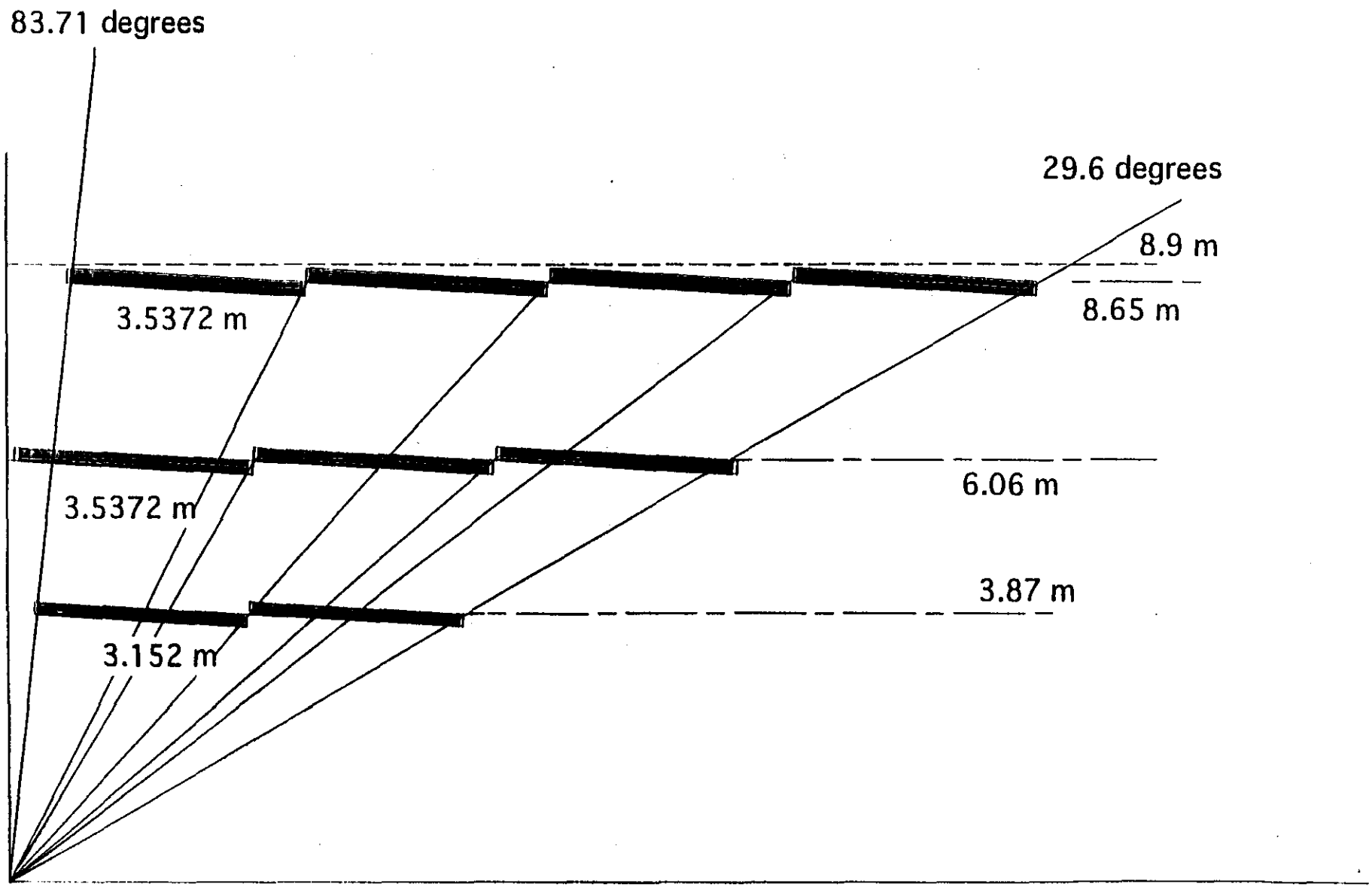
83.71 degrees
29.6 degrees
8.9 m
8.65 m
3.5372 m
3.5372 m
6.06 m
3.87 m
3.152 m

Test Beam Plans

Phase I:

(1) tests of 40x40 cm^2 6-layer chamber

- in B-field:
  - μ radiation / high energy beam
  - Lorentz-angle studies
  - resolution vs angle and position
  - electronics evaluation
  - punch-through studies

(2) test of full-scale chamber 1.2 x 3.5 m^2

- spatial resolution
- time resolution
- intra-layer alignment
- electronics studies

Phase II:

(1) integrated tests of chambers, support, alignment

- false sagitta
- time resolution
- trigger studies
- system resol'n vs position/chamber boundaries

(2) integrated tests of muon system with CT, calorimeter

Cathode-Strip Chamber Tests
GEM Muon Detector

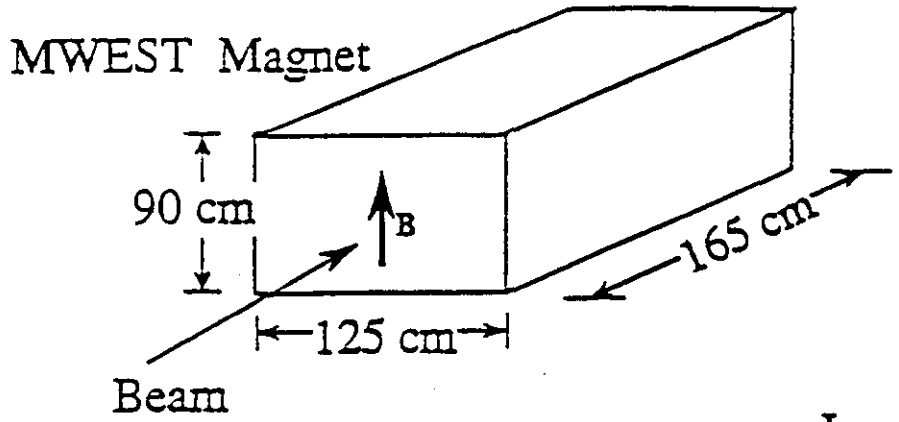

Six-Plane Chamber

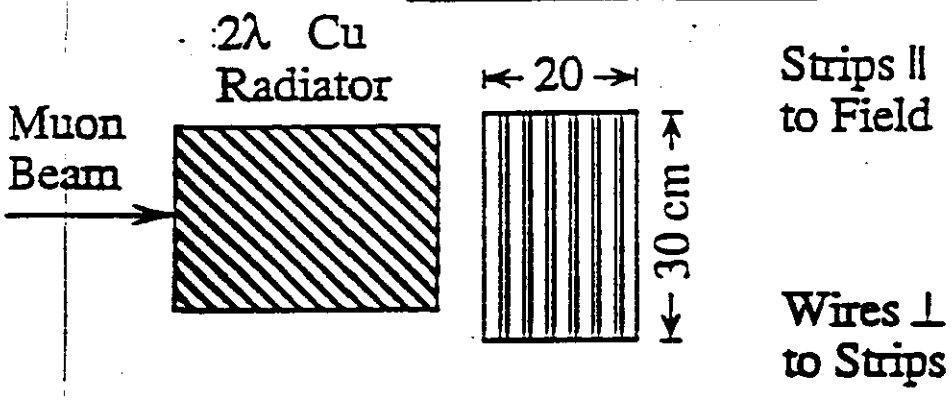

Lorentz Angle and Resolution Studies

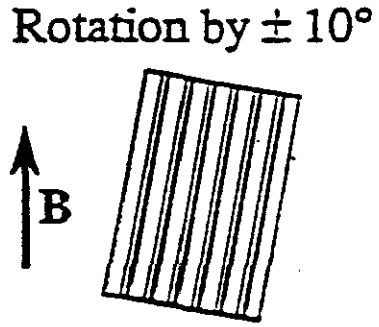

Resolution Studies from 0 to 50° Polar Angle

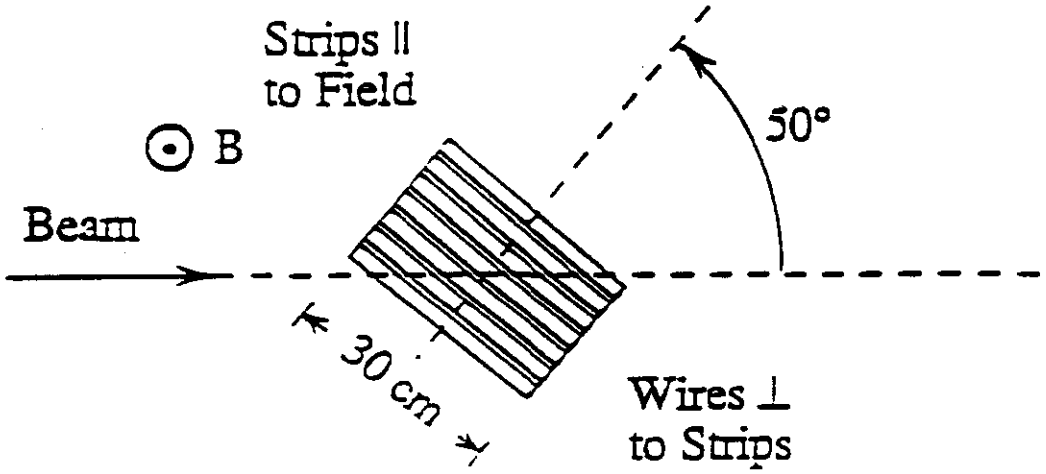

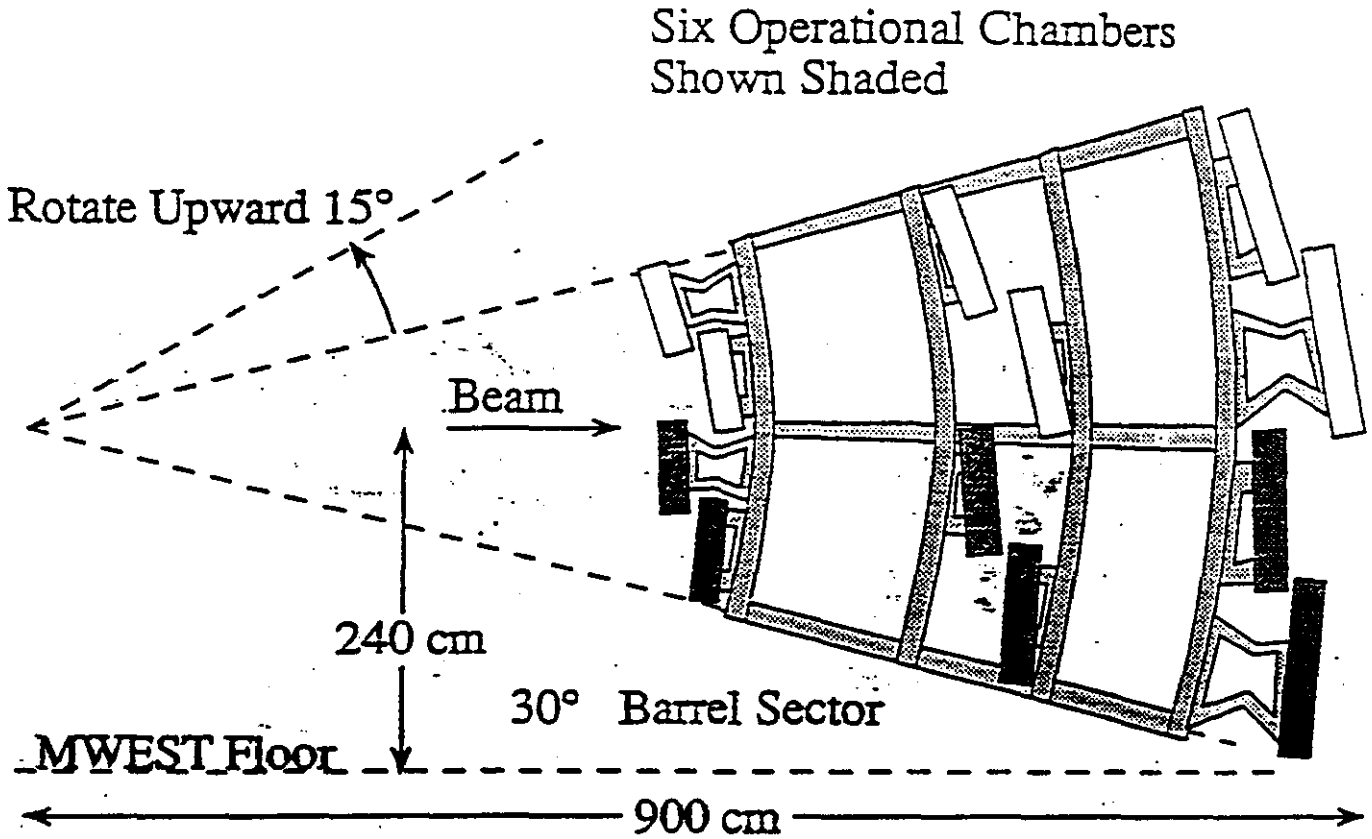
Six Operational Chambers
Shown Shaded
Rotate Upward 15°
Beam
240 cm
30° Barrel Sector
MWEST Floor
900 cm

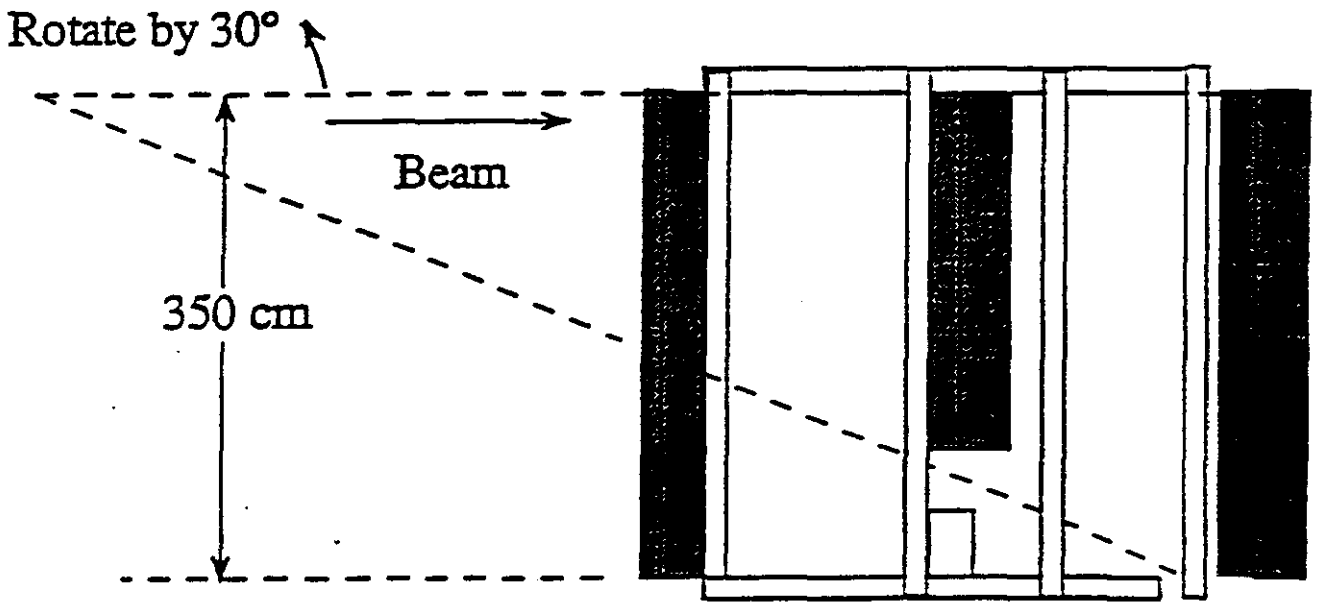
Rotate by 30°
Beam
350 cm

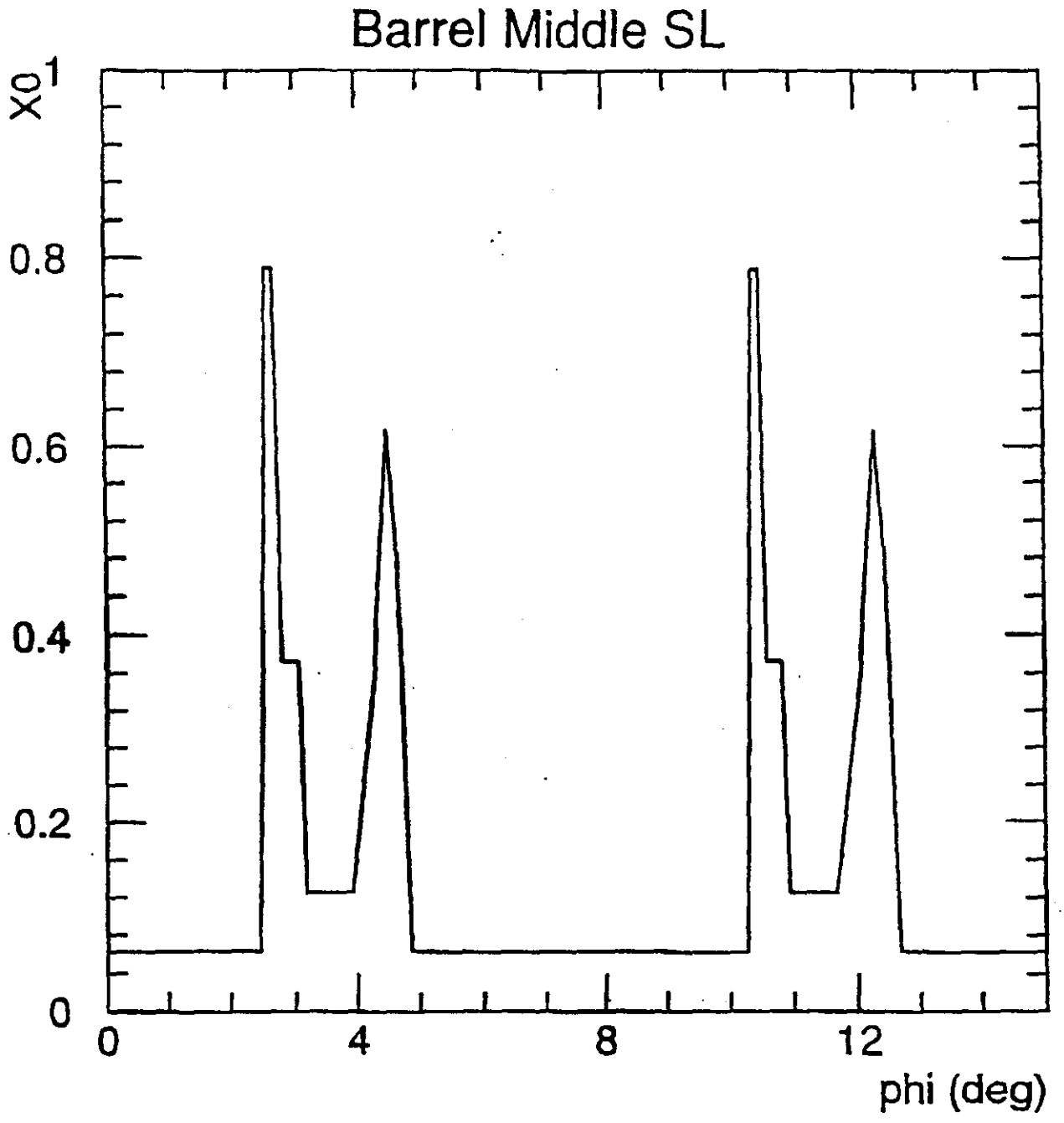
Barrel Middle SL
X_0^{-1}
0.8
0.6
0.4
0.2
0
0
4
8
12
phi (deg)

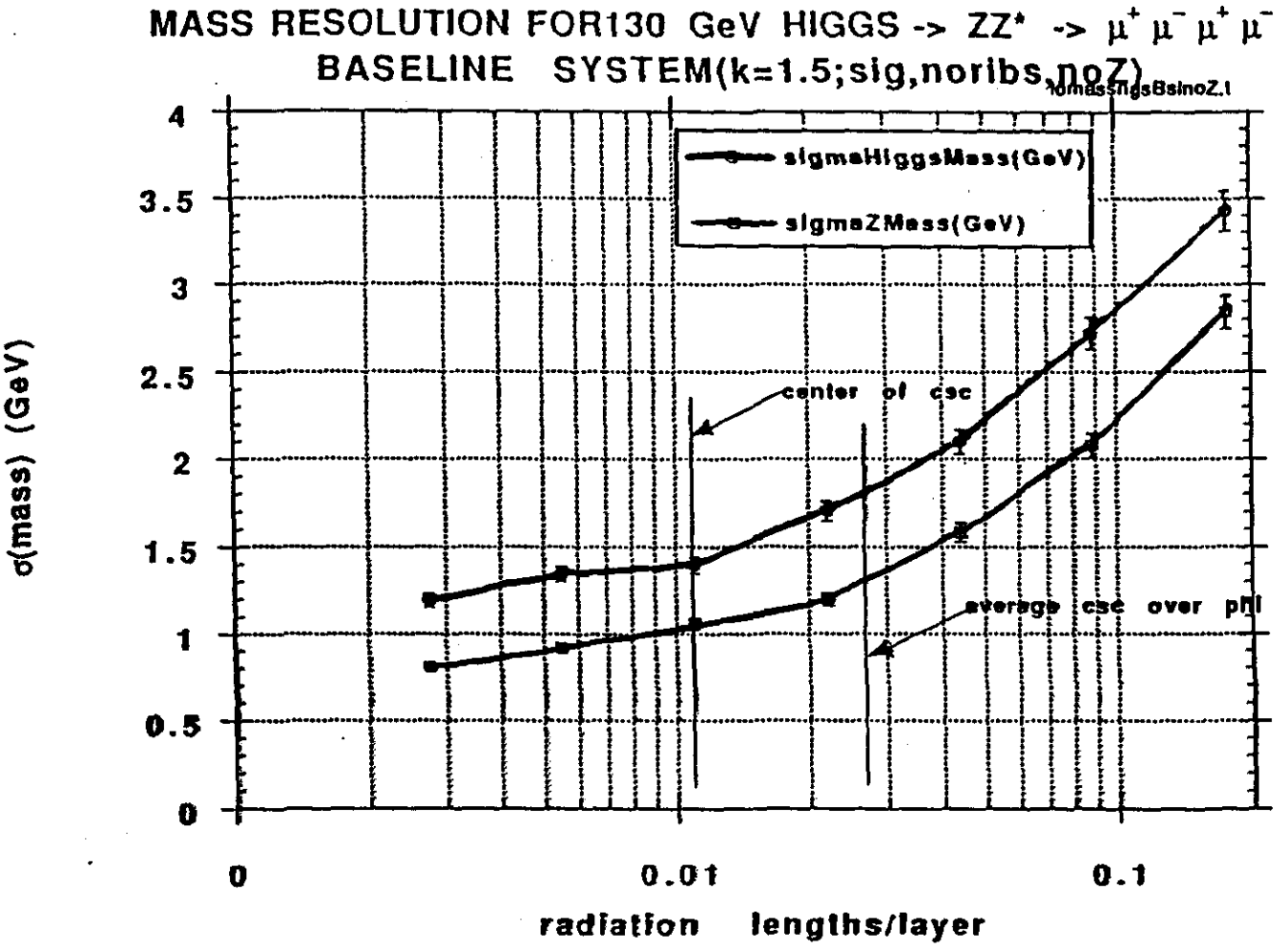

Of order 10 events could be detected / ssc year at $\mathcal{L} \simeq 10^{33}\ cm^{-2}\ s^{-1}$.

C-LINE #62037
CLEAR TOPPER

p_T−resolution for μ^+ with p_T = 25 GeV/c $N_{seg} \geqq 3$

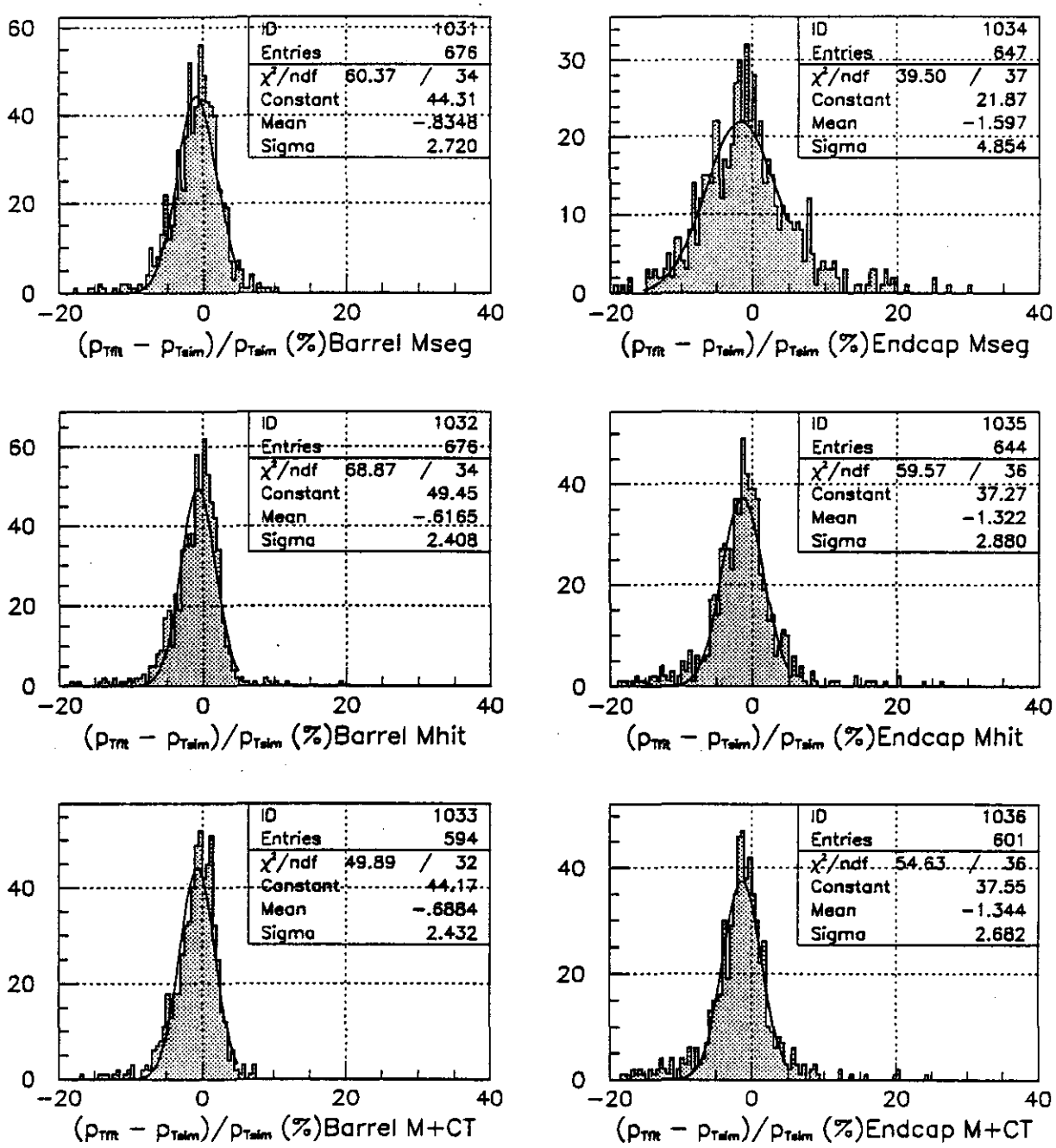

gem

γeμ

Presentation by:

C. Baltay

CENTRAL TRACKER REPORT

1. Design for the Fermilab
   18° Sector Test

2. Brookhaven Test Beam Results
   Jenny Thomas

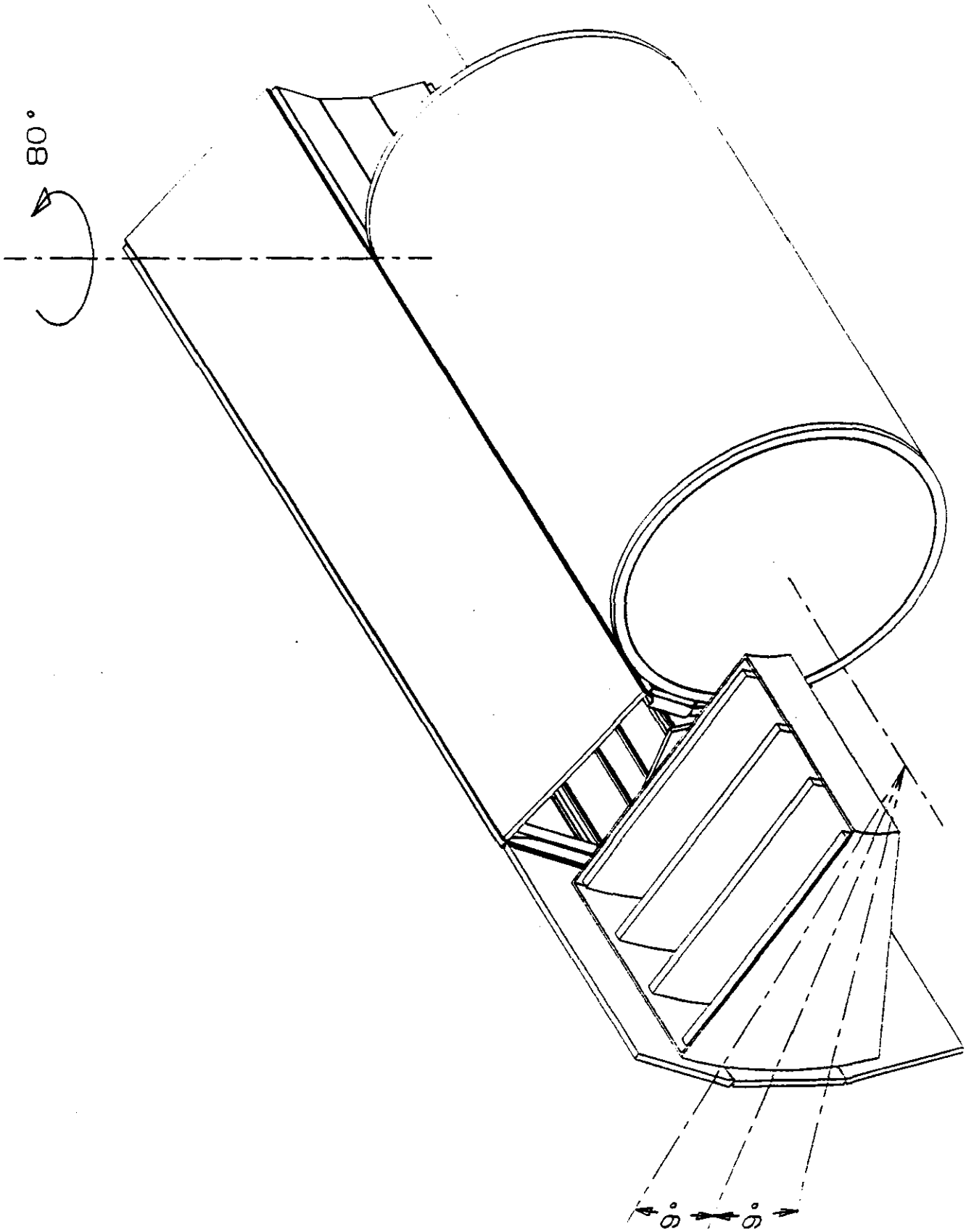
80°
8°
8°

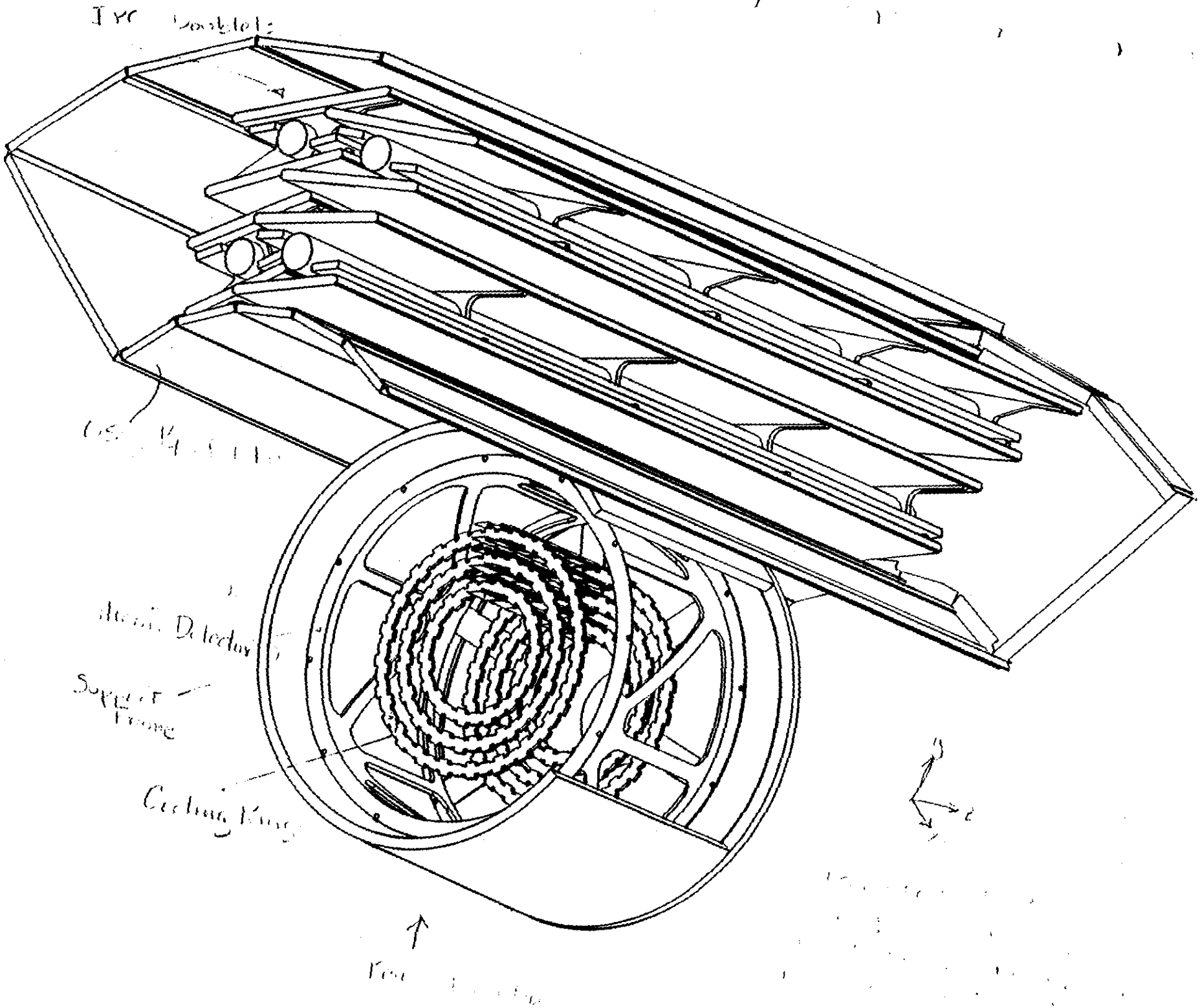
Support Frame
Cooling Ring

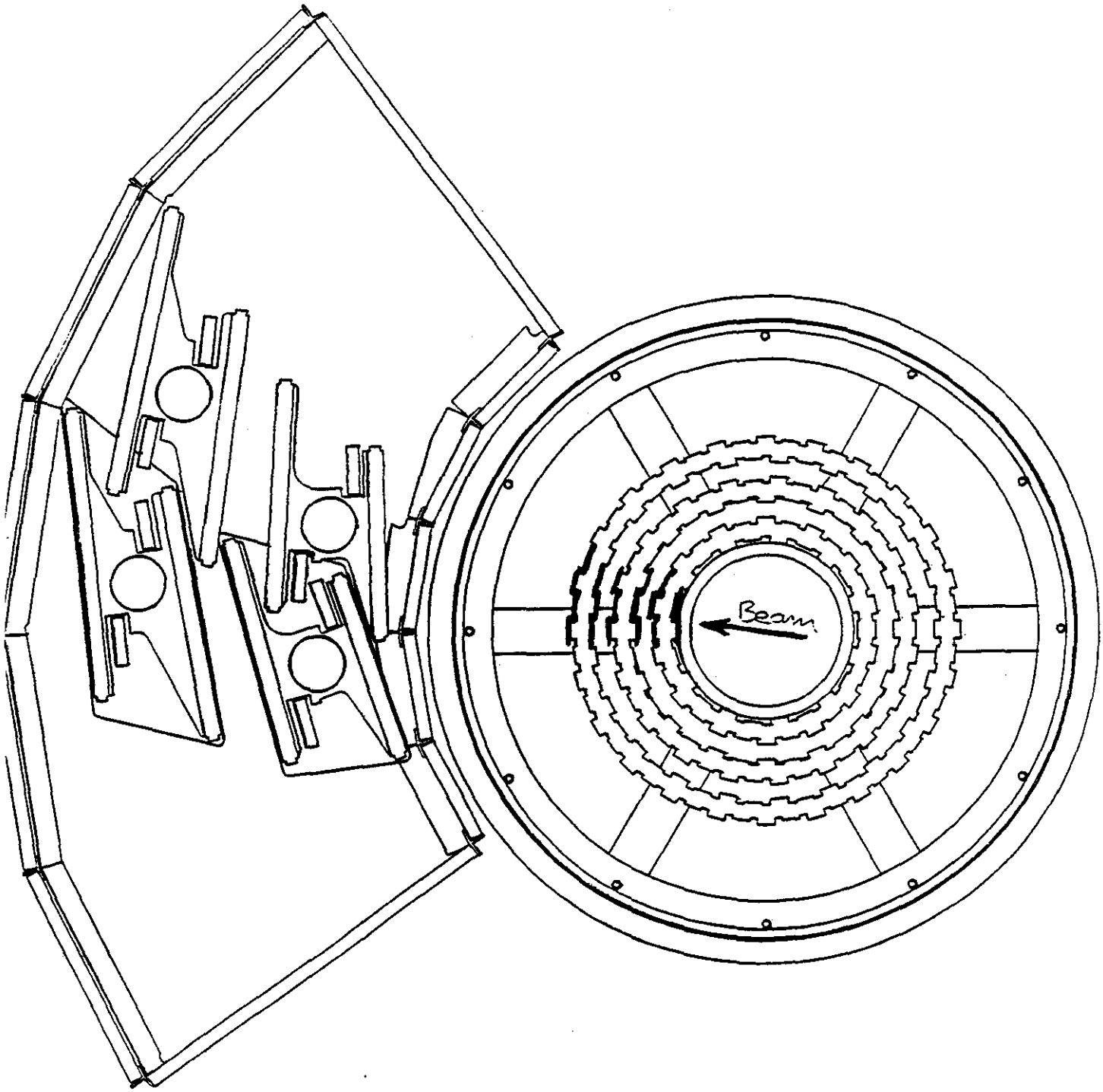
Beam

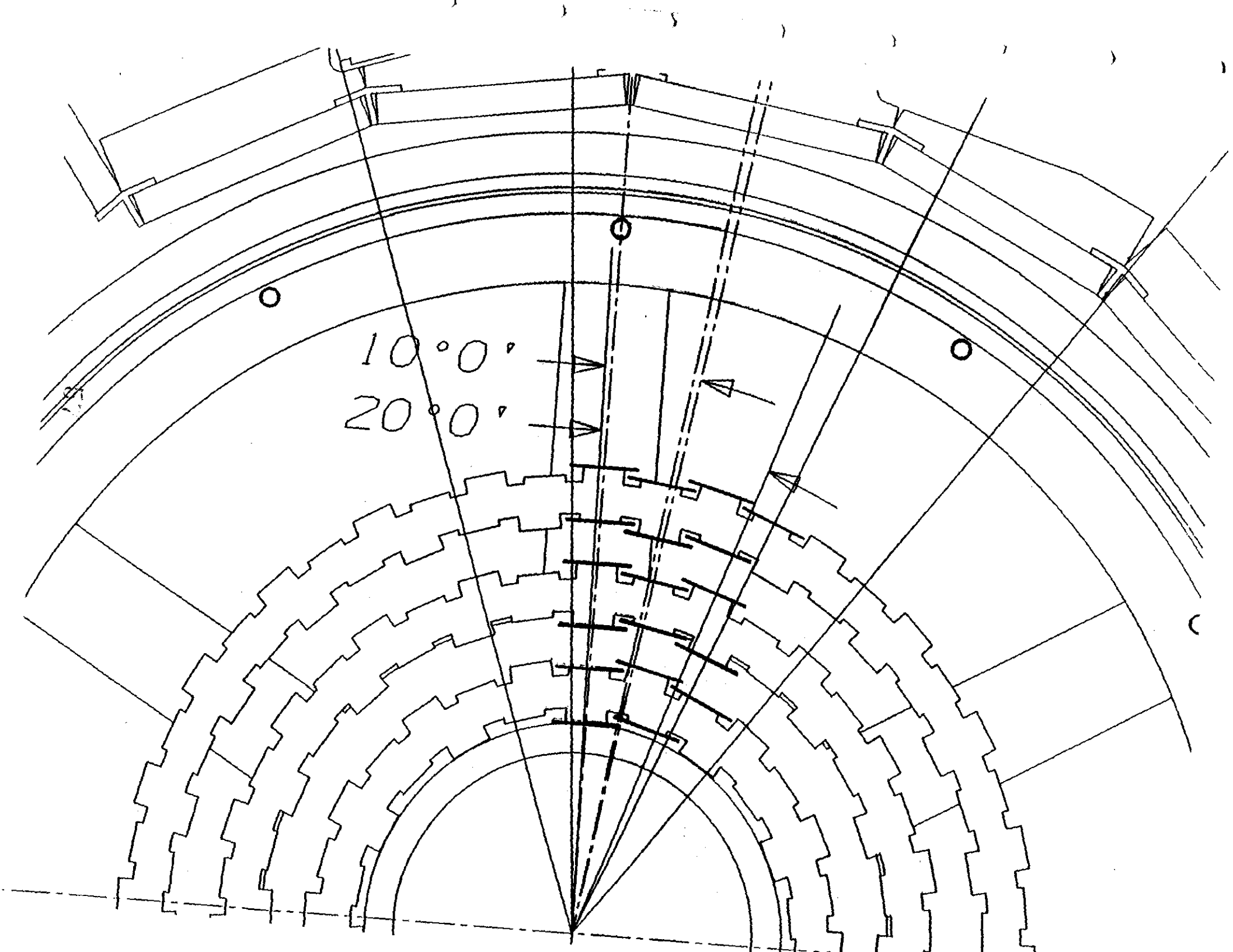
10°0'
20°0'

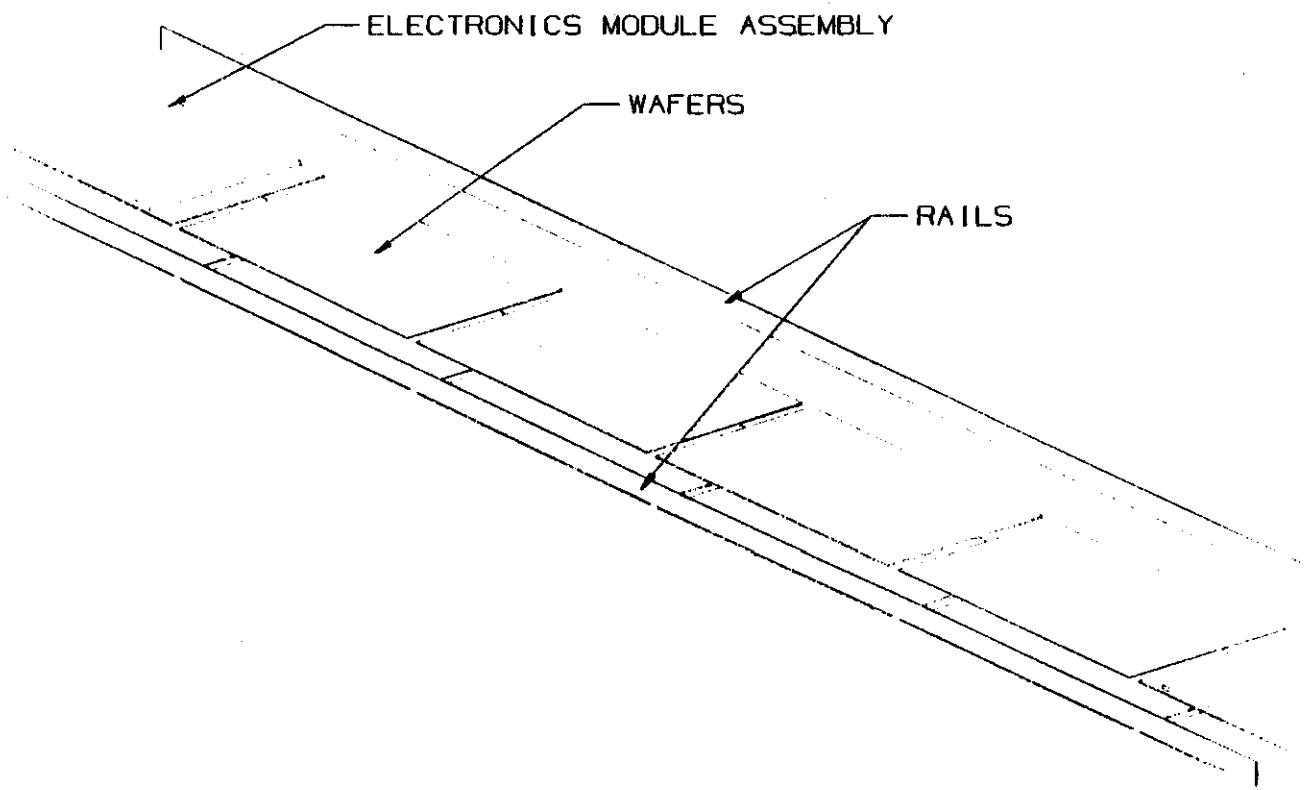
ELECTRONICS MODULE ASSEMBLY
WAFERS
RAILS

1.2

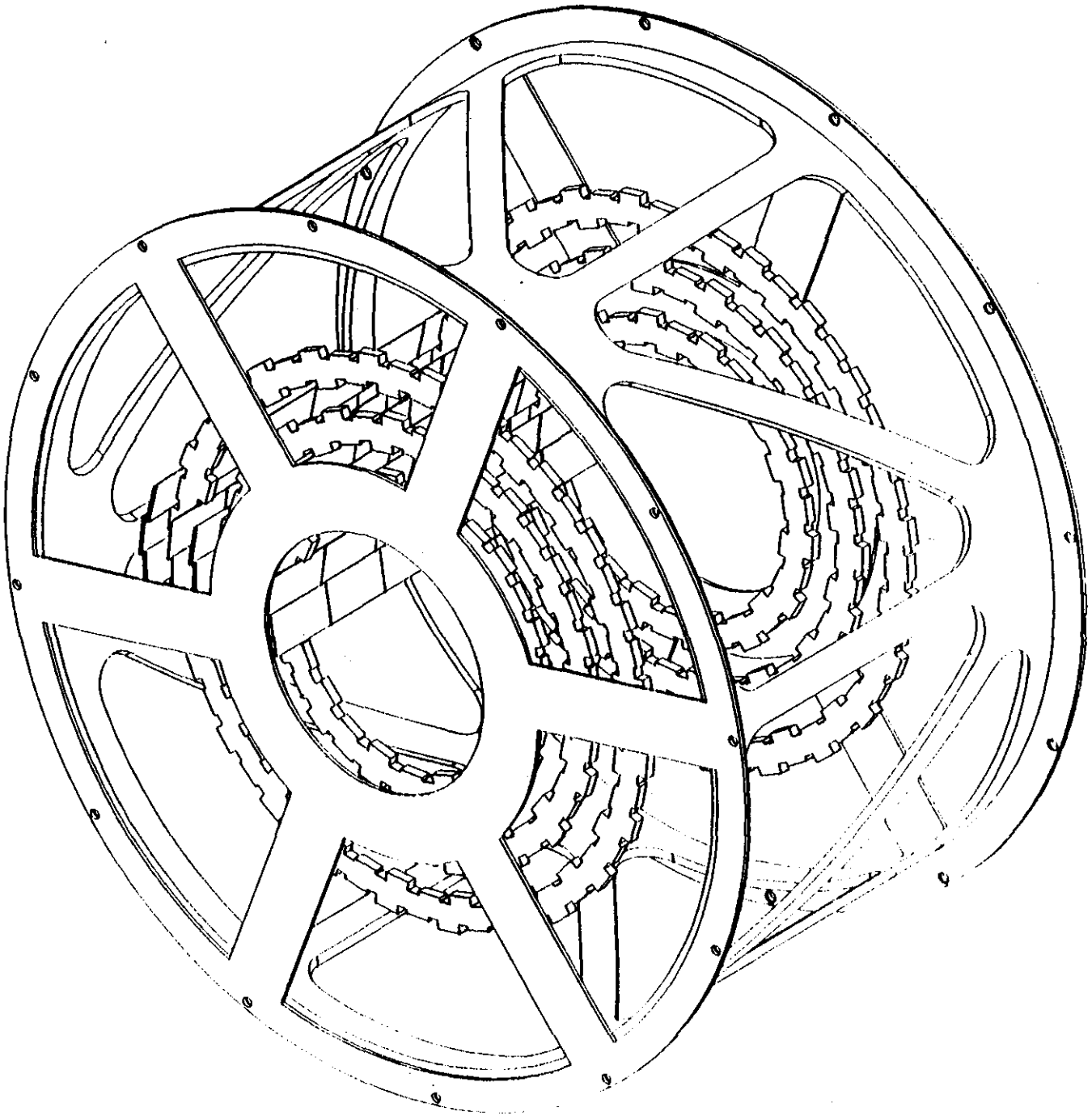

gem

γeμ

Presentation by:

C. Baltay/J. Thomas

PRELIMINARY RESULTS FROM FIRST TEST OF FULL SIZE BARREL PROTOTYPE AT BNL AGS TEST BEAM

INDIANA

C. BOWER J. MUSSER

LOS ALAMOS

M. BROOKS D. LEE R. MARTIN G. MILLS
J. ROMERO

SSC LAB

H. FENKER K. MORGAN R. SHYPIT J. THOMAS

SUNY @ ALBANY

B. NEMATTI , J. O'NEILL , H. SEVERINI

YALE

C. BALTAY B. BRRAKET E. WOLIN

BNL

B. YU

THANKS TO H. GORDON, V. POLYCHRONAKIS

PREVIEW

- INTRODUCTION
- EQUIPMENT
- SETTING UP
- TWO TRACK STUDY
- SILICON PERFORMANCE
- IPC RESULTS
- CONCLUSIONS

INTRODUCTION

- PLAN WAS TO TEST FULL SIZE BARREL IPC PROTOTYPE & MEASURE RESOLUTION
- SEPARATELY TO MEASURE TWO TRACK RESOLUTION USING MINI-CHAMBERS OF SIMILAR DESIGN

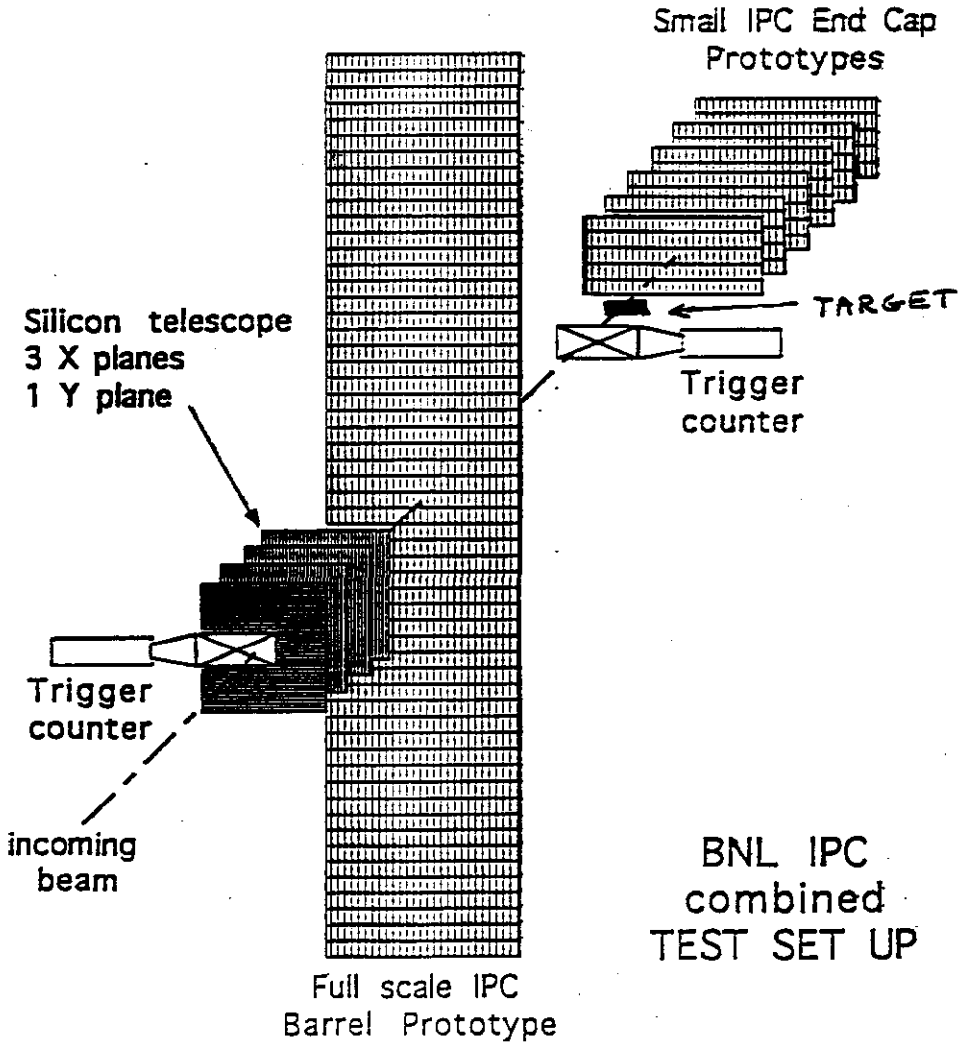

BNL IPC combined TEST SET UP

- FIRST OPPORTUNITY TO GET THE HARDWARE & PEOPLE TO WORK TOGETHER

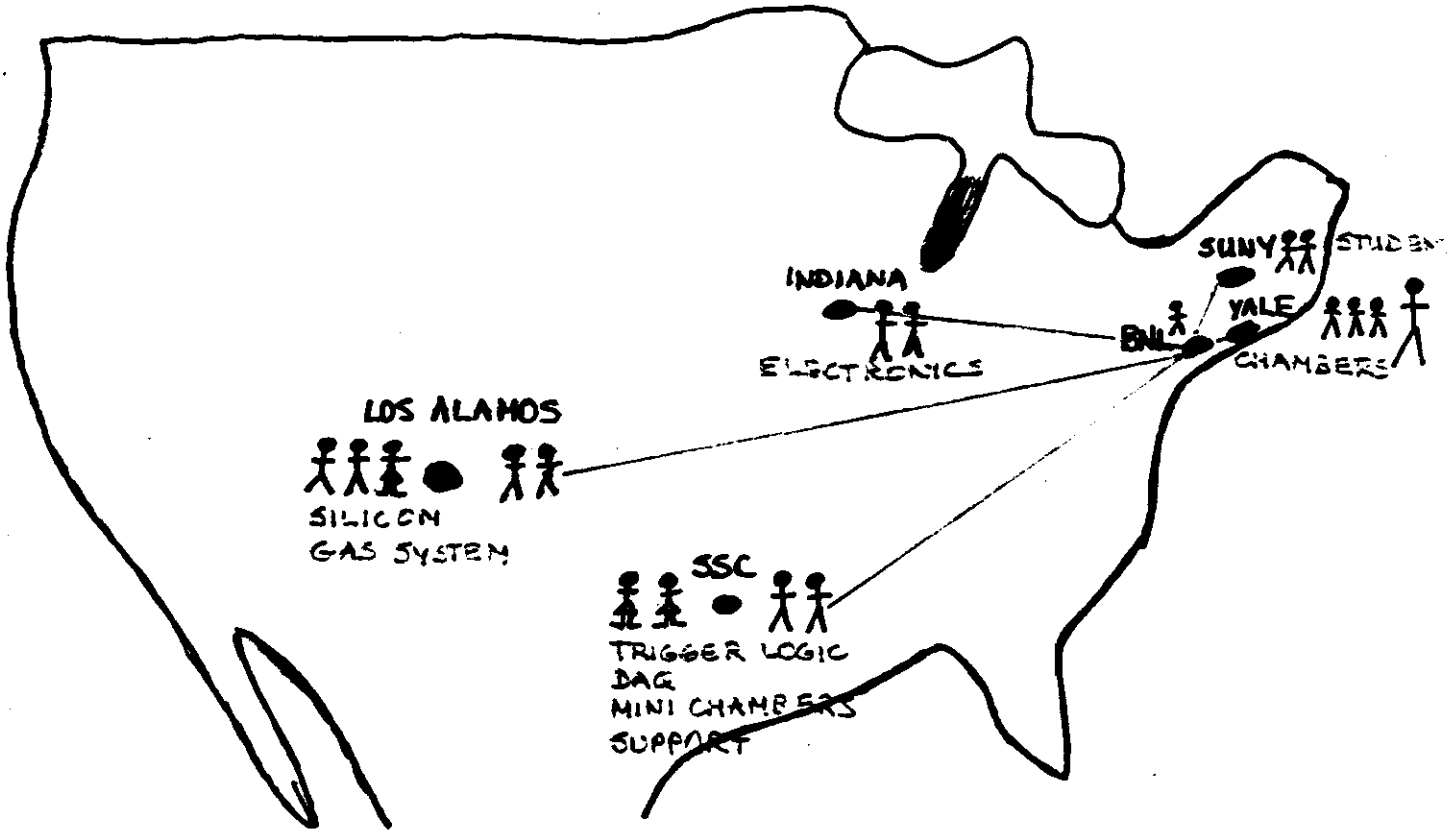

- TOTAL OF 17 PEOPLE FROM 5 INSTITUTIONS

TWO TRACK STUDY

- 6 MINI-CHAMBERS + TARGET USED TO MAKE & FIND 2 TRACKS
- 2 CHAMBERS HAVE STEREO GEOMETRY
- IDEA: IDENTIFY TRACKS AT LAYER 6 WITH GOOD SEPARATION - EXTRAPOLATE BACK TO EXPLORE INTERESTING REGION

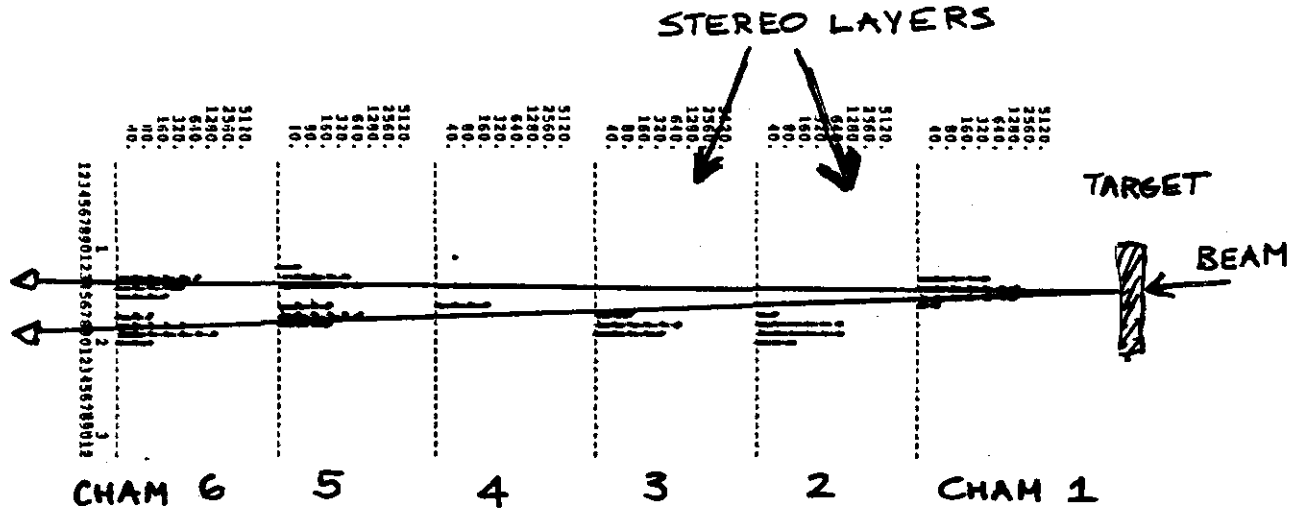

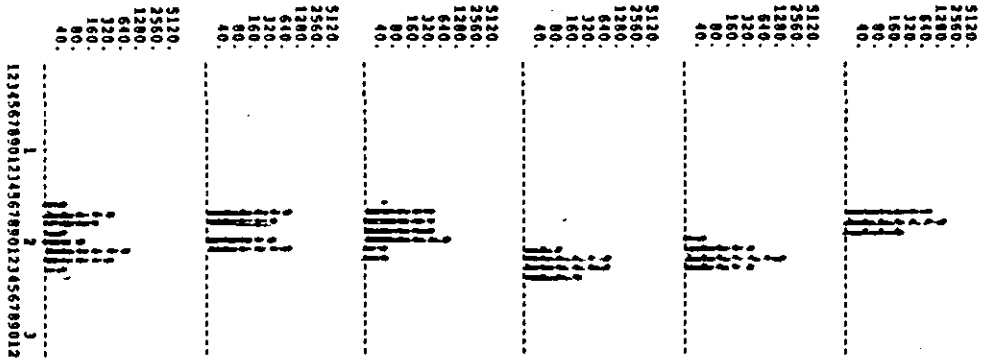

TYPICAL EVENT DISPLAYS.

SILICON PERFORMANCE

- USE SILICON INFORMATION TO FIND A TRACK.
- ONE MEASUREMENT IN Y & 3 IN x
- PROJECT TRACK IN SILICON INTO IPCs

FIT RESIDUALS

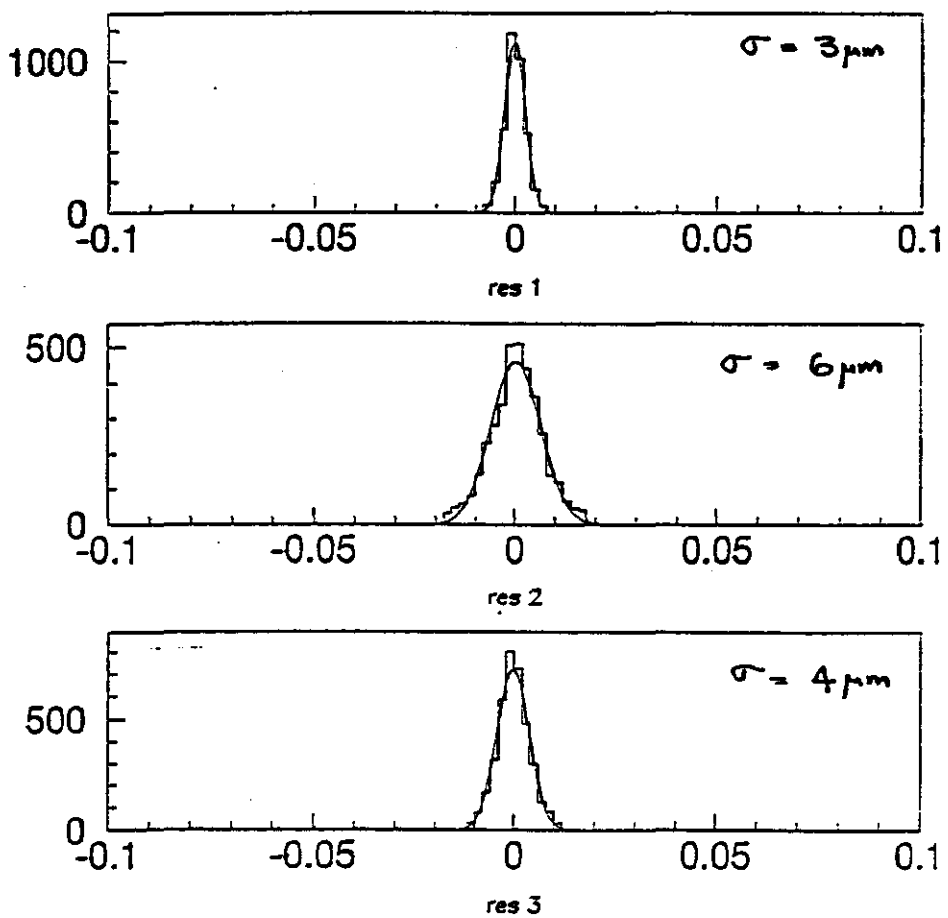

LAYER 1

LAYER 2

LAYER 3

IPC SCHEMATIC

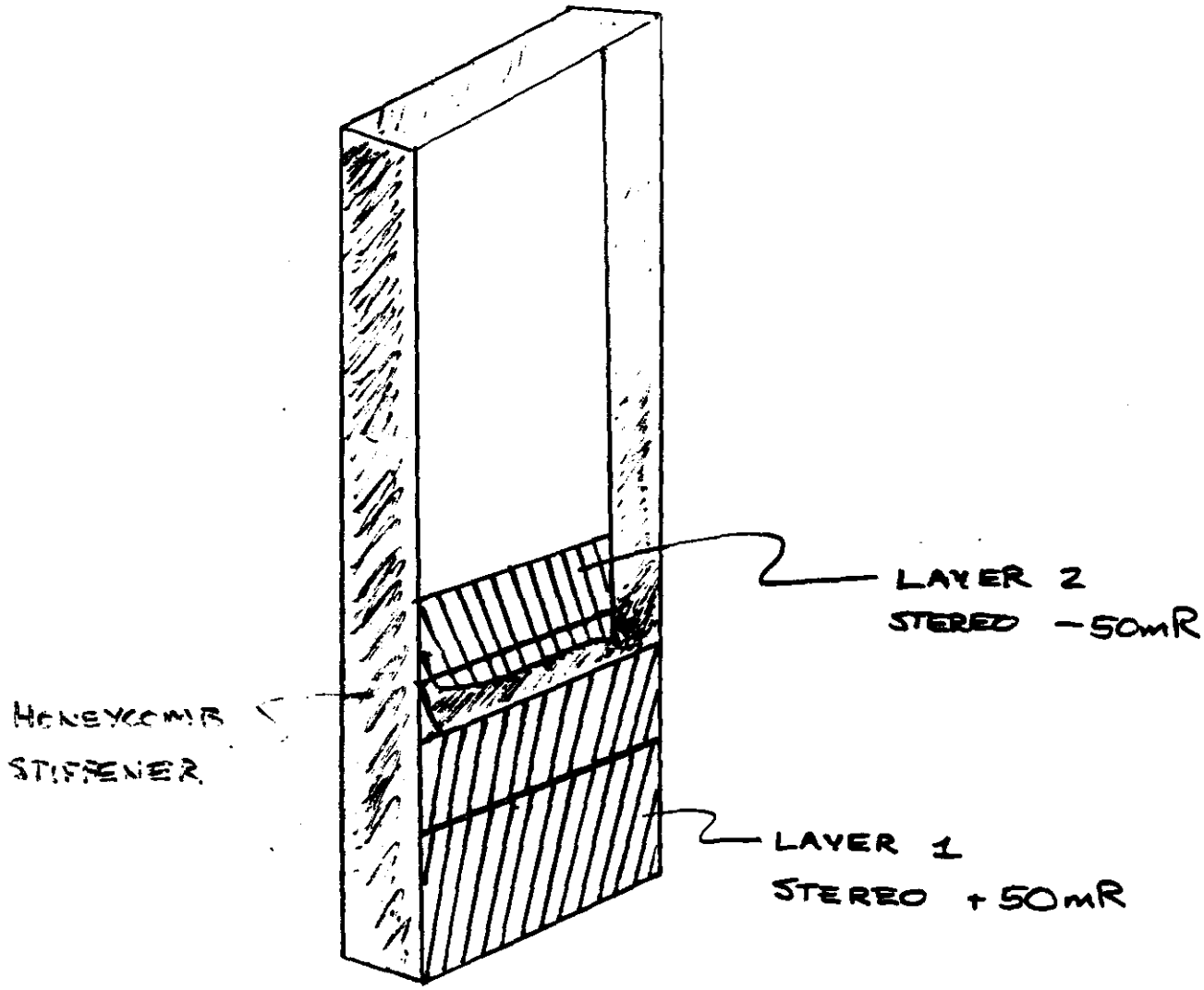

IPC RESULTS

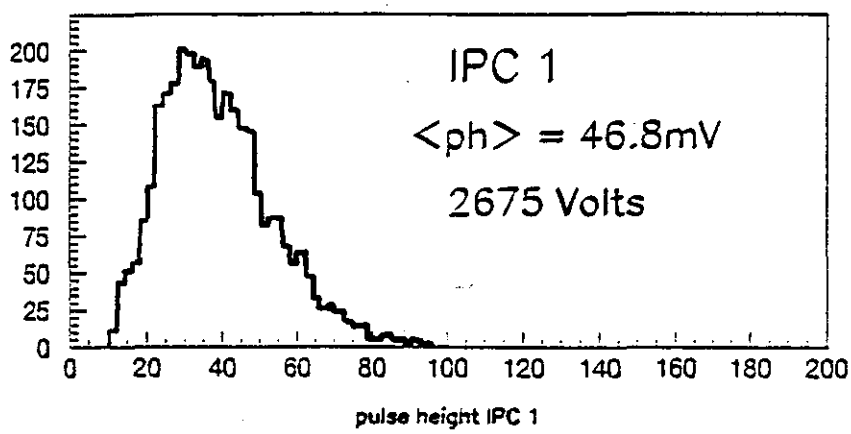

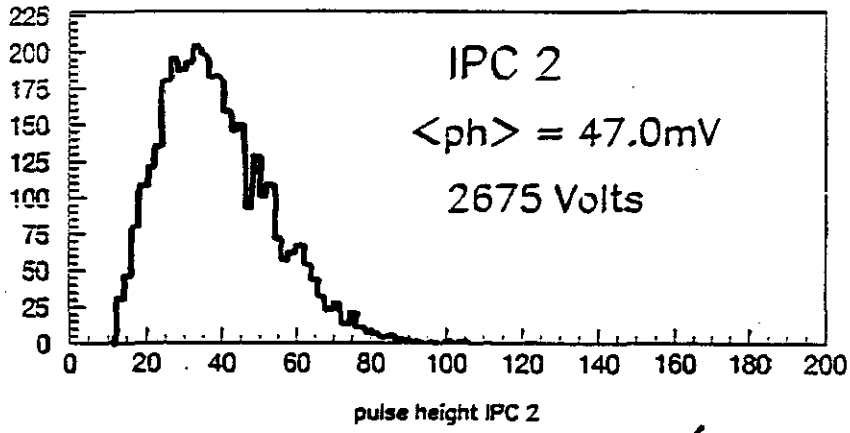

$\langle PED \rangle \simeq 10-20$ ADC /2000

$\sigma_{E.N.} \simeq 4-5$ ADC

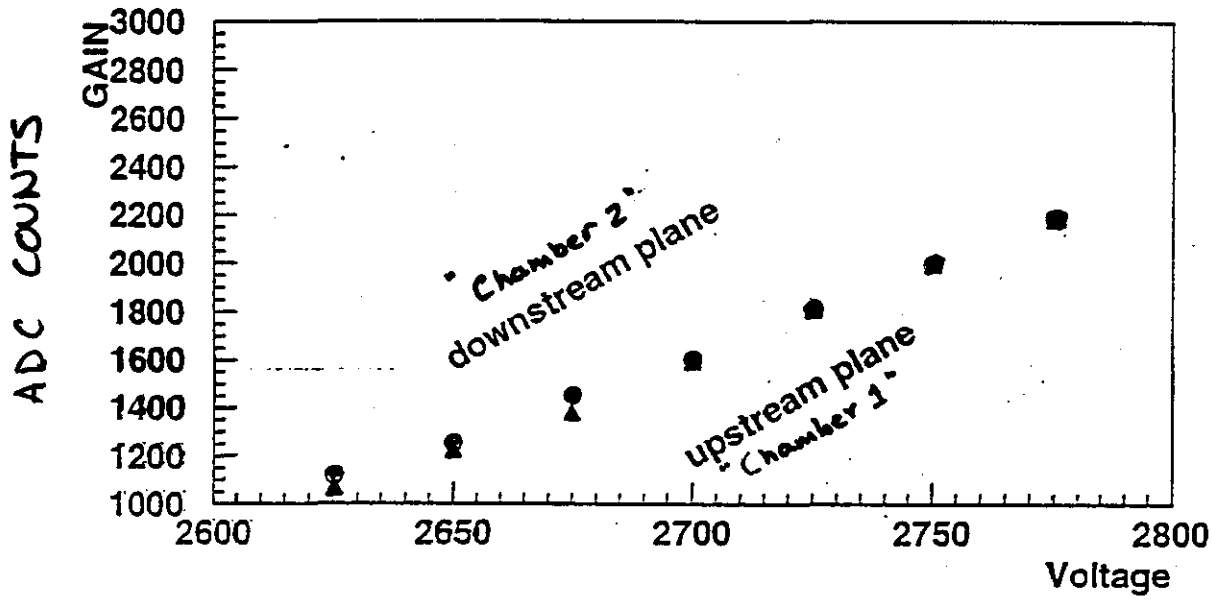

- SEVERAL SOURCES OF UNCERTAINY IN THE PROJECTED POSITION OF TRACK

  → 2mR BEAM DIVERGENCE IN Y
  $\simeq 20\,\mu m$

  → MULTIPLE SCATTERING AT LAST LAYER OF SILICON
  $\simeq 10\,\mu m$

  → VIBRATION OF IPC IN STRUCTURE
  $\simeq 25 - 50\,\mu m$ (?)

- COLLECTED ~ 200K EVENTS TOTAL
  20% PASS CUTS

  → HITS IN ALL 4 SILICON (=1 IN Y)

  → NON SATURATED HIT IN 1 IPC

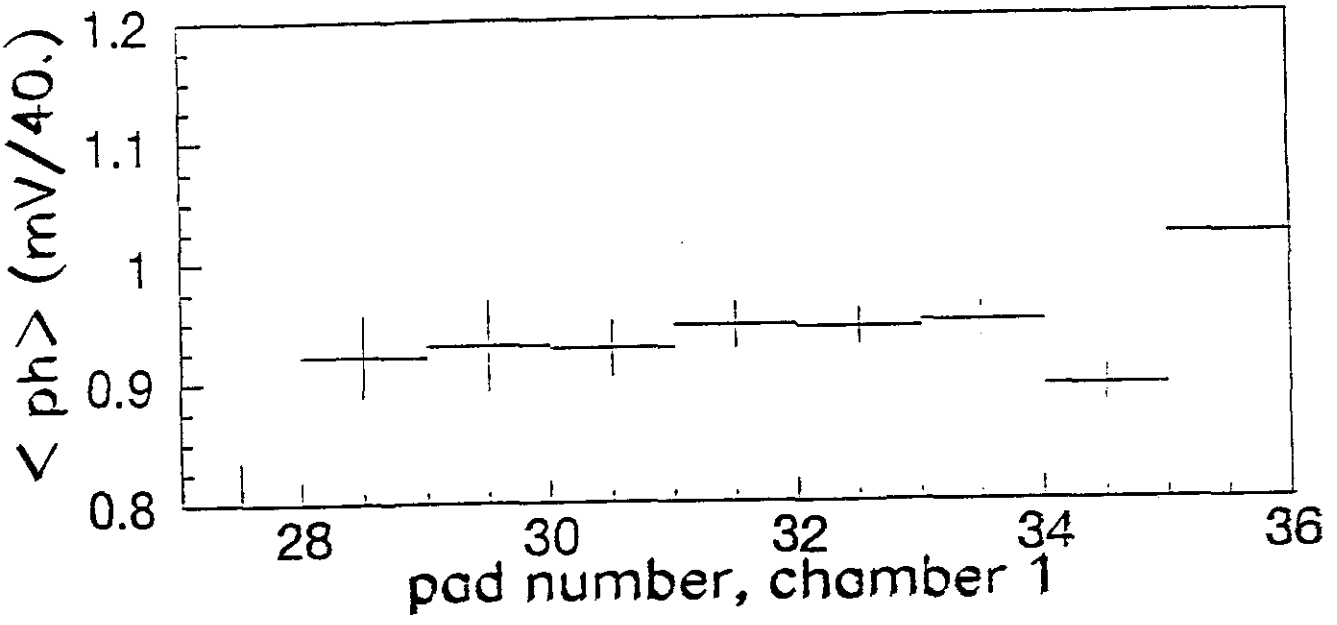
1.2
1.1
1
0.9
0.8
< ph> (mV/40.)
28
30
32
34
36
pad number, chamber 1

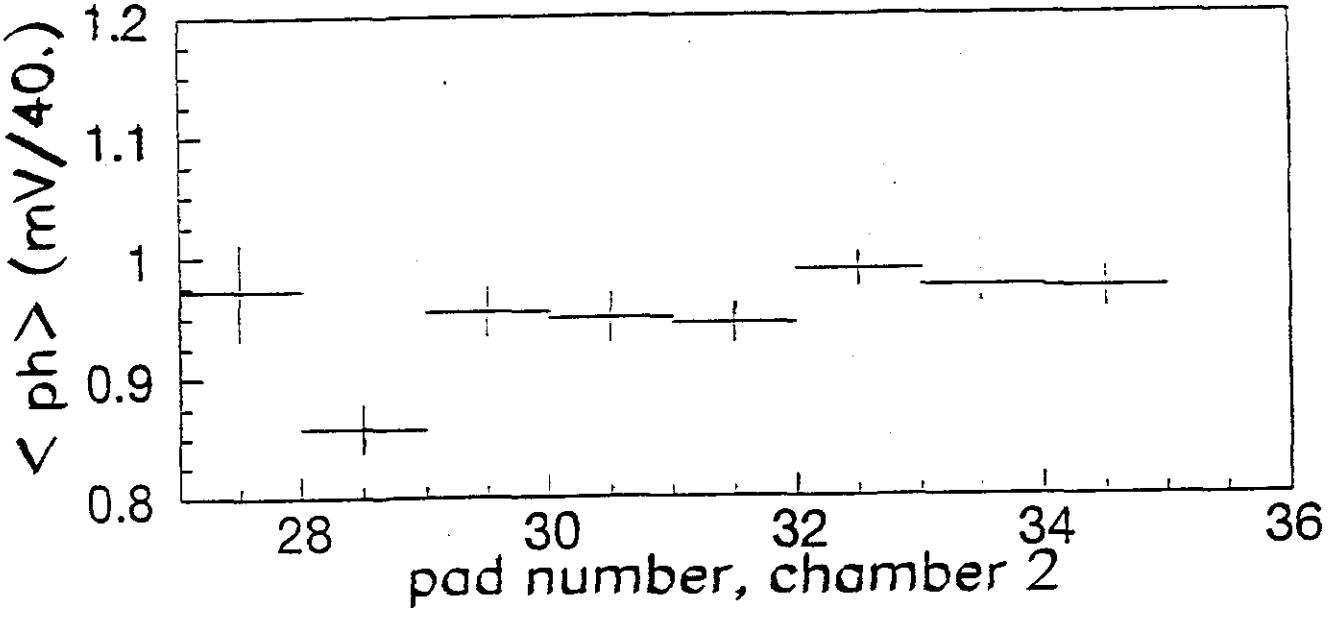
1.2
1.1
1
0.9
0.8
< ph> (mV/40.)
28
30
32
34
36
pad number, chamber 2

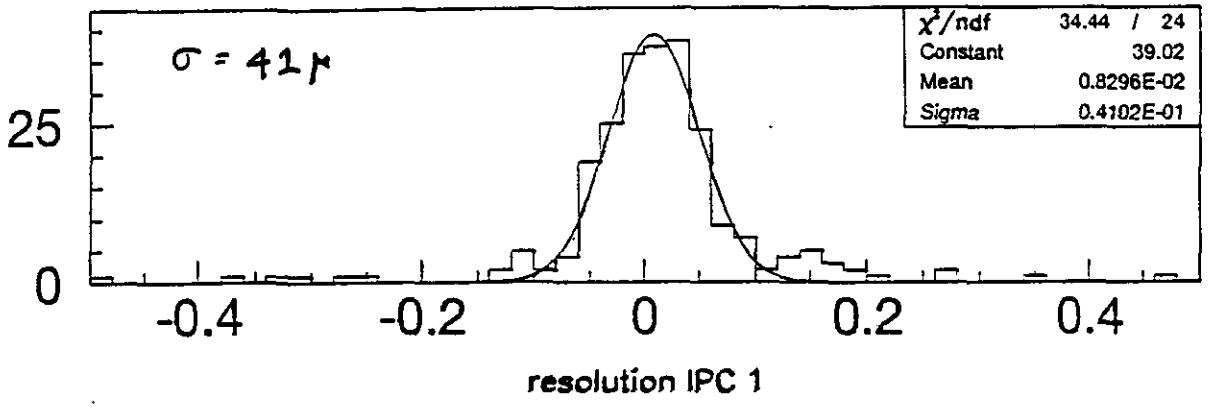
σ = 41 μ
χ²/ndf 34.44 / 24
Constant 39.02
Mean 0.8296E-02
Sigma 0.4102E-01
25
0
-0.4
-0.2
0
0.2
0.4
resolution IPC 1

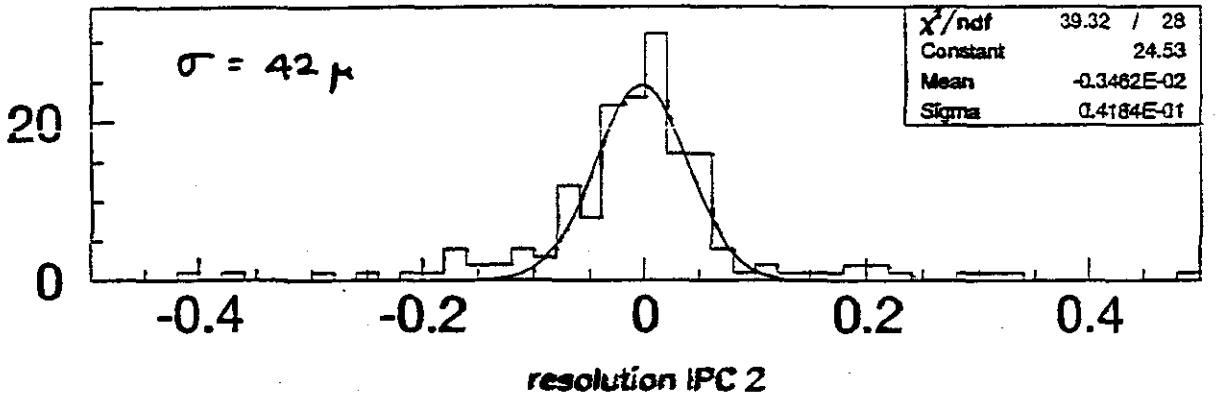
σ = 42 μ
χ²/ndf 39.32 / 28
Constant 24.53
Mean -0.3462E-02
Sigma 0.4184E-01
20
0
-0.4
-0.2
0
0.2
0.4
resolution IPC 2

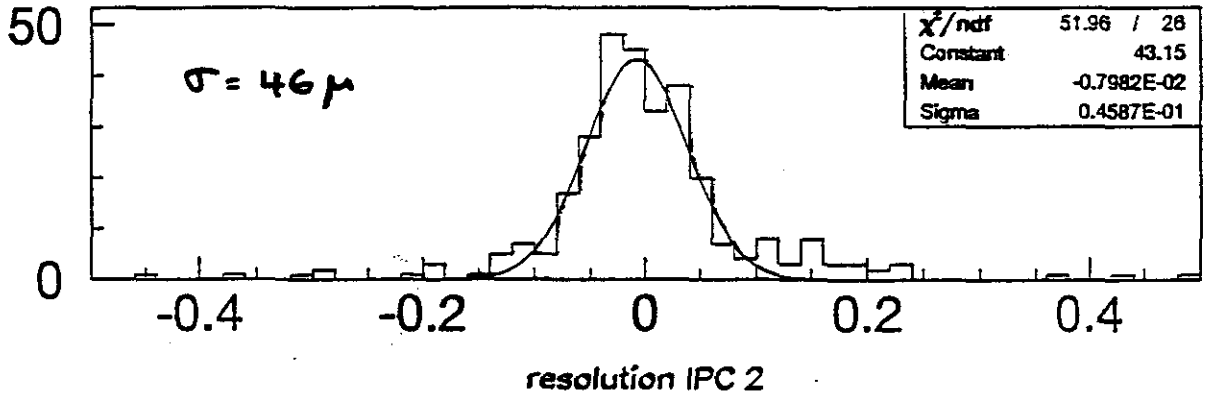
σ = 46 μ
χ²/ndf 51.96 / 26
Constant 43.15
Mean -0.7982E-02
Sigma 0.4587E-01
50
0
-0.4
-0.2
0
0.2
0.4
resolution IPC 2

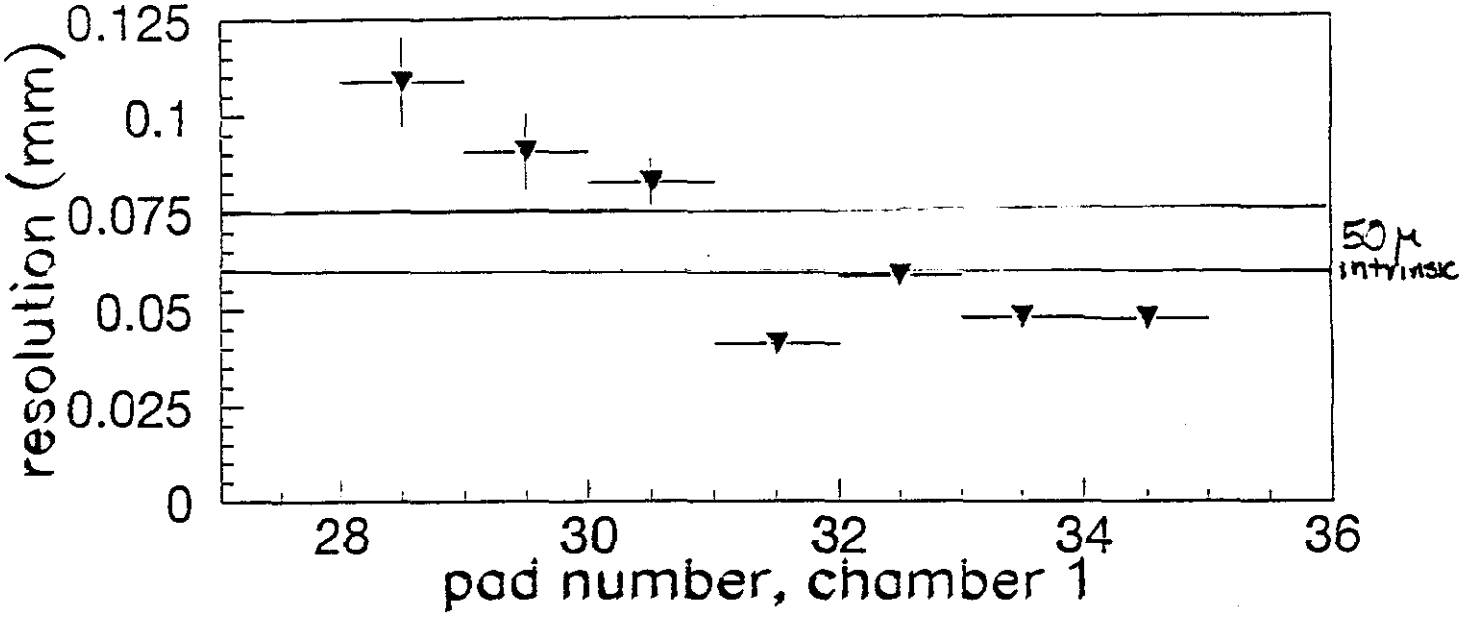
0.125
0.1
0.075
0.05
0.025
0
resolution (mm)
28
30
32
34
36
pad number, chamber 1
50 μ
intrinsic

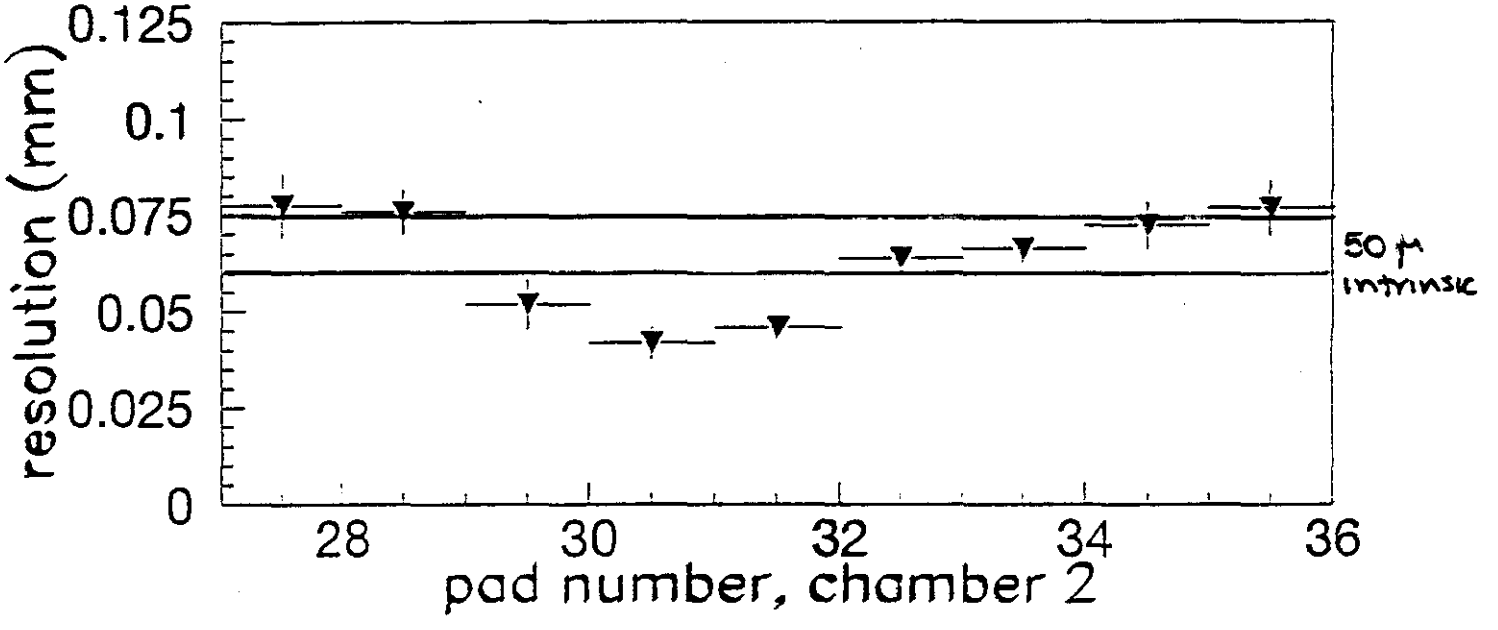
0.125
0.1
0.075
0.05
0.025
0
resolution (mm)
28
30
32
34
36
pad number, chamber 2
50 μ
intrinsic

EQUIPMENT

- 2 IPC PROTOTYPES : 2m LONG
  20 CM WIDE
  (2.5mm pads) TWO STEREO LAYERS ± 50mR

- 4 SILICON WAFERS 1 y , 3 x
  AC COUPLED "OPAL" DETECTORS
  SVXD ELECTRONICS (FROM CDF)
  USE ANALOGE INTERPOLATION

- 72 CHANNELS OF BNL HYBRID BASED FAST PREAMP / SHAPER + 11 BIT ADCS
  (FUNCTIONALLY IDENTICAL TO FINAL DESIGN WITHOUT READOUT SAMPLING)

- DAQ – TTR BASED SYSTEM WITH 68040 μP + 2 SPARC WORKSTATIONS IN VME

- 6 MINI-CHAMBERS + ELECTRONICS FOR TWO-TRACK STUDY

- 2 RACKS OF TRIGGER LOGIC + ASSOCIATED ELECTRONICS

- RECYCLABLE GAS SYSTEM TO CLEAN & REUSE CO_2 CF_4 GAS

CONCLUSIONS

- FIRST LOOK AT RESULTS SHOWS 50 μm RESOLUTION ACHIEVABLE

- MORE WORK NEEDED TO UNDERSTAND CALIBRATION

- THOROUGH UNDERSTANDING OF TWO TRACK RESOLUTION IS UNDERWAY (~ 10 - 20K USEFUL EVENTS)

gem

γeμ

Presentation by:

H. Yamamoto

GEM TN-93-???

Measurement of CP-violation using $B_d^0 \to J/\Psi + K_S^0$ decay mode with GEM Detector

Hiro Yamamoto

Lauritsen Laboratory
California Institute of Technology
Pasadena, CA 91125

July 19, 1993

Abstract

The feasibility to measure CP-violation in B-meson system with the GEM detector at SSC has been studied. In this report, $B_d^0 \to J/\Psi + K_s^0 \to \mu^+\mu^-\pi^+\pi^-$ decay mode was studied using high p_t muons for the B-tagging.

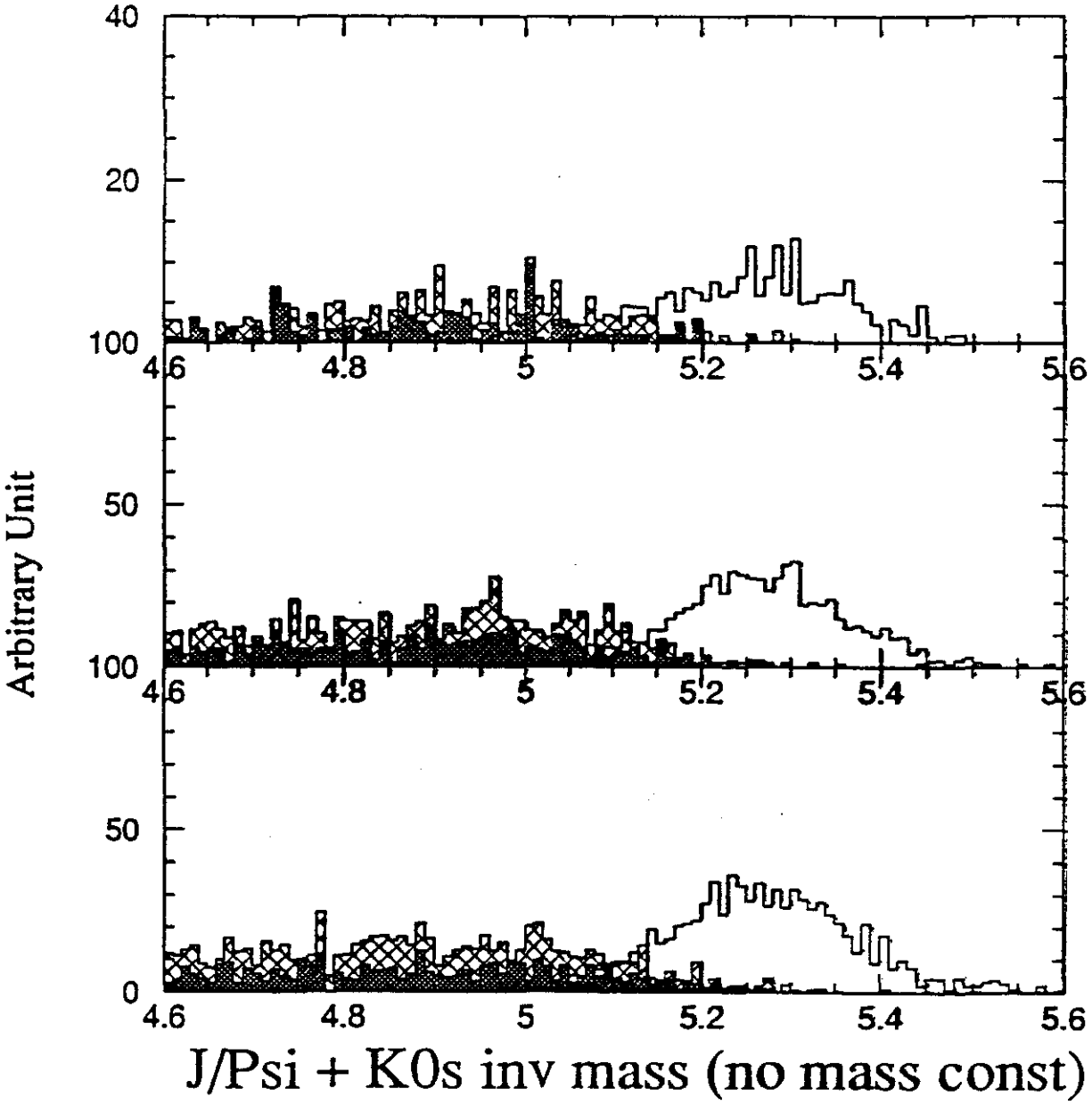
Arbitrary Unit
40
20
100
50
100
50
0
4.6
4.8
5
5.2
5.4
5.6
J/Psi + K0s inv mass (no mass const)

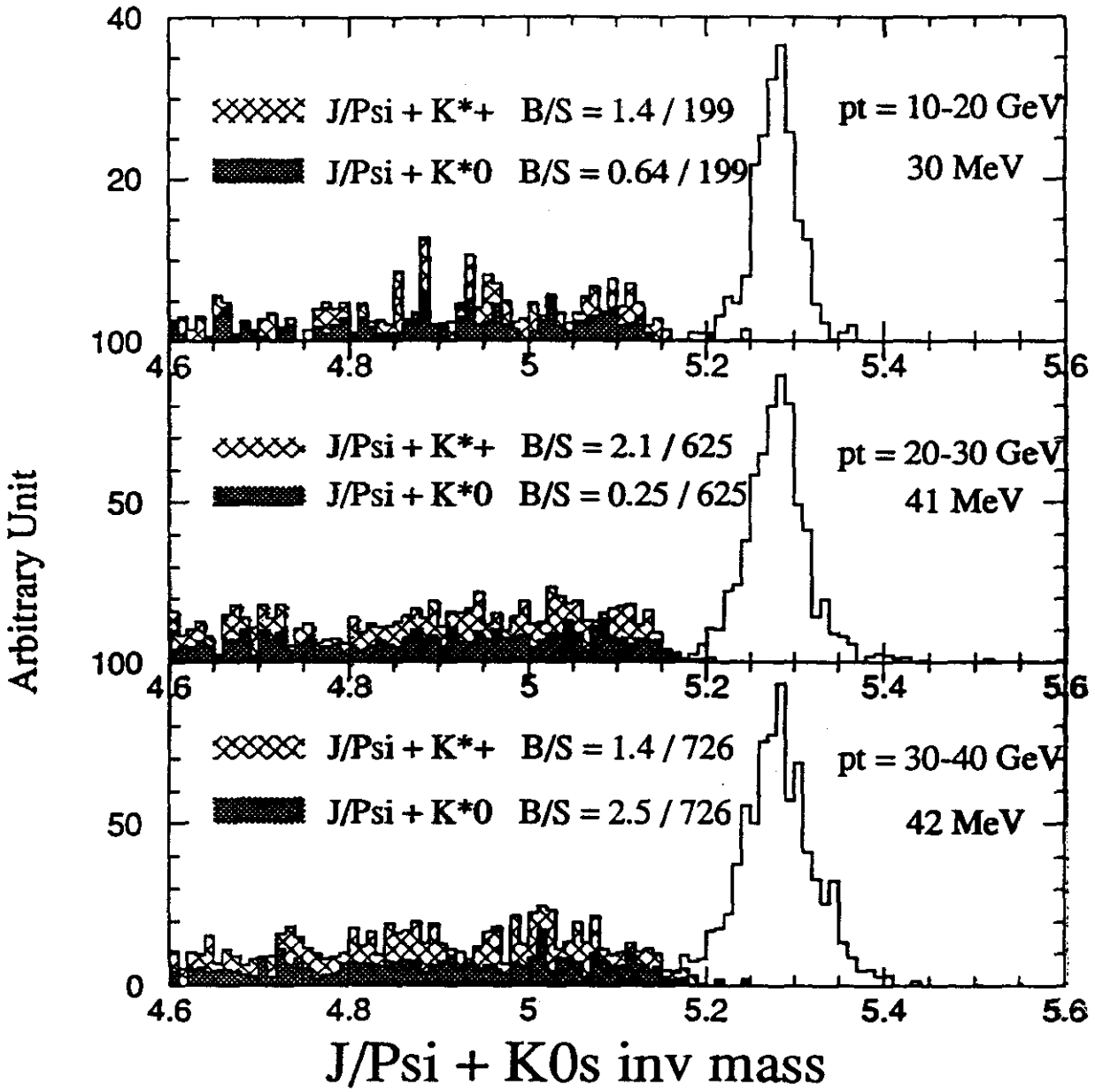
J/Psi + K*+ B/S = 1.4 / 199
J/Psi + K*0 B/S = 0.64 / 199
pt = 10-20 GeV
30 MeV
J/Psi + K*+ B/S = 2.1 / 625
J/Psi + K*0 B/S = 0.25 / 625
pt = 20-30 GeV
41 MeV
J/Psi + K*+ B/S = 1.4 / 726
J/Psi + K*0 B/S = 2.5 / 726
pt = 30-40 GeV
42 MeV
Arbitrary Unit
J/Psi + K0s inv mass

ATLAS

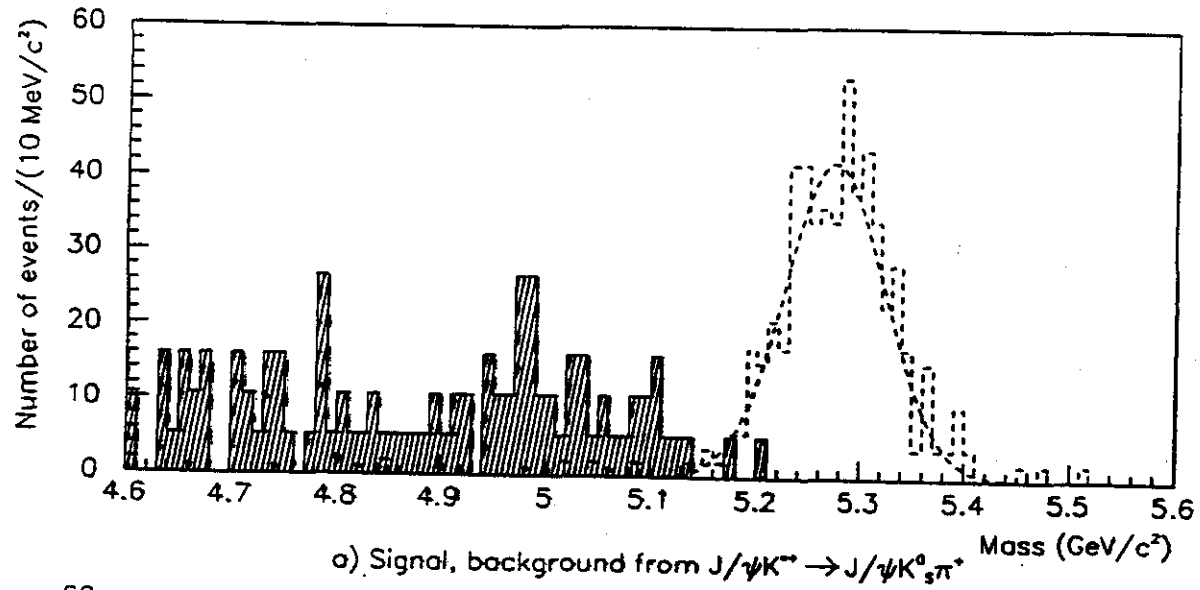

a) Signal, background from $J/\psi K^{*+} \rightarrow J/\psi K^0_s \pi^+$

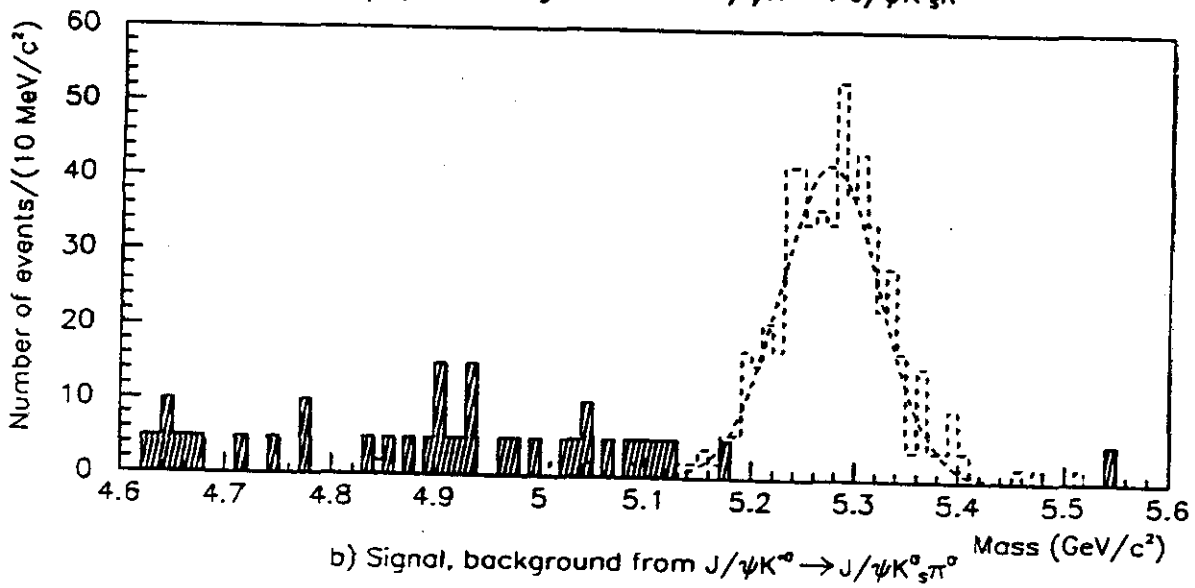

b) Signal, background from $J/\psi K^{*0} \rightarrow J/\psi K^0_s \pi^0$

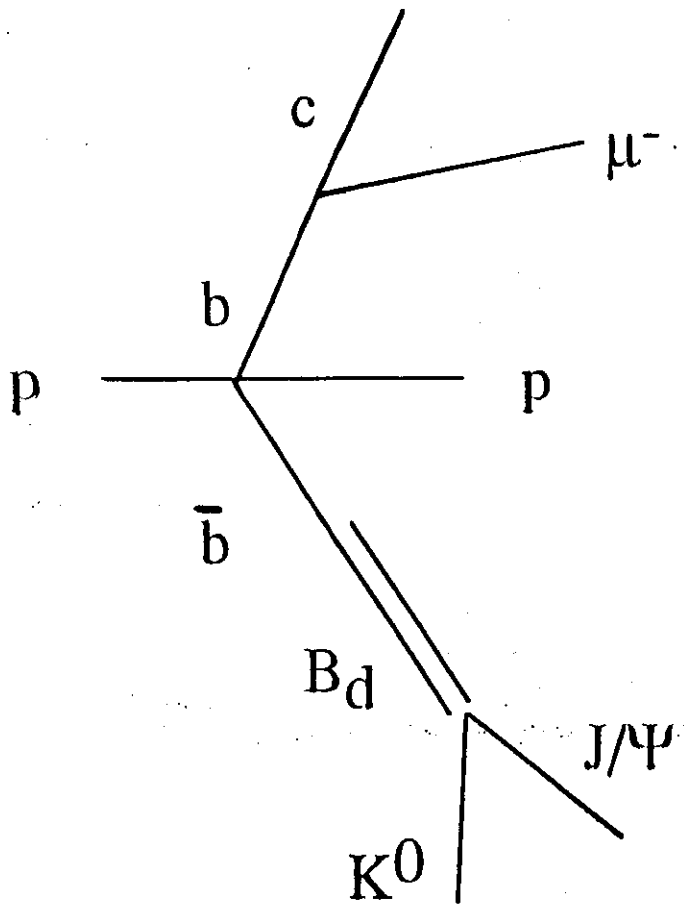

vs

$$b + \overline{B}_d \rightarrow J/\Psi + K^0$$

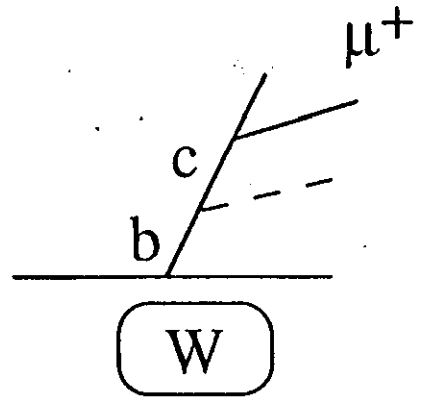

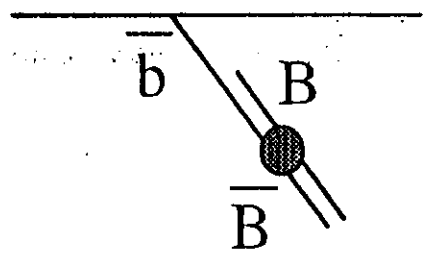

$x^2 / (1 + x^2)$

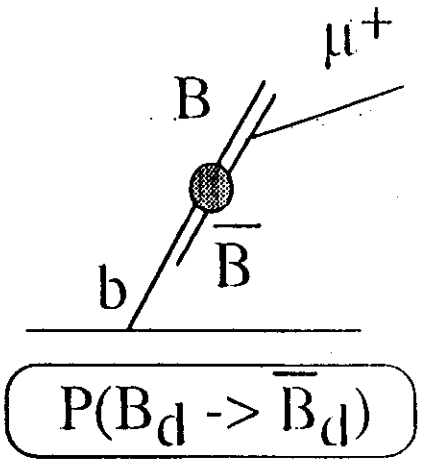

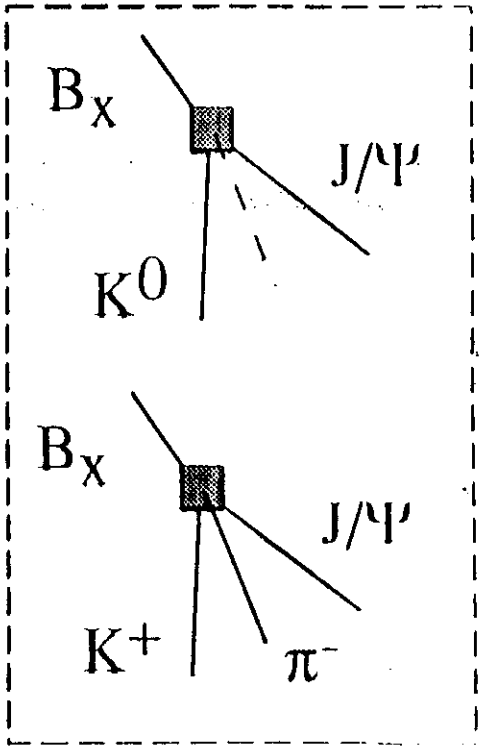

$K^* \pi\pi \rightarrow K_s$

2 Signature of $B_d^0 \to J/\Psi + K_s^0 \to \mu^+\mu^-\pi^+\pi^-$

The CP violation is measured by the difference of the branching ratios of B_d and $\overline{B}_d$ [1] decaying into the same CP eigenstate $J/\Psi\ K^0$ in the production of b–$\bar{b}$ pair production in proton-proton collision. The identity of the B-meson, either B_d or $\overline{B}_d$, is identified by the leptons decaying from the other B hadron.

The significance of the measurement of the angle β is affected by various factors:

1. The $b - \bar{b}$ pair production cross section
2. The flavor identification of B_d meson
3. The detector acceptance
4. The background

2.1 Error of sin2β

The error of the measured β is expressed as follows.

$$\delta(sin2\beta) \simeq \frac{1}{D' \times x/(1+x^2) \times \sqrt{N_{rec}}}, \quad sin2\beta << 1, \tag{1}$$

where

$$x = \frac{\Delta m}{\Gamma} = 0.71 \pm 0.11, \tag{2}$$

$$\begin{aligned} D' &= \frac{N(correcttag) - N(wrongtag)}{N(correcttag) + N(wrongtag)} \\ &= 1 - 2 \times W', \end{aligned} \tag{3}$$

$$\begin{aligned} W' &= f^+ \times W \\ &+ f^0 \times (P(B_d \to B_d) \times W + P(B_d \to \overline{B}_d) \times (1 - W)) \\ &+ f^s \times 0.5, \end{aligned} \tag{4}$$

and

$$\begin{aligned} N_{rec} &= N_{rec}(J/\Psi K_s \ell^+) + N_{rec}(J/\Psi K_s \ell^-) \\ &= N_{gen}(b\bar{b}) \times Br(b \to \ell^\pm) \times Br(B_d \to J/\Psi K \to \mu^+\mu^-\pi^+\pi^-) \times \epsilon_{eff}. \end{aligned} \tag{5}$$

[1] In this note, "B" is used to refer to bottomed hadrons, and "b" is used to refer to bottom quark, if not otherwise specified.

PYTHIA 5.6

- LUDECY modified to include polarizarions in B decays

GEMFAST / GEMGEN

- Signle particle generator in $\eta < 2.5$
- Assume sec vertex finding 100 % if 2 tracks are reconstracted by CT
- No loss due to track overlapping

$J/\Psi \rightarrow \mu\mu$

- Energy loss in CA

  Use average energy loss if $\Delta R(\mu\mu) < 0.15$, otherwise use L3 method

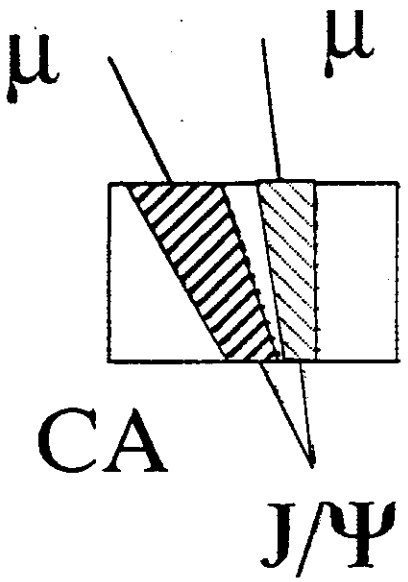

Mass constraint fit for Ks and J/Ψ

$M0 = M(p1,p2)$

2 free parameters, $|p1|$ and $|p2|$

$\chi 2 = (\Delta p1/\sigma 1)**2 + (\Delta p2/\sigma 2)**2$

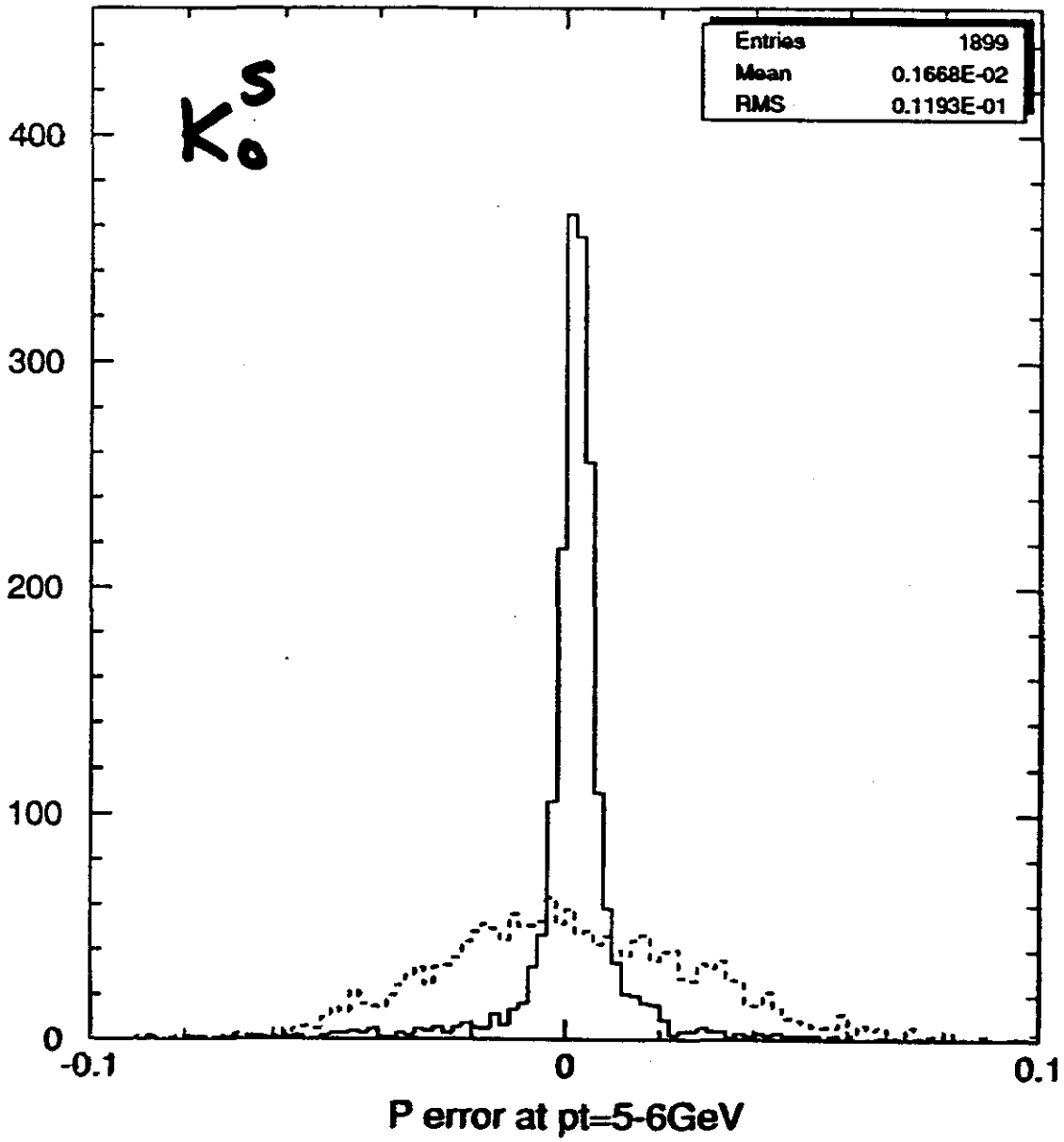
K_0^S
Entries 1899
Mean 0.1668E-02
RMS 0.1193E-01
400
300
200
100
0
-0.1
0
0.1
P error at pt=5-6GeV

Particle Properties

	dp / p (%)	Efficiency	σ (mass)	Comments
π	$0.115p \oplus 3.5$	0.97		
μ	3.5 -> 2	0.80		low pt acceptance in GEMFAST ??
J/Ψ	1.5 -> 2 mass cns at low μ res at high	0 -> 0.45 ~ 0.55 ($\chi^2 < 20$) low pt efficincy	77 -> 83 MeV	Mass : 2.8 - 3.4 GeV $\chi^2 < 20$ E_{loss} : use <los> if dR<0.15
K_s^0	1 -> 0.5 mass cns imprv by factor of 4-5	0.75 -> 0.20 ($\chi^2 < 5$) decay vertex finding	9.9 -> 10.7 MeV	Mass : 0.45 - 0.55 GeV $\chi^2 < 20$
B_d		0 -> 0.1 low pt J/Ψ long flight pass of K	30 -> 42 MeV mass cns imprvs by factor of 2.5-3	bck / sig (%) 5.2-5.36 $J/\Psi\ K^{*0} \to J/\Psi\ K^0\pi^0 < 0.5$ $J/\Psi\ K^{*+} \to J/\Psi\ K^0\pi^+ < 0.5$ w/o V vertex req $J/\Psi\ K^{*0} \to J/\Psi\ K^+\pi^- < 20$ $J/\Psi\ K^+\pi^- < 2$

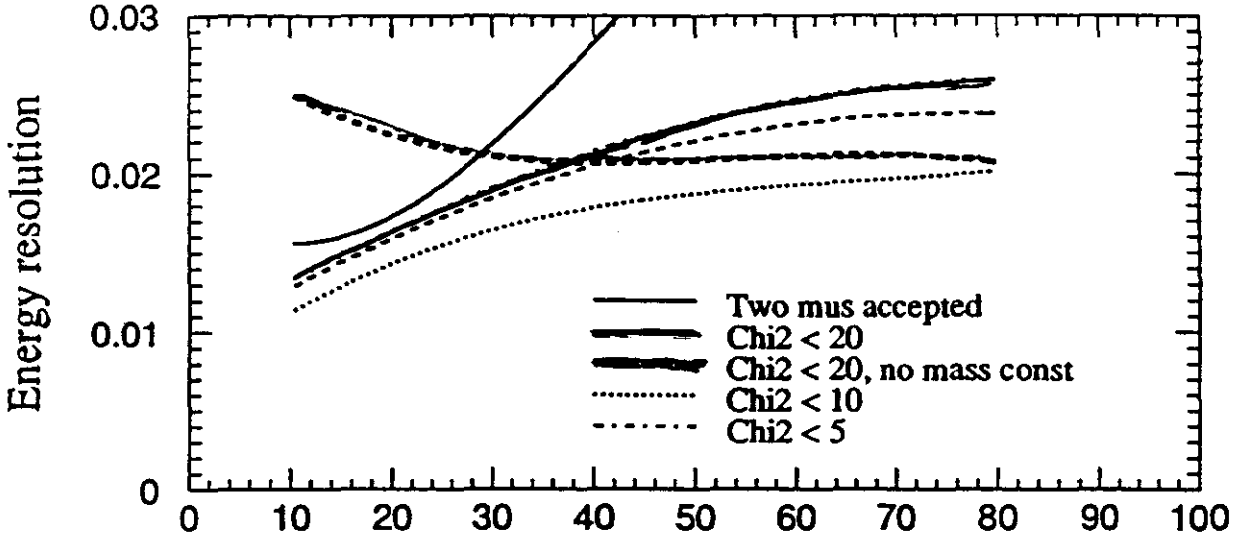

(a) Momentum Resolution vs Pt of J/Psi

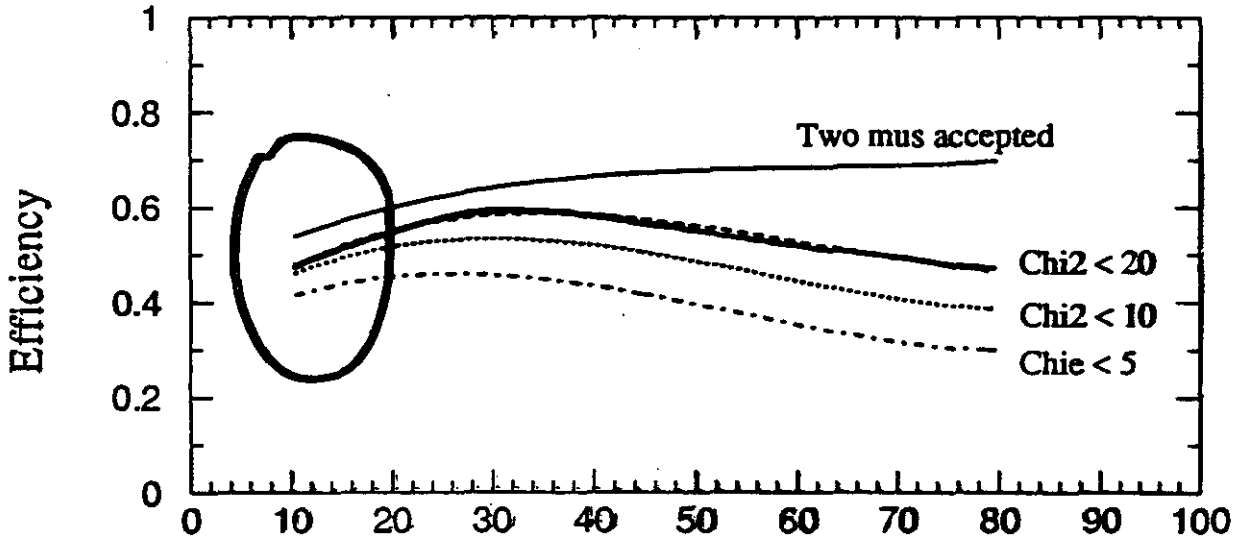

(b) Efficincy vs Pt of J/Psi

Resolution and Efficiency of J/Psi

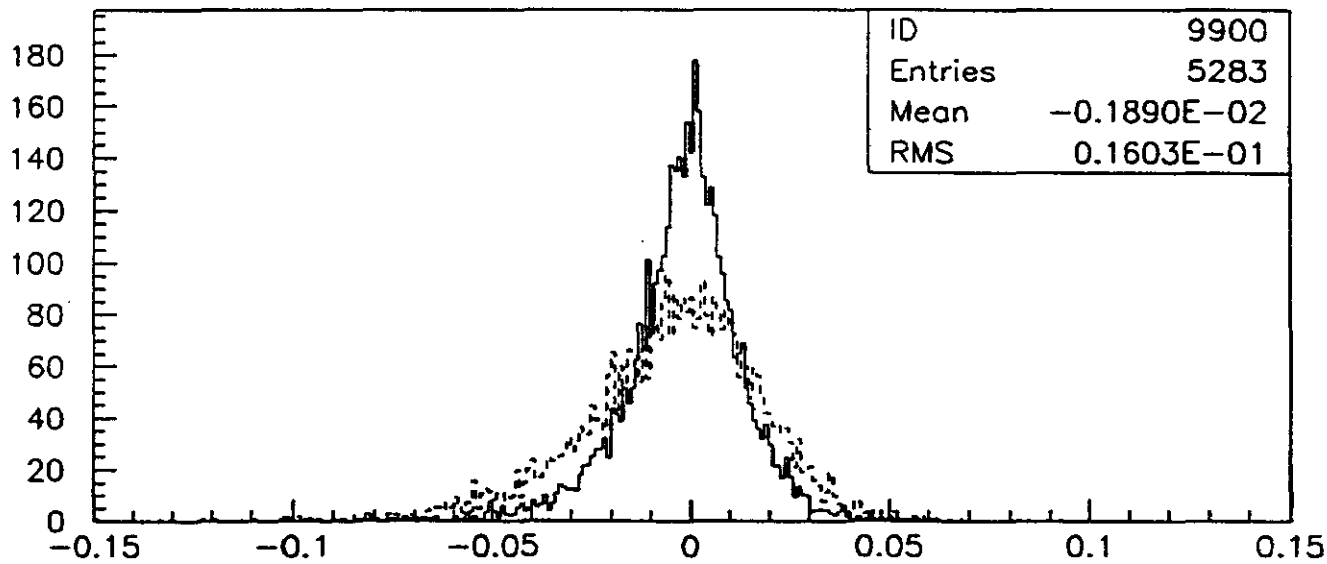

P resolution pt=10−25 GeV

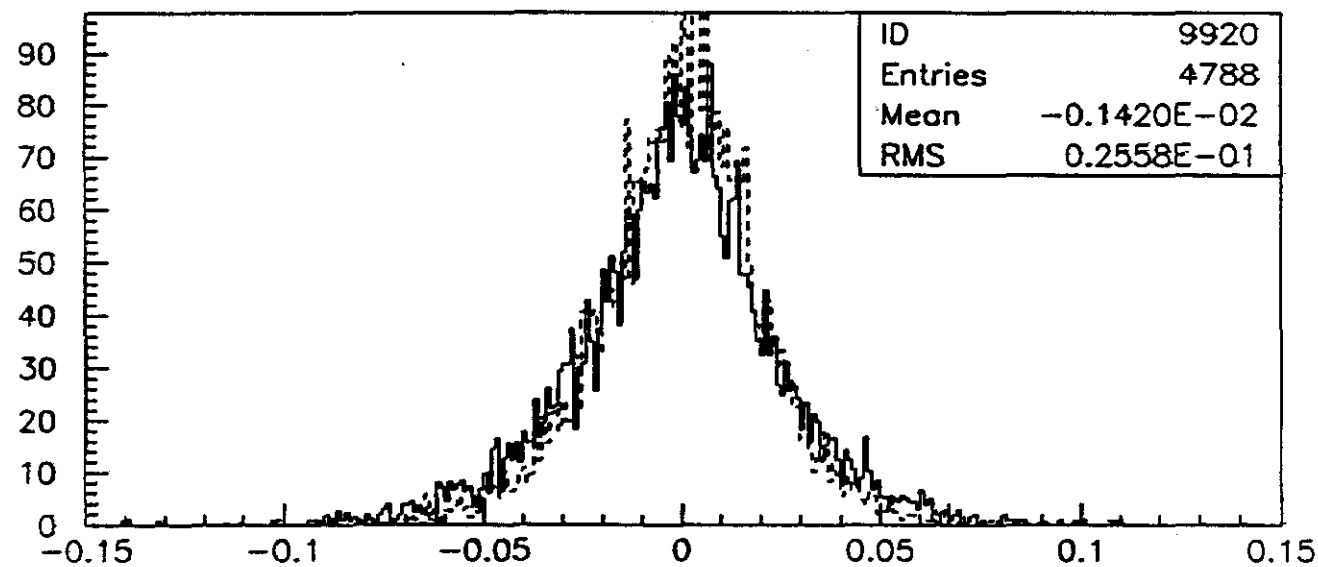

P resolution pt=60−75 GeV

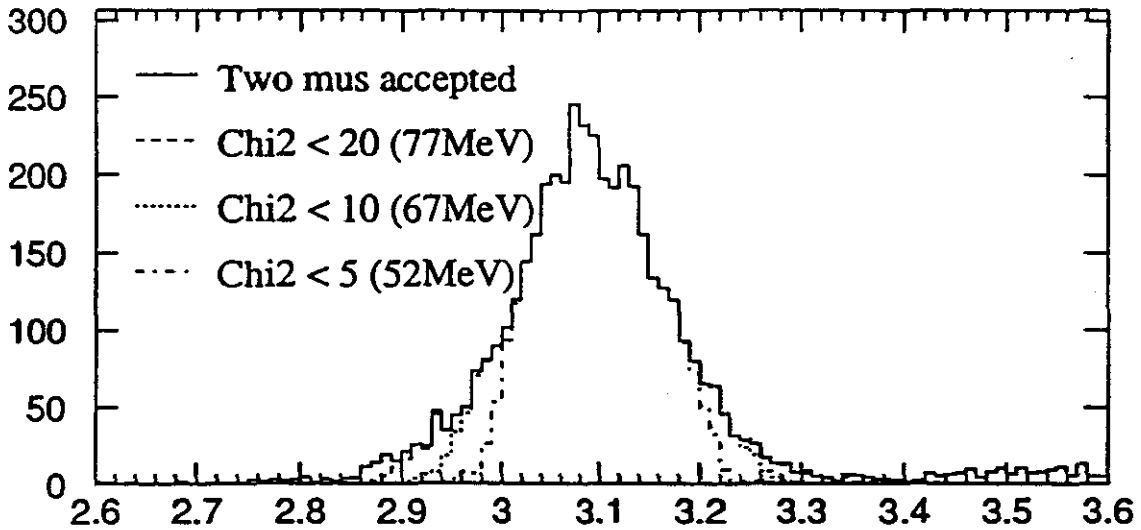

(a) mu-mu mass (pt=10-25 GeV)

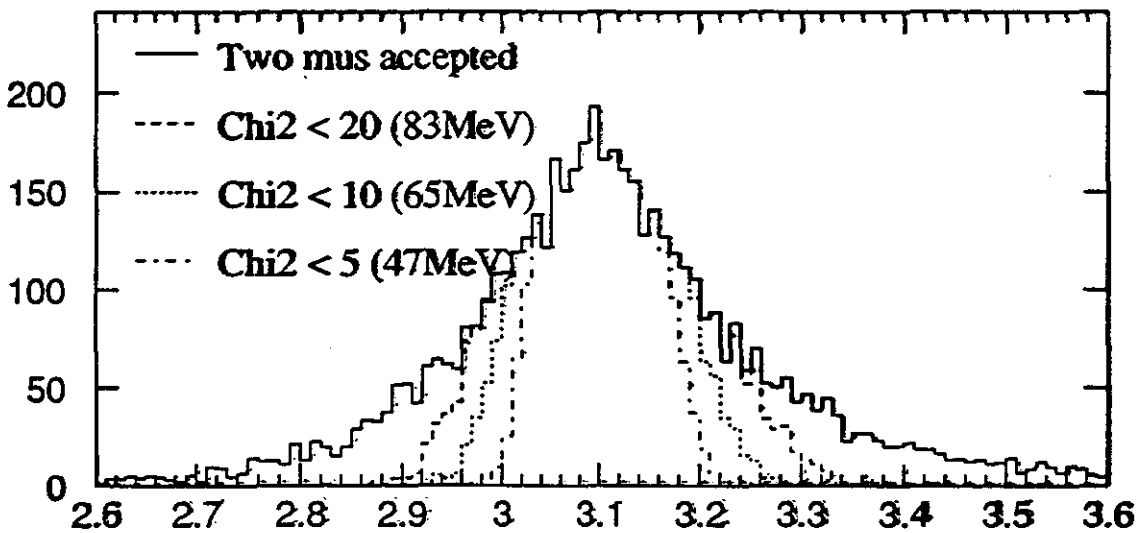

(b) mu-mu mass (pt=60-75 GeV)

mu-mu mass (GeV)

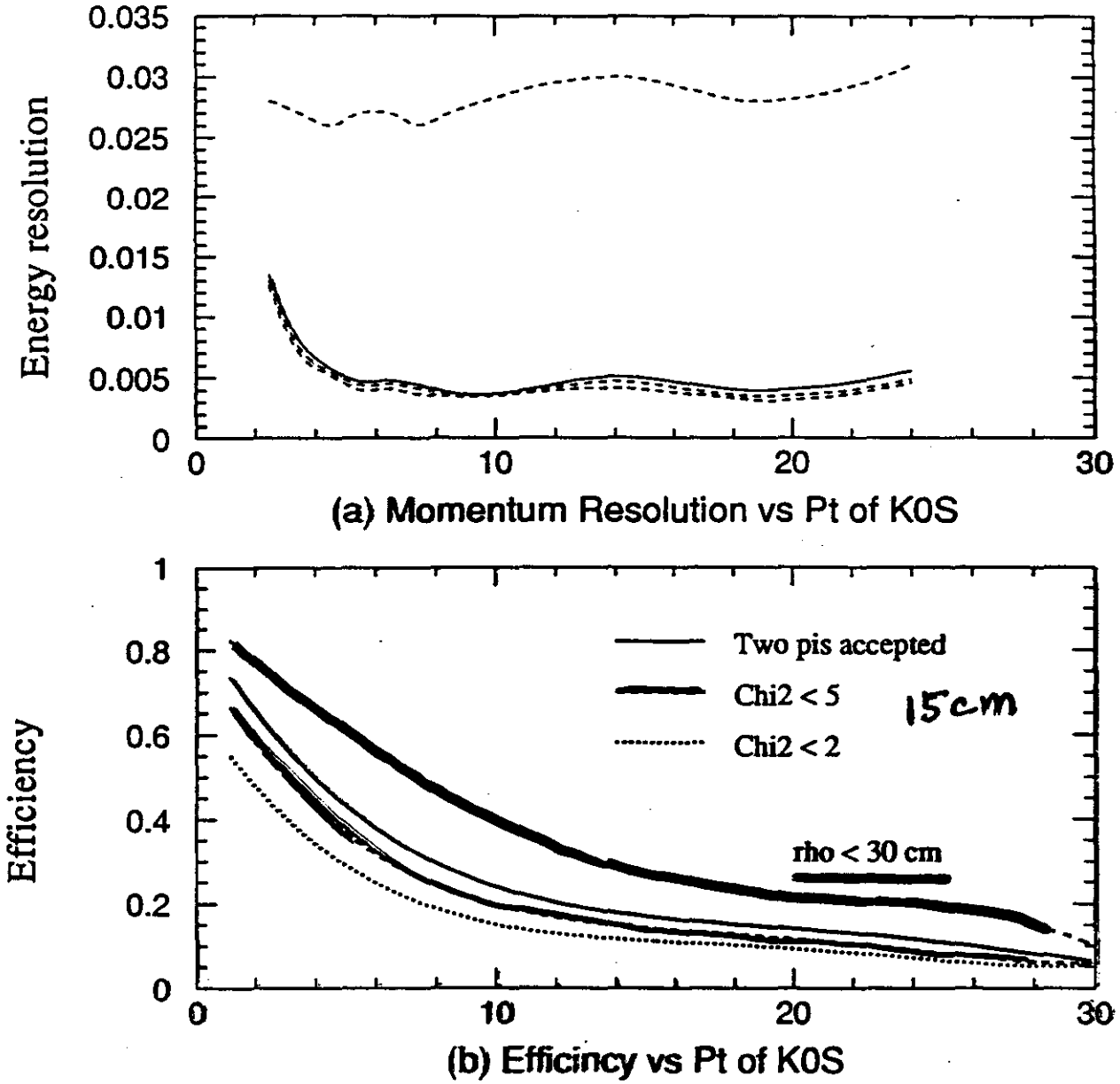

Resolution and Efficiency of K0S

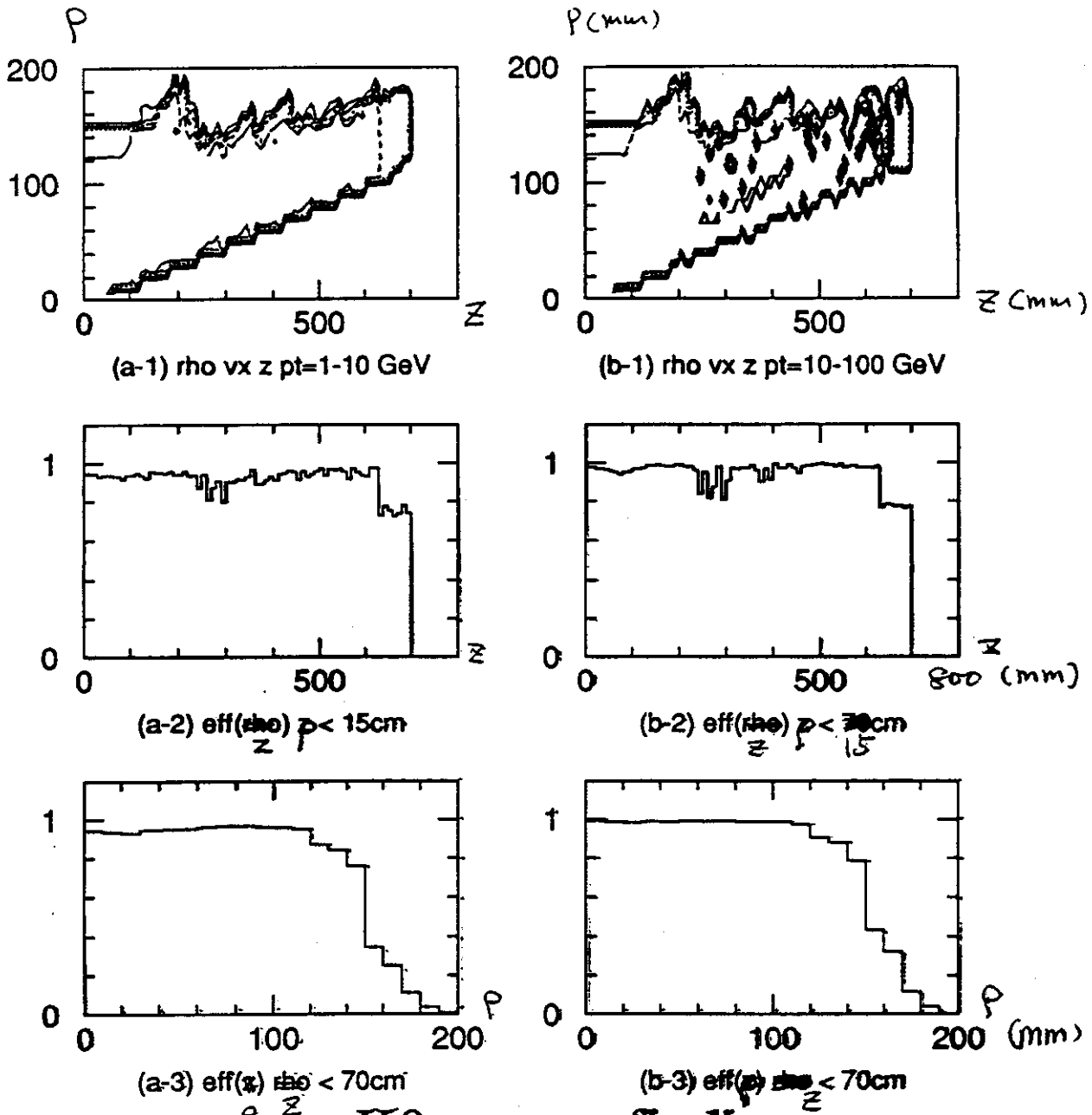

K0s vertex finding

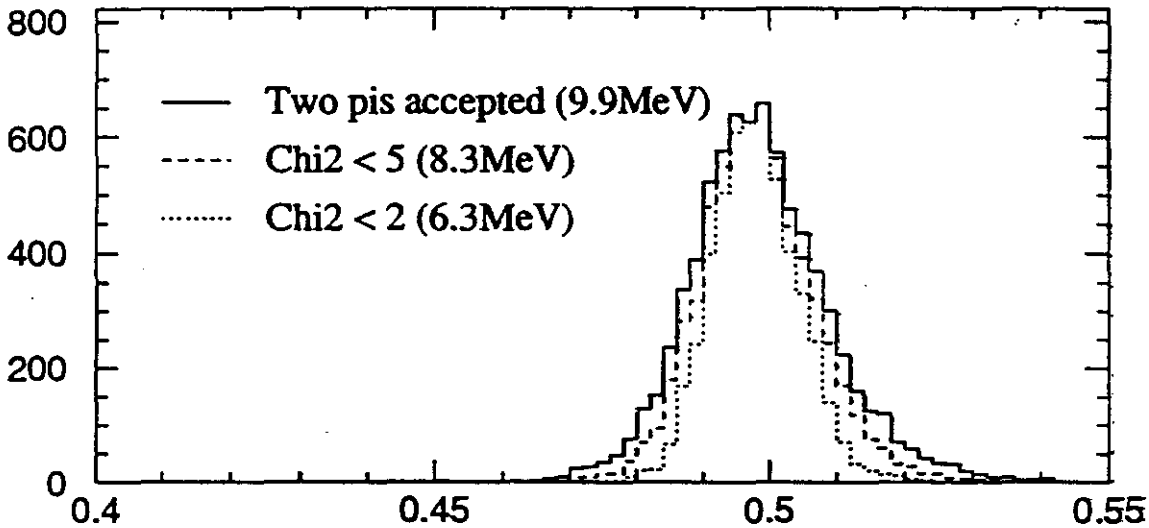

(a) pi-pi mass (pt=3-6 GeV)

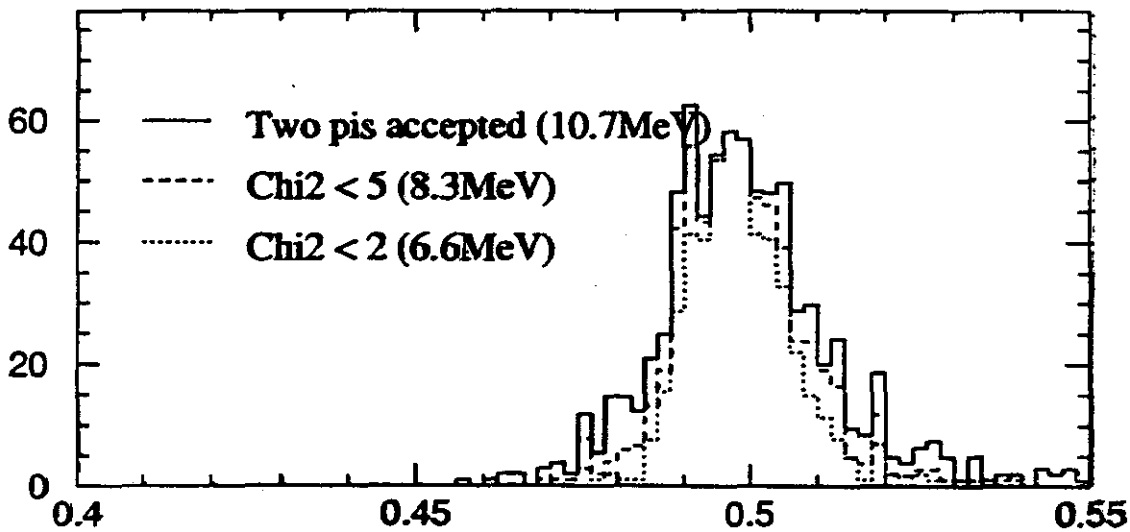

(b) pi-pi mass (pt=15-25 GeV)

pi-pi mass (GeV)

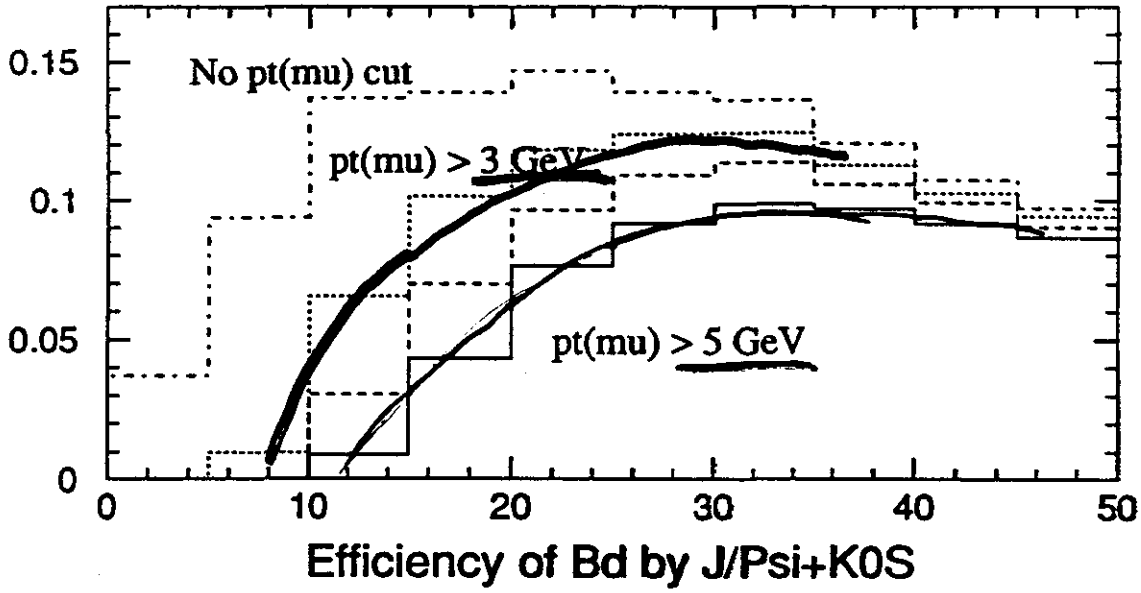
No pt(mu) cut
pt(mu) > 3 GeV
pt(mu) > 5 GeV
0.15
0.1
0.05
0
0
10
20
30
40
50
Efficiency of Bd by J/Psi+K0S

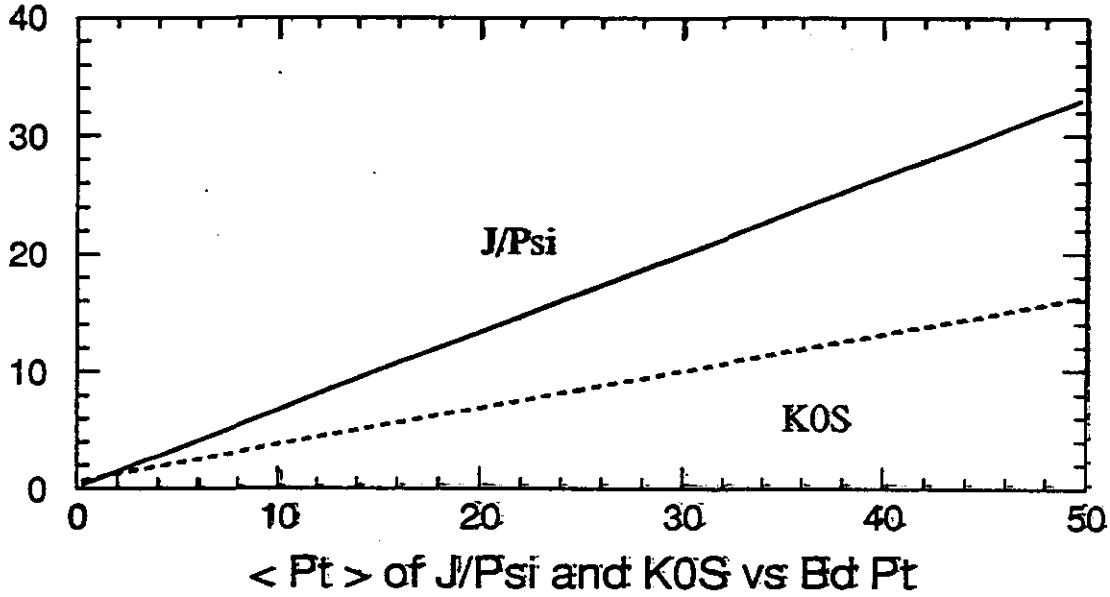
J/Psi
K0S
40
30
20
10
0
0
10
20
30
40
50
< Pt > of J/Psi and K0S vs Bd Pt

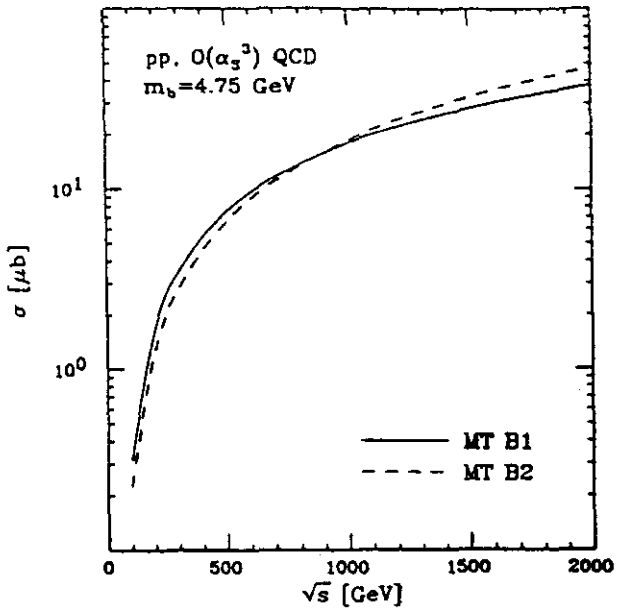

FIG. 8. The calculated cross section $\sigma(pp \to b\bar{b}X)$ at order α_s^3 in QCD is shown as a function of $\sqrt{s}$ for $100 < \sqrt{s} < 2000$ GeV. The solid line is obtained from the parton densities of the MT set $B1$ ("nonsingular" gluon), and the dashed curve from the MT set $B2$ ("singular" gluon).

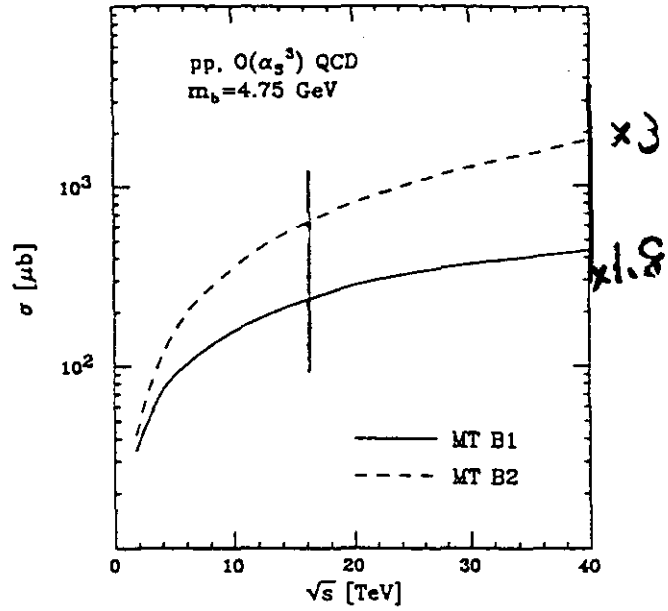

FIG. 9. As in Fig. 8 but for $\sqrt{s} \geq 2$ TeV.

$\sqrt{s} = 630$ GeV and $\sqrt{s} = 1.8$ TeV. Shown also are data of the UA1 [13] and Collider Detector at Fermilab (CDF) [14] collaborations. The selections on rapidity, $|y| < 1.5$ at $\sqrt{s} = 630$ GeV and $|y| < 1$ at $\sqrt{s} = 1.8$ TeV, are the same as those made in the analyses of the data. The solid curves in Figs. 6 and 7 are obtained from the MT set $B1$ with a "nonsingular" gluon density, $M_b = 4.75$ GeV, and $\mu^2 = M_b^2 + (p_T^{\min})^2$. The band delimited by the dotted lines shows the range of theoretical predictions we obtained by adding in quadrature the differences obtained from the central solid curve when we varied separately the bottom-quark mass, $4.5 < M_b < 5.0$ GeV; the renormalization scale, $\frac{1}{4}[M_b^2+(p_T^{\min})^2] < \mu^2 < 4[M_b^2+(p_T^{\min})^2]$; and the gluon density, substituting MT sets S and $B2$ for set $B1$. The range of values of p_T and y explored at the CERN and Fermilab colliders ($x > 0.01$) do not offer an opportunity to discriminate between the very small x behaviors of $xG(x,\mu)$ incorporated in MT sets S, $B1$, and $B2$.

Comparisons of the theoretical curves in Figs. 6 and 7 with data show good agreement at $\sqrt{s} = 630$ GeV but perhaps as much as a factor of 2 to 3 disagreement at $\sqrt{s} = 1.8$ TeV. The calculations of Collins and Ellis indicate that resummation effects are negligible at $\sqrt{s} = 630$ GeV but may enhance the theoretical cross sections at $\sqrt{s} = 1.8$ TeV by factors of 1.2 to 1.5 depending on the choice of the gluon densities. Taken at face value, the discrepancy at $\sqrt{s} = 1.8$ TeV suggests that a substantially different form for the gluon density may be appropriate for $x < 0.03$.

In Figs. 8 and 9, we provide calculations of the integrated inclusive cross section $\sigma(pp \to b\bar{b}X)$ obtained by integrating the inclusive yield over all rapidity and transverse momentum. In these computations we use $\mu^2 = M_b^2 + p_T^2$. For the energy range 100 GeV $< \sqrt{s} <$ 2 TeV shown in Fig. 8, the singular and nonsingular parametrizations of the gluon density yield similar results. The differences become increasingly significant as $\sqrt{s}$ increases above $\sqrt{s} = 2$ TeV, as shown in Fig. 9.

A 20 TeV proton beam incident on a fixed proton target provides a center-of-mass energy $\sqrt{s} = 200$ GeV. For this SSC fixed-target option, we calculate $\sigma(b\bar{b}X) = 1.25$ μb for the singular MT set $B2$ and 1.65 μb for the nonsingular MT set $B1$. Including uncertainties associated with variations of μ and M_b, we estimate

$$\sigma(b\bar{b}X, \sqrt{s} = 200 \text{ GeV}) = 1.0 \text{ to } 2.0\ \mu\text{b}. \tag{12}$$

At $\sqrt{s} = 40$ TeV, the calculations yield $\sigma(b\bar{b}X) \simeq 0.45$ mb for set $B1$ and nearly 9 mb for set $B2$. However, at this energy, resummation effects are expected to be very significant, providing enhancement factors [9] of ~ 4 for a nonsingular gluon starting distribution [$xG(x) \to$ constant] and ~ 1.5 for a singular distribution [$xG(x) \sim x^{-1/2}$]. Using these factors, we may multiply our $O(\alpha_s^3)$ results at $\sqrt{s} = 40$ TeV, obtaining $\simeq 1.8$ mb for set $B1$ and $\simeq 3$ mb for set $B2$. Including estimates of other uncertainties, we quote

$$\sigma(b\bar{b}X, \sqrt{s} = 40 \text{ TeV}) = 1 \text{ to } 3 \text{ mb}. \tag{13}$$

Similar reasoning leads to an estimate appropriate at the LHC energy $\sqrt{s} = 15.4$ TeV:

$$\sigma(b\bar{b}X, \sqrt{s} = 15.4 \text{ TeV}) = 0.5 \text{ to } 0.9 \text{ mb}. \tag{14}$$

In Figs. 10 and 11 we present calculations of the integral transverse momentum spectrum $\sigma(p_T \geq p_T^{\min})$ at $\sqrt{s} = 40$ TeV. In Fig. 10 the cross section is integrated over all rapidity, whereas in Fig. 11 the selection $|y| < 1$ is imposed. These figures demonstrate that the influence of the more singular gluon density is felt most strongly at small p_T ($p_T < 25$ GeV) at $\sqrt{s} = 40$ TeV. Because enhancements associated with resummation were discussed

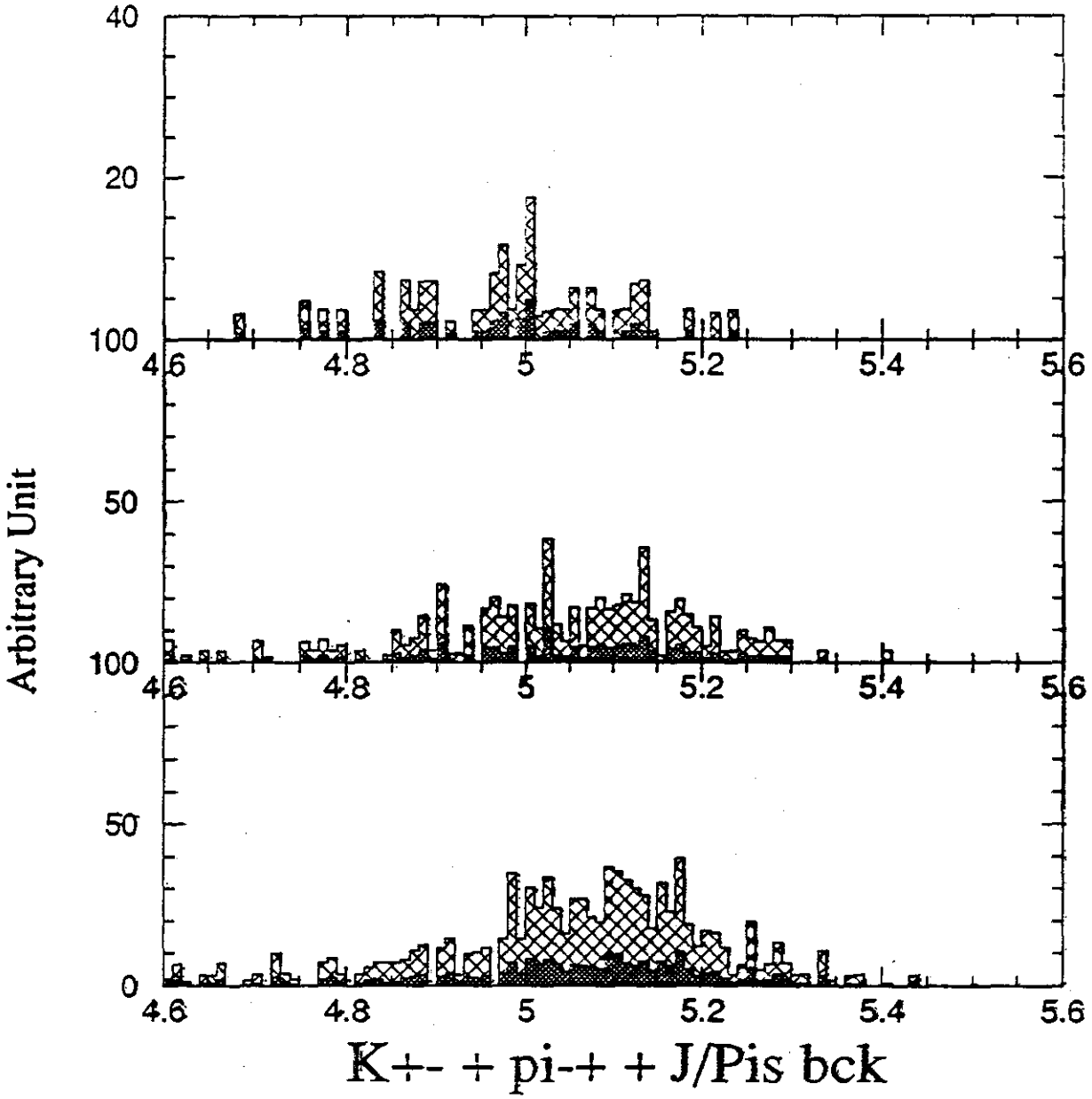
Arbitrary Unit
40
20
100
50
100
50
0
4.6
4.8
5
5.2
5.4
5.6
K+- + pi-+ + J/Pis bck

Table 1: $b-\bar{b}$ production cross sections

PDF	$b-\bar{b}$	g - g	g - q	Total	$b-\bar{b}$	g - g	g - q	Total	5+5+5	5+5+13
					$P_t(b,\bar{b}) \geq 10$ GeV				P_t of μ's in $\lvert\eta\rvert \leq 2.5$	
	(mb)								(pb)	
CTEQ1L	0.46	0.43	0.28	1.2	0.033	0.050	0.044	0.13	7.7	3.7
MT B2	1.2	0.64	0.51	2.3	0.049	0.064	0.057	0.17	8.1	4.2

Table 2: Efficiency

Contribution	Acceptance Factor	Comment
b $\rightarrow \mu$ for flavor tagging	0.23	
η(tag μ) ≤ 2.5	0.50	
b $\rightarrow$ B_d	0.4	
$B_d^0 \rightarrow J/\Psi + K_s^0 \rightarrow \mu^+\mu^-\pi^+\pi^-$	1.7×10^{-5}	
3μ's in $\eta \leq 2.5$	0.66	
Trigger p_t (μ) $\geq$ 8 GeV	0.12	13GeV, $\times$1/4(all), $\times$1/2(5GeV min)
3μ's with $p_t \geq 5$ GeV	0.056	4GeV, $\times$1.7
$\eta(\pi^\pm) \leq 2.5$	0.96	
p_t ($\pi^\pm$) $\geq$ 0.5 GeV	0.76	
z(K_s^0decay) $\leq$ 70 cm	0.72	100 cm, $\times$1.07
ρ(K_s^0decay) $\geq$ 1 cm	0.98	
ρ(K_s^0decay) $\leq$ 15 cm	0.35	30 cm, $\times$1.6
p_t (K_s^0) $\geq$ 1 GeV	1.0	
p_t (J/Ψ) $\geq$ 10 GeV	1.0	
$\theta(\vec{p_J}, \vec{p_K}) \leq 45°$	0.99	
Sub total	7.3×10^{-10}	
μ acceptance	$(0.8)^3$	
π acceptance	$(0.95)^2$	
χ^2 cuts and other expences	$\sim$ 0.8	
Grand total	2.7×10^{-10}	6500 evts / 10^{33}

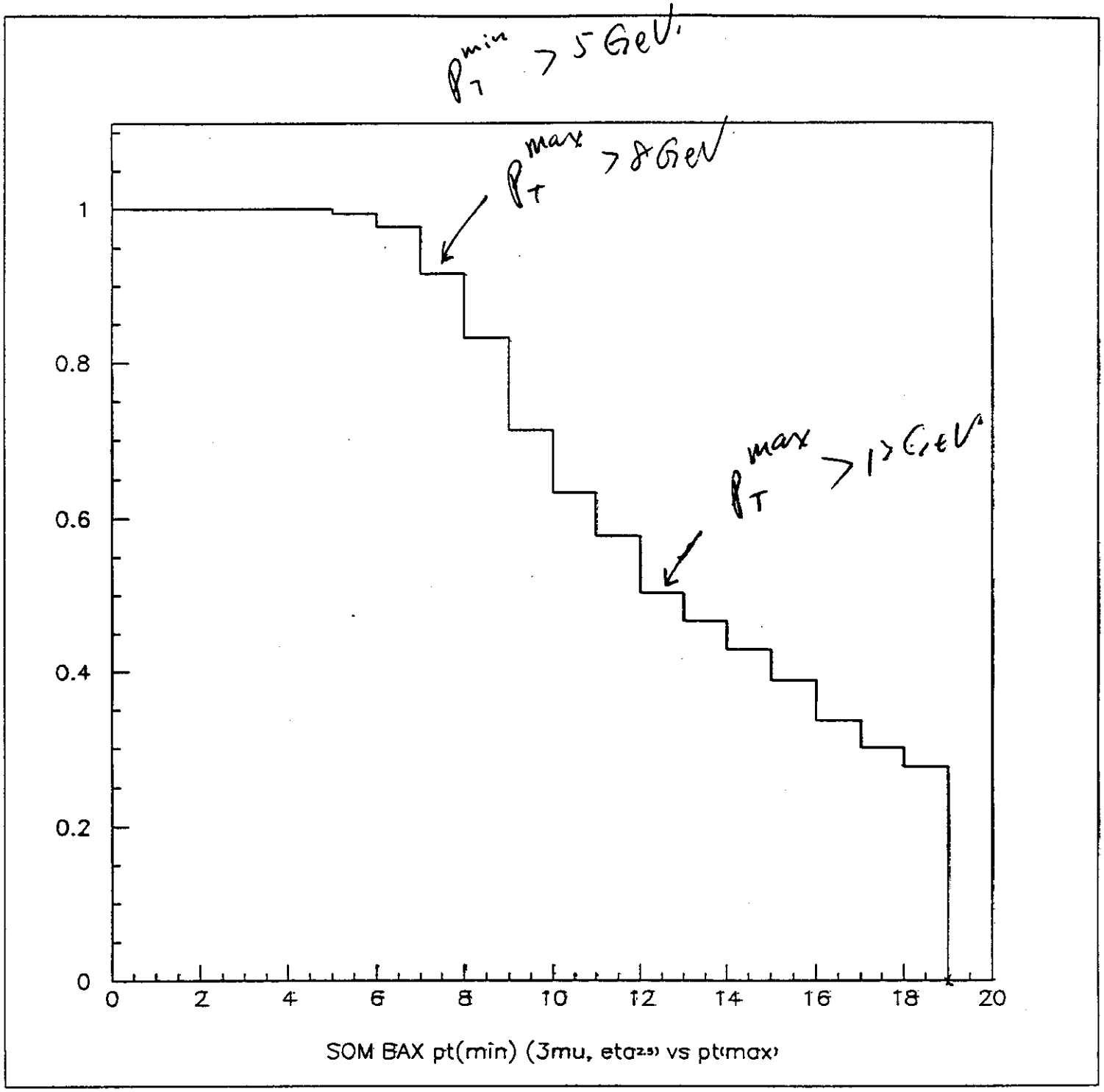
$p_T^{min} > 5$ GeV
$p_T^{max} > 8$ GeV
$p_T^{max} > 12$ GeV
1
0.8
0.6
0.4
0.2
0
0
2
4
6
8
10
12
14
16
18
20
SOM BAX pt(min) (3mu, eta<2.5) vs pt(max)

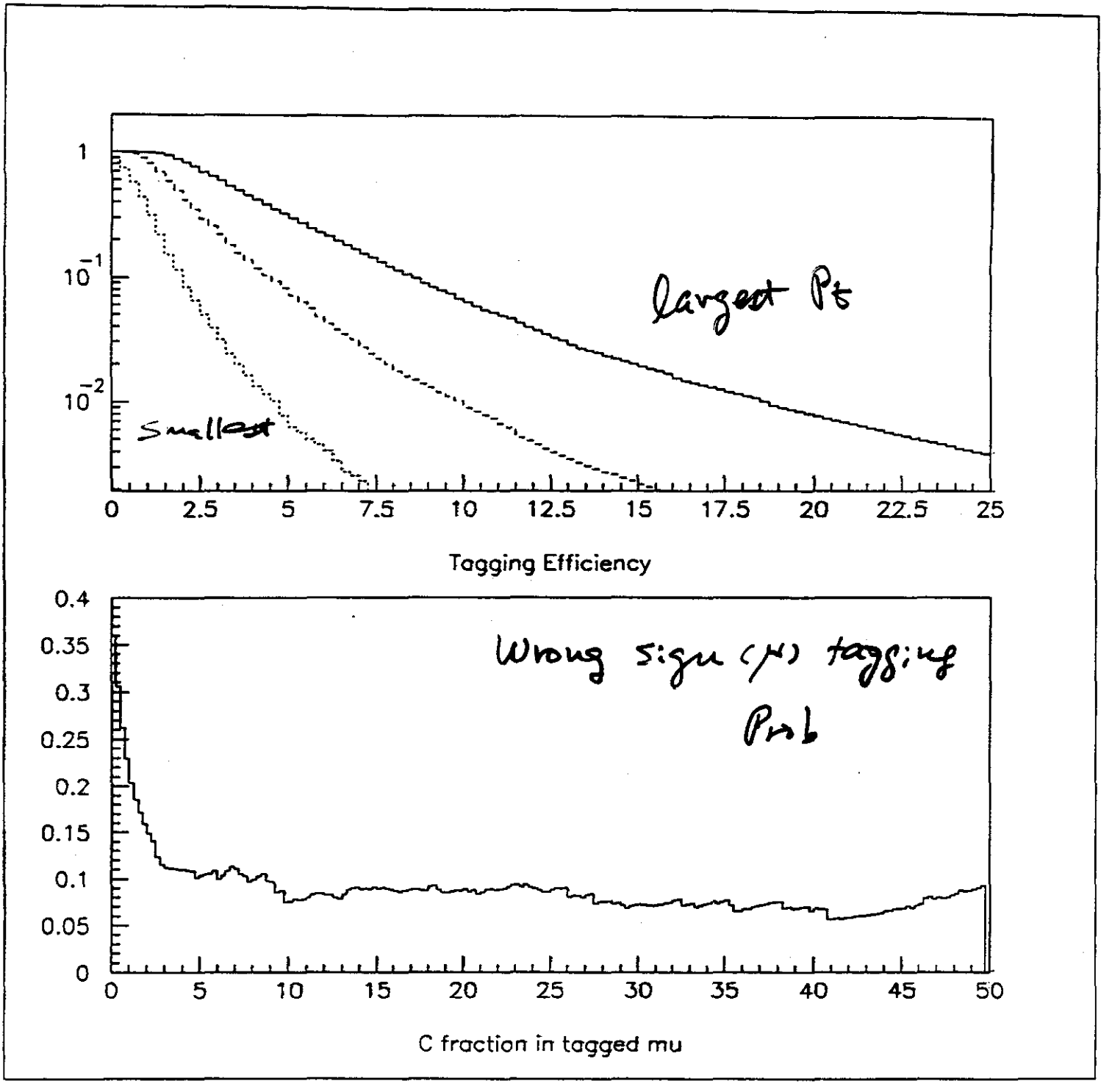
1
10^{-1}
10^{-2}
largest Pt
smallest
0
2.5
5
7.5
10
12.5
15
17.5
20
22.5
25
Tagging Efficiency
0.4
0.35
0.3
0.25
0.2
0.15
0.1
0.05
0
Wrong sign (μ) tagging Prob
0
5
10
15
20
25
30
35
40
45
50
C fraction in tagged mu

Conclusion

1. Momentum resolution is not problem

2. May take 2 - 3 times longer due to

   - Smaller CT
   - Large energy loss in the calorimeter

     $P_T(\mu) > 5$ GeV

gem

γeμ

Presentation by:

P. Dingus

Peter Dingus
SSCL 8/5/93

Pattern Recognition Issues

The fundemental problems in pattern recognition are dependent on the types and density of the backgrounds associated with the signal. These in turn depend upon:

A) Materials comprising the muon chambers.

B) The momentum magnitude of the muon .

C) The physical layout of the experiment.

Only correlated background will be considered in detail.

Then a couple of track reconstruction senarios

will be considered in the presence of these backgrounds.

We will consider three files of 3500 isolated muons of momentums;

1 TeV, 500 GeV , and 100 GeV Pt which were uniformly distributed throughout the GEM detector. The Sigem simulation V1.3 (Y.Fisyak , GEM TN-162) was used with 10KeV cuts.

MATERIALS – 1.9 CM NOMEX
– 0.5, 0.7, 1.0 CM $CF_4 CO_2$ (SL 1, 2, 3)
– 0.05 CM G10
– 0.0017 CM Cu

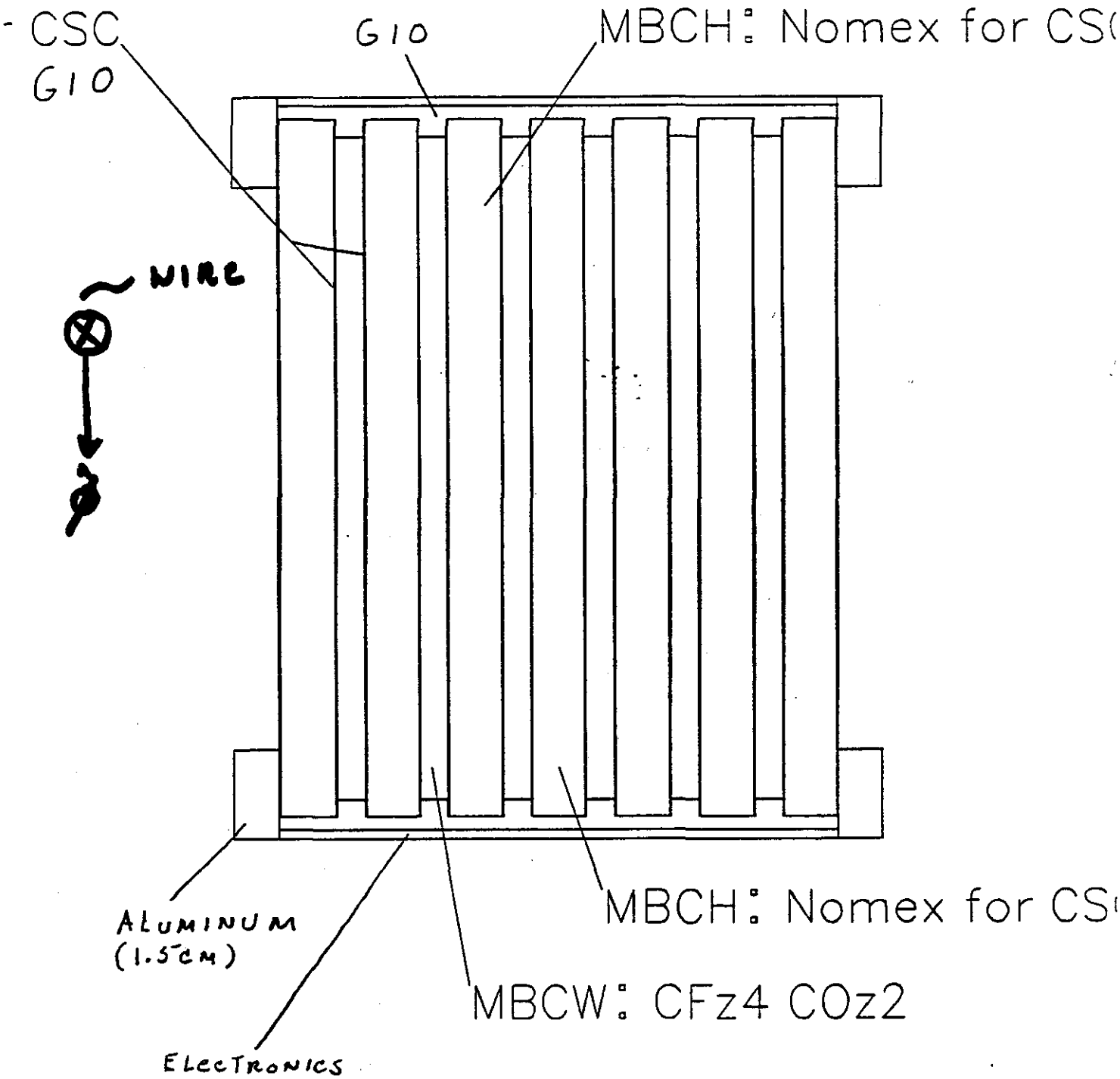

CSC CHAMBER

SIGEM V1

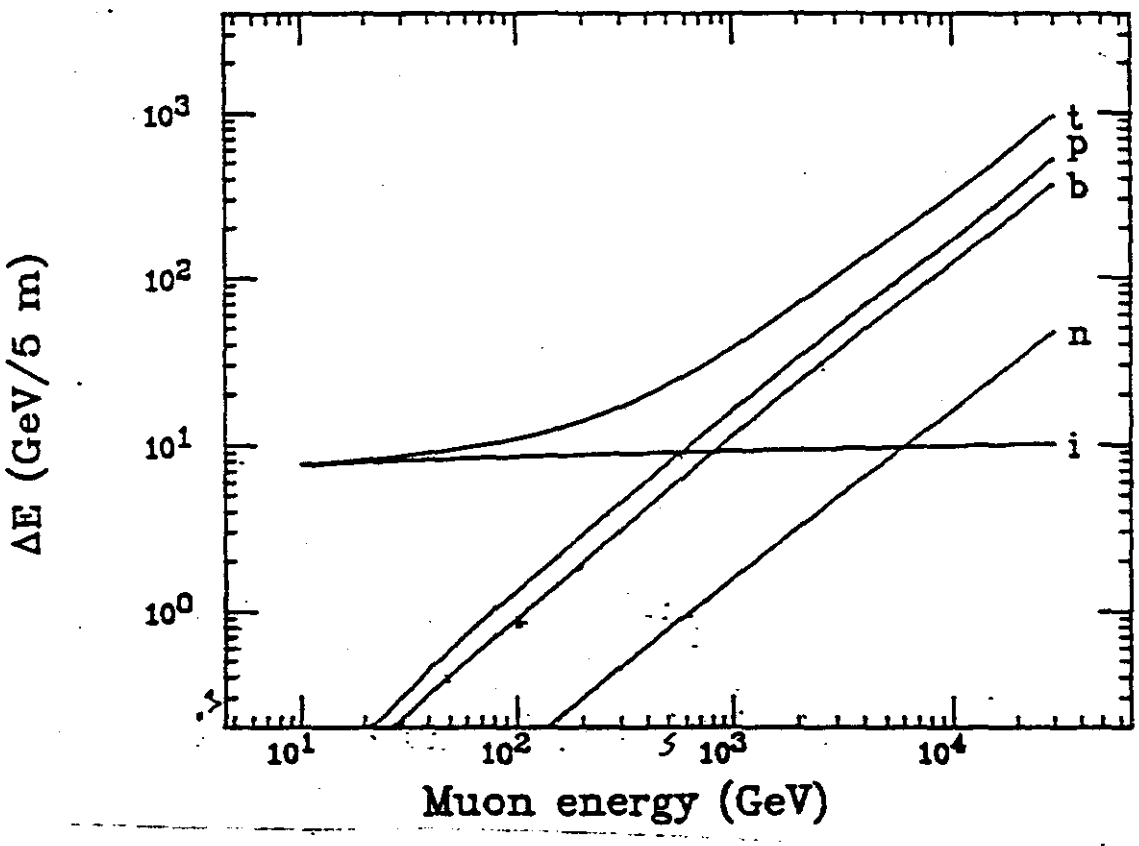
ΔE (GeV/5 m)
Muon energy (GeV)
t
p
b
n
i

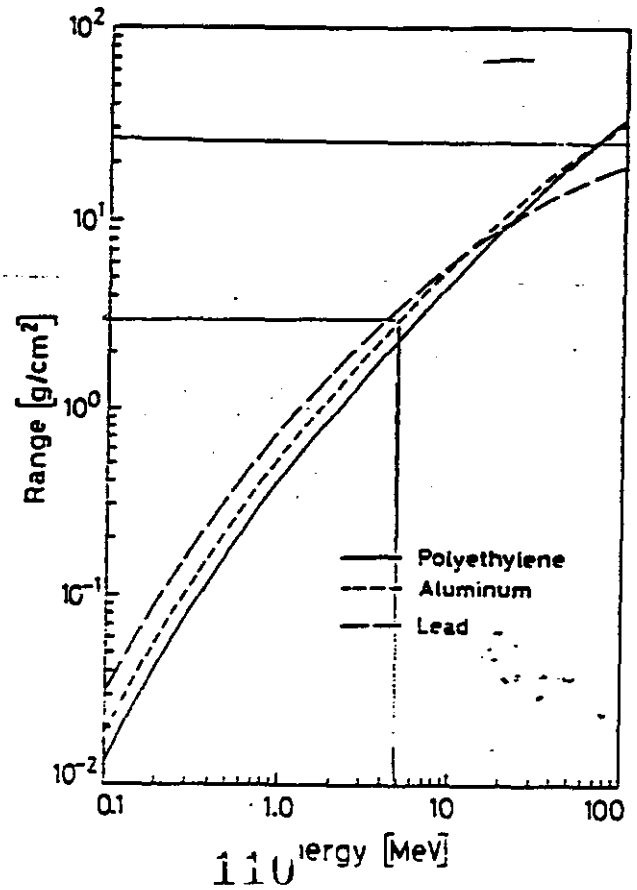
Range [g/cm²]
Polyethylene
Aluminum
Lead

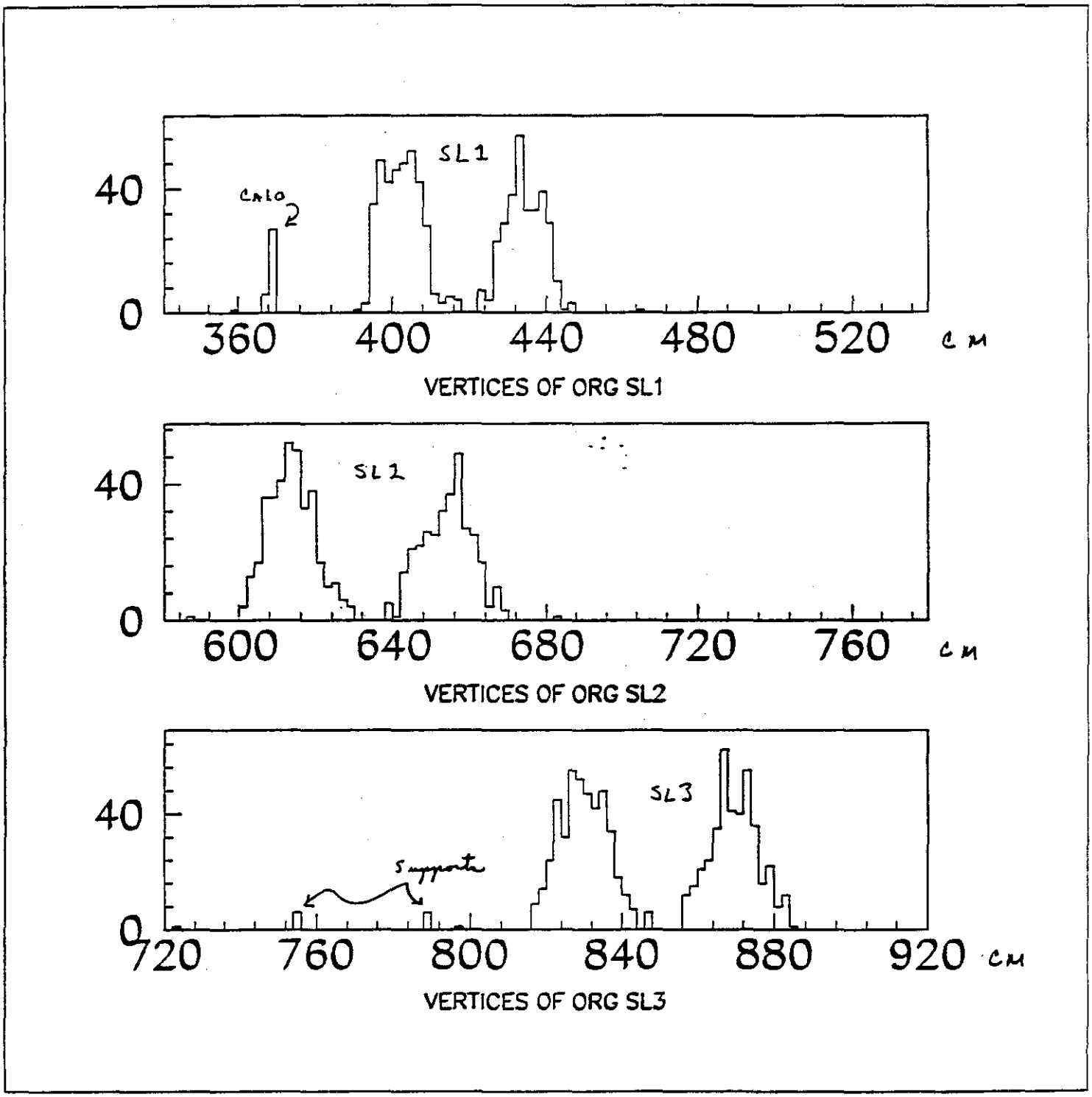

1 TeV P_T IN THE BARREL

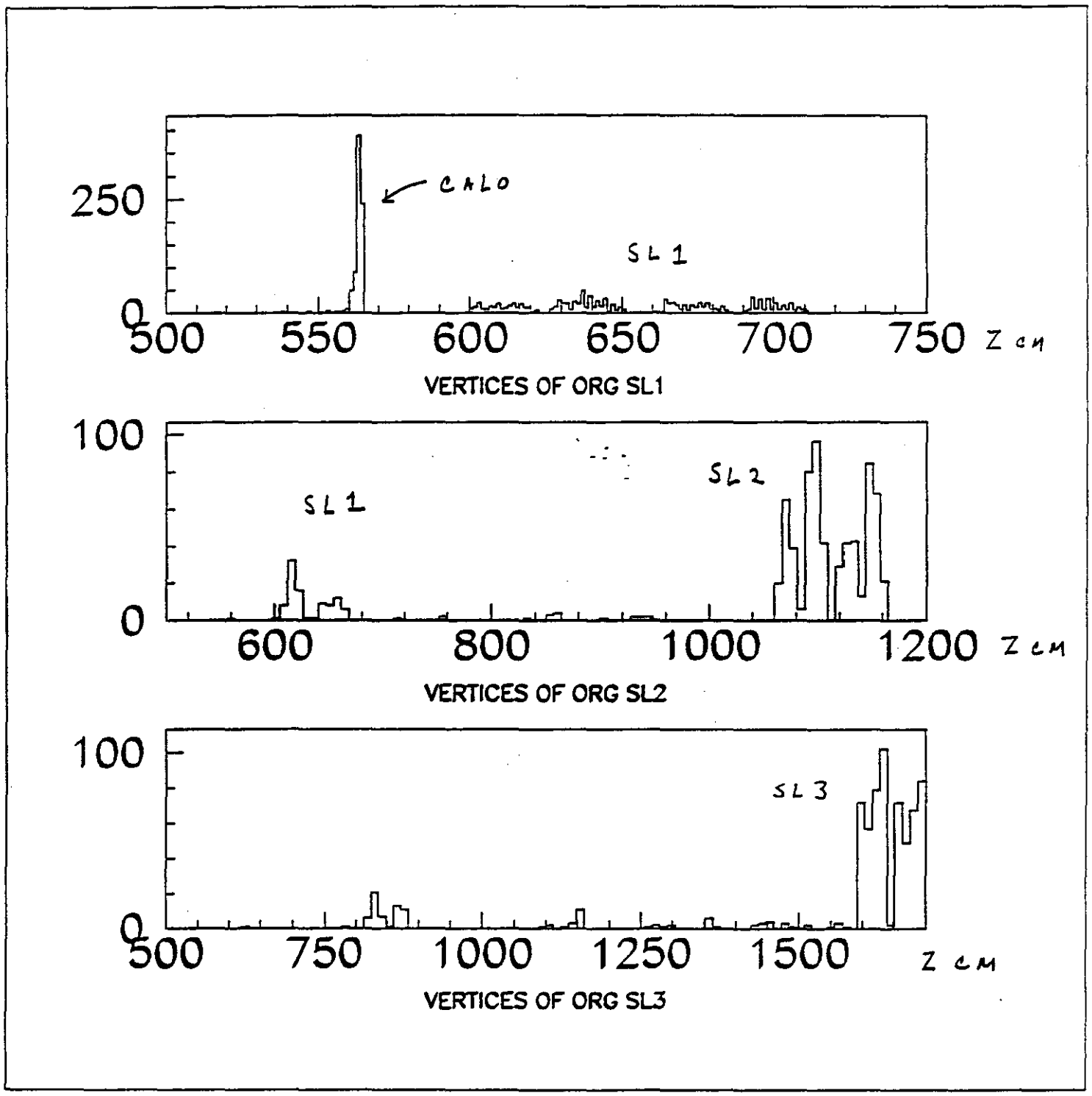

1 Tev P_T, ENDCAP

The Background

The background consist of EM debris produced by muons both at the top of the calorimeter and in the material of the Muon System. The types of background that can produce hits in the CSC chambers are :

A) Electrons/Positrons or hadrons from the calorimeter.

B) Delta rays and Gamma conversions from the muon.

For 100 MeV gamma's produced by muon showering in copper only about 40% produced at a depth of 3.5cm escape the calorimeter. Thus only the last few cm's at the top of calorimeter are important in generating EM debris that escapes the calorimeter.

Of cource this becomes more important as the energy of the muon is is increased. At E(muon) = 700 GeV ionization loss = loss by bremsstrahlung.

A) In the barrel muon system (eta between 0.1 and 1.4) only about 10% of the background on the first superlayer originated from the calorimeter, while 50% of the background hits on the first superlayer of the endcap originated in the calorimeter.

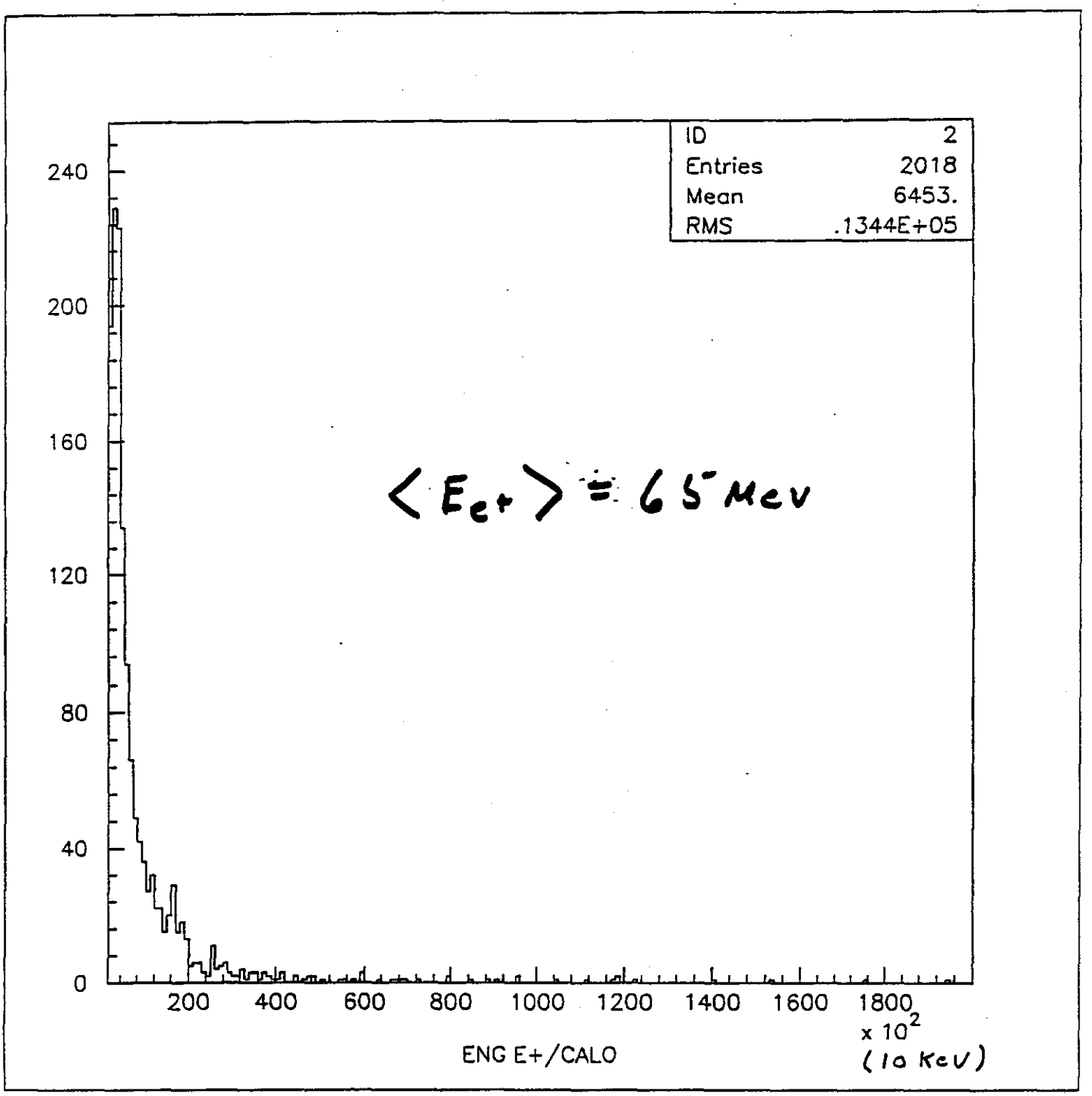
ID 2
Entries 2018
Mean 6453.
RMS .1344E+05
240
200
160
120
80
40
0
200
400
600
800
1000
1200
1400
1600
1800
x 10^2
(10 KeV)
ENG E+/CALO
<E_e+> ≐ 65 MeV

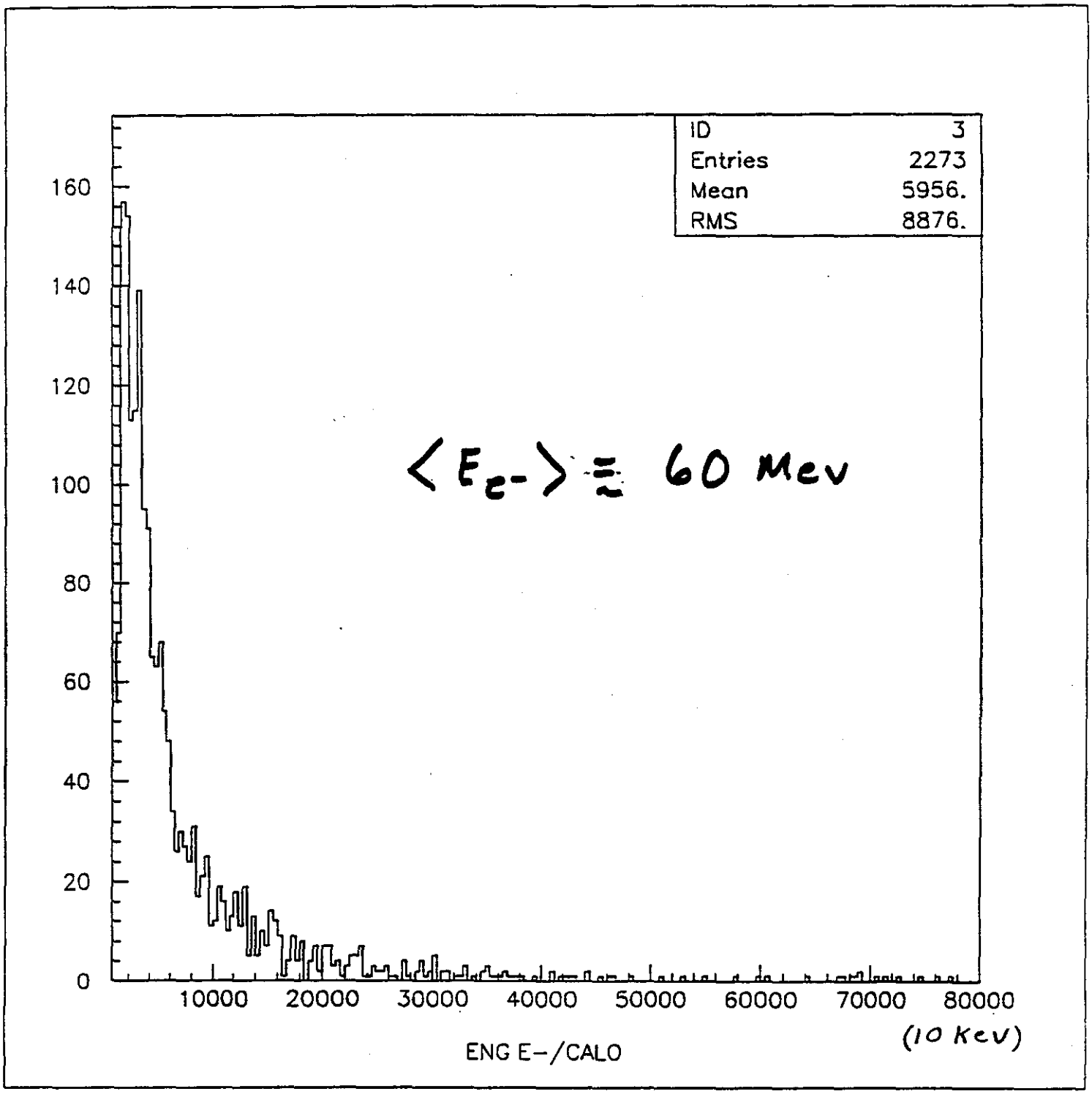
ID 3
Entries 2273
Mean 5956.
RMS 8876.
160
140
120
100
80
60
40
20
0
10000
20000
30000
40000
50000
60000
70000
80000
(10 KeV)
ENG E-/CALO
$\langle E_{e^-} \rangle \cong 60$ MeV

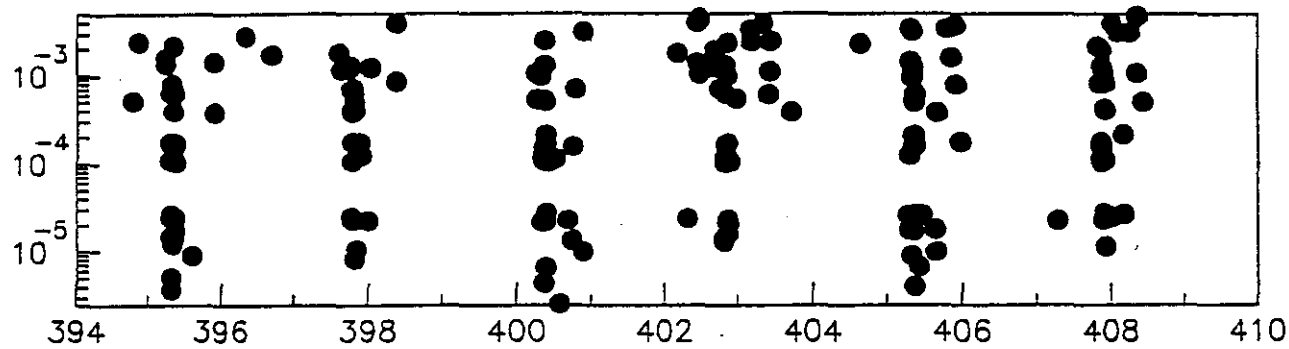

EH VS VERTICES OF ORG SL1

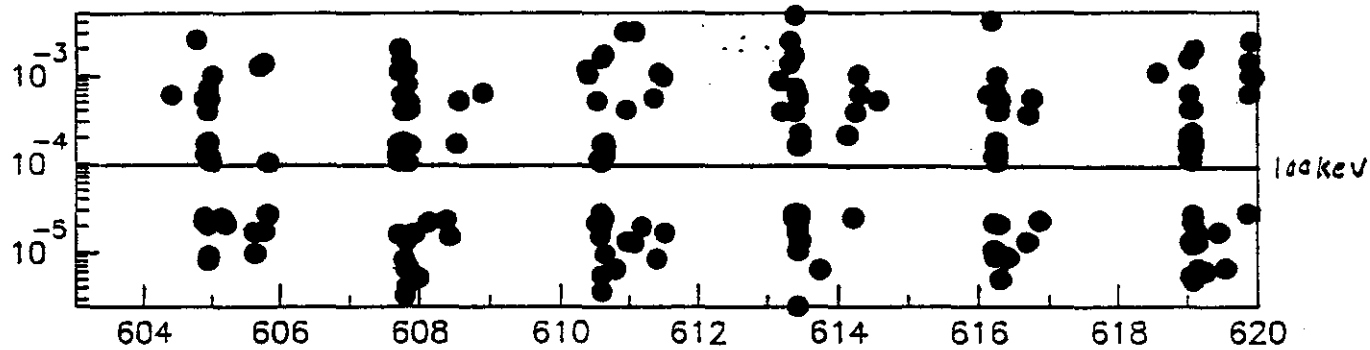

EH VS VERTICES OF ORG SL2

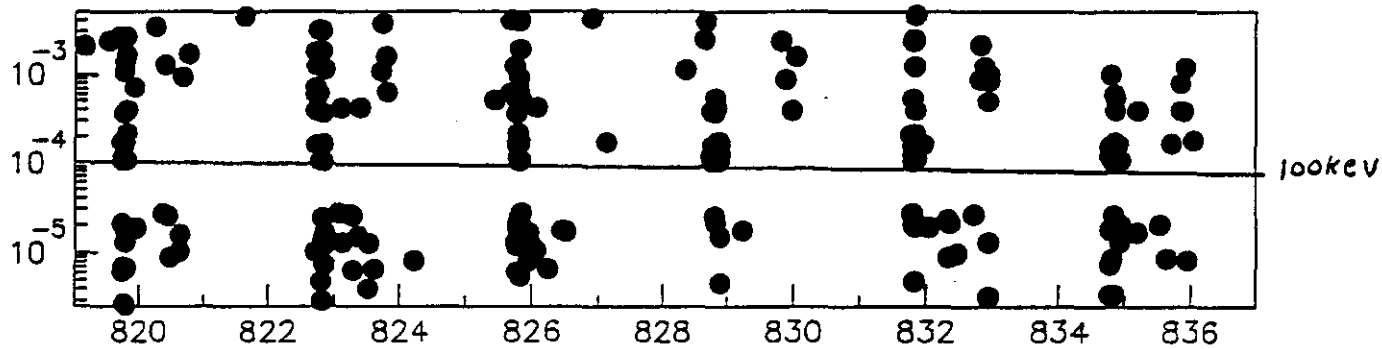

EH VS VERTICES OF ORG SL3

1 Tev G $\theta = 60°$

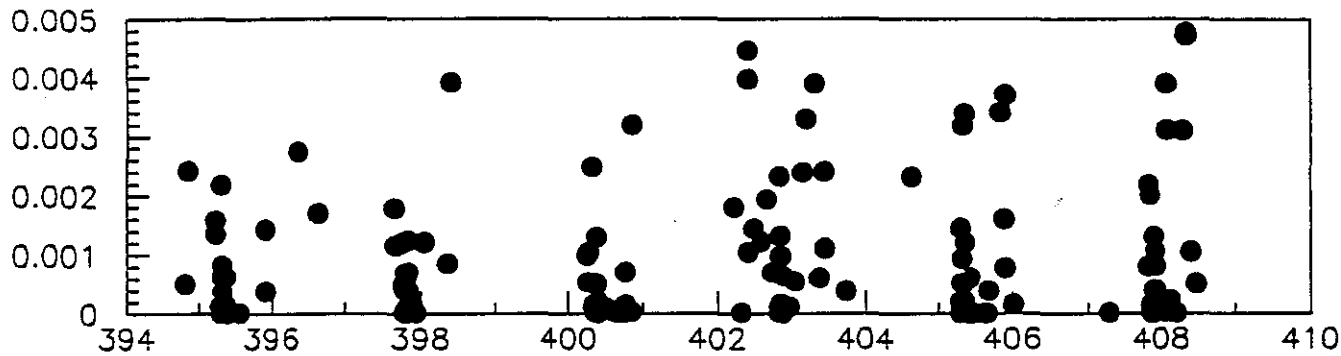

EH VS VERTICES OF ORG SL1

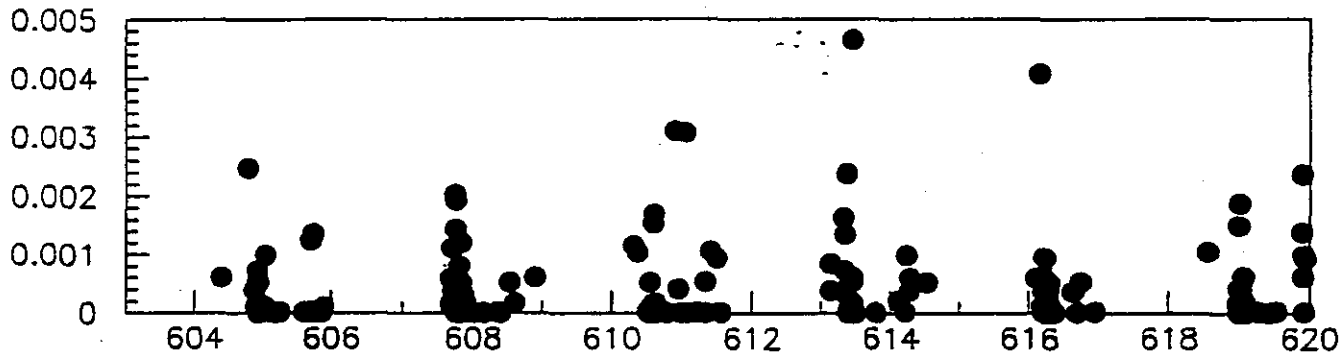

EH VS VERTICES OF ORG SL2

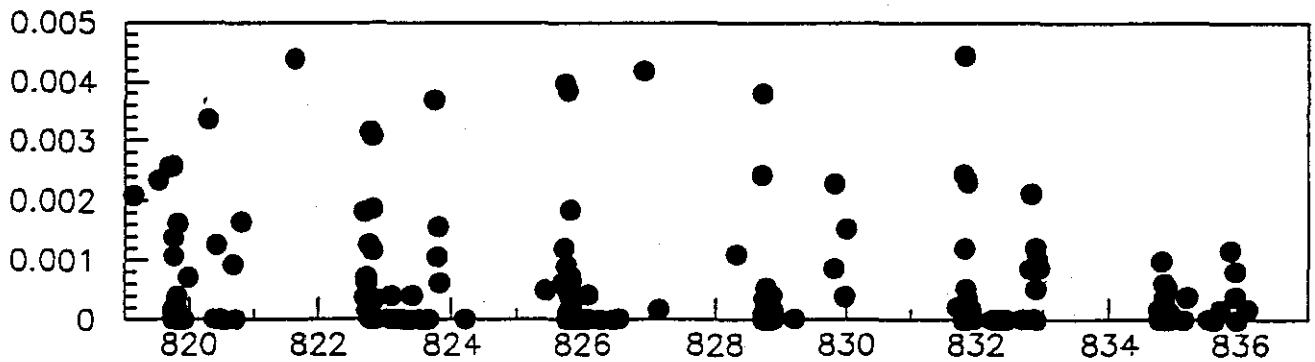

EH VS VERTICES OF ORG SL3

1 Tev G $\theta = 60°$

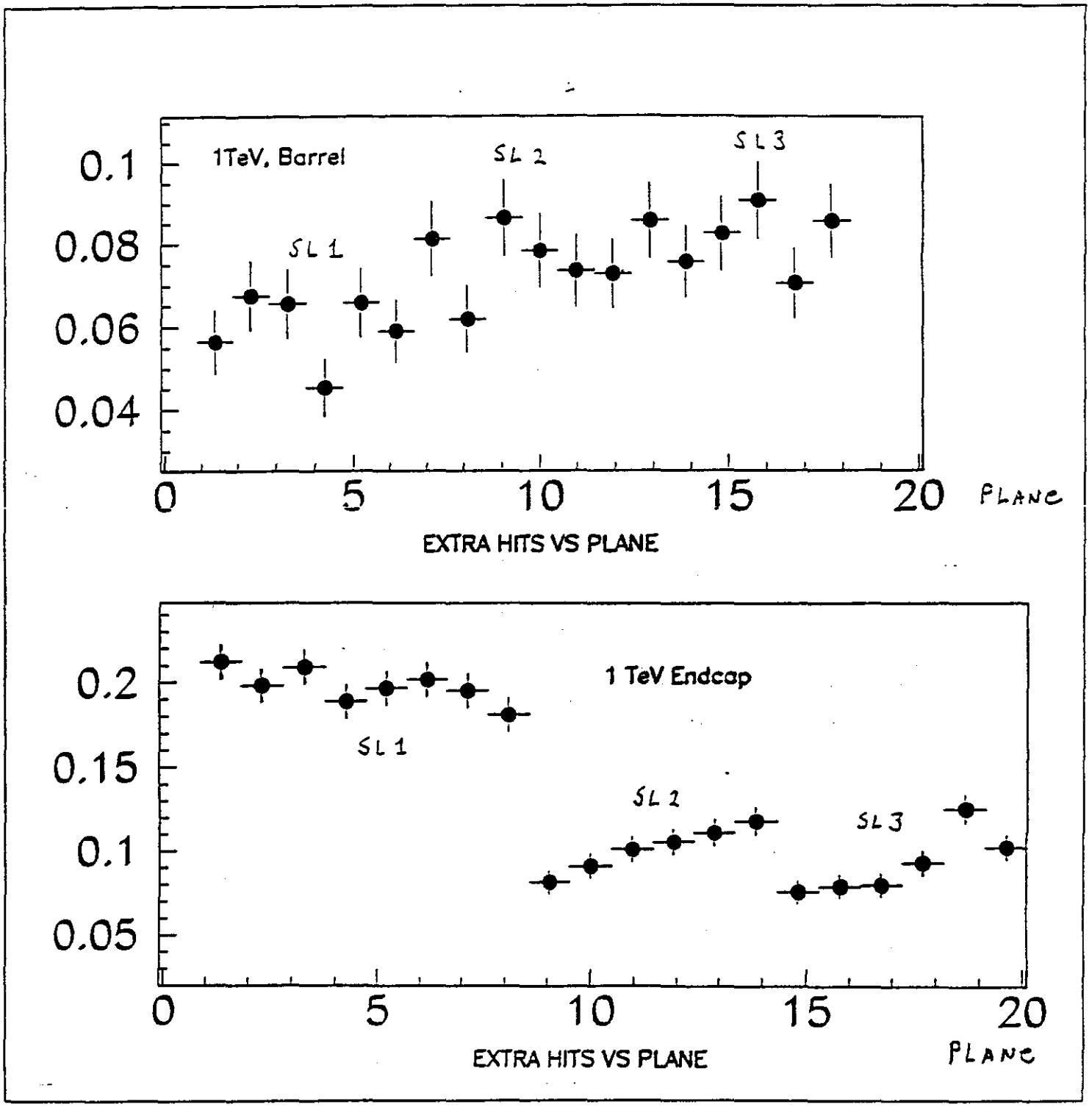

Figure 6) Occupancy of charged background within the "standard interval", as defined in the text, as a function of chamber in the barrel and endcap.

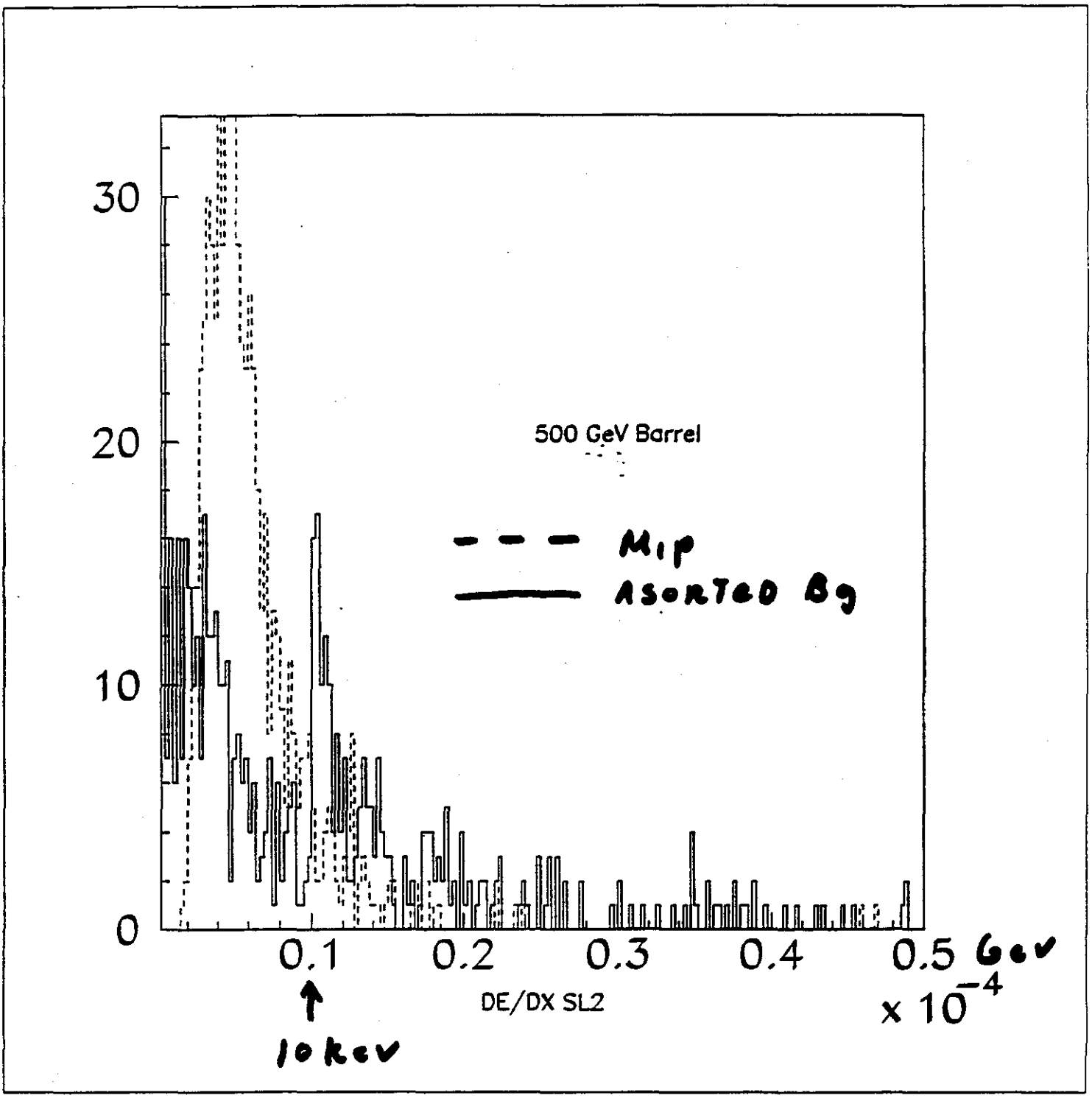
30
20
10
0
500 GeV Barrel
Mip
ASORTED Bg
0.1
0.2
0.3
0.4
0.5 GeV
DE/DX SL2
x 10^-4
10 keV

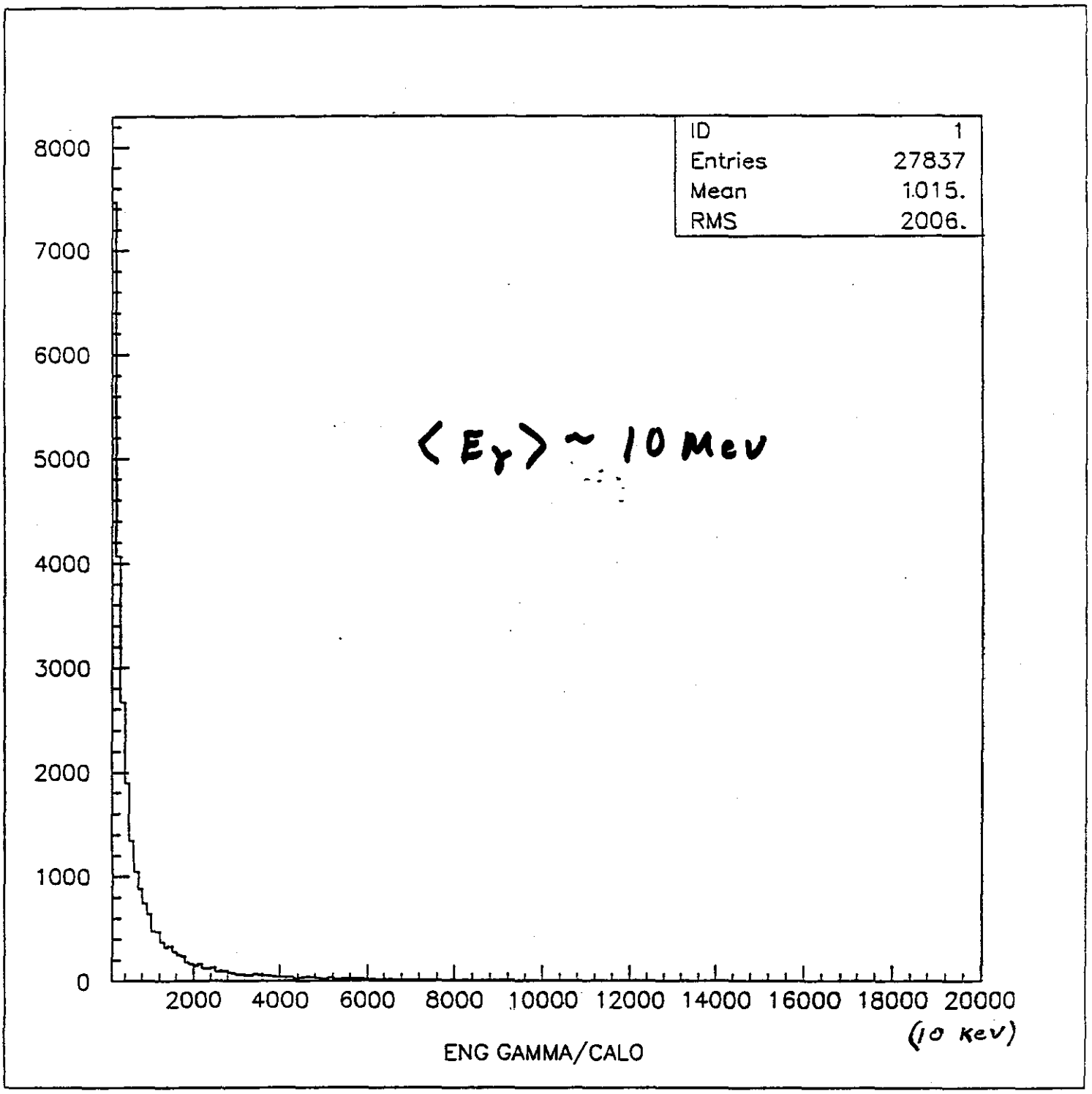
ID 1
Entries 27837
Mean 1015.
RMS 2006.
8000
7000
6000
5000
4000
3000
2000
1000
0
2000 4000 6000 8000 10000 12000 14000 16000 18000 20000
(10 KeV)
ENG GAMMA/CALO
⟨Eγ⟩ ~ 10 MeV

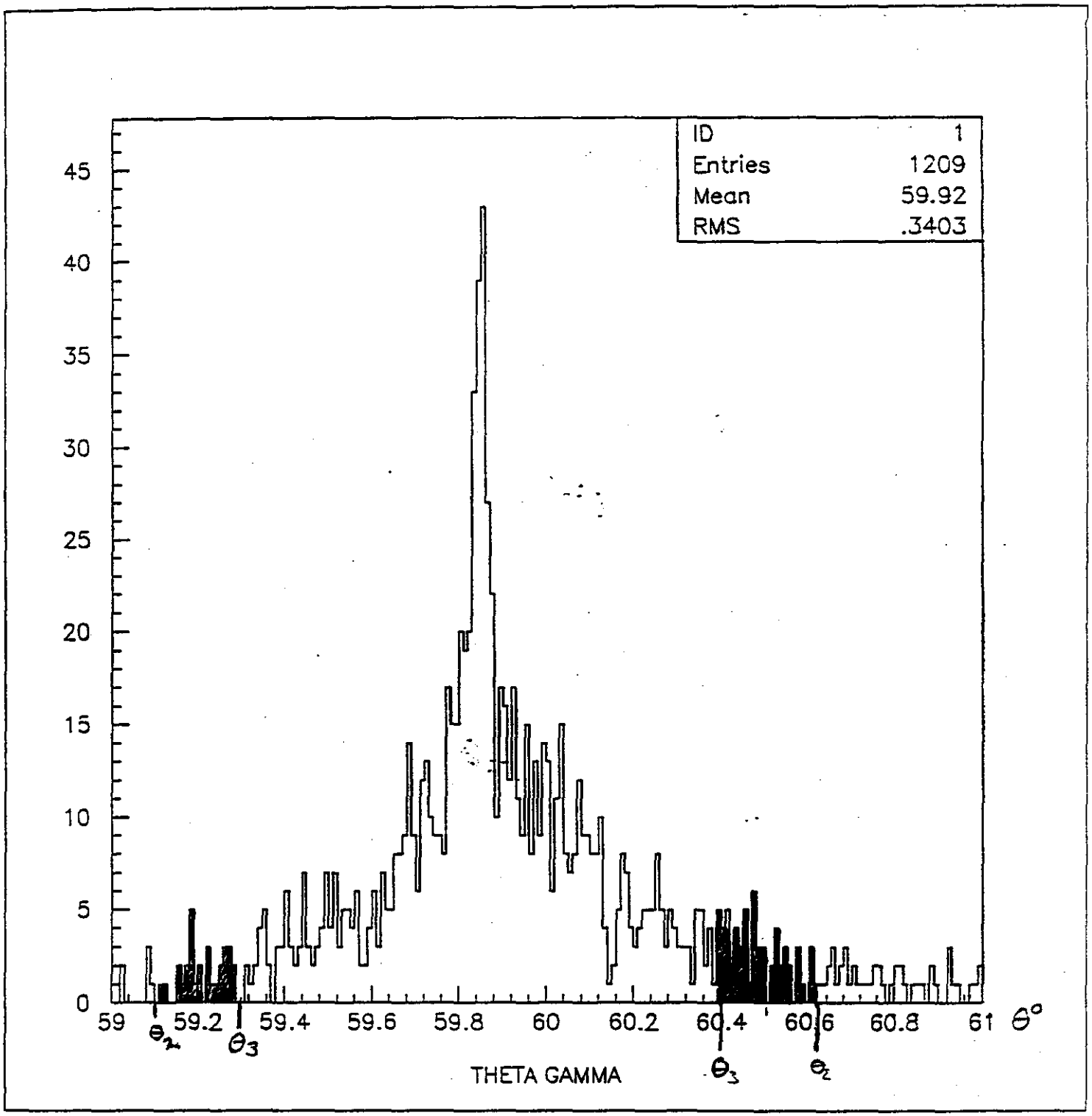

1 TeV μ @ θ = 60°

▨ = EXTRA γ's SEEN ON SL2 COMPARED TO SL3 FOR TWO PAD WIDTHS

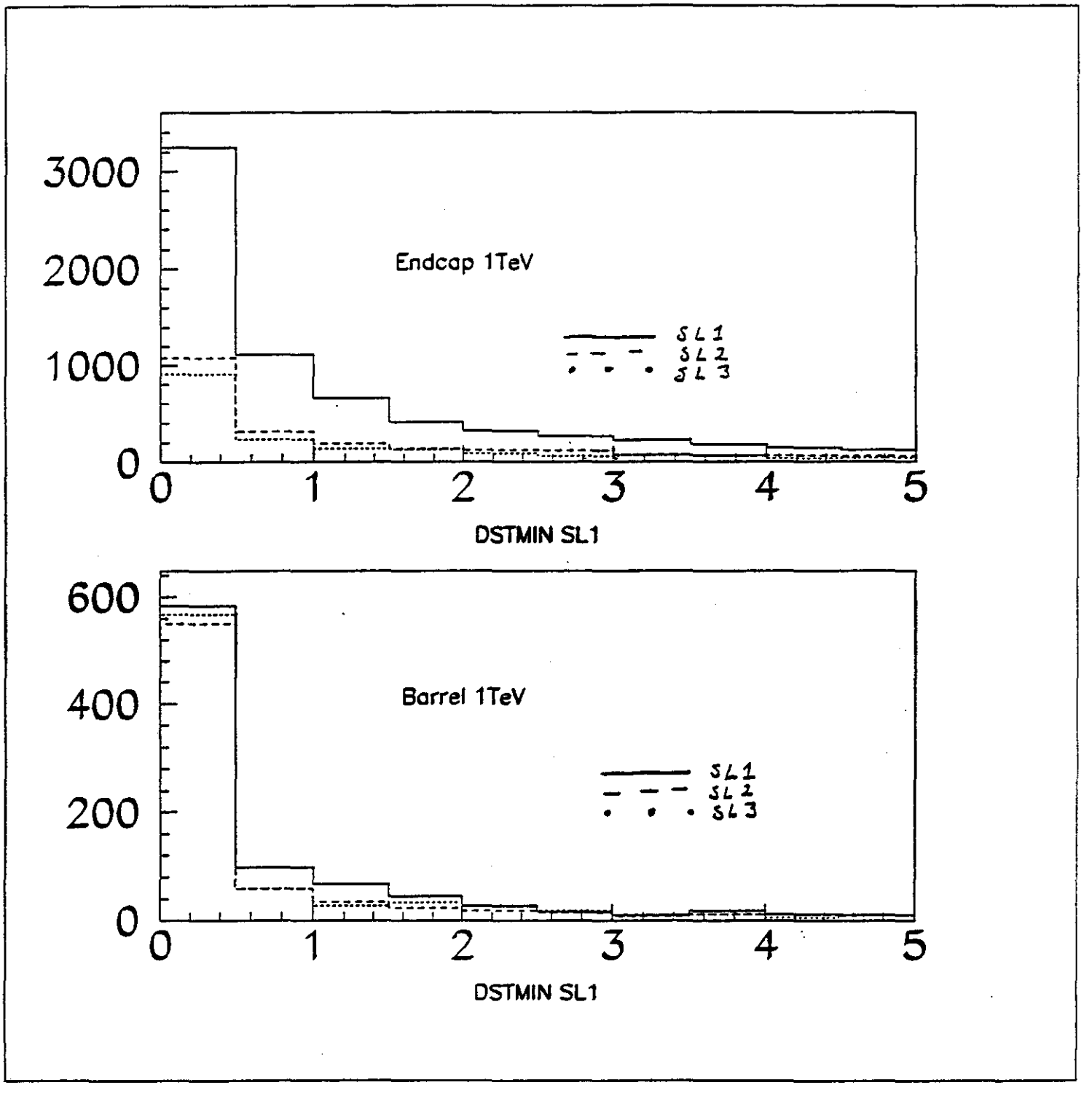
3000
2000
1000
0
Endcap 1TeV
SL1
SL2
SL3
0
1
2
3
4
5
DSTMIN SL1
600
400
200
0
Barrel 1TeV
SL1
SL2
SL3
0
1
2
3
4
5
DSTMIN SL1

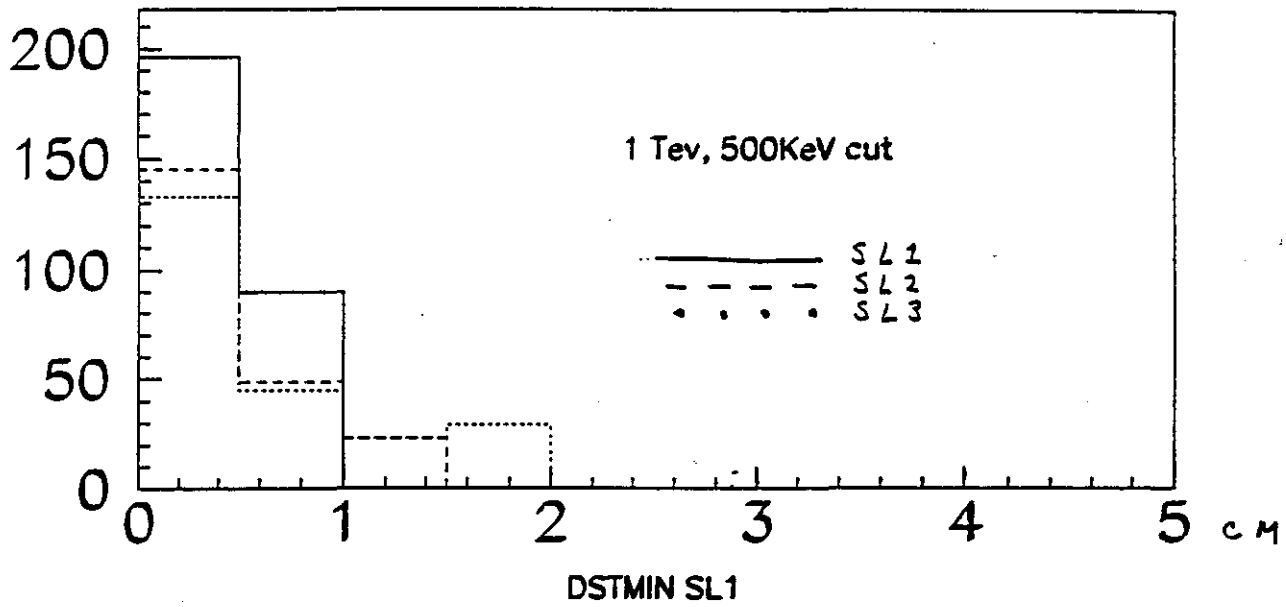
200
150
100
50
0
0
1
2
3
4
5
cm
1 Tev, 500KeV cut
SL1
SL2
SL3
DSTMIN SL1

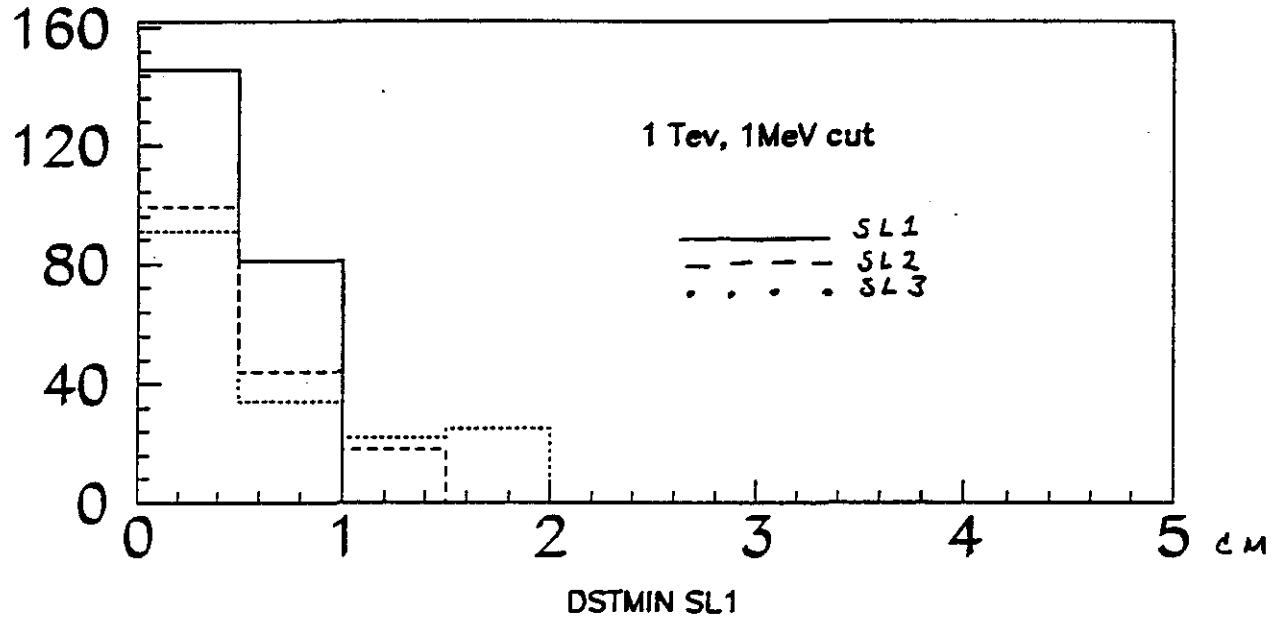
160
120
80
40
0
0
1
2
3
4
5
cm
1 Tev, 1MeV cut
SL1
SL2
SL3
DSTMIN SL1

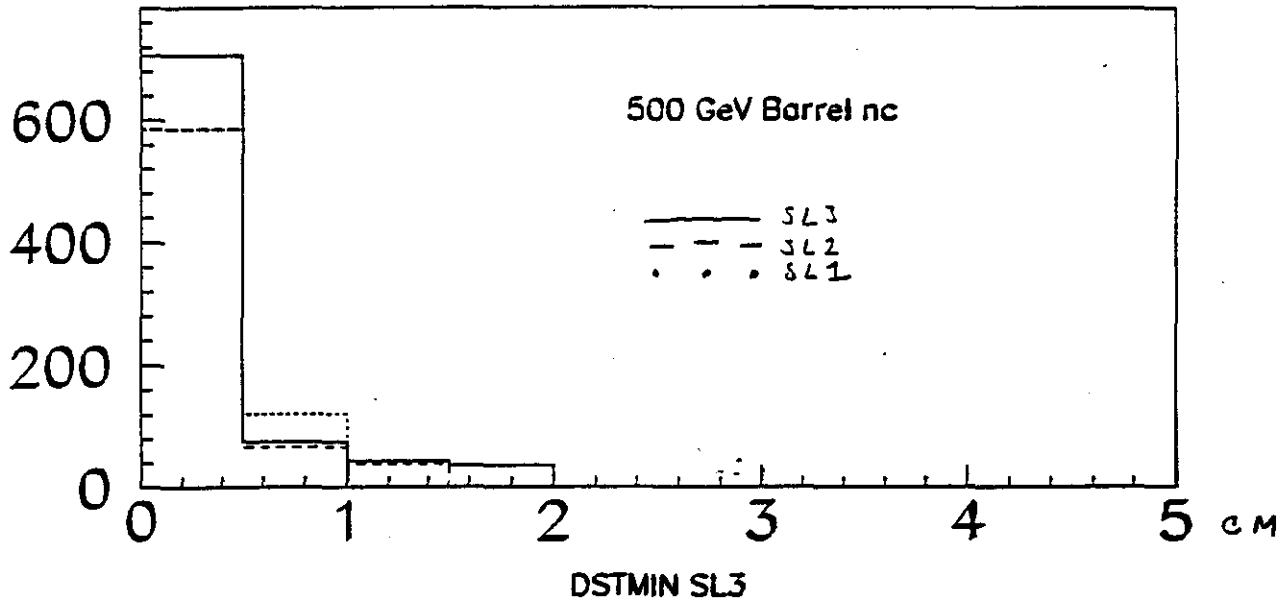
500 GeV Barrel nc
SL3
SL2
SL1
600
400
200
0
0
1
2
3
4
5
cm
DSTMIN SL3

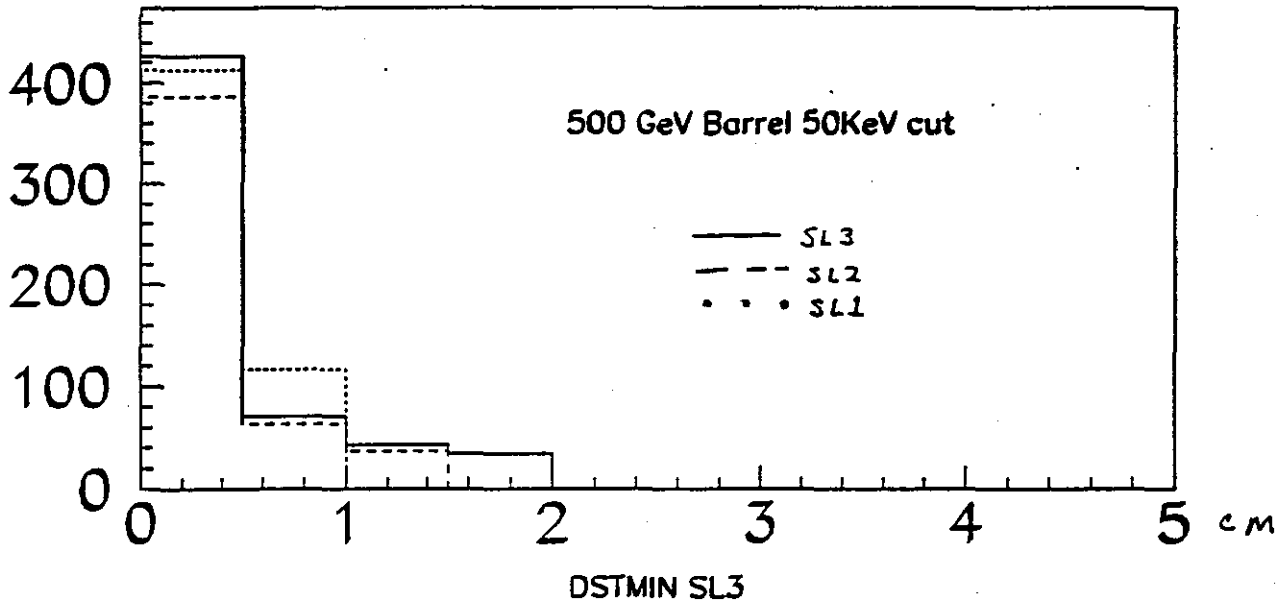
500 GeV Barrel 50KeV cut
SL3
SL2
SL1
400
300
200
100
0
0
1
2
3
4
5
cm
DSTMIN SL3

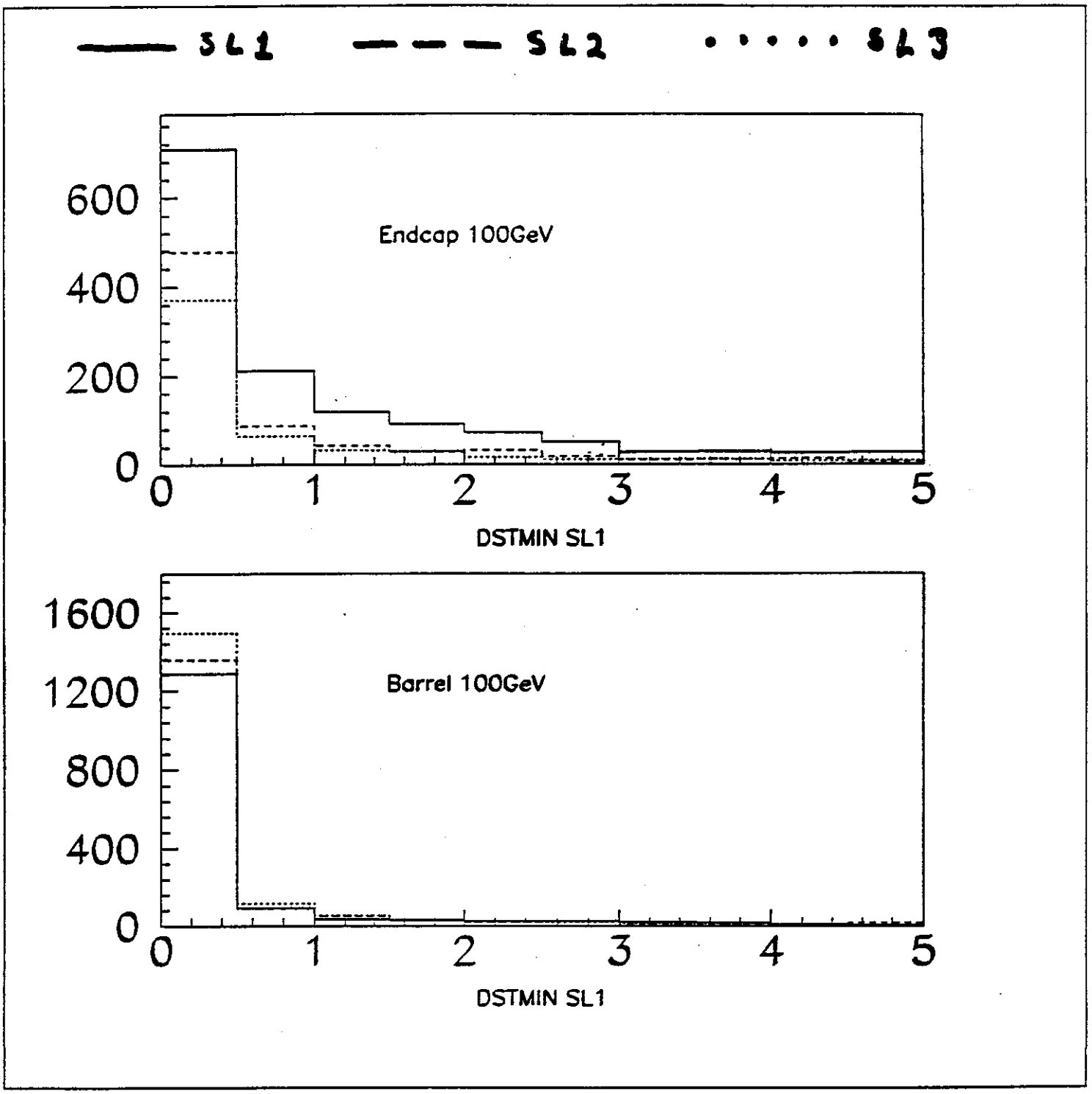
SL1
SL2
SL3
600
400
200
0
Endcap 100GeV
0
1
2
3
4
5
DSTMIN SL1
1600
1200
800
400
0
Barrel 100GeV
0
1
2
3
4
5
DSTMIN SL1

B) For gamma conversions, the gamma direction tends to be close to the muon:

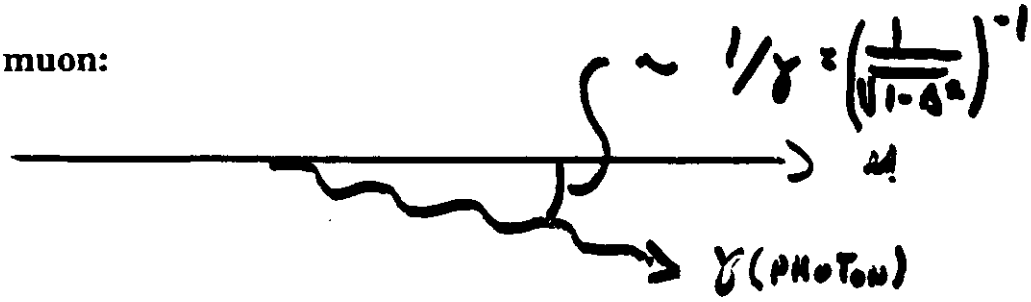

Taking this into consideration and photon attenuation length in 0.5X0 of G10, we expect about 70% of the 10 MeV photons available for conversion on SL2 to be available on SL3.

We find 60%+/- 20% for the 1 TeV sample at theta=60.

A large amount of the charged background close to the muon is soft and produced in the gas of the CSC chambers.

A 500 KeV cut on background associated with the 1TeV sample shows a 66% reduction in the population of background within 0.5 cm of the muon while for the region between 0.5 and 1.0cm it was 10%. For a 1MeV cut it was 75% and 20%.

Table 1, Compromised Plane Distributions

Detector	Barrel			Endcap		
Superlayer	1	2	3	1	2	3
Plane	Compromised Plane Probability, 100 GeV.					
0	0.689	0.654	0.606	0.597	0.704	0.737
1	0.930	0.909	0.880	0.819	0.899	0.91
2	0.988	0.981	0.992	0.912	0.961	0.966
3	0.998	0.997	0.998	0.948	0.979	0.982
4	0.998	0.999	0.999	0.964	0.989	0.988
5	1.0	0.999	1.0	0.977	0.994	0.994
6	1.0	1.0	1.0	0.984	1.0	1.0
7	-	-	-	0.989	-	-
8	-	-	-	1.0	-	-

Detector	Barrel			Endcap		
Superlayer	1	2	3	1	2	3
Plane	Compromised Plane Probability, 500 GeV.					
0	0.642	0.565	0.540	0.528	0.670	0.70
1	0.917	0.919	0.882	0.749	0.893	0.91
2	0.968	0.984	0.974	0.832	0.948	0.955
3	0.986	0.994	0.993	0.874	0.973	0.974
4	0.992	0.996	0.996	0.906	0.984	0.978
5	0.995	0.999	0.996	0.932	0.991	0.989
6	1.0	1.0	1.0	0.949	1.0	1.0
7	-	-	-	0.963	-	-
8	-	-	-	1.0	-	-

Detector	Barrel			Endcap		
Superlayer	1	2	3	1	2	3
Plane	Compromised Plane Probability, 1000 GeV.					
0	0.624	0.564	0.542	0.521	0.657	0.693
1	0.871	0.866	0.859	0.705	0.867	0.883
2	0.953	0.963	0.960	0.781	0.939	0.939
3	0.976	0.989	0.986	0.821	0.965	0.964
4	0.986	0.994	0.994	0.858	0.974	0.980
5	0.993	0.997	1.0	0.886	0.987	0.987
6	1.0	1.0	1.0	0.910	1.0	1.0
7	-	-	-	0.928	-	-
8	-	-	-	1.0	-	-

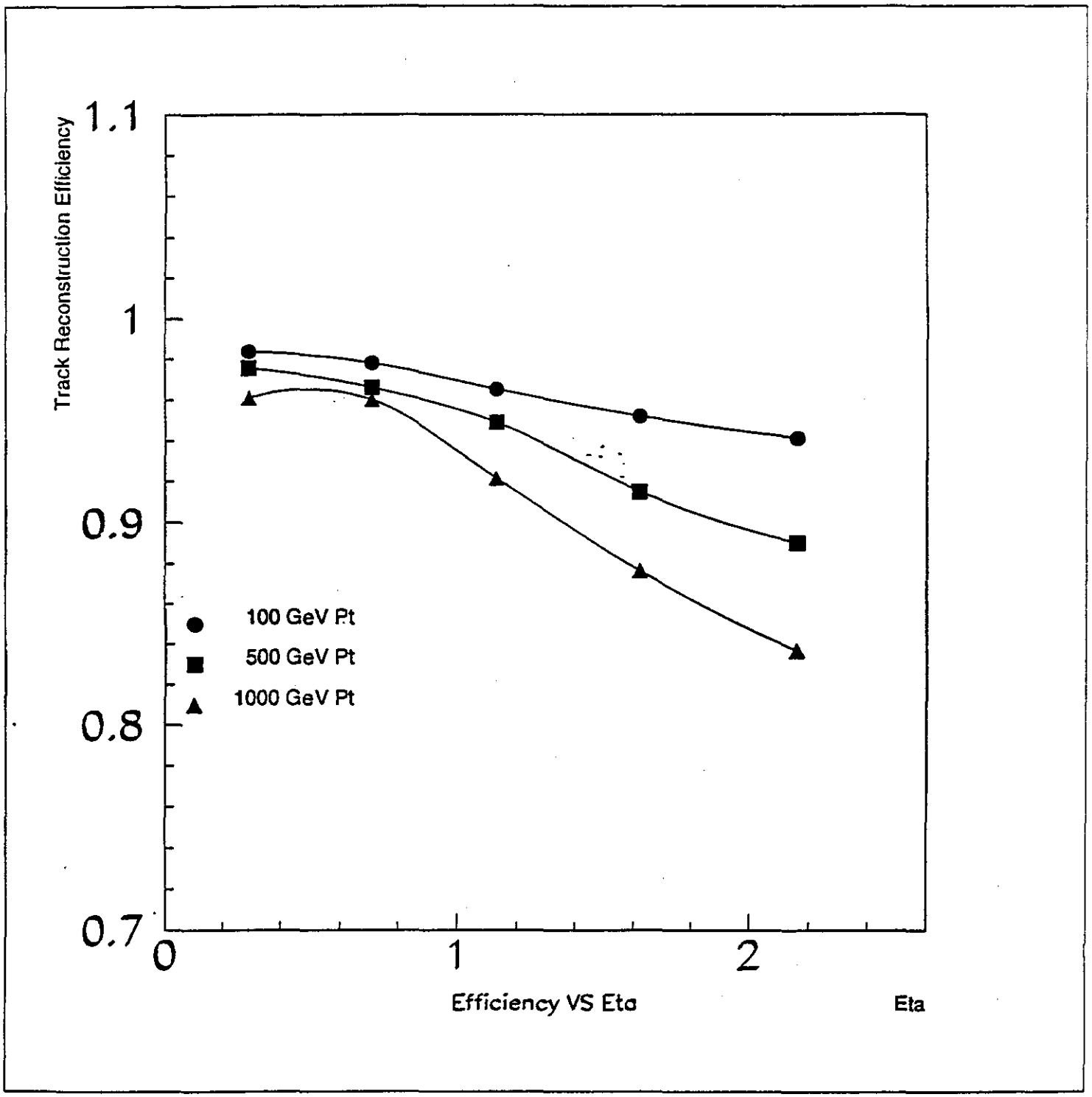
Track Reconstruction Efficiency
1.1
1
0.9
0.8
0.7
0
1
2
100 GeV Pt
500 GeV Pt
1000 GeV Pt
Efficiency VS Eta
Eta

We will define a "standard interval" which will define our ability to reconstuct tracks in the presence of charged background.

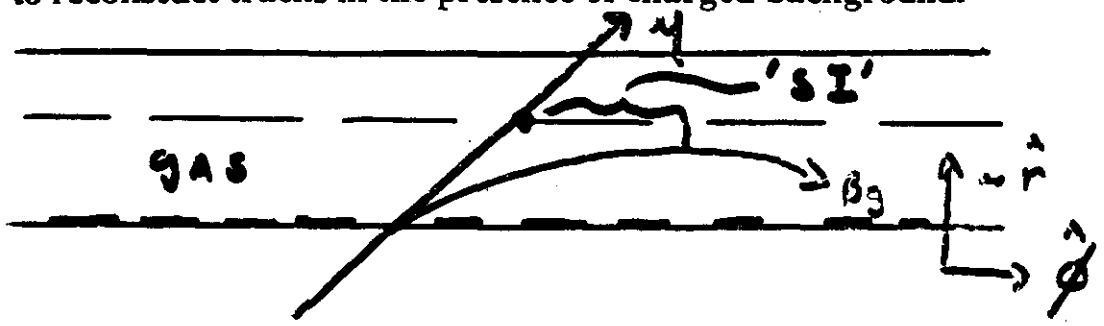

SI => 0.02cm < Δ < 2 Strip-widths, this definition is consistent with the measured resolution of a charged track in the CSC chambers in the presence of another charged particle.

We will consider two senarios:

A) At least 3 "good hits" per superlayers constitutes a track segment. We require 3 "good segments" per track to to count as a reconstructed track.

B) We use a track "cluster-merge" reconsturction program (JCW, GEM TN-93-416) to find tracks, with the criterion that there be;

1) At least 3 good hits per superlayer

2) At least 4 good hits on SL3 and at least 2 good hits on SL1 and SL2.

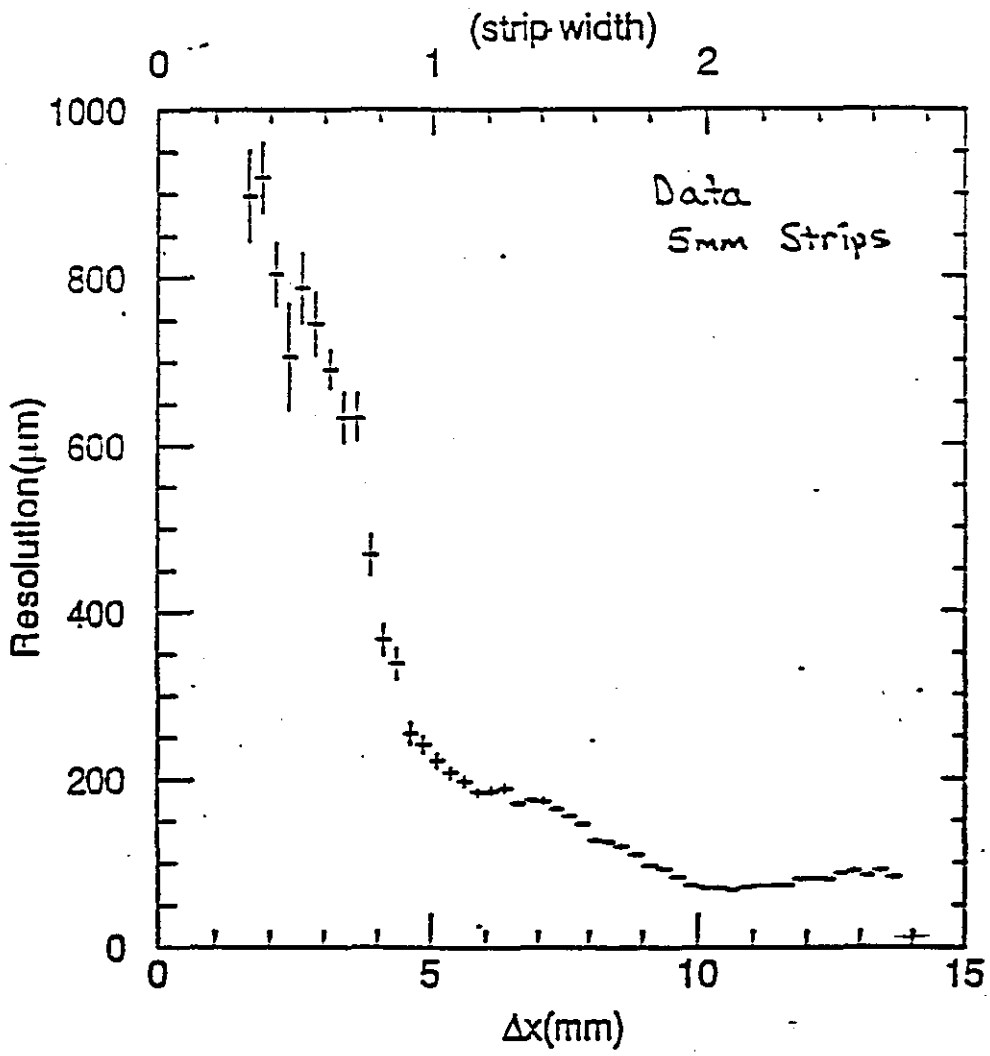

Figure 19) Chamber resolution of a charged hit in the presence of another charged hit as a function of the distance between the two hits, defined as the "Two Track Resolution" in the text.

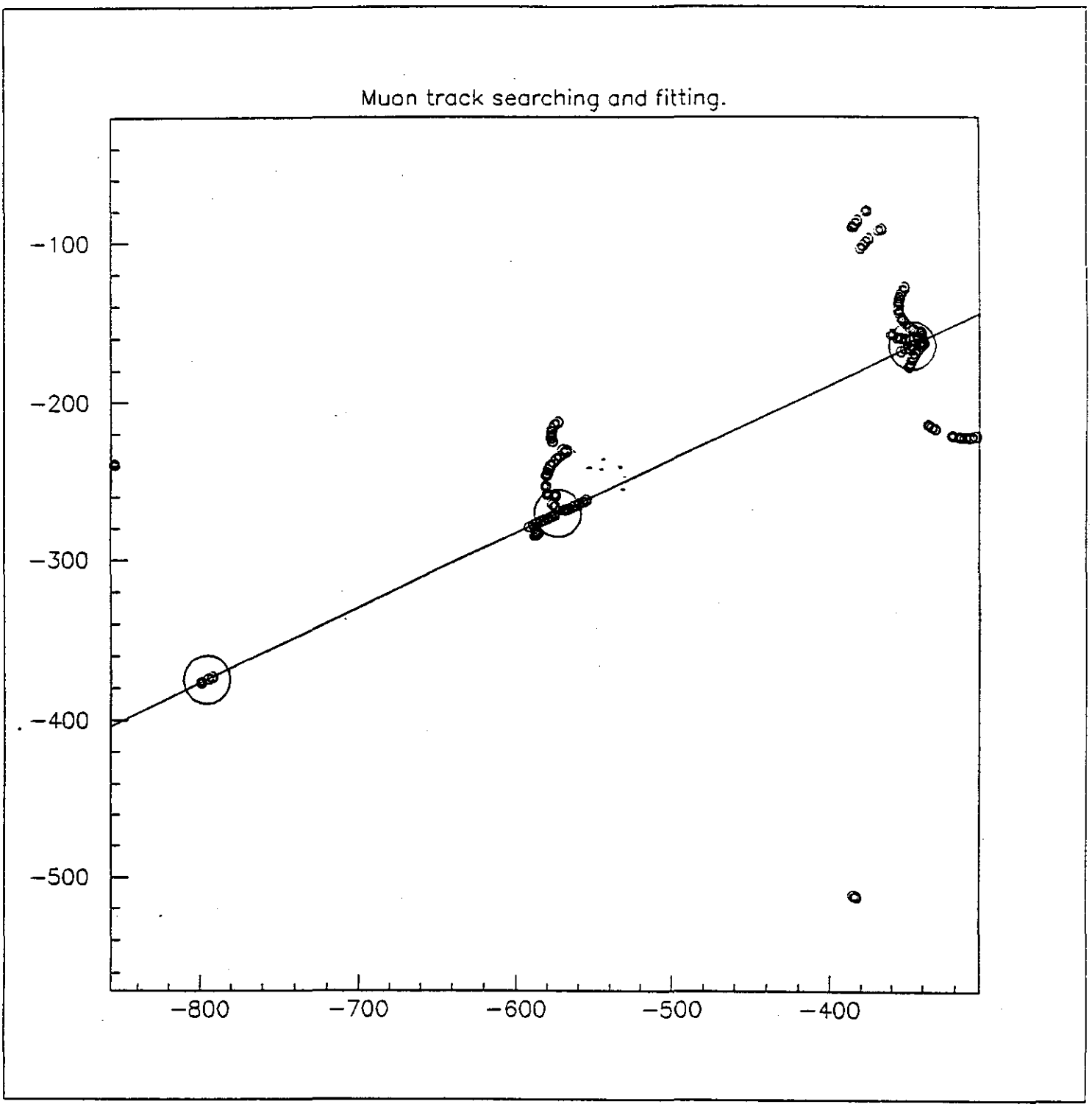
Muon track searching and fitting.
-100
-200
-300
-400
-500
-800
-700
-600
-500
-400

JCW

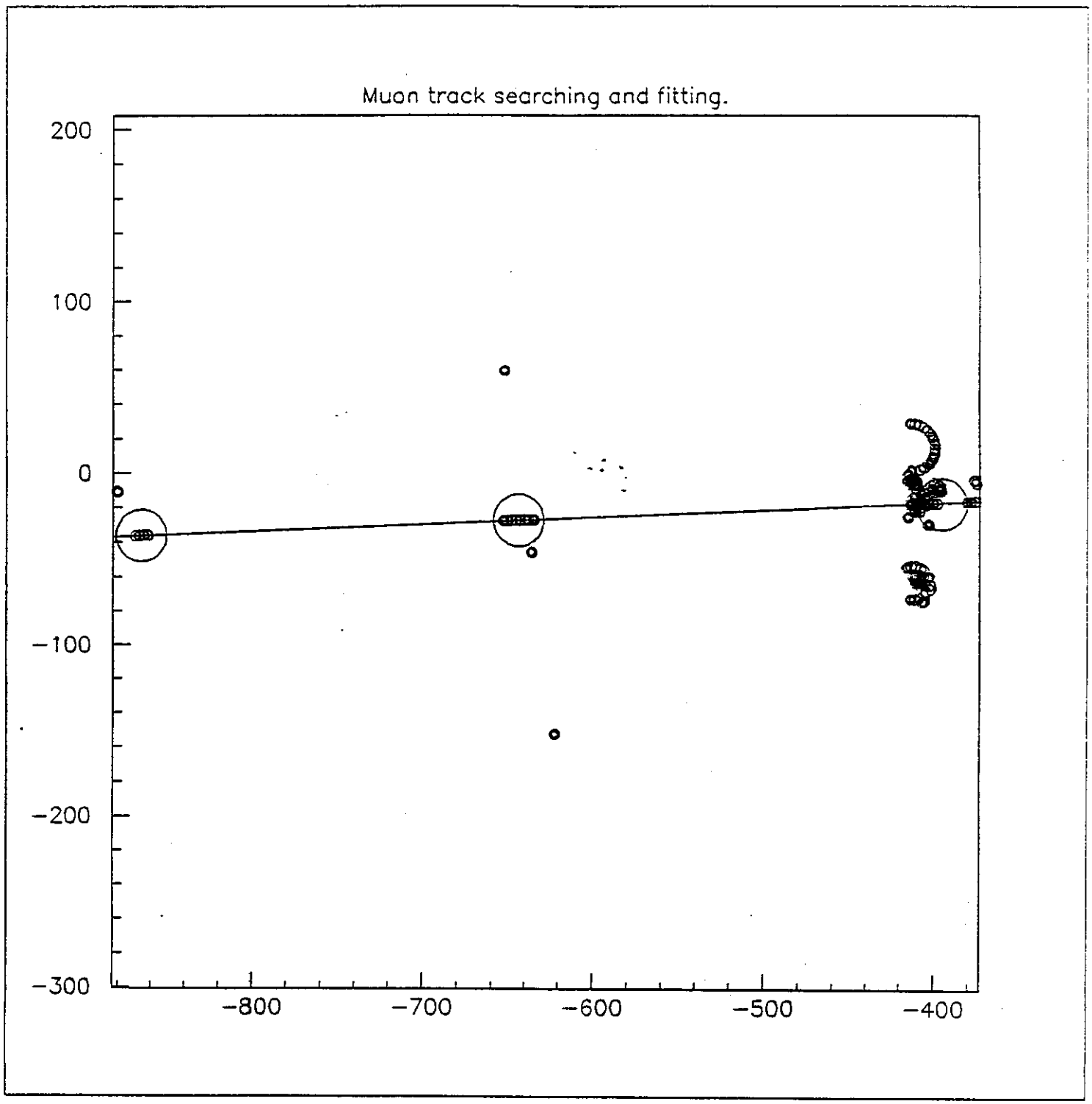
Muon track searching and fitting.
200
100
0
−100
−200
−300
−800
−700
−600
−500
−400

JCW

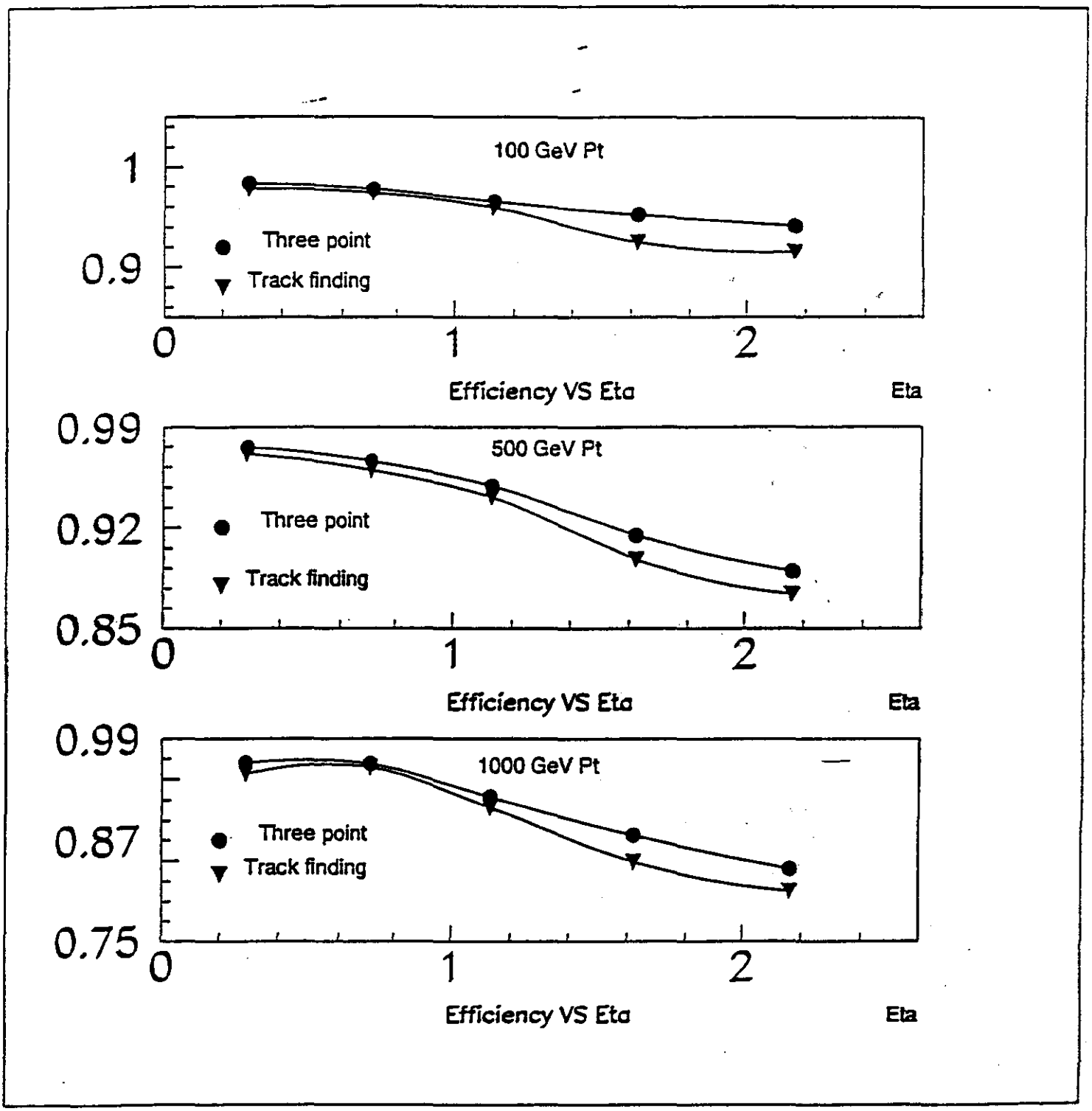

Figure 10) Comparison of the track finding efficiency using the "three good hits" method and the cluster search-merge algorithm discribed in the text. The comparison is made by using a preselected data set where three "good" hits had already been found, thus showing the inefficiency of the cluster-algorithm. The cluster algorithm is shown to be very efficient .

Track Reconstruction Efficiency

100 GeV P_t Isolated muons.			
η	3 good	T.F. (senario 1)	T.F. (senario 1+2)
0.08-0.5	0.9836	0.9779	0.9866
0.5-0.92	0.978	0.974	0.9846
0.92-1.34	0.965	0.959	0.9714
1.38-1.86	0.952	0.925	0.9598
1.86-2.46	0.9412	0.915	0.9594

500 GeV P_t Isolated muons.			
η	3 good	T.F. (senario 1)	T.F. (senario 1+2)
0.08-0.5	0.9757	0.971	0.9807
0.5-0.92	0.966	0.9598	0.9683
0.92-1.34	0.9488	0.941	0.9547
1.38-1.86	0.9148	0.898	0.9415
1.86-2.46	0.89	0.874	0.9215

1000 GeV P_t Isolated muons.			
η	3 good	T.F. (senario 1)	T.F. (senario 1+2)
0.08-0.5	0.9581	0.948	0.9714
0.5-0.92	0.9643	0.956	0.9648
0.92-1.34	0.9212	0.909	0.9488
1.38-1.86	0.8764	0.845	0.8935
1.86-2.46	0.8367	0.81	0.8475

SENARIO 1 ≡ 3 "GOOD HITS" / SL

SENARIO 2 ≡ $(\geq 2, \geq 2, \geq 4)$
SL1 SL2 SL3

OCCURENCE OF FAKE TRACK FOR 10 GeV ROAD IS 10 TIME GREATER FOR (3,3,3) AS FOR (2,2,4)

MUONS IN b JETS

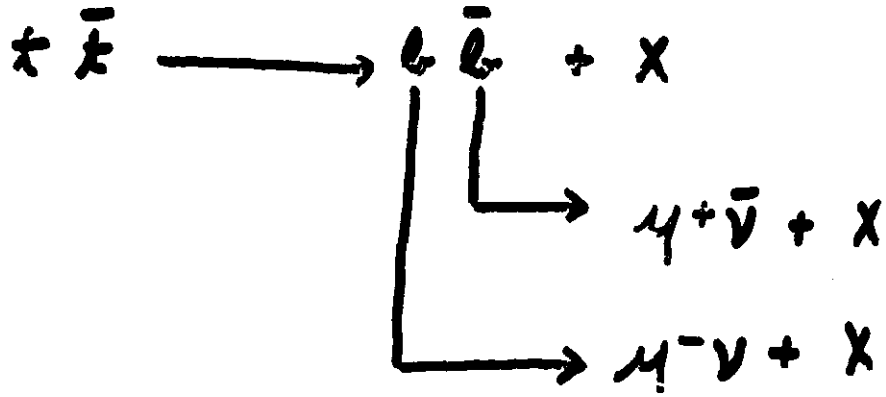

Where the mass of the top was set to 250 GeV . Since the muon is is typically close to the jet axis for b jets, this is a good enviroment to look at noisy, relatively low energy , muons. A cone in eta and phi is made around the muon and all generated particles in that cone with Pt > 3 GeV are passed to the simulation with very low cuts (10 KeV).

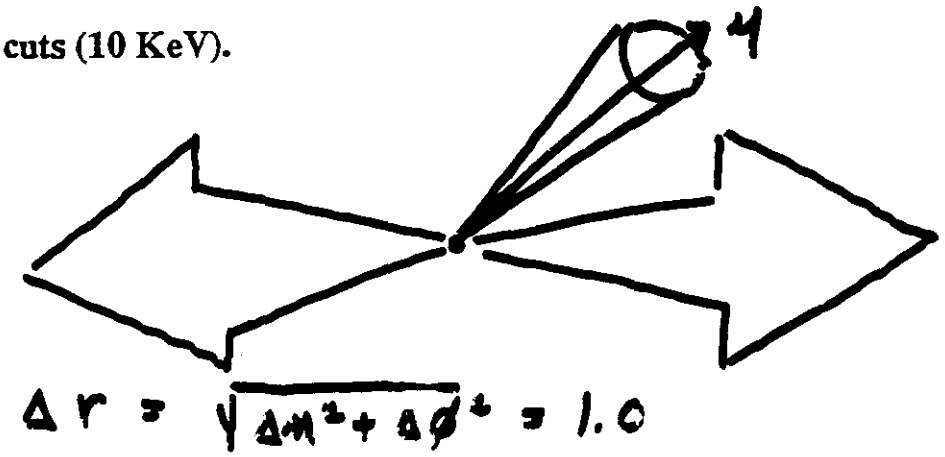

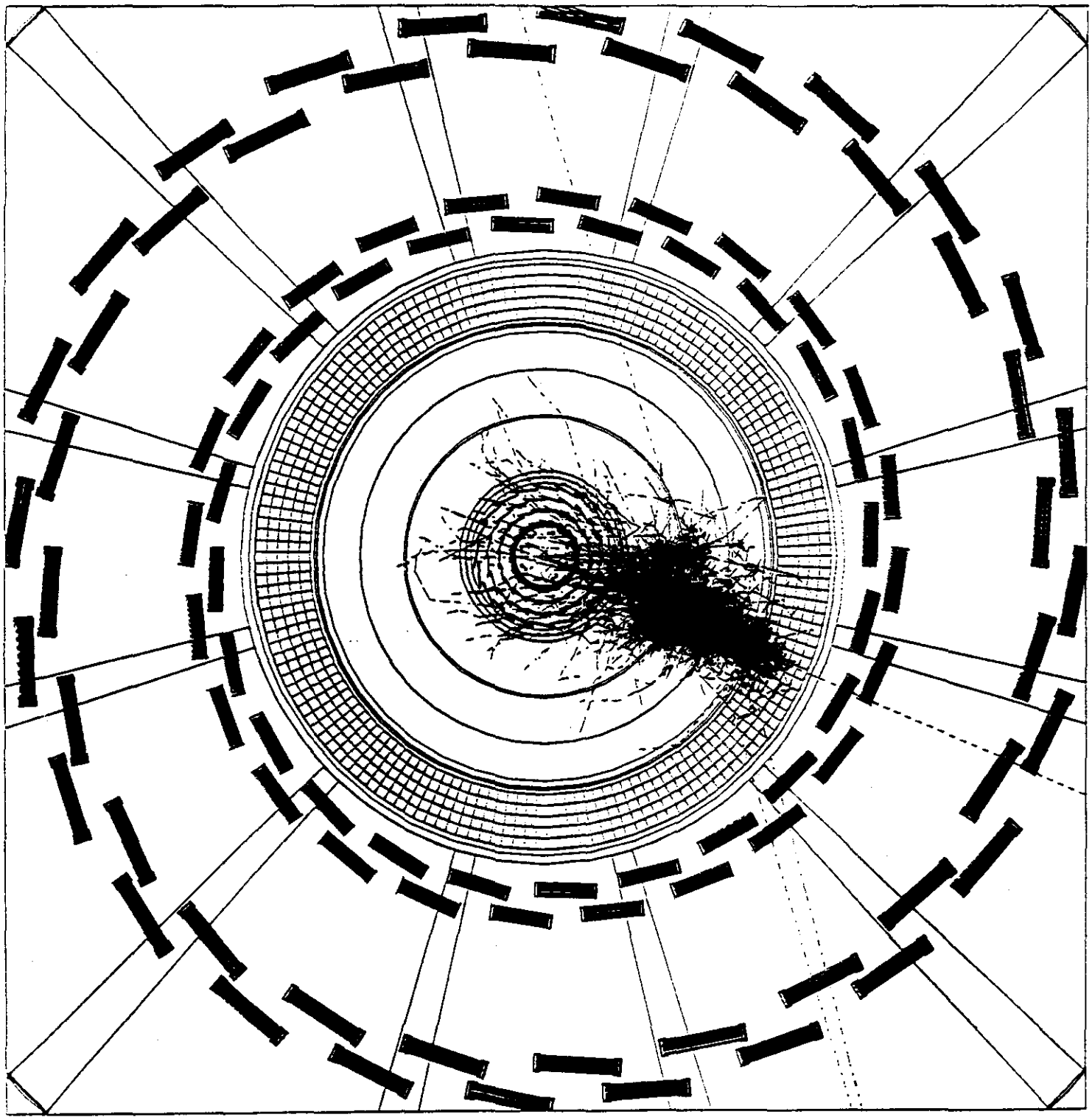

500 GeV μ WITH AN
800 GeV π IN THE CONE
AROUND μ

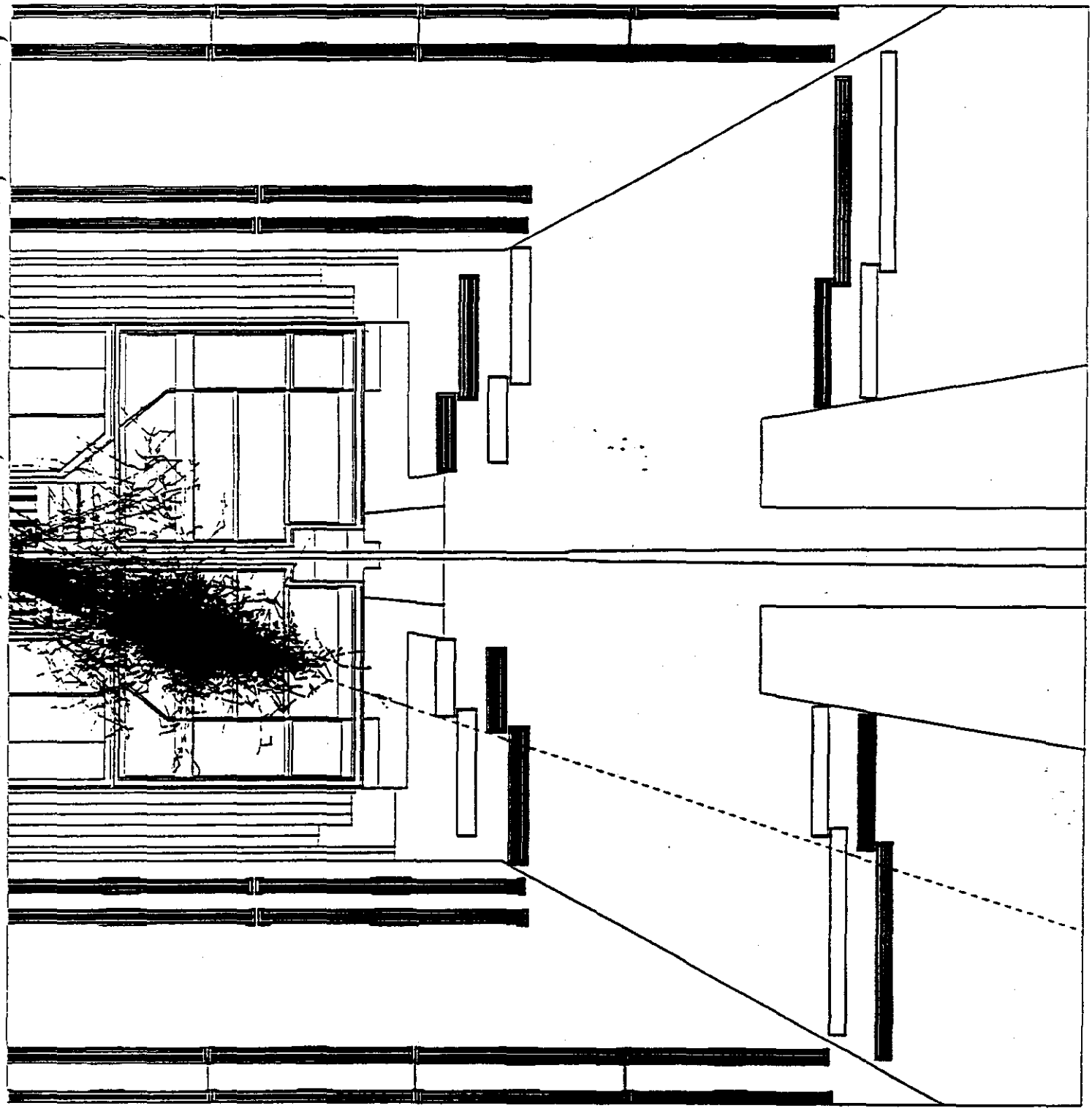

135 GeV μ WITH 745 GeV π^+ IN
THE CONE ($C = \sqrt{\Delta\eta^2 + \Delta\phi^2} = 1.0$) AROUND μ

$t\bar{t} \longrightarrow b\bar{b} \longrightarrow \bar{u}, \bar{c} + \mu^+\nu$
$\quad\quad\quad

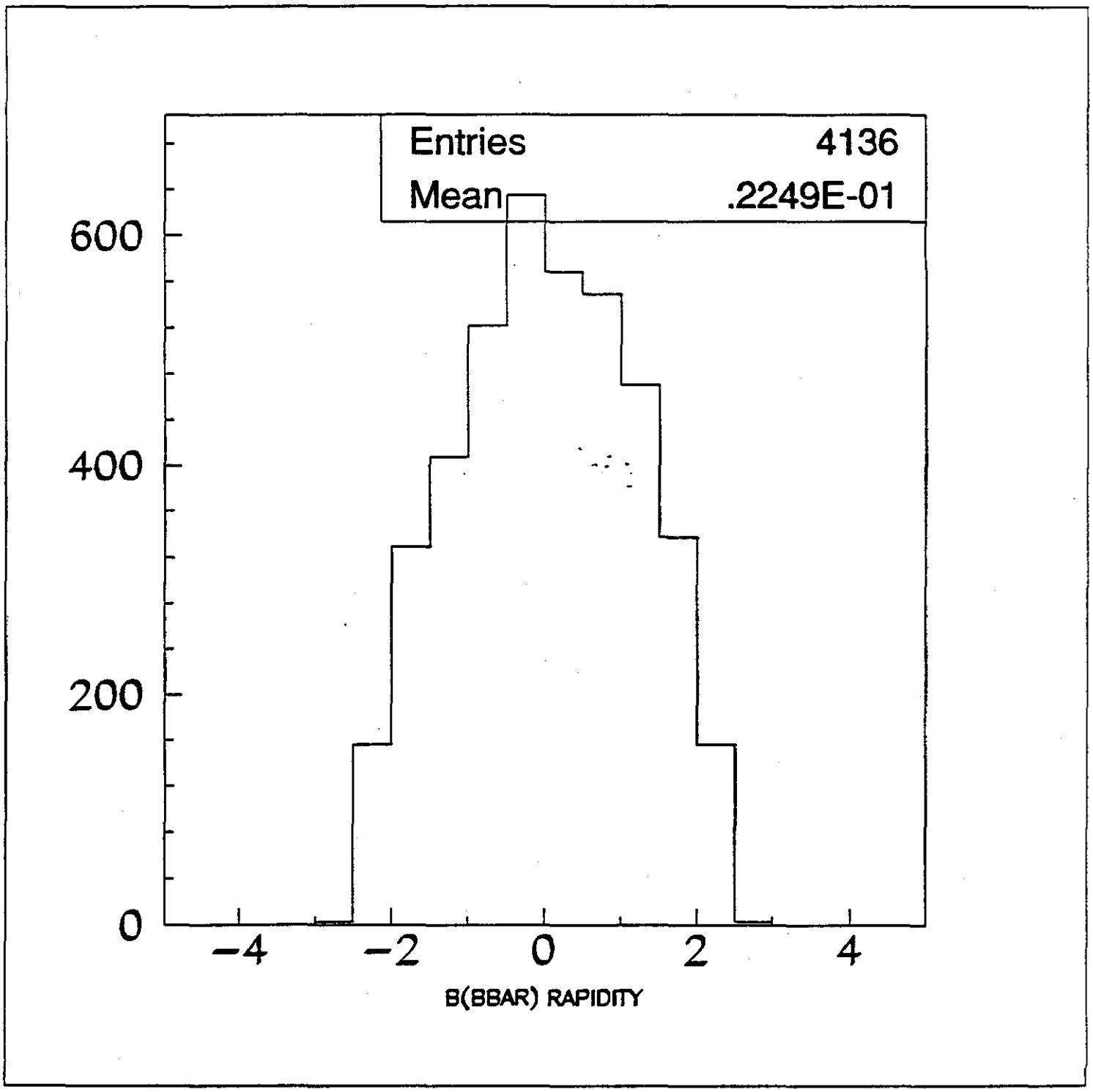
Entries 4136
Mean .2249E-01
600
400
200
0
−4
−2
0
2
4
B(BBAR) RAPIDITY

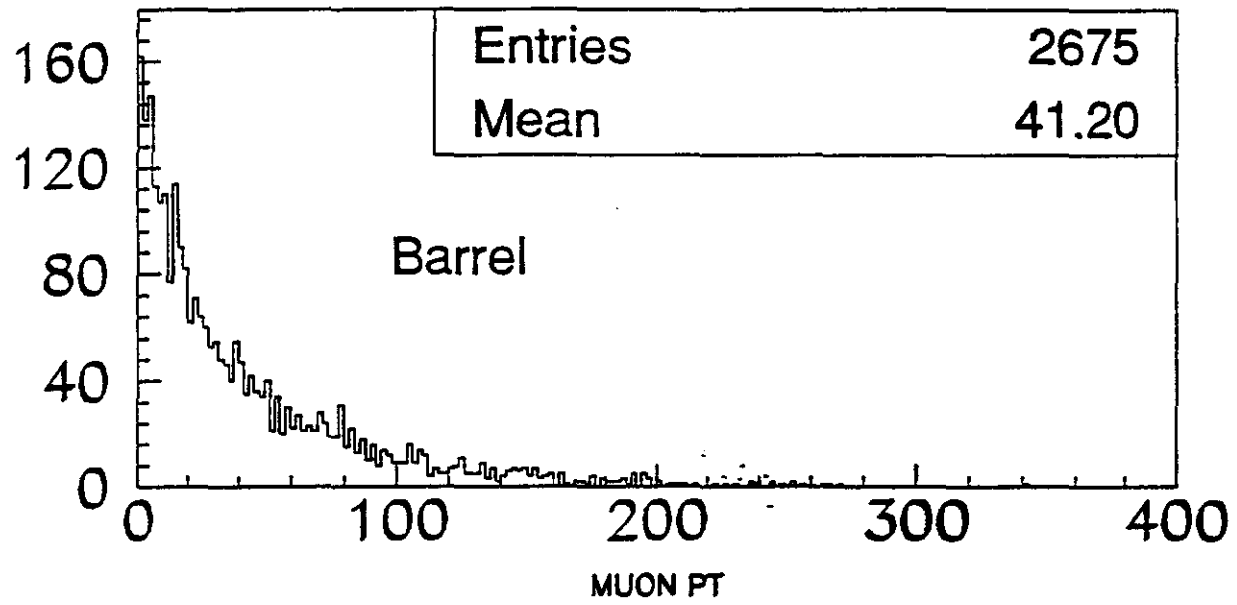
Entries 2675
Mean 41.20
Barrel
160
120
80
40
0
0
100
200
300
400
MUON PT

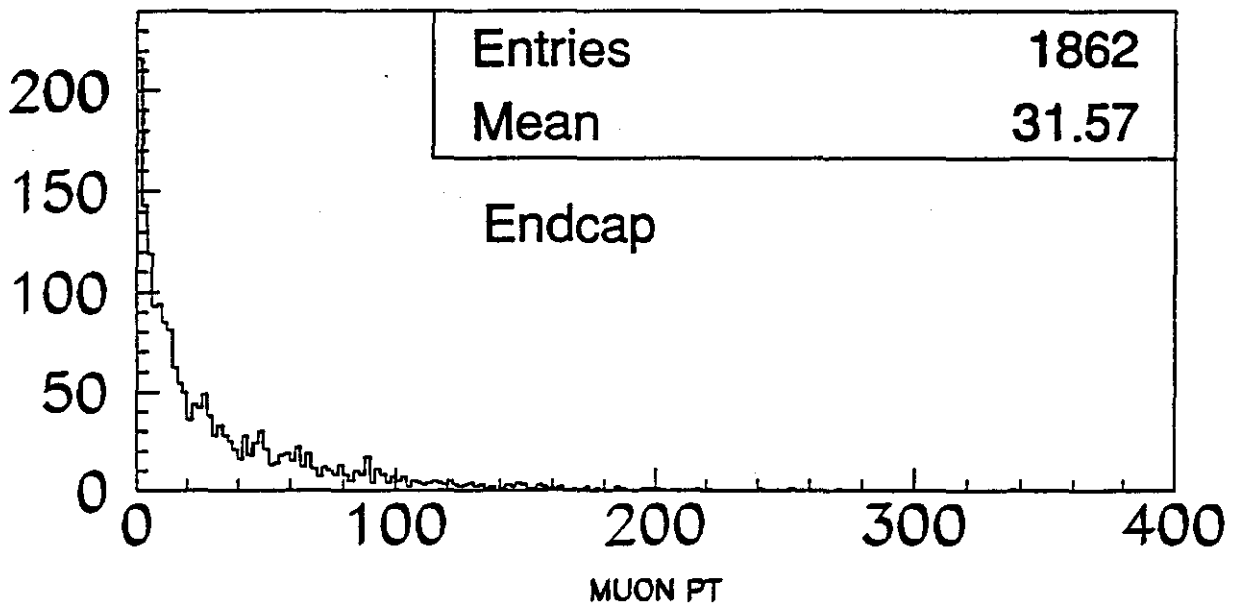
Entries 1862
Mean 31.57
Endcap
200
150
100
50
0
0
100
200
300
400
MUON PT

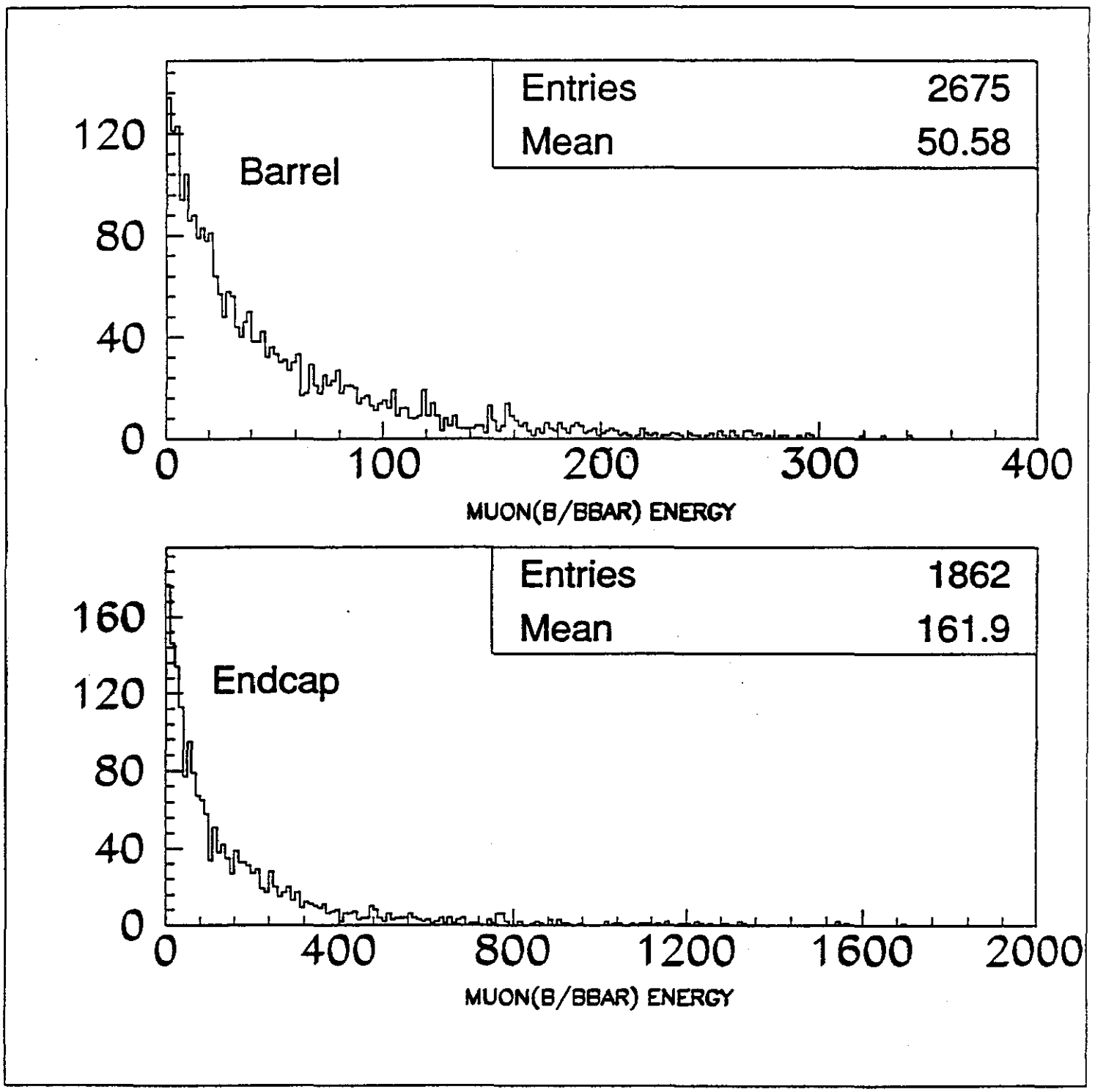
Entries 2675
Mean 50.58
Barrel
120
80
40
0
0
100
200
300
400
MUON(B/BBAR) ENERGY
Entries 1862
Mean 161.9
Endcap
160
120
80
40
0
0
400
800
1200
1600
2000
MUON(B/BBAR) ENERGY

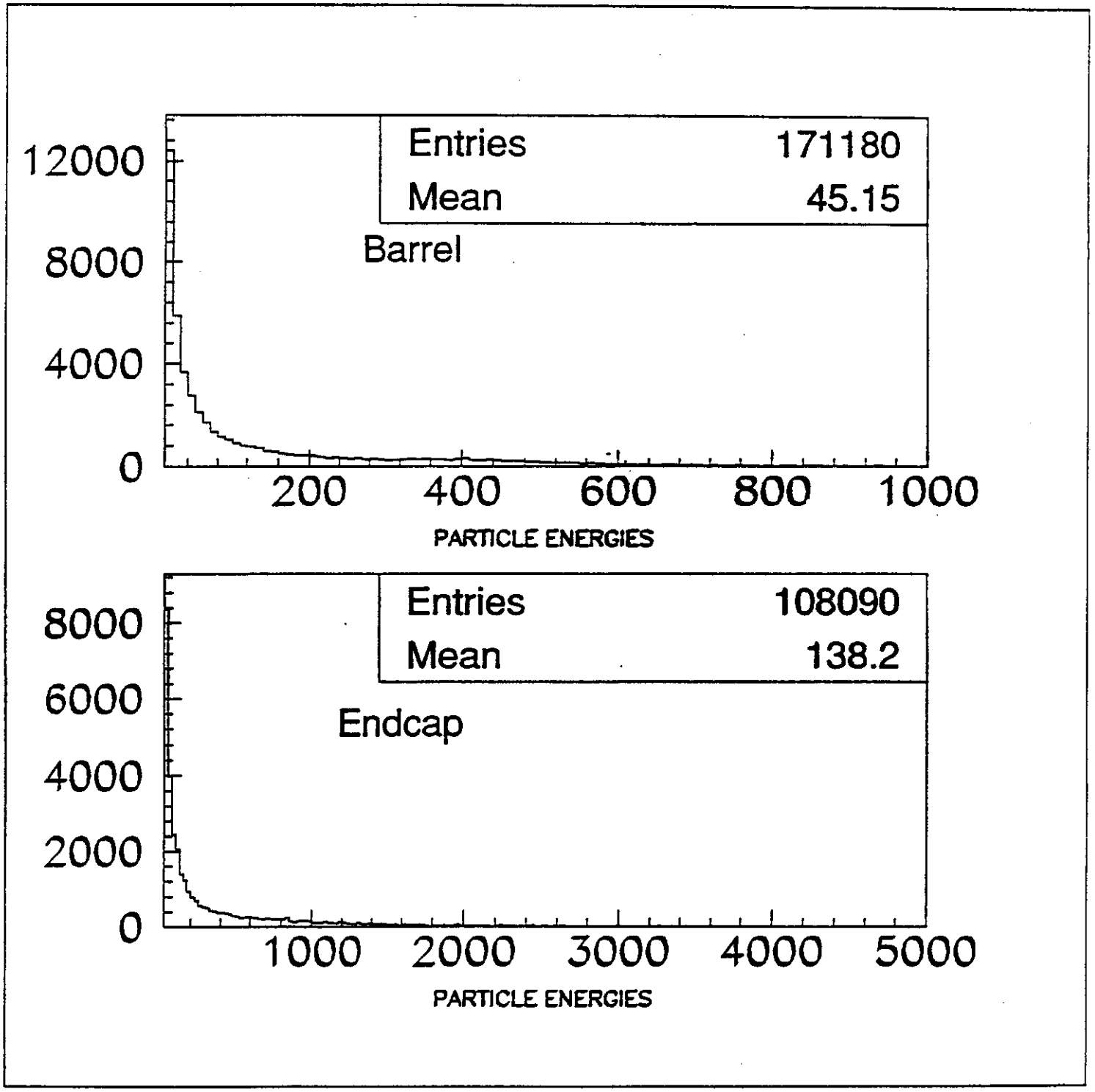

Energies of particles in a cone around η, $\sqrt{\Delta\eta^2+\Delta\phi^2}=1$

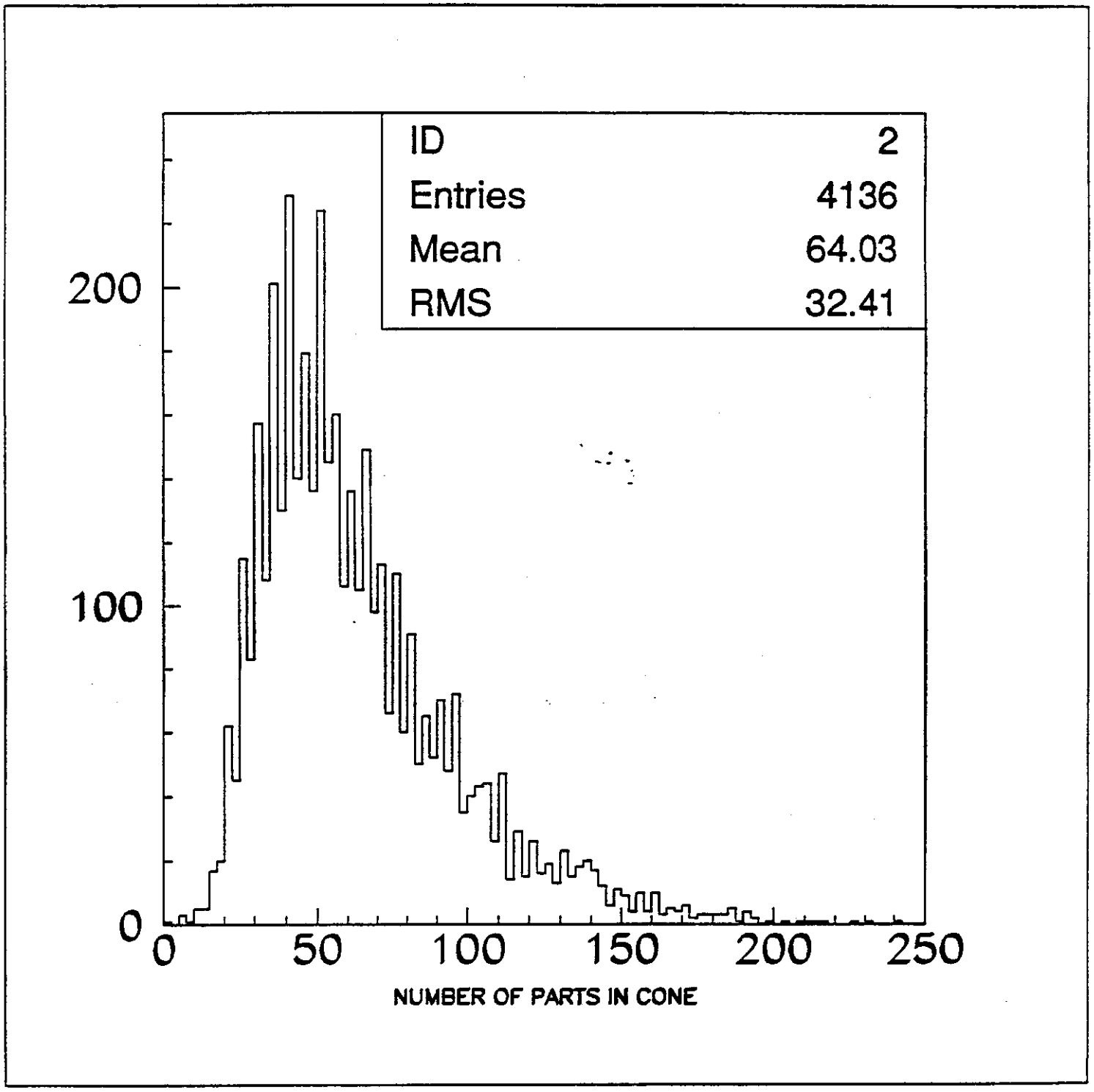
ID 2
Entries 4136
Mean 64.03
RMS 32.41
200
100
0
0
50
100
150
200
250
NUMBER OF PARTS IN CONE

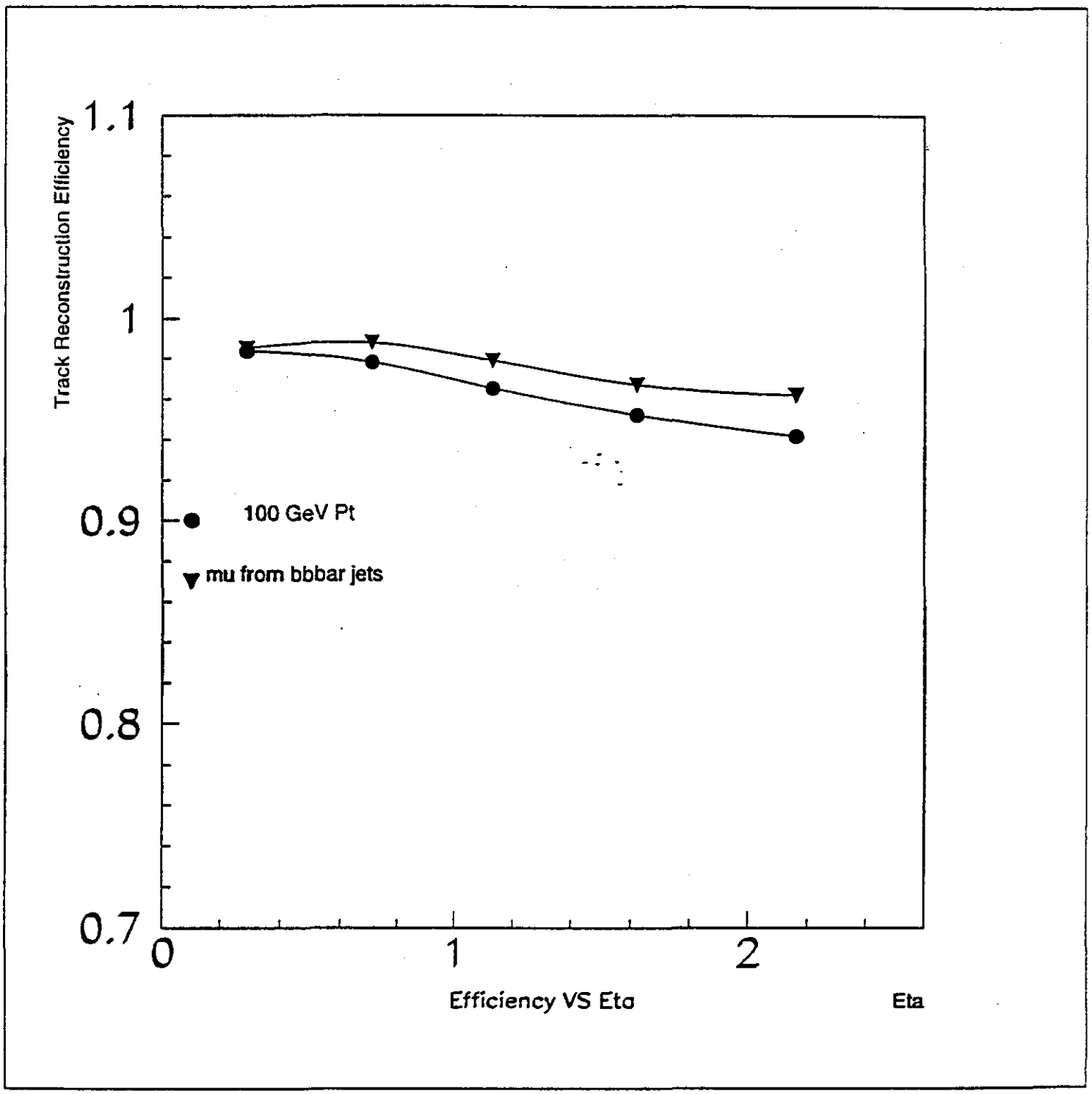
Track Reconstruction Efficiency
1.1
1
0.9
0.8
0.7
0
1
2
100 GeV Pt
mu from bbbar jets
Efficiency VS Eta
Eta

this implimentation we have taken the tracking vector to include; $(\frac{1}{\rho}, vl, wl, v, w)$. These five parameters uniquely define a track, they are defined as follows:

- $\frac{1}{\rho}$ is the curvature of the track.
- vl is the slope of the track in a plane containing the unit vector in the measurement plane, v, and the unit vector normal to the measurement plane, u, where (u, v, w) form an orthonormal local coordinate system for the current measurement plane.
- wl is the same as vl but in the (u, w) plane.
- v is the v component of the hit on the local measurement plane, this direction is taken as the CSC strip direction of the CSC chamber.
- w is the w component of the hit on the local measurement plane and is taken as the wire direction of the CSC chamber.

The Kalman filter minimizes the following χ^2 :

$$\chi^2 = \sum_{i}^{planes} (x_i - \theta)^T V_i^{-1} (x_i - \theta) + (P_i - \theta)^T W_i^{-1} (P_i - \theta)$$

where :

- x = vector of measured track parameters.
- θ = fitted vector of track parameters.
- P = predicted vector of track parameters.
- V = measurement covariance matrix.
- W = Tracking covariance matrix.
- $\sigma = \sigma^2$, this definition is made so as not to overly burden the notation.
- i = measurement plane index.

Geane provides the following facilities;

$$P_i = F_{i,i-1}\theta_{i-1} \tag{6}$$
$$\sigma_{P_i} = T_i^T \sigma_{\theta_{i-1}} T_i + W_i \tag{7}$$

These two equations represent first the perdiction of the track parameters on plane i given their values on plane i-1, and second the tracking covariance matrix of the predicted values on plane i. In the above formula $F_{i,i-1}$ swims the track parameters between planes i and i-1 and $T_i = T_{i,i-1}$ is the transport matrix between planes i and i-1 defined as;

$$T_i = \frac{\partial P_i}{\partial \theta_{i-1}} \tag{8}$$

The Kalman filter proceeds in two steps, first it loops over all the hit planes in a track candidate. This is the filter step where it makes a first estimate of the fitted track vector, $\bar{\theta}_i$ and the associated covariance matrix:

$$\bar{\theta}_i = \sigma_{\bar{\theta}_i}(\sigma_{P_i}^{-1} P_i + V_i^{-1} x_i) \tag{9}$$
$$= \frac{(\sigma_{P_i}^{-1} P_i + V^{-1} x_i)}{\sigma_{\bar{\theta}_i}^{-1}} \tag{10}$$
$$\sigma_{\bar{\theta}_i}^{-1} = \sigma_{P_i}^{-1} + V_i^{-1} \tag{11}$$

Notice that the initial estimate of track parameters is just the weighted mean of the predicted and measured track parameters. Once the filtering is done we loop through all the planes a second time in the reverse order to that of the filtering so as to use information about the fitted and perdicted track vectors on the next plane, i+1, to corrected the fitted value on plane i. This is called smoothing, and is done in the follow iterative way;

$$\theta_i = \bar{\theta}_i + A_i(\theta_{i+1} - P_{i+1}) \tag{12}$$
$$\sigma_{\theta_i} = \sigma_{\bar{\theta}_i} + A_i(\sigma_{\theta_{i+1}} - \sigma_{P_{i+1}})A_i \tag{13}$$

where:

$$A_i = \sigma_{\bar{\theta}_i} T_{i+1} \sigma_{P_{i+1}}^{-1} \tag{14}$$

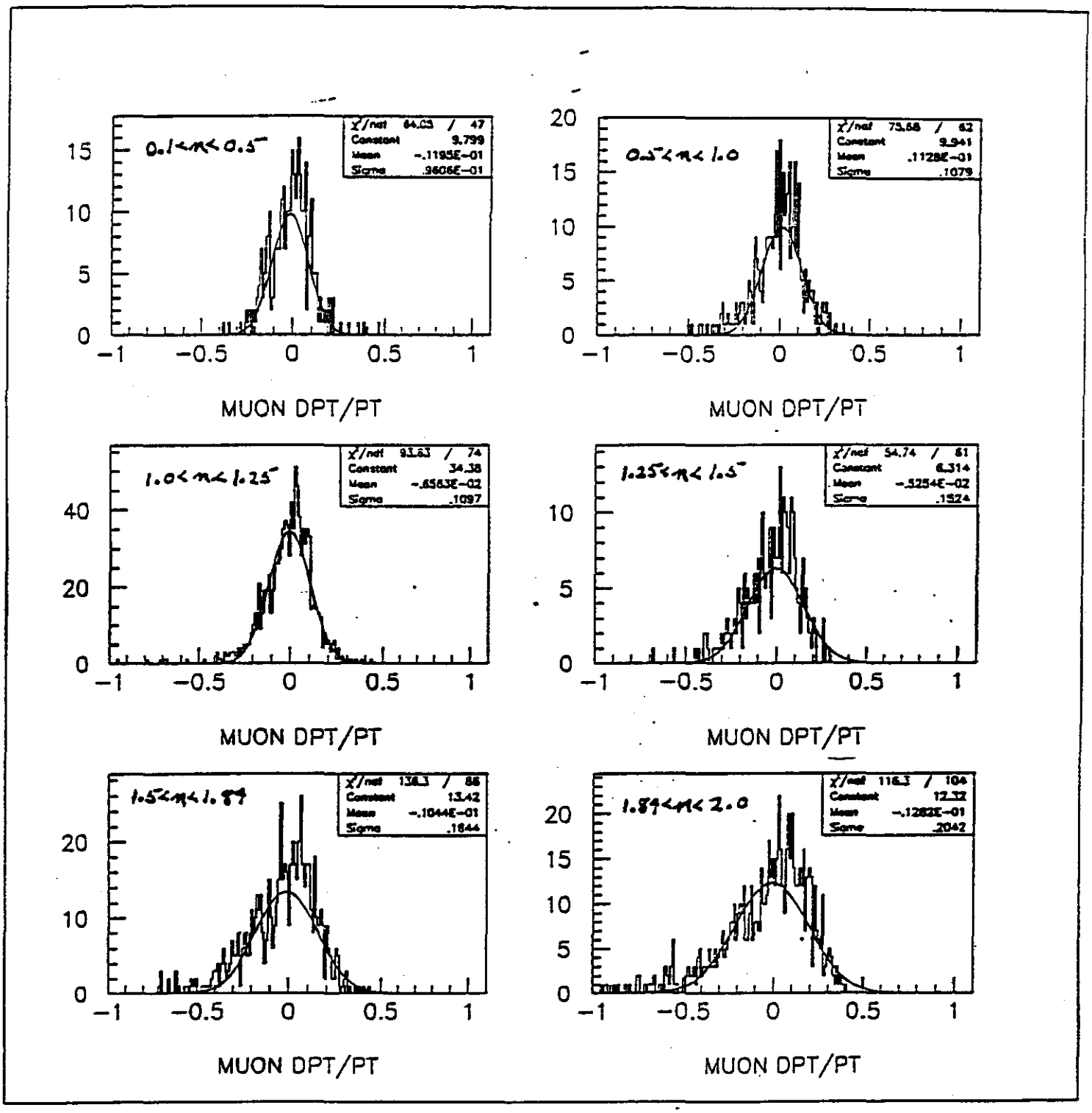

Figure 15a) Resolution distributions as a function of η for the isolated 1 TeV P_t muon sample, including all correlated backgrounds, computed by the Kalman Filter .

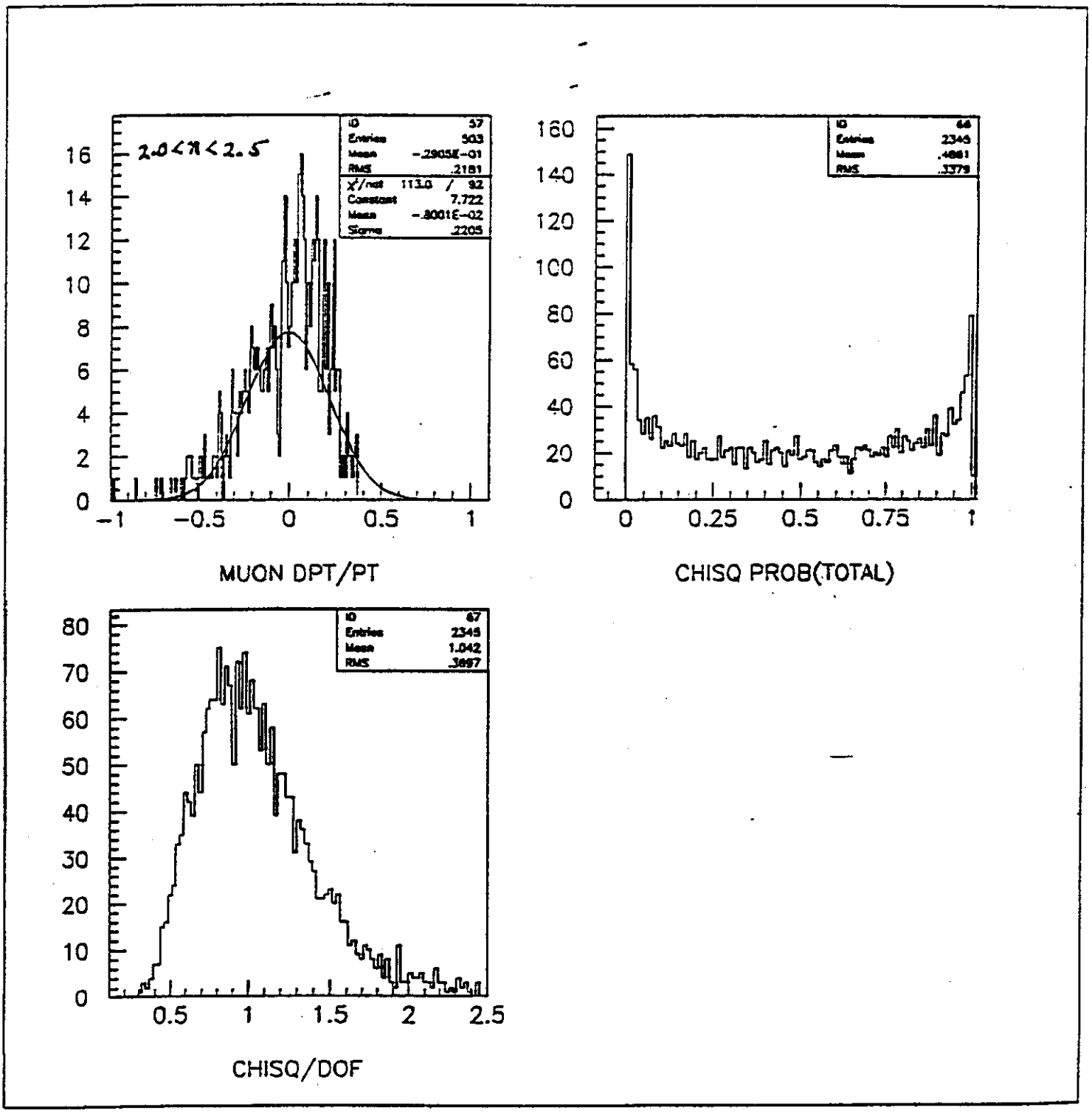

Figure 15b) Distributions of χ^2 probability and $\frac{\chi^2}{DOF}$ resulting from the Kalman Filter track fit for the 1 TeV muon sample with background .

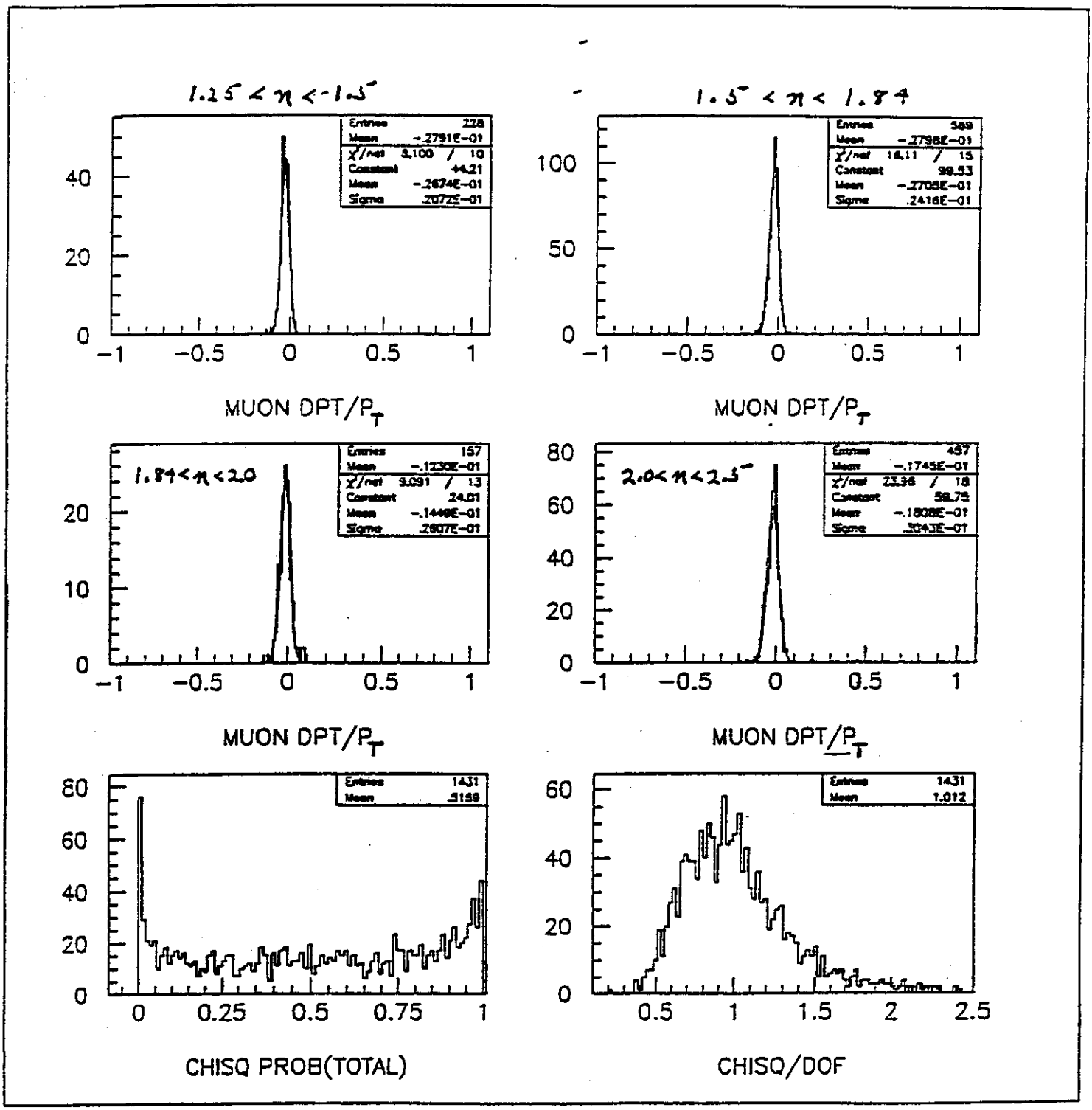

Figure 20) Track resolution distributions and quality of fit for the structure-free 100 GeV P_t sample of muons in the endcap. This sample of muon events scanned the detector in η but not in ϕ in order to access the effect of the staggering of chambers in ϕ and of chamber supports.

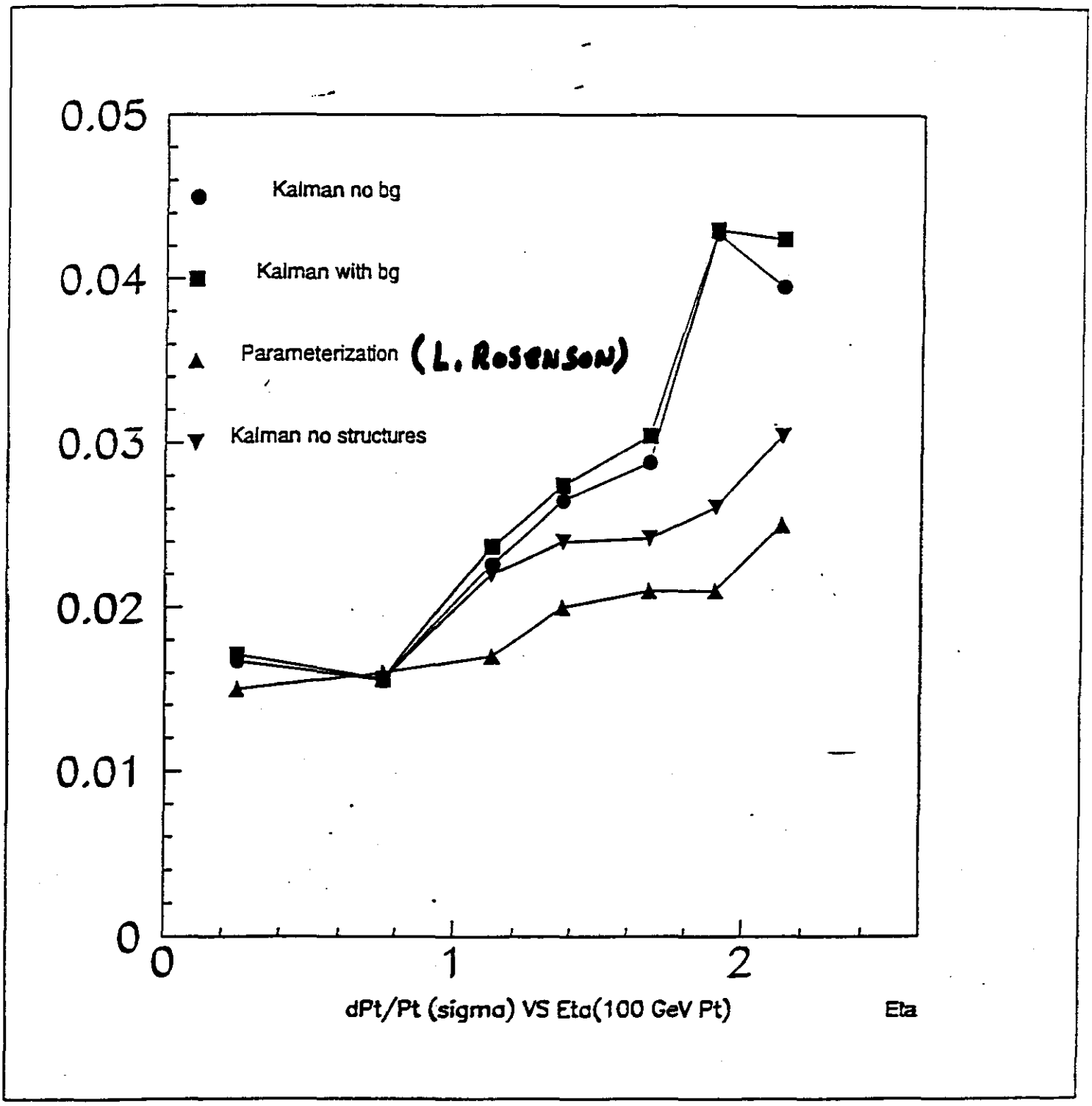

Figure 16) Track resolution plot as a function of η for the 100 GeV P_t muon sample using the Kalman Filter .

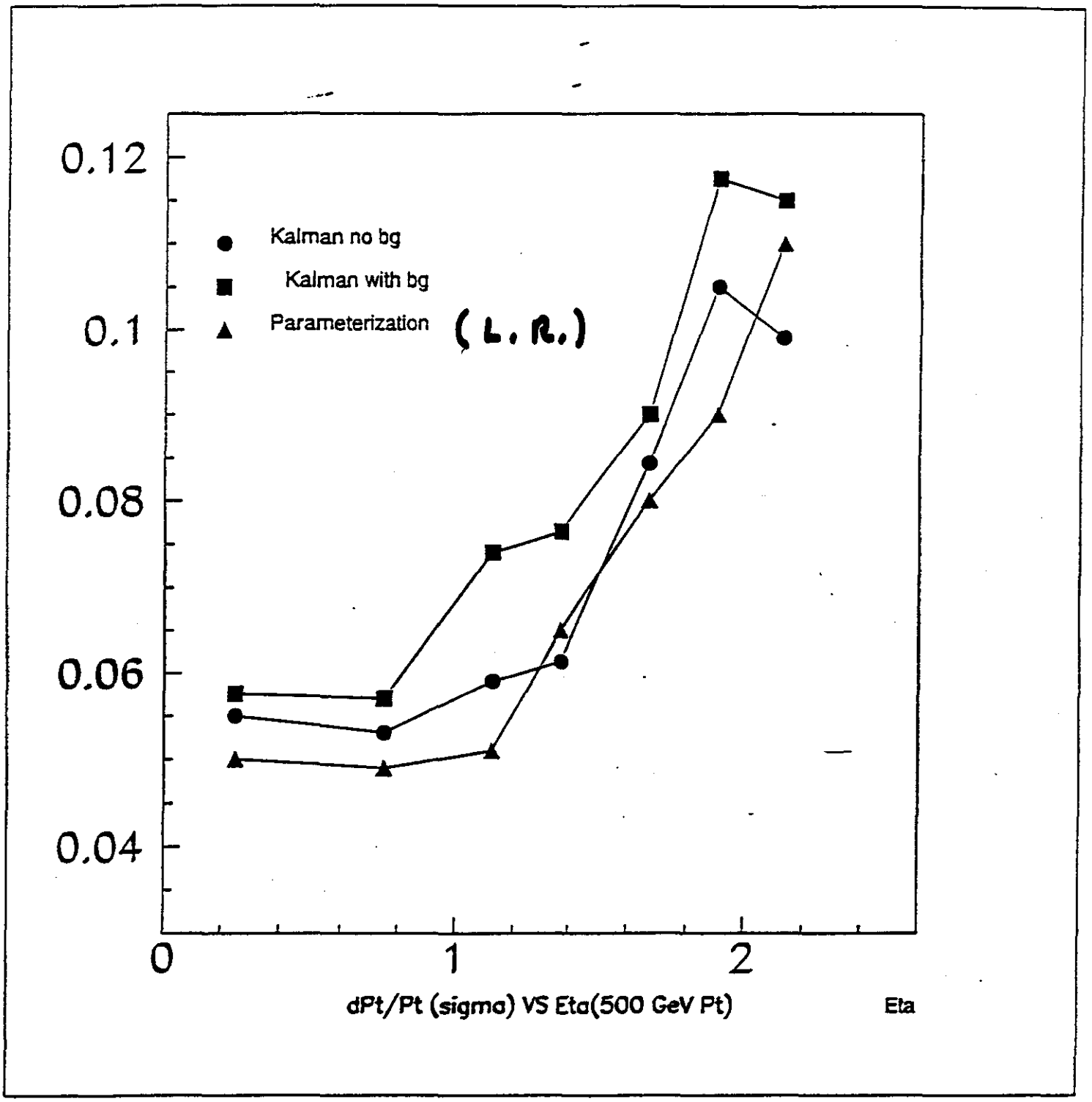

Figure 17) Track resolution plot as a function of η for the 500 GeV P_t muon sample using the Kalman Filter .

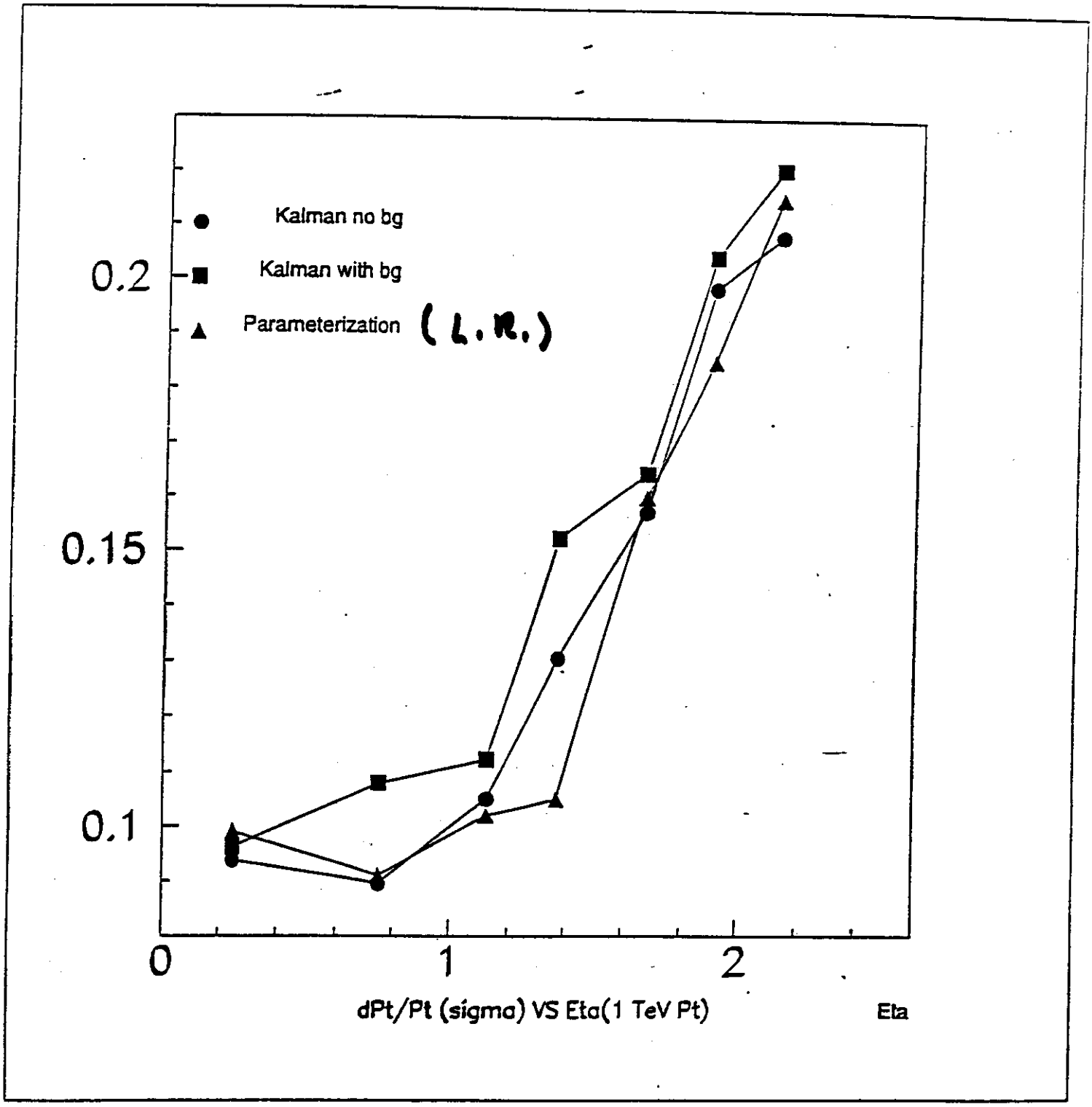

Figure 18) Track resolution plot as a function of η for the 1 TeV P_t muon sample using the Kalman Filter .

Pattern Recognition Issues

The fundemental problems in pattern recognition are dependent on the types and density of the backgrounds associated with the signal. These in turn depend upon:

A) Materials comprising the muon chambers.

B) The momentum magnitude of the muon .

C) The physical layout of the experiment.

Only correlated background will be considered in detail.

Then a couple of track reconstruction senarios

will be considered in the presence of these backgrounds.

We will consider three files of 3500 isolated muons of momentums;

1 TeV, 500 GeV , and 100 GeV Pt which were uniformly distributed throughout the GEM detector. The Sigem simulation V1.3 (Y.Fisyak , GEM TN-162) was used with 10KeV cuts.

PHYSICS SIMULATIONS UPDATE

John Womersley 8/4/93

MUCH WORK CONTINUES TO BE DONE

STANDARD HIGGS

$H \to \gamma\gamma$ Drell-Yan / $Z \to ee$ background

- radiative background $ee\gamma$... (Daniel Froidevaux at PAC)
  now understood & agreed to be small
  (Ren-Yuan Zhu + B. Ward YFS3 MC.)

- electron faking γ
  new study of e/γ discrimination using CT
  (Yan-Lin Ye)
  $\to$ A_γ 85–90% and $R(\gamma/e) < 0.2\%$
  possible with cut on N_{hit} or N_{layer}
  (+ better still in Si alone)
- $H \to \gamma\gamma$ trigger strategy (Henk Uijterwaal)

$H \to 4\mu$

- muon acceptance, resolution
  (Torre Wenaus)
  investigate effects of closing gaps in barrel + 30°

	muons	TDR	now	w/o gaps
$m_H = 150$	3SL	43%	36%	73%
$H \to 4\mu$	2,3SL	54%	55%	
	2,3SL+CT	87%	90%	

σ_H = 1.6 GeV (3SL) $\to$ 2.4 GeV (2,3SL+CT)
but $S/\sqrt{N}$ goes up by factor 3.

New improved E loss correction by Vladimir Gavrilov.

* For each event, straight lines are defined to connect the event vertex and the Cal. bumps. A cone can be defined around a straight line by

$$\frac{\ell^2}{R^2} < \Delta^2 = 0.03^2 \quad (0.02^2 \rightarrow 0.05^2)$$

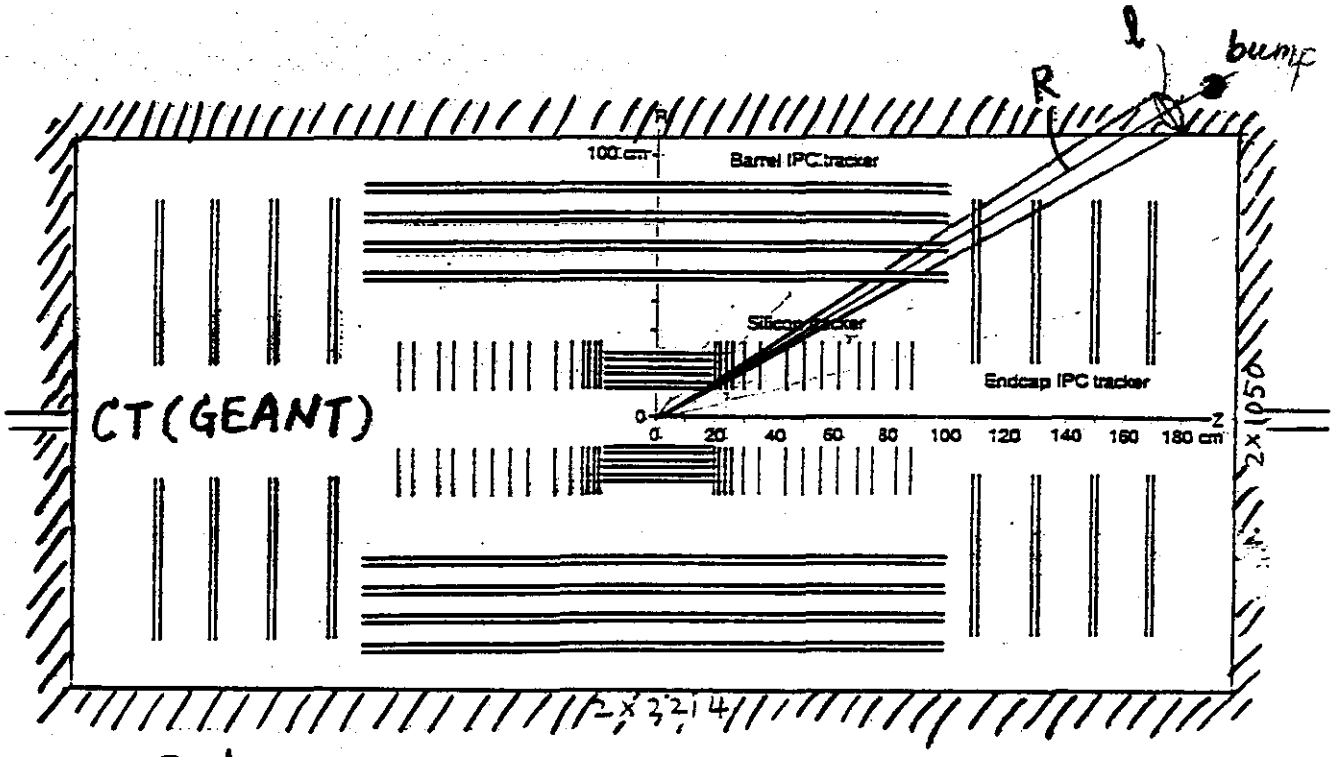

Cal. (GEMFAST)

Counting : N_{hit} — number of hits within the cone

N_{layer} — number of detector layers hit within the cone

	Cut on Nhit			Cut on Nlayer		
	Ncut	A_γ(%)	Ae(%)	Lcut	A_γ(%)	Ae(%)
Si+Pad	2	84.4	0.0140	2	85.1	0.0392
	4	85.0	0.0168	4	87.0	0.0477
	6	86.0	0.0757	6	89.3	0.126
	8	86.7	0.193	8	93.8	0.266
	10	87.9	0.297	10	95.8	0.373
	12	88.8	1.88	12	97.3	2.93
Si only	2	94.9	0.07	2	95.8	0.07
	4	95.7	0.07	4	97.1	0.07
	5	96.0	3.64	5	98.0	3.94
	6	96.3	34.6	6	99.1	48.0

* Conclusion: $R(\gamma/e) < 0.2\%$ can be achieved for $A_\gamma \sim 90\%$.

GEM Level 2.

* Processor farm with 100 to 1000 500 SSCUP processors, processors are used for L2 and L3 algorithms.

* 10 to 100 kHz Level 1 trigger rate.

* 1 to 10 ms available for the L2 trigger algorithms.

Algorithms.

* 3 layers:

1) Use data of a single component to extract trigger primitives: e/γ, jet, E_t, tracks, muon.

2) Combine data from 2 or 3 components: CT-track + e/γ-candidate.

3) Extract global physics quantities: Invariant mass of 2 objects.

* Studies in progress are:

1) e/γ finding, trigger for $H^0 \rightarrow \gamma\gamma$ (and a few other processes). Relatively simple algorithm but a lot of data to process. (Every cell in the EM-CAL).

2) Jet-finding. More complex algorithm but less data to process (sums of EM- and HAC-CAL cells). Will be presented in a next talk.

93/07/07 14.12

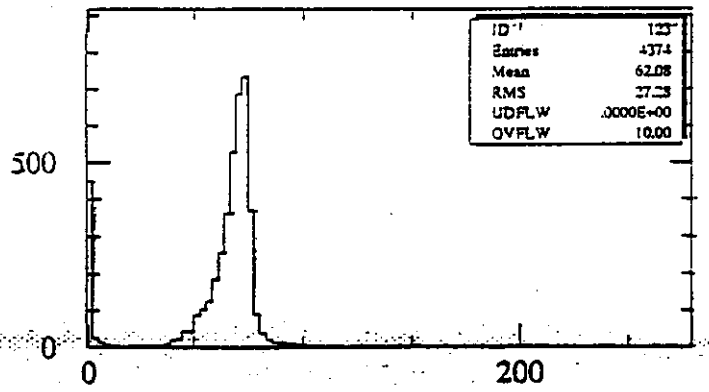

Level 1 (1+2 photon trigger)

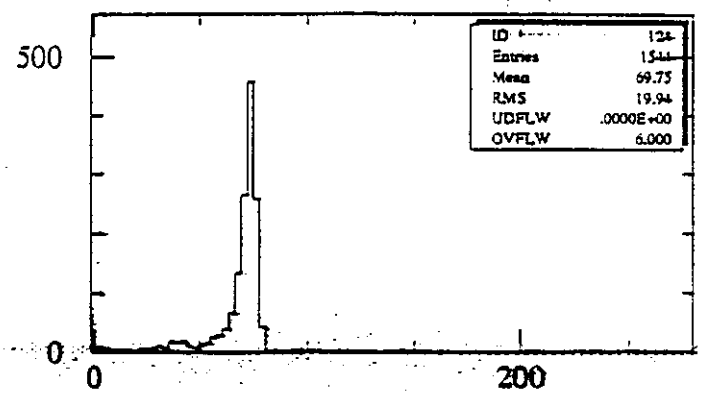

Level 2 (1+2 photon trigger)

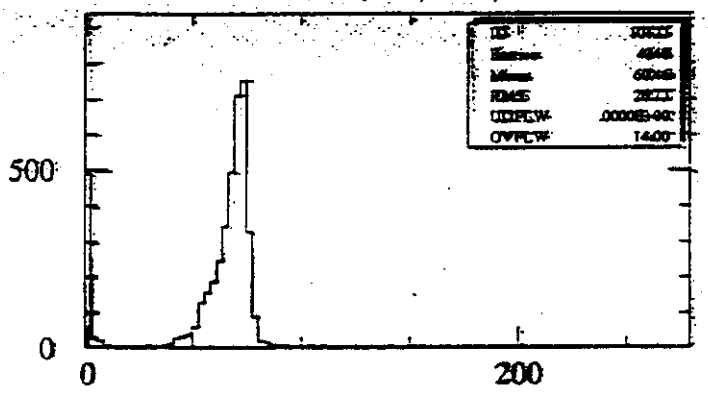

Level 1 (1+2 photon trigger)

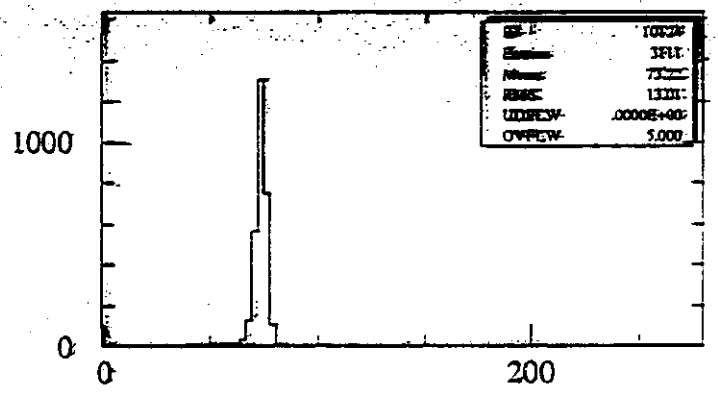

Level 2 (1+2 photon trigger)

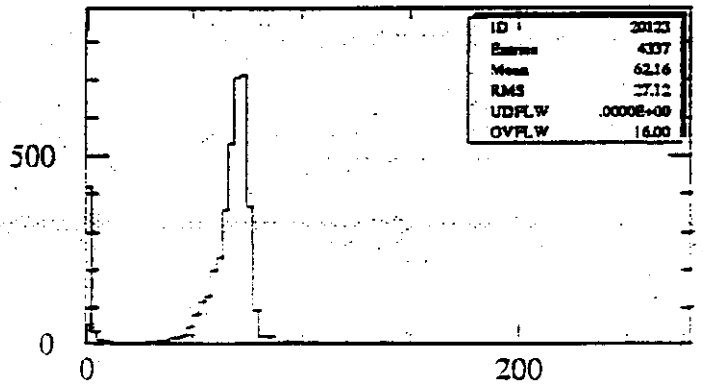

Level 1 (1+2 photon trigger)

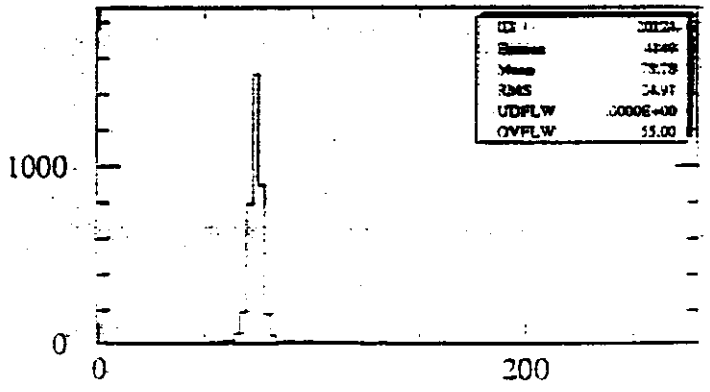

Level 2 (1+2 photon trigger)

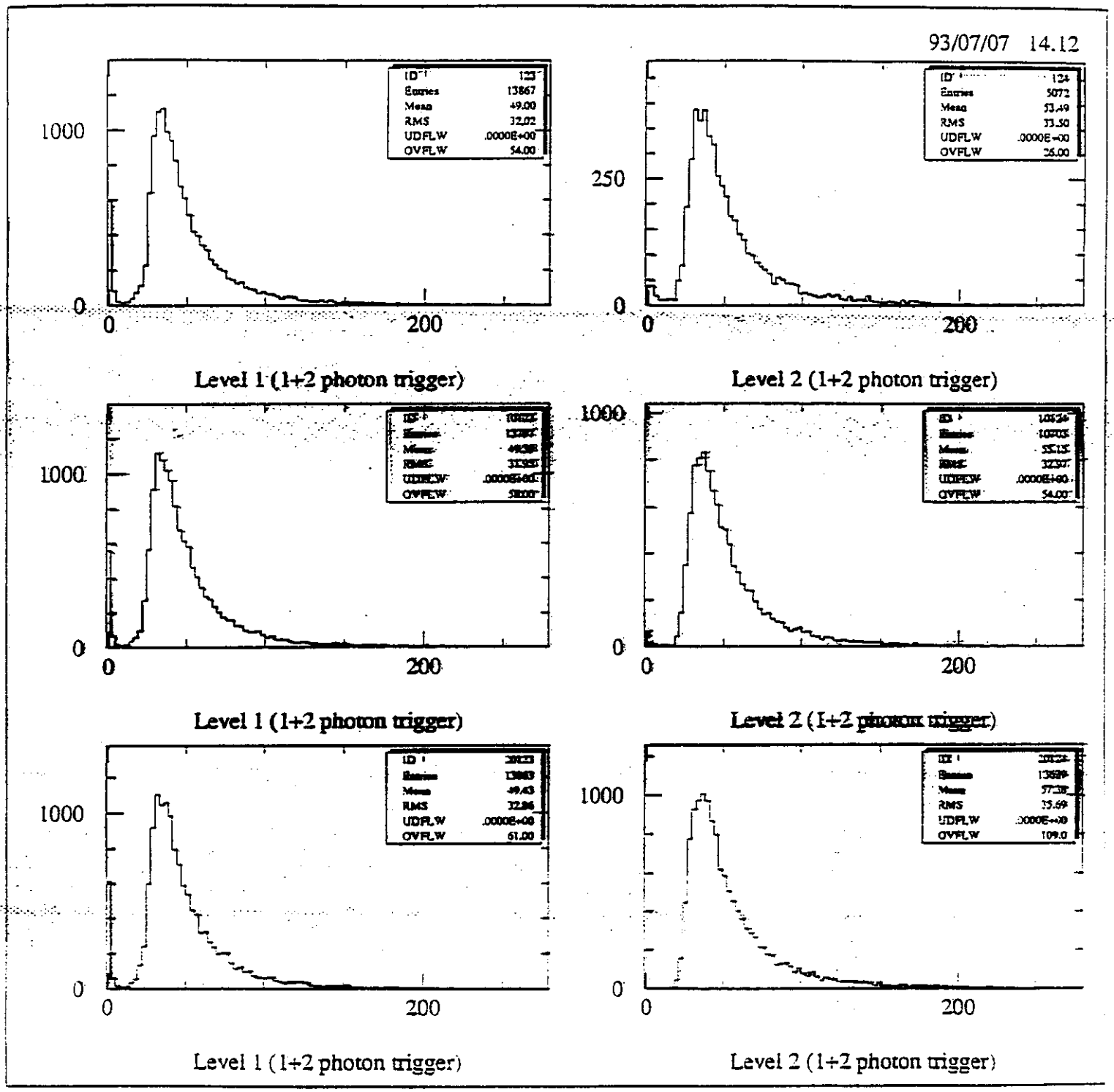
93/07/07 14.12
ID 123
Entries 13867
Mean 49.00
RMS 32.02
UDFLW .0000E+00
OVFLW 54.00
1000
0
0
200
Level 1 (1+2 photon trigger)
ID 124
Entries 5072
Mean 33.49
RMS 33.50
UDFLW .0000E+00
OVFLW 26.00
250
0
0
200
Level 2 (1+2 photon trigger)
1000
0
0
200
Level 1 (1+2 photon trigger)
1000
0
0
200
Level 2 (1+2 photon trigger)
ID
Entries
Mean
RMS
UDFLW
OVFLW
1000
0
0
200
Level 1 (1+2 photon trigger)
ID
Entries
Mean
RMS
UDFLW
OVFLW
1000
0
0
200
Level 2 (1+2 photon trigger)

Conclusions.

1. This can be used as a trigger for $H^0 \rightarrow \gamma\gamma$.
2. The algorithm can be executed in the time available for a L2 algorithm.

Next:

1. Do the same for a jet trigger algorithm.
2. Test the performance of a "realistic setup": e/γ and/or jet-finding depending on the L1 trigger bits.
3. Use CT and Muon data.

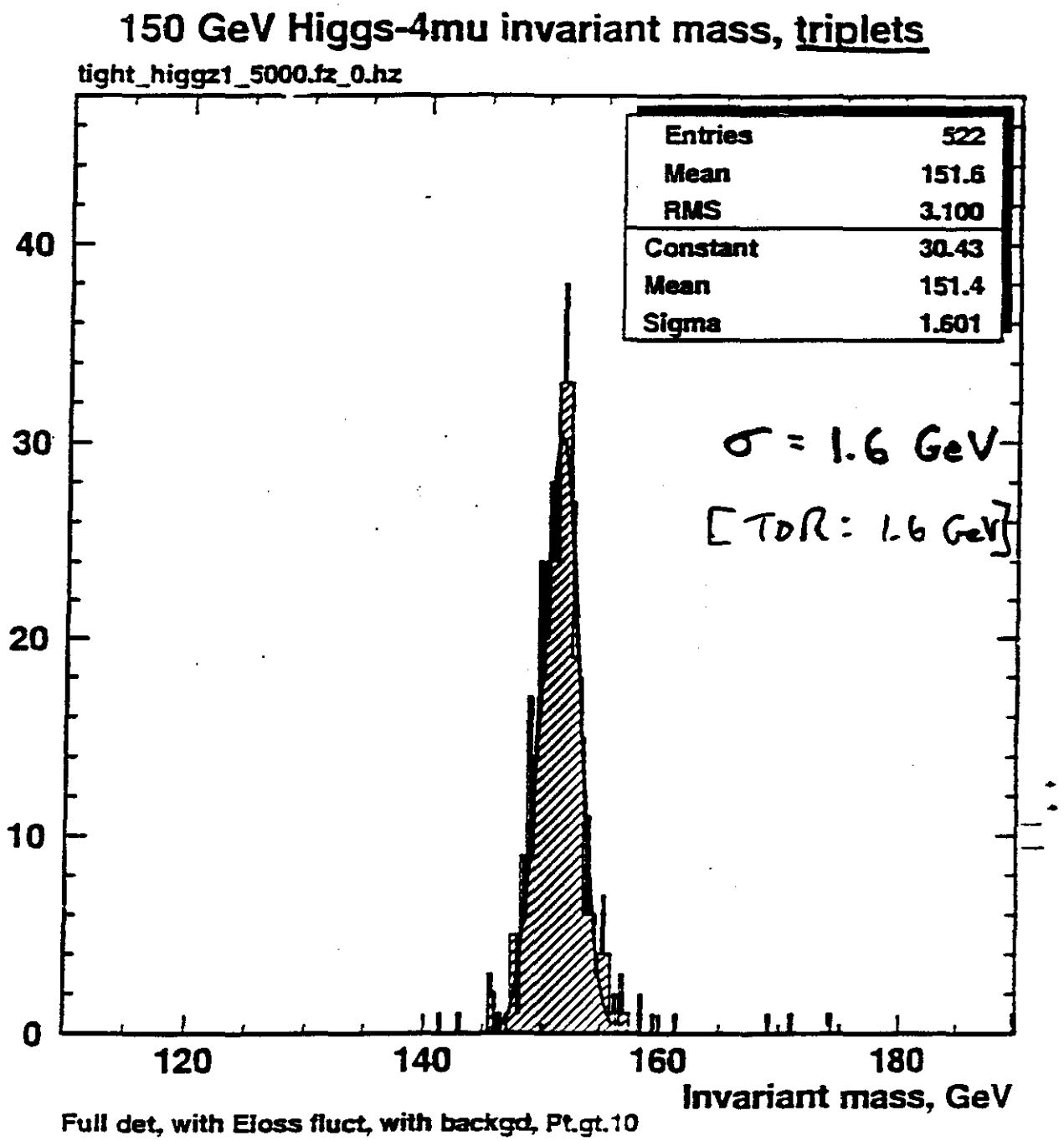
150 GeV Higgs-4mu invariant mass, triplets
tight_higgz1_5000.fz_0.hz
Entries 522
Mean 151.6
RMS 3.100
Constant 30.43
Mean 151.4
Sigma 1.601
σ = 1.6 GeV
[TDR: 1.6 GeV]
40
30
20
10
0
120
140
160
180
Invariant mass, GeV
Full det, with Eloss fluct, with backgd, Pt.gt.10

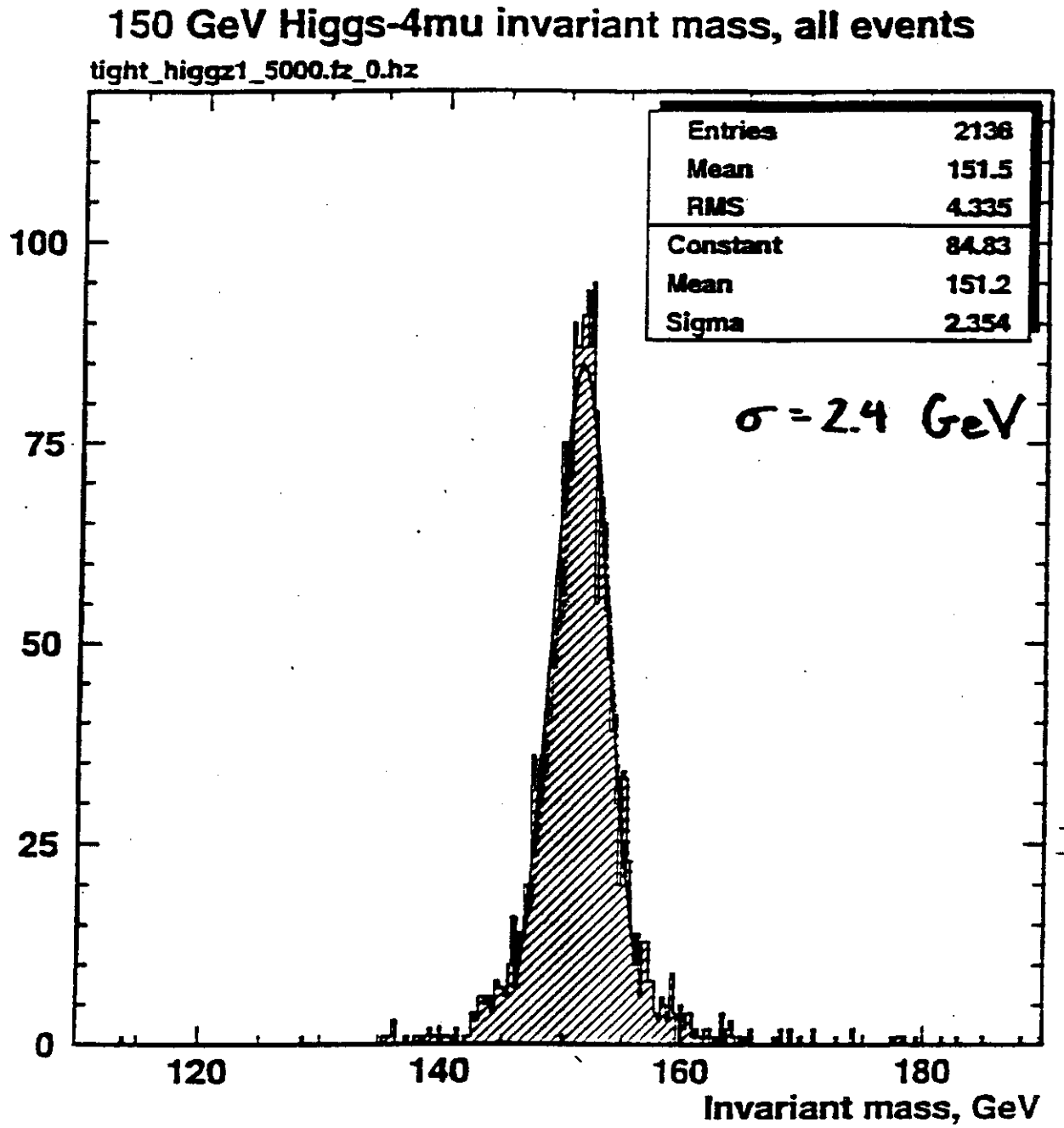

full det, with Eloss fluct, with backgd, Pt.gt.10, CT used

CALO E LOSS CORR'N -
VLADIMIR'S METHOD.

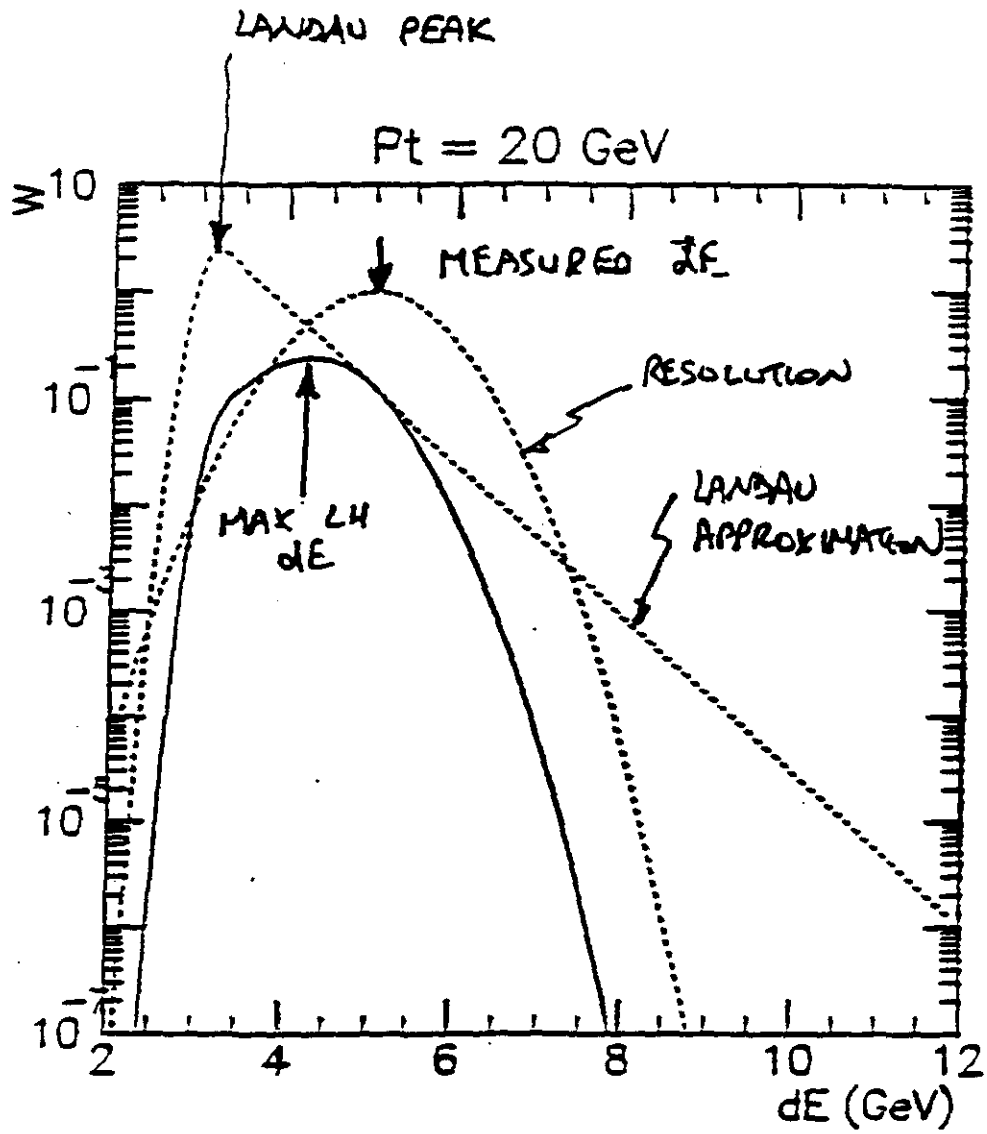

V. GAVRILOV

E LOSS CORRECTION

20 GeV p_T, BARREL ($\theta \sim 75°$)

σ OF dE/E =

2.9% FOR dE = UNCORRECTED E LOSS

2.3% FOR $\frac{\text{MEAS}}{\text{PROB}}$ RATIO CORR.

→ 1.8% FOR MAX LH CORR. + $\frac{\text{MAXLH}}{\text{PROB}}$ RATIO

IN PROGRESS:

- INTEGRATING CT SIMU/RECO OF MELYNDA et al INTO SIGEM + MY μ RECO
- IMPLEMENTING MODEL OF NEW μ SYSTEM DESIGN FOR RESOLUTION + ACCEPTANCE STUDIES
  - WHEN DESIGN 'STABILIZES' WILL RELEASE GEMFAST μ PARAMS UNLESS THERE IS DEMAND FOR IT EARLIER
  - GEMFAST PARAM WILL INCLUDE DOUBLETS, VTX CONSTRAINT, CT

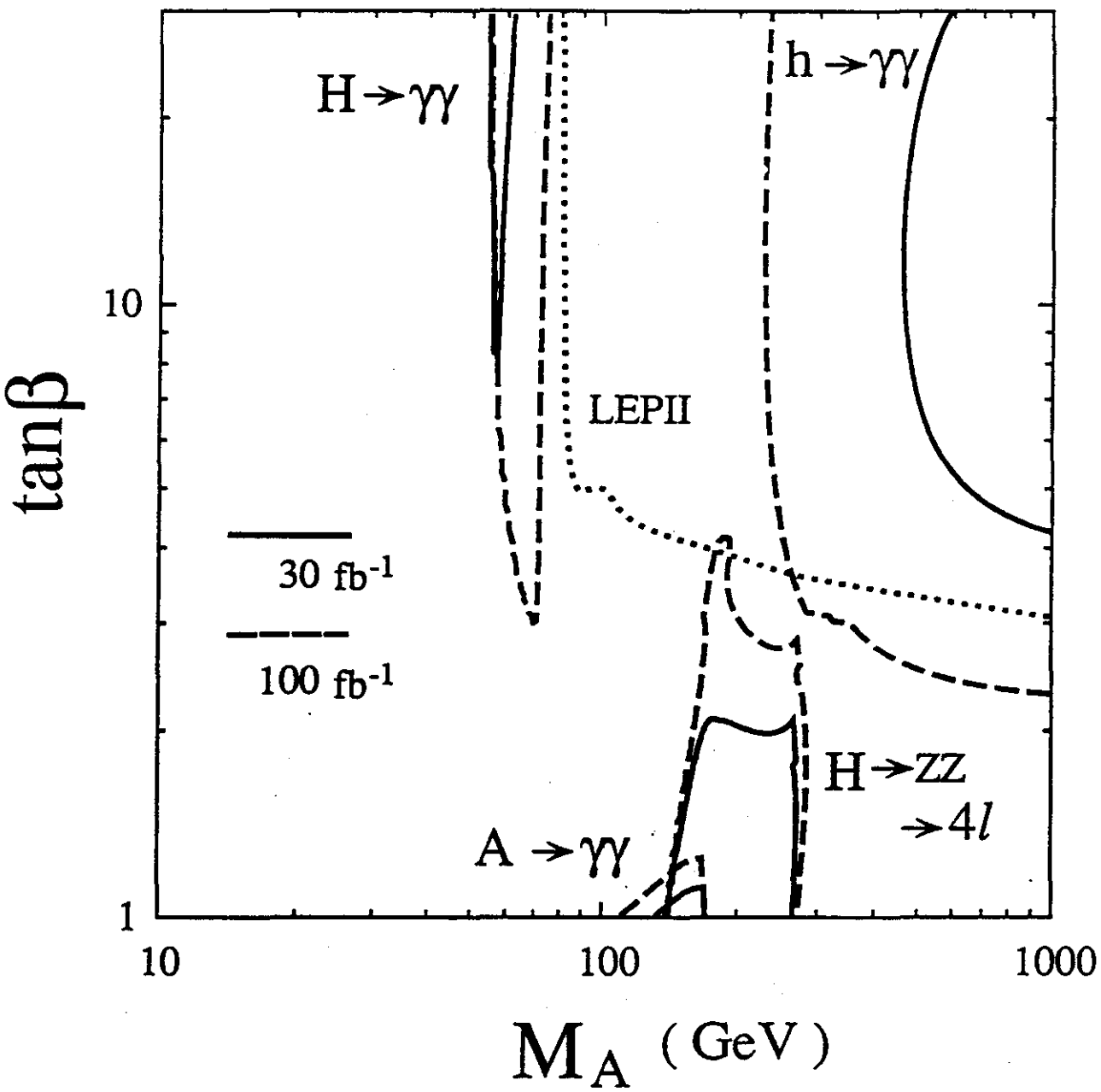

Figure 2: GEM's 5σ discovery contour curves for 30 (solid) and 100 (dash) fb^{-1} in the $(m_A, \tan\beta)$ plane, obtained by using $\gamma\gamma$ and $\ell^+\ell^-\ell^+\ell^-$ decay channels. Also shown is a discovery contour obtainable at LEPII with an integrated luminosity of 500 pb^{-1} and at a center of mass energy of 190 GeV.

gem

γeμ

Presentation by:

J. Rutherfoord

GEM Collab. Council
2/2/93

First Beam Test of LAr Tube Electrode Structure

Virtues

Clean electrical geometry - fast, simple readout

Easy to maintain small gap

Straightforward segmentation

BNL/AGS B2 Test Beam July '93

8, 6, 4, & 2 GeV/c e^-, μ^-, π^-

0.4, 1.4, & 3.4 degrees

Material in front

Cerenkovs, GEM Tracker, SDC Tracker, PHENIX Tracker

GEM FCal EM SECTION

Brass, quartz, argon: Only materials in very high radiation field

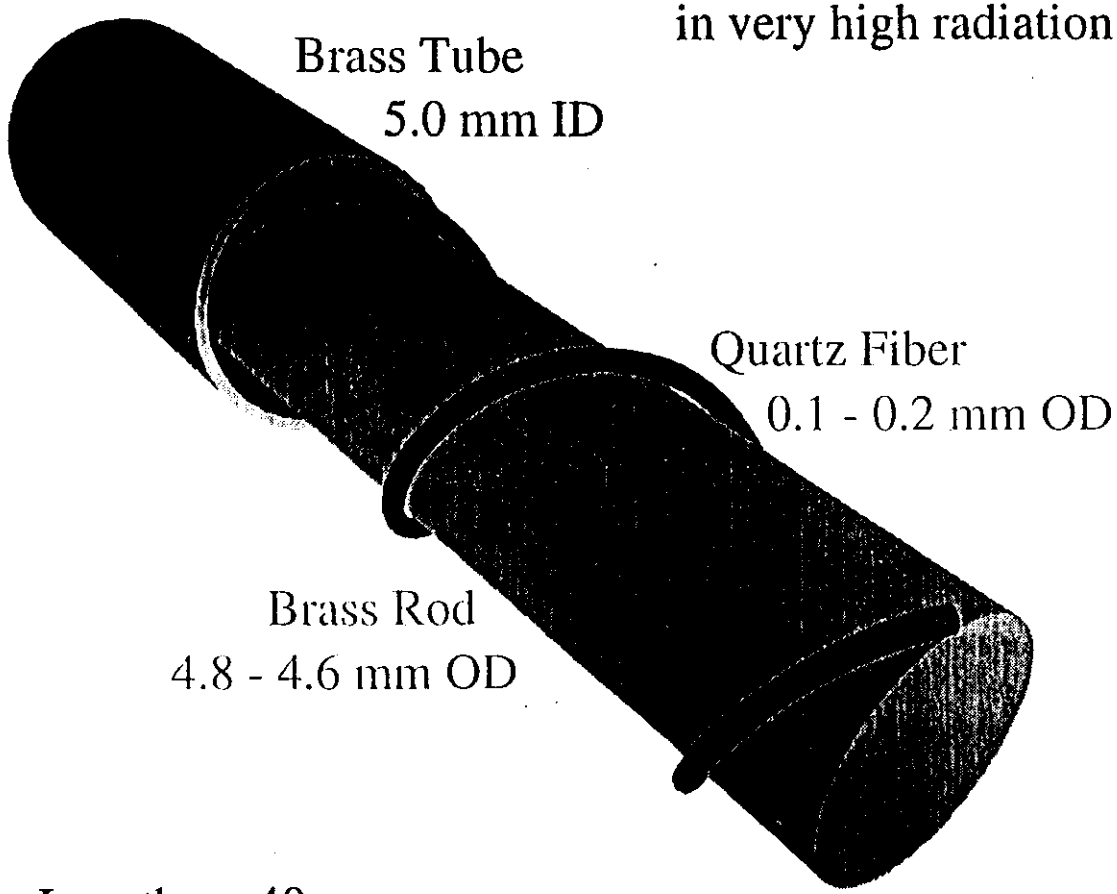

Length	40	cm	
Gap	100	200	μm
Impedance	2	4	Ω
Capacitance	800	400	pF
Sampling fraction	0.6	1.2	%
Electronics Noise	1.6	0.4	GeV in $2R_M$

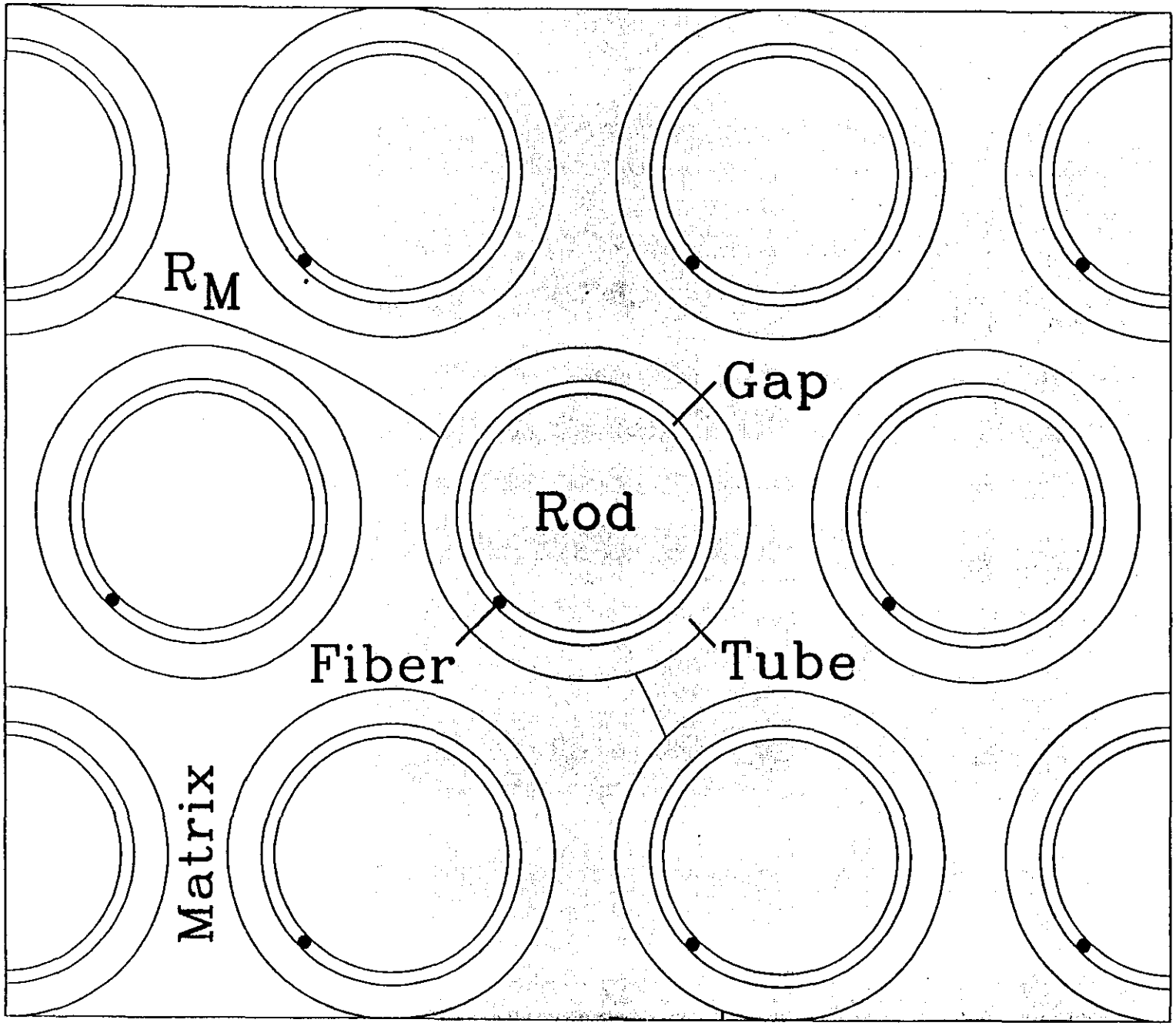
R_M
Gap
Rod
Fiber
Tube
Matrix

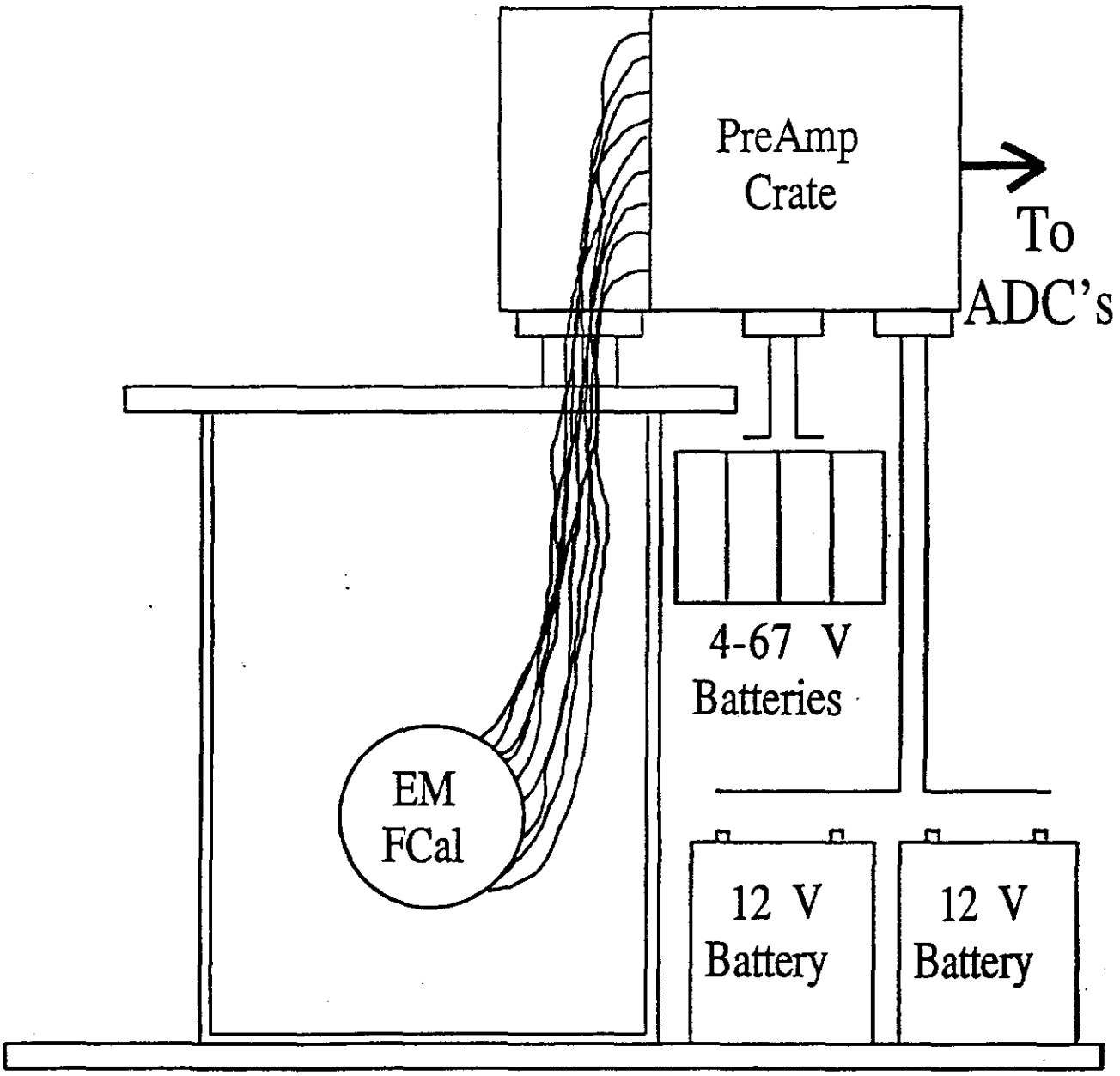
PreAmp
Crate
To
ADC's
4-67 V
Batteries
EM
FCal
12 V
Battery
12 V
Battery

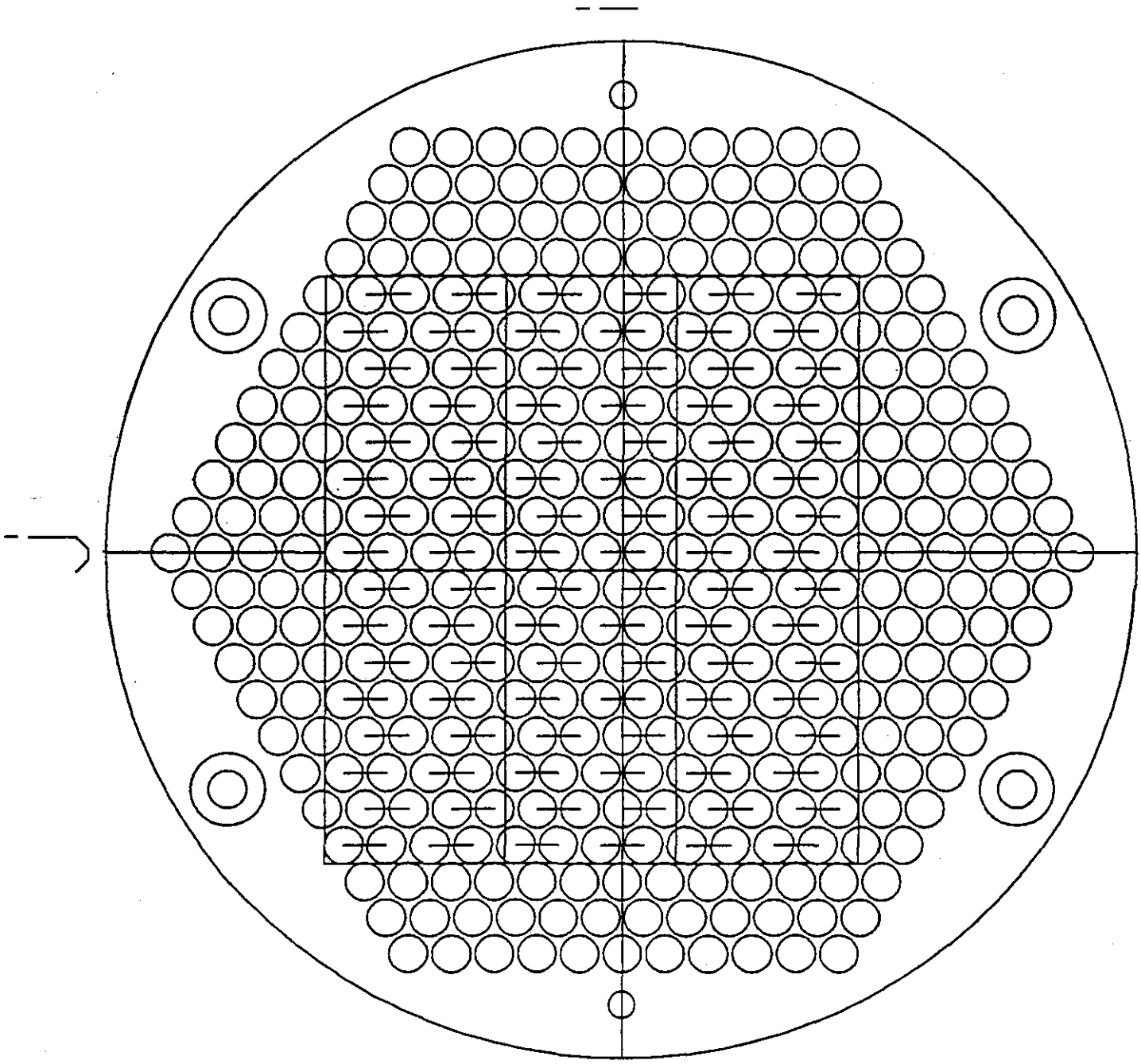

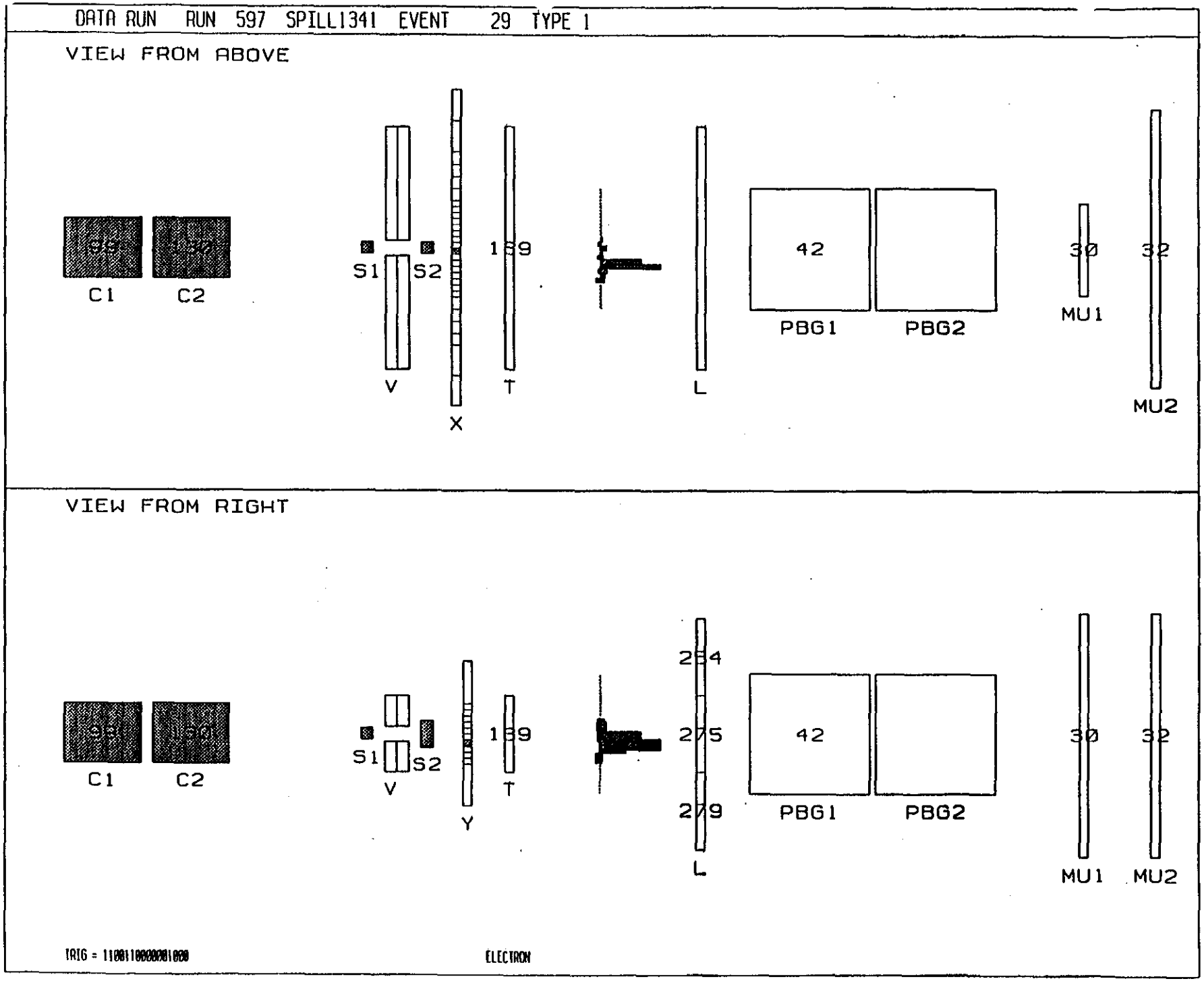
DATA RUN RUN 597 SPILL1341 EVENT 29 TYPE 1
VIEW FROM ABOVE
C1
C2
S1
S2
V
X
T
L
42
PBG1
PBG2
MU1
MU2
VIEW FROM RIGHT
C1
C2
S1
S2
V
Y
T
L
42
PBG1
PBG2
MU1
MU2
ELECTRON

DATA RUN Run 504 Spill 12 Event 92 Type 1

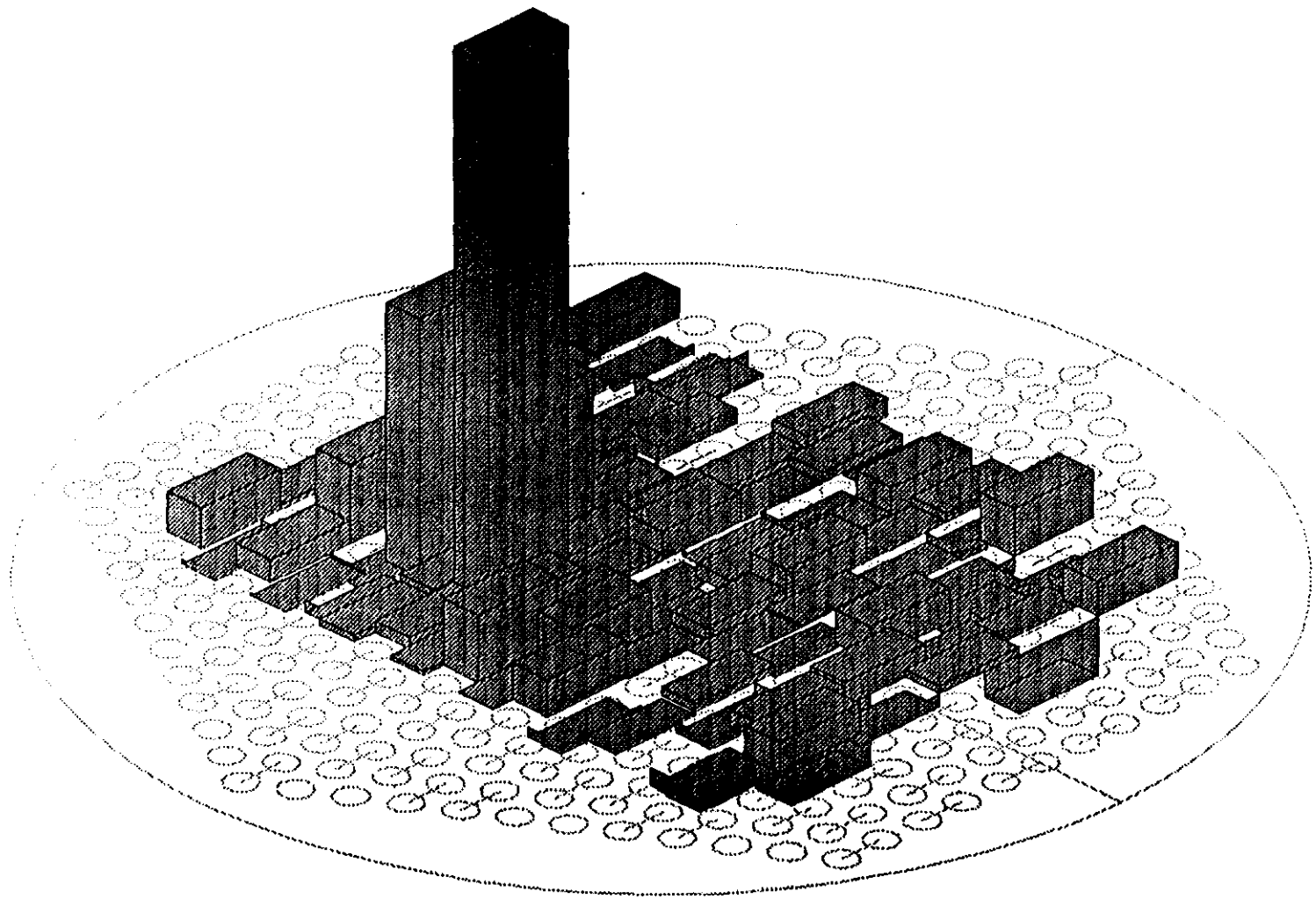

Trig = 1100110000001000 ELECTRON

Collected Charge from Ionization Sampling Calorimeter (unity gain)

$W = 25.1\ eV/e^-$ at 10 kV/cm

Induced charge in read-out is half produced charge

f_S	dE/dx weighted sampling fraction	0.0154
e/mip	"transition effect" Ar/Brass	0.90
B	Ballistic deficit (drift time 50 ns, shaping time 50 ns)	0.055
A	Attachment due to impurities	0.034
Q	Collected Charge	

$Q = f_S\ (e/mip)\ (1-B)\ (1-A)\ /\ 2W = 252{,}000\ e^-/GeV$

At 8 GeV, $Q = 2{,}020{,}000\ e^-$

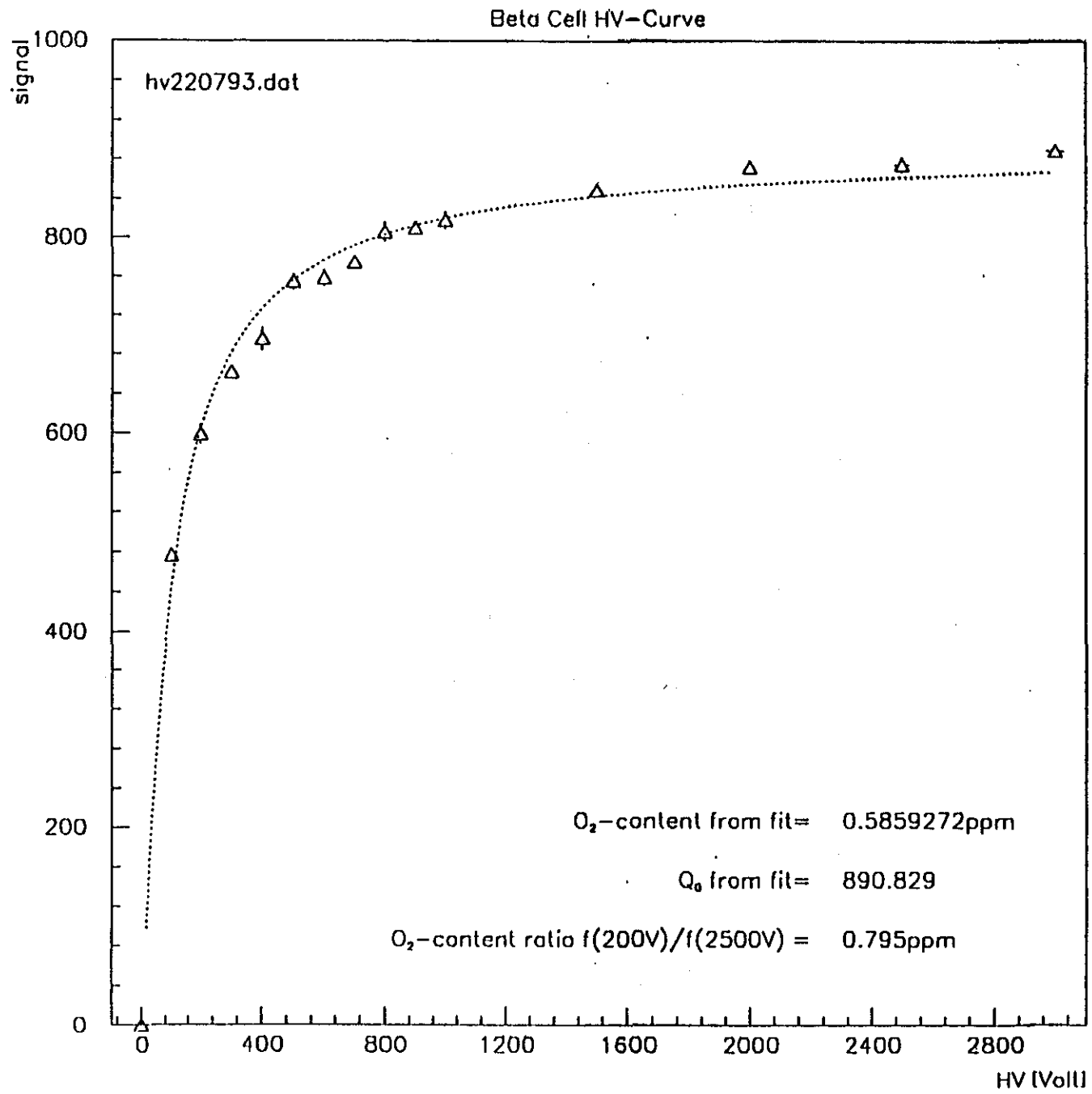
Beta Cell HV-Curve
hv220793.dat
signal
1000
800
600
400
200
0
0
400
800
1200
1600
2000
2400
2800
HV [Volt]
O_2-content from fit= 0.5859272ppm
Q_0 from fit= 890.829
O_2-content ratio f(200V)/f(2500V) = 0.795ppm

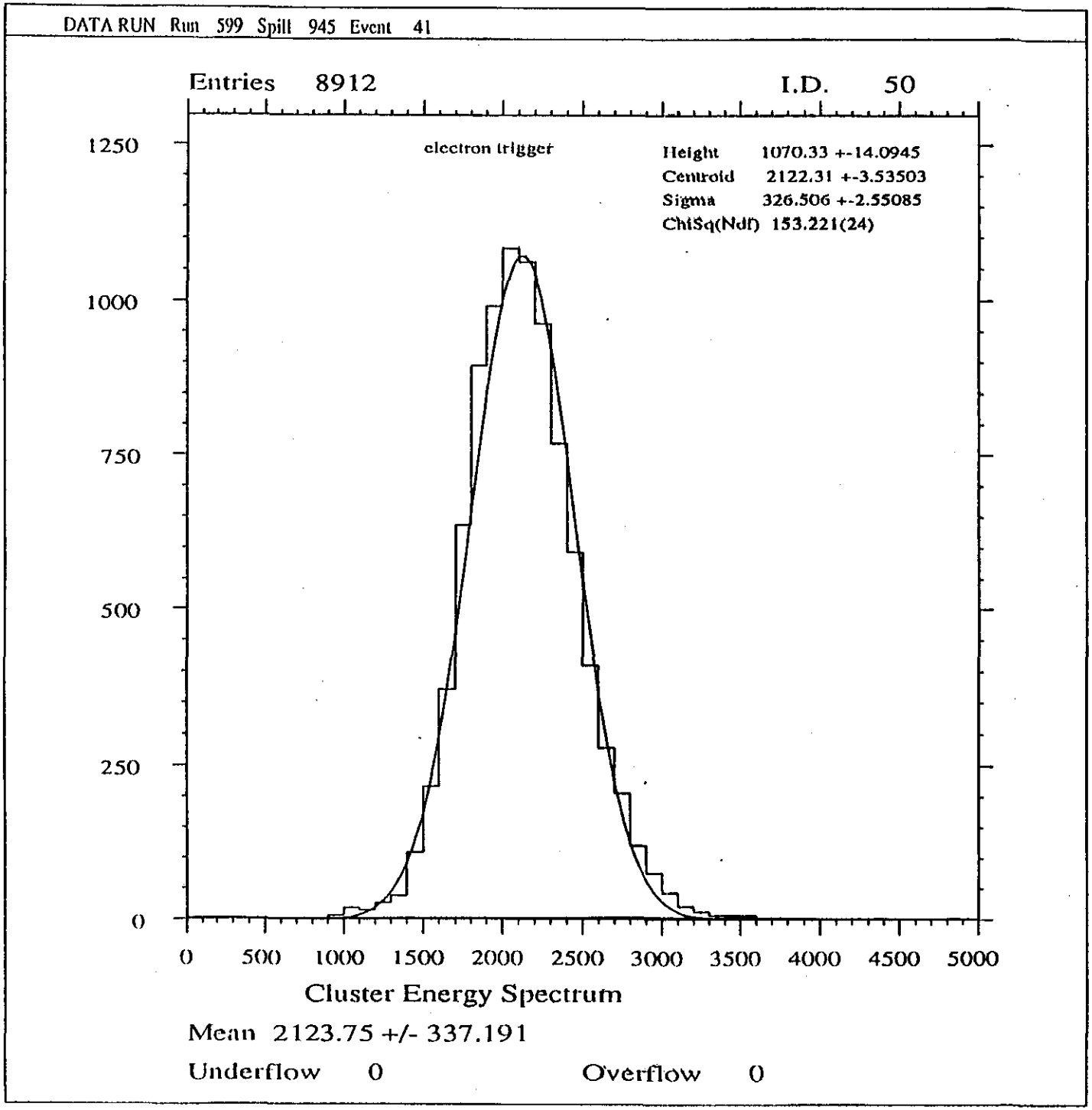
DATA RUN Run 599 Spill 945 Event 41
Entries 8912
I.D. 50
electron trigger
Height 1070.33 +-14.0945
Centroid 2122.31 +-3.53503
Sigma 326.506 +-2.55085
ChiSq(Ndf) 153.221(24)
1250
1000
750
500
250
0
0 500 1000 1500 2000 2500 3000 3500 4000 4500 5000
Cluster Energy Spectrum
Mean 2123.75 +/- 337.191
Underflow 0
Overflow 0

JAGUAR

gem

γeμ

Presentation by:

G. Word

GEM Collaboration Council Meeting Computing Report

Gary B. Word

Superconducting Super Collider Laboratory

August 5, 1993

Recent progress of computing projects:

Focus: GEM Test Beam (TB) at FNAL

Goal: Provide complete support for TB, from DAQ to Analysis, consistent with long term GEM design

General Coordinators:

- G. Word (SSCL)
- J. Dunlea (U. of Roch., lives @ FNAL)

Project areas:

- Project Management (very brief)
- TB Global Control System
- TB Data Acquisition System
- TB Data Storage
- Data Analysis (skip)
- List of Computing Projects (brief)
- Simulation and Reconstruction (brief, Geometry Builder as example)

TB Global Control System

- Leader: Tom Kozlowski
- Project Members:
  - Tracker: ?. (Been busy @ BNL)
  - Muon: V. Glebov
  - Calorimeter TB: W. Wisniewski
    - Cal. Cryogenics: J. Voyles
    - Cal. TB Transporter: C. Timmer
    - Cal. Monitoring: J. Rutherfoord? / Milind
  - DAQ: H. Uijterwaal
  - EPICS: B. Dalesio, Y-Z Zhou
  - Calibration, threshold: L. Parlier
  - GUI: T. Kozlowski, G. Word
  - nonGEM parts (EPICURE, Cherenkov, Syncrotron, Misc. Scintillators):A. Morelos
- Recent Activities & Documents:
  - 93/7/6 Workshop at SSCL
    - Agenda: Article 36 of ssc.gem.comp
    - Transparencies: GEM TN-93-434
    - Summaries: GEM TN-93-434
    - Synopsis:
      - Interface Coordinators determined; some in-

terface questions addressed.

- Several Cal. and Muon requirements stated.
- EPICS use in TTR discussed as possibility.
- Several EPICS questions to be addressed.
- EPICS test-stand promised "soon."
- Lots of "action items."

– 93/7/28 Initial rough draft by Kozlowski of a GCS System Requirements Specifications and of a System Project Management Plan (limited circulation)

– 93/8/3 Long awaited **EPICS test-stand** finally **shipped** to SSCL; should arrive "any day now."

• Next general meeting: end of August?

Test Beam Data Acquisition System

- Leaders: J. Dunlea, G. Word
- Project Members:
  - H. Uijterwaal, M. Botlo, M. Jagielski, A. Romero, M. Bowden, V. Kappor, Carrel, S. McCorkle, H. Takai
- Recent Activities & Documents:
  - 93/6/16-17 Test Beam Workshop at FNAL
    - Agenda: GEM TN-93-418
    - Transparencies: GEM TN-93-418
    - Summaries: ?
    - Synopsis: (DAQ was small part of meeting.) Some possible DAQ tools were discussed. Decision was made to query the subsystems for their DAQ requirements by July 1 and to DECIDE on the basic DAQ model on July 8-9.
  - 93/7/1 DAQ Requirements Workshop
    - Agenda: Article 3 in ssc.gem.testbeam
    - Transparencies: ?
    - Summary: Article 4 in ssc.gem.testbeam
    - Subsystems Survey Summary: Articles 10 and 13
    - Synopsis: Data rates are expected to be on the order of 10 KB/s, probably at a rate of 100 Hz.

More significantly, D. Marlow proposed that the Test Beam DAQ be modelled after the proposed production DAQ system.

- 93/7/8-9 DAQ Design Workshop at FNAL & SSCL
  - Agenda: Article 5 in ssc.gem.testbeam
  - Transparencies: ?
  - Summaries: Article 8
  - Synopsis: GEM Test Beam at FNAL DAQ will employ a two-level architecture, both VME based, one for **subsystem-level crates**, the other, a master crate for data collection, event building and data distribution. The baseline option for the **master crate** will employ a **hardware switch**, similar conceptually to the GEM production DAQ.
    - **Sean McCorkle** will lead the subsystem-level crate projects.
    - **Michi Botlo** will lead the master crate projects.
    - DAQ & Computing Chapters of RDT coordinated by G. Word
- 93/7/12 Proposal for a switch based event-builder (M. Botlo, M Bowden, H. Uijterwaal)
  - Proposal: Article 9 in ssc.gem.testbeam.
- 93/8/2 Draft MOU between GEM Elec./DAQ Subsystem and PRD Elec. Dept. (coord. by D. Trainer)

Test Beam Data Storage

- Leader: G. Word (acting)
- Project Members: J. Hilgart, L. Cormell
- Recent Activities & Documents:
  - 93/6/2 Memo from L. Cormell requesting specific cpu and data storage requirements (p. 117 in GEM TN-93-418)
  - 93/6/16-17 In transparencies for GEM Test Beam Meeting at FNAL (GEM TN-93-418), statements of requirements for data acces and data storage system design goals/directions can be found. (pp. 111, 115-116)

    - Synopsis: The proposed Test Beam System Design introduces a File Builder which collects events and creates data "files" in the data storage system in "final form". Design goals include:
      - central data repository, probably at SSCL
      - common access to data for all post-File Builder processes
      - transparent access to data; data migration to/from tape by storage system
  - 93/7/? Expression of interest in collaborating with PASS was extended by J. Hilgart, which appeared to be warmly, but cautiously received.

- Request to subsystems:

In order to properly respond to Cornell's request, more information is needed from the detector subsystem groups. Specifically, we need subsystem *documents* which address the following:

1. Event size (available from DAQ survey).
2. Total number of events that will be taken each year.
3. Descriptions of the analysis processes which include:
   - number of people analyzing the data
   - descriptions of expected analysis activities
   - tolerable times for servicing various analysis requests

List of Computing Projects (Draft)

1. Framework Projects (coordinated by I. Sheer and G. Word)
   - Job Control Parameters
   - Software Technology Choices
   - Data Modelling and Module Definition
   - Data Analysis Toolkit and Environment
2. Detailed GEM Detector Simulation and Reconstruction projects (coordinated by J. Womersley)
   - Geometry Builder
   - Describe GEM using the Geometry Builder
   - Describe 1995 Test Beam setup using the Geometry Builder
   - Monte Carlo Generators and interfaces, including simulation of
   - Particle Transporter through the GEM detector
   - Digitization
   - 3D Event Display
   - Full GEM Reconstruction

3. Test Beam (TB) specific projects (coordinated by G. Word):

- TB Global Control System
- TB Data Acquisition / TB Online
- TB Reconstruction
- TB Data Analysis
- TB Database(s)
- Calibration Studies
- Data Storage

For details, see Article 61 in ssc.gem.comp.

Request to add projects to the list should be made to K. McFarlane.

ALL GEM computing efforts should be represented.

Simulation and Reconstruction (briefly)

- Leader: J. Womersley

One recent activity of this project has been focussing on a "Geometry Builder." The next four slides are John's summary of a Working Meeting which occurred here two days ago.

GEOMETRY BUILDER WORKING MEETING
(8/3/93)

16 attendees including 3 from accelerator

John Womersley

Introduction, Overview, Priorities, Risks

Yuri Fisyak

Title constants used in SIGEM (Zebra TZ)

Dale Orth

Modeling of Accelerator (mechanical, shielding) + video

Toby Burnett

GISMO objects : mediums, volumes, graphics

Laurie Waters

SABRINA graphical interface to MCNP/LAHET

Saul Youssef

Review of geometric part of simulation; system of primitives used in GVerify package

Geometry Builder

Initial requirements
Later developments

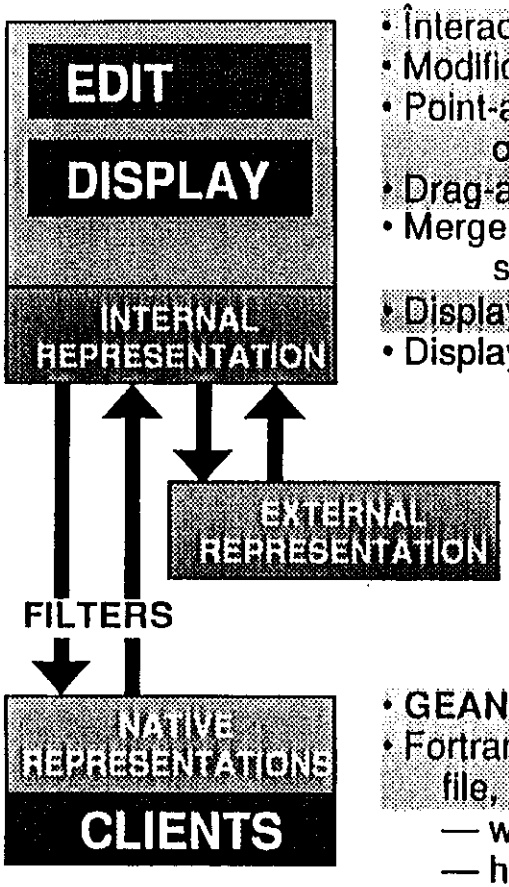

- Interactive geometry creation on the screen with a GUI and mouse
- Modification and positioning of volumes interactively on the screen with GUI
- Point-and-click selection of volumes on the screen, with display of parameters, positioning, materials, media and rotations.
- Drag-and-repositioning with mouse
- Merge geometries from various sources (e.g. to add a CAD model of a support structure, input from an IGES file, to a previously created GEANT model)
- Display in 2D, with slices and projections
- Display in 3D, rotatable, hidden line removal

- Persistent objects?
- ASCII file describing the geometry in some well-defined, human readable format.

- **GEANT** geometry in a GSAVE RZ file and/or
- Fortran code (calls to GSVOLU and GSPOS) list of parameters available as an ascii file, must include creation of materials, tracking media and rotation matrix calls.
  - — with optimization of GEANT geometry tree
  - — handling of magnetic fields in tracking media
- **GISMO**
- **CAD** modeler (IGES file —compatible with AutoCAD, Intergraph & Pro-Engineer)
- **CALOR89**
- **MCNP**
- **Event display, reconstruction, . . .**

USEFUL DISCUSSIONS

— Do we need to define an ASCII geometry language?
can a more generic system (ADAMO, Cheetah) be used?

— Do we want to define our own "internal representation"
(our own solid model) + filters to other representations
or
Choose one existing representation (GISMO? SABRINA?)
as our internal

— Need to think more about needs of clients other than
particle transport — event display, reconstruction, etc.

— Question of making geometry persistent

NEXT MEETING: AUGUST 25-26, FERMILAB

- understand more about GISMO (All)
  → Atwood's television show next week

- understand more about SABRINA (J.W, B.M.)

- scheme for ASCII file based on Cheetah (G.W.)

- poll users — needs, desires

Call for Participation

- Development of computing system is ongoing.
- News of computing projects can be found in the **ssc.gem.comp** and **ssc.gem.testbeam** newsgroups.
- The Computing Subsystem is holding meetings around the time of Council meetings. Each detector subsystem should plan to send a representative to these meetings.
- Needs participation from collaboration at large.
- Further information can be obtained from:
  - K. McFarlane
  - G. Word
  - I. Sheer
  - J. Womersley